https://ntrs.nasa.gov/search.jsp?R=19880001756 2020-03-20T08:35:00+00:00Z

Contract No.: NAS-9-17486
DRL No.: T-1951
Line Item No.: 7
DRD No.: MA-183TH
Tracor Document No.: T86-01-9561-U

FINAL REPORT OF INCIPIENT FAULT DETECTION STUDY FOR ADVANCED SPACECRAFT SYSTEMS

Submitted to:

National Aeronautics and Space Administration
Johnson Space Center
Houston, Texas 77058

November 30, 1986

Submitted by:

G. Martin Milner
Principal Scientist

Michael C. Black
Engineer Scientist IV

J. Mike Hovenga
Engineer Scientist IV

Dr. Paul F. McClure
Consultant

Approved by:

Homer E. Wieland
Division Vice President

Tracor Applied Sciences, Inc.

DISTRIBUTION LIST

Delivery Address:

NASA Lyndon B. Johnson Space Center
Attn: (Mail Code/Name)
Houston, Texas 77058

Quantity	Mail Code	Attention of
1	BE4	Brenda Traylor
1	AL32	Technology Utilization Office
1	JM2	Technical Library
15	EC3	Patrice S. Miller

ABSTRACT

A feasibility study to investigate the application of vibration monitoring to the rotating machinery typical of planned NASA advanced spacecraft components is described. Factors investigated include: 1) special problems associated with small, high RPM machines, 2) application across multiple component types, 3) microgravity, 4) multiple fault types, 5) eight different analysis techniques including signature analysis, high frequency demodulation, cepstrum, clustering, amplitude analysis, and pattern recognition are compared, and 6) small sample statistical analysis is used to compare performance by computation of probability of detection and false alarm for an ensemble of repeated baseline and faulted tests. Both detection and classification performance are quantified. Vibration monitoring is shown to be an effective means of detecting the most important problem types for small, high RPM fans and pumps typical of those planned for the advanced spacecraft. A preliminary monitoring system design and implementation plan is presented.

TABLE OF CONTENTS

TABLE OF CONTENTS (Cont'd)

TABLE OF CONTENTS (Cont'd)

LIST OF TABLES

LIST OF FIGURES

LIST OF FIGURES (Cont'd)

ABBREVIATIONS

ASC	-	Advanced Spacecraft
BB	-	Baseband
Boeing	-	Boeing Aerospace Company
BPFI	-	Ball Pass Frequency - Inner Race
BPFO	-	Ball Pass Frequency - Outer Race
ECLSS	-	Environmental Control and Life Support System
ETRI	-	ETRI, Inc.
FFT	-	Fast Fourier Transform
FRF	-	Fundamental Rotational Frequency
HFD	-	High Frequency Demodulation
Hz	-	Hertz
IFD	-	Incipient Fault Detection
k	-	Unit of One Thousand
LSI	-	Life Systems, Inc.
Machine Spec	-	Tracor's identification for the machine being tested
Micropump	-	Micropump, Inc.
MUX	-	Multiplexer
PCB	-	PCB Piezotronics, Inc.
P_D	-	Probability of Detection
P_{FA}	-	Probability of False Alarm
Raw	-	Uncorrected Vibration Data
Refit	-	U.S. Navy terminology for a set of vibration readings within an experiment
RPM	-	Revolutions Per Minute
TRW	-	TRW, Inc.
VAX	-	Trademark of Digital Equipment Corporation's Computer Systems at Tracor Applied Sciences, Inc.
VMS	-	Vibration Monitoring System

EXECUTIVE SUMMARY

Theoretical and experimental investigations were performed to assess the feasibility of applying vibration monitoring techniques to advanced spacecraft. Approaches and techniques were developed to enhance the reliability of small rotating machinery components.

Over 200 documents were obtained and reviewed during the Conceptual Study Phase of the effort and thirteen major vibration analysis techniques were identified for investigation. Little practical information on realistic fault and failure modes for representative rotating components was obtained from manufacturers and the literature survey. Tracor and LSI engineering evaluations resulted in several potential fault/failure modes to be investigated.

Vibration analysis was demonstrated to be an effective means of early detection for a majority of the problems associated with small, high speed machines. The most severe problem types investigated (impeller fault, large imbalance, loss of bearing lubrication, and bearing race faults) were shown to be detectable with very low probabilities of false alarm (P_{FA}). The expected number of false alarms during a specified period is proportional to the product of P_{FA}, vibration sample rate, and total number of machines sampled. Values of P_{FA} were sufficiently small for the severe problems to allow frequent sampling of numerous machines.

A methodology for quantifying and comparing vibration analysis techniques was developed and demonstrated which allows assessment in both absolute and relative terms for small-sample laboratory experiments. Both detection and classification functions were quantified.

An effective classification capability for some problem types was demonstrated even though the primary focus of the study was problem detection. Continued development would significantly improve classification capability. It is expected that a majority of problem types can be classified effectively.

The most promising technique over a wide range of problem types was shown to be the weighted sum of the baseband power spectra. This technique is generic in approach but can be systematically matched to individual problems. The use of reference baseline data on each individual machine is very important in order to significantly increase problem detectability.

Processing of high frequency demodulation (HFD) data was shown to be of marginal value for problem types other than bearing race faults. A clustering algorithm to detect harmonics combined with HFD increased the detection probability to 0.99 versus 0.90 for baseband analysis of fan outer race faults. Attempts to select "optimum" bandpass center frequencies appeared to have little effect. Cepstrum analysis provided no significant problem detection enhancement for the problem types investigated. Likelihood ratio processing of time series in the full analysis bandwidth provided no significant increased detection capability. This technique was expected to be superior to most amplitude statistical processing including kurtosis and peak detection.

Theoretical and experimental investigations to assess the effects of a microgravity environment on the performance of vibration monitoring techniques were performed. Gravitational effects on bearing preload were shown to be significant and must be taken into account when comparing vibration monitoring technique performance at one g with microgravity performance.

Theoretical and experimental investigations were conducted to assess the applicability of vibration monitoring techniques across a range of dissimilar machines of the same basic type. Correction factors for machine size, construction details and operating speed were developed and shown to be applicable to vibration monitoring techniques designed to detect rotor imbalance in two different size fans by responding to changes in mean square acceleration.

A preliminary monitoring and analysis plan was developed which demonstrated the feasibility of implementing an automated Vibration Monitoring System (VMS) onboard advanced spacecraft. System component design, incorporation of pattern detection/classification techniques, database management, and expert system utilization were described which would form the basis of a final VMS.

1.0 INTRODUCTION

1.1 Background

The purpose of the Incipient Fault Detection Study for Environmental Control and Life Support Systems (ECLSS) was to investigate the feasibility of applying vibration monitoring techniques to small rotating machinery components, and to recommend and develop approaches and techniques that enhance reliability and maintainability. This investigation included a Conceptual Study, an Application Study, and the development of a Monitoring/Analysis Plan.

The advanced spacecraft (ASC) will contain numerous small rotating machines critical to the mission. These components will be required to operate over extended periods of time and will be subject to failures due to wear during normal operation, as well as early failures due to manufacturing or installation errors.

Previous experience with rotating machinery has demonstrated that vibration monitoring and analysis can significantly reduce the cost of maintenance, increase reliability, and decrease the probability of catastrophic failure. However, this previous experience has been limited primarily to large rotating machines such as power generators, turbines, and associated support equipment. Examples include the Navy vibration monitoring programs to improve the reliability/maintainability of rotating machines onboard submarines and surface ships and the utilization of vibration monitoring techniques by power generating companies and large industrial operations.

The planned use of very small rotating machines (fractional horsepower) in the ASC to provide critical functions and the requirement to operate without failure over extended periods has resulted in the need to investigate techniques for increasing reliability and maintainability of small machines. Vibration monitoring and analysis is an excellent candidate technique.

1.2 Report Organization

This document is a final report summarizing the approach that was implemented, results and conclusions, and recommendations for future work. Sections 2.0 and 3.0 describe the Conceptual Study and the Application Study that were performed and present detailed results of

these studies. A preliminary design for a vibration monitoring system (VMS) is presented in Section 4.0, together with a monitoring plan. Results, conclusions, and recommendations are summarized in Section 5.0.

A comprehensive list of references is provided, which incorporates all references contained in the intermediate deliverables as well as references contained in other related reports and publications produced during the study. A list of all deliverables and related reports produced during the effort is provided as reference in Appendix A. Appendices B and C are detailed reports describing investigations of microgravity effects and dissimilar machine effects. Appendix D provides details related to feasibility testing and overall results. Appendix E contains a detailed description of the derivation of likelihood ratio weights for vibration spectra and Appendix F contains a description of the clustering algorithm used to detect and analyze harmonic series.

The Final Conceptual Study Report is provided as Volume II.

2.0 CONCEPTUAL STUDY

2.1 Introduction

The Conceptual Study addressed major aspects of vibration monitoring as they apply to increased reliability/maintainability of rotating components of the ASC. A systematic approach was implemented for the selection of potential vibration monitoring techniques. The approach includes: 1) definition and ranking of six specific vibration monitoring functions, 2) definition and ranking of fault types, 3) identification of all important vibration characteristics, and 4) identification of thirteen major processing techniques and ranking according to functions performed, fault types addressed, performance potential, and other factors. Statistical analysis methods applicable to small sample experiments typical of vibration analysis experiments were developed. An expert system approach was developed during the Conceptual Study to provide automatic vibration signature analysis.

Section 2.2 provides an overview of the Preliminary Conceptual Study. A comprehensive description of the Conceptual Study is contained in Volume II of this report. Sections 2.3 through 2.5 summarize Conceptual Study efforts performed since completion of the Preliminary Conceptual Study. These efforts are:

1. An extended evaluation of selected analysis techniques,
2. A theoretical investigation of microgravity effects,
3. A theoretical investigation of dissimilar machine effects, and
4. An investigation of machine size effects.

2.2 Preliminary Conceptual Study Overview

An overview of technical issues addressed during the Preliminary Conceptual Study is presented in Sections 2.2.1 through 2.2.7. Topics include:

1. Selection of components for testing,
2. Identification of vibration monitoring functions,

3. Identification of component faults, failure modes, and related vibration characteristics,
4. Analysis techniques,
5. Quantification of performance,
6. Automation, and
7. Concept analysis, ranking, and scaling rationale.

2.2.1 Selection of Components for Testing

Selection of components for testing began with a survey of the proposed ASC systems and hardware. A detailed description of the selection process is contained in Section 2.2 of Volume II, Final Conceptual Study Report. Boeing Aerospace and Life Systems Incorporated (LSI) completed surveys of ASC equipment. The Boeing study focused on selection of fans and the LSI study focused on selection of pumps. Both subcontractors also performed general surveys of all ASC equipment. Reports submitted by each subcontractor are included as Appendix A (Boeing) and Appendix B (LSI) to Volume II of this report.

Functional partitioning of the ASC was divided into seven categories:

1. Atmosphere Revitalization System (ARS)
2. Atmosphere Pressure and Composition Control System
3. Module Temperature and Humidity Control System
4. Water Management System
5. Waste Management System
6. Extravehicular Activity (EVA) Support
7. Safe Haven

The surveys of equipment conducted by Boeing and LSI revealed clear choices for test components based on the number and type of rotating components. The Boeing survey of Space Shuttle ECLSS components also revealed that all rotating machinery components were

powered from a three phase, 400 Hz source and that test components should therefore meet these specifications in order to be representative. Table 3.1 in Section 3.0 of this report lists the rotating components used for testing and provides a summary of their characteristics.

2.2.2 Identification of Vibration Monitoring Functions

A comparison of relative merits and performance optimization of analysis techniques requires clear definitions of the vibration monitoring functions to be performed. Also, selection of candidate techniques for the same function requires concise definitions of measures of success (e.g. probability of detection (P_D), probability of false alarm (P_{FA}), probability of correct classification, error bounds for estimated parameters, and others). Vibration monitoring/analysis techniques can be used during three phases of a given component life cycle: design, acceptance testing, and operational phases.

Initial design phase monitoring at the development test level could help eliminate inherent design problems which cause imbalance, misalignment, or rubbing. Investigation of this use of vibration monitoring, although possibly very effective, was considered beyond the scope of this study. In general, investigation of vibration monitoring for acceptance testing was also considered to be beyond the scope of this study. However, successful application of vibration monitoring to detect operational problems will require a complete program of acceptance testing and operational monitoring. Therefore, most of the proposed operational vibration monitoring techniques begin with an acceptance test prior to operational monitoring.

Two levels of functionality were defined to assess and rank vibration monitoring functions. A high level of functionality was defined to rank importance and a more concise level was defined for design and study. The higher level vibration monitoring functions defined for this study are:

1. Continuous Protection Against Catastrophic Failure,
2. Early Detection of Machine Abnormalities,
3. Accurate Diagnosis of Problem/Given a Detected Machine Abnormality,
4. Assessment of Level of Severity/Given a Detected Machine Abnormality,
5. Accurate Prediction of Future Machine Condition versus Time (Including Time to Failure)/Given a Detected Machine Abnormality, and

6. Provision of Feedback Information for Control of Machine Operational Characteristics.

Section 4.0 of this report describes three levels of processing: level zero, level one, and level two. With the exception of "continuous protection against catastrophic failure" which is a level zero function, the six functions listed here may be performed as either level one or level two processing which are periodically performed at regular intervals. The distribution of functions over level one or level two depends on the performance levels that can be achieved with a given sample rate.

2.2.3 Identification of Component Faults, Failure Modes, and Related Vibration Characteristics

Six separate sources were used during the Conceptual Study to obtain information related to ECLSS component faults and failure modes:

1. Boeing survey of the Orbiter Problem Record database,
2. LSI survey of failure rate tables for ECLSS rotating components, published by Hamilton Standard,
3. Detailed engineering evaluation conducted by LSI,
4. General literature survey conducted by Tracor,
5. Engineering analysis conducted by inspection of test components, and
6. Repair experience of Texas Process Equipment--the major service center for Micropumps and Micropump, Inc..

The Orbiter Problem Record database was accessed by Boeing to identify failures which have been reported in the ECLSS subsystems over the past ten years. Failure reports were provided to Tracor to identify the number and types of failures that have been experienced. The overall results and conclusions drawn from these observations are as follows:

1. The NASA quality control process is excellent;
2. The Space Shuttle missions are too short (with respect to mechanical life expectancy) to induce faults and mechanical failure "due to normal operation" conditions;
3. Additional data is needed on post-flight inspection and disassembly of 1981 and later Space Shuttle flights;
4. A long term life expectancy test program of mechanical components should be undertaken or data from such a test be made available. Proper measurement and analysis of long term vibration characteristics of these components should be an integral part of these life expectancy tests.

Computations of unit failure rates were developed by LSI from subcomponent failure rates published by Hamilton Standard. These failure rate values may be used to estimate the units most likely to fail. However, they should not be interpreted as indicative of the probability that a given unit will develop an incipient fault detectable by vibration monitoring.

Engineering evaluation was performed by LSI to estimate the most likely faults or failures for ECLSS components. The fault types--balance, alignment, rubbing wear, and breakage--were defined as candidates. The ECLSS subcomponents were listed and the possibility of a given fault type in a given subcomponent was identified.

The extensive literature survey conducted during the Conceptual Study provided no useful published information regarding the likelihood or importance of specific faults due to wear for small, high-speed, rotating machines. This result supports the conclusion that a long term life expectancy test program for mechanical components should be undertaken. Pump and fan components selected for IFD testing were disassembled and inspected in order to identify possible fault types. Information regarding fault and failure identification for motor driven pumps was sought by contacting Texas Process Equipment--the major service center for Micropumps and Micropump, Incorporated, the units selected for testing. The vibration characteristics of each test components' fault type were identified and defects were ranked according to severity and likelihood of occurrence.

2.2.4 Analysis Techniques

A review of current vibration analysis literature resulted in the identification of thirteen major techniques that may be useful for analysis of vibration data from ECLSS rotating machines. A list of these techniques and references for each technique are presented in Table 2.1. The first eight techniques listed in Table 2.1 were investigated during this study. Techniques nine through twelve were not investigated due to the unique equipment required for implementation. The Hilbert transform, used primarily as a means of implementing demodulation processing, was judged to have minimal applicability and was not investigated.

2.2.5 Quantification of Performance

Comparison of diverse algorithms with diverse outputs was an important requirement. The approach consisted of entering measured values for baseline and faulted results in a computational algorithm to compute bounded values of P_D and P_{FA}. These quantities were determined by the mean (μ) and variance (σ^2) for the baseline versus the mean and variance for faulted, and the number of repeated trials. Values of P_D for each algorithm were compared at fixed values of P_{FA}. Values of P_D and P_{FA} were computed by integration of Gaussian densities. The assumption of Gaussian statistics is based on the knowledge that the algorithm outputs are obtained by a summation of independent variates so that the central limit theorem may be applied, and the fact that the underlying experimental variables are the ensemble of many possible fault variations.

Often only four baseline cases and four faulted cases were analyzed in the laboratory. Estimates of μ and σ may be very poor for this small sample, however, they may also be sufficient to clearly quantify algorithm performance. Small sample analysis is a difficult area in the field of statistics because there are no generalized theories. A Monte Carlo based program was developed to analyze the small sample statistics. Measured values of μ and σ are used as input and confidence limits are computed. Tables 2.2 and 2.3 contain example computations for representative values of baseline and faulted μ and σ for spectrum analysis of a tone.

Two sets of example values for median P_D are given in Tables 2.2 and 2.3 for four versus eight experiments. These values may be used to quantify the information gained in this

Table 2.1 - Major Vibration Analysis Techniques

VIBRATION TECHNIQUE	REF.	EXPLANATION	VIBRATION TECHNIQUE	REF.	EXPLANATION
1. Signature	[1]	Examine acceleration power spectrum with bandwidth	8. Transient Analysis	[8]	Process data to detect and capture short duration effects that may t effect average quantities such power spectra.
					se a tach signal to obtain and ocess vibration records synched ith the machine rotation rate.
					se two or more accelerometers id measure coherence or other oss properties and identify phase lations.
					se an impedance transducer to easure net flow of energy rather an vibrational energy.
					orm a two dimensional spectrum o measure crosspower between wo frequencies and their sum to letect nonlinear effects.
					means of extracting envelope formation from a modulated time ignal.

Table 2.2 - Example Computation of Confidence Bounds for Probability of Detection (P_D) and Probability of False Alarm (P_{FA}) for Four Repeated Trials

		μ	σ
Baseline Values	70, 72, 77, 71	72.50	3.11
Faulted Values	85, 89, 83, 94	87.75	4.86

P_{FA}	P_D		
	Assume μ, σ are True Values	Median Value for Four Trials	90% Confidence Value for Four Trials
.5	.9991	.997	.85
.3	.998	.990	.74
.1	.990	.97	.57
.01	.95	.87	.10

Table 2.3 - Example Computation of Confidence Bounds for Probability of Detection (P_D) and Probability of False Alarm (P_{FA}) for Eight Repeated Trials

	μ	σ
Baseline Values	72.50	3.11
Faulted Values	87.75	4.86

P_{FA}	P_D Median Value for Eight Trials
.3	.992
.1	.983
.01	.92

example by increases in repeated trials. For example, if values of $P_{FA} \cong .01$ and $P_D \cong .9$ are of interest and computed results for two candidate algorithms yield results that differ by more than $\Delta P_D = .05$, then four experiments are sufficient. If the difference is less than .05, then an increased number of trials is required to reliably select the best algorithm.

2.2.6 Automation

Vibration analysis methods requiring manual monitoring are incompatible with the ASC environment. Vibration parameters must be automatically monitored onboard by system software. An autonomous maintenance prediction system should be in the form of signal processing to detect features followed by an expert system to complete the diagnosis and recommend actions. Additional details concerning automation of vibration monitoring techniques are provided in Section 4.0 of this report.

2.2.7 Concept Analysis, Ranking, and Selection Rationale

Concept analysis, ranking, and selection rationale address:

1. ECLSS Component Selection,
2. Vibration Monitoring Functions,
3. Fault/Failure Modes,
4. Performance Potential,
5. Development Difficulties, and
6. Information Display and Interpretation.

A method of ranking performance potential was developed during the Conceptual Study. The ranking method, described fully in Reference [11], incorporated the factors of 1) number of monitoring functions performed, 2) number of fault types detectable, 3) preliminary assessment of performance, 4) technical risk, 5) difficulty of testing, and 6) difficulty of complete development. Based on this ranking method, the highest ranked analysis techniques during the Conceptual Study were narrowband spectral analysis or signature analyses, high frequency demodulation, statistical analysis of amplitude (e.g. likelihood ratio processing), and process modeling (e.g. autoregressive moving averages modeling). Results obtained during the Application Study (see Section 3.0 of this report) demonstrate that post-processing of vibration signatures does provide significant detection and diagnostic capability, and that HFD is a valuable technique for certain problem types. However, statistical analysis of amplitude and process modeling appear to have substantially less potential than these highest ranked techniques.

2.3 Extended Evaluation of Selected Analysis Techniques

In conjunction with the Application Study, several vibration analysis techniques were implemented and examined in detail. These techniques fall into two categories: 1) post-processing of narrowband vibration power spectra, and 2) processing of alternate data types. The techniques examined are listed below for each category.

Post-Processing of Narrowband Vibration Power Spectra

1. Likelihood ratio weighted summation
2. Modified likelihood ratio weights
3. Single frequency signature analysis
4. Multiple frequency signature analysis
5. Spectral continuum analysis
6. Cepstrum analysis
7. Automatic frequency clustering

Processing of Alternate Data Types

8. High frequency demodulation
9. Analysis of amplitude statistics

Summary definitions and descriptions for each of the techniques listed above are contained in section 2.3.1 through 2.3.9. Section 2.3.10 provides a description of the methods used to compare the performance of each technique.

2.3.1 Likelihood Ratio Weights

The likelihood ratio weighted sum of vibration power spectra was demonstrated to be clearly superior in detection performance to other algorithms investigated during this study. A detailed derivation and discussion of the application of the technique is presented in Appendix E of this report. A summary description is provided in this section.

The equation for the likelihood ratio weights used for this study is:

$$W_i = \frac{m_{bi} - m_{gi}}{\sigma_i}$$

where

m_{bi} = mean value at frequency bin i for bad machines

m_{gi} = mean value at frequency bin i for good machines

σ_i = standard deviation at bin i for all machines.

The test statistic is given by

$$L = \sum_{i=1}^{m} (s_i - m_i) W_i$$

where

$$m_i = m_{bi} + m_{gi}/2$$

s_i = value for a given vibration power spectrum at bin i, and

m = total number of spectral lines.

If,

$L > 0$, machine is called BAD

$L \leq 0$, machine is called GOOD.

The procedure is intuitively reasonable. Power spectra are obtained for a set of machines in good condition and for a set of machines in faulted condition. The values for m_{bi}, m_{gi}, and σ_i are computed and the bins with the largest mean shift ($m_{bi} - m_{gi}$) as compared to their stability (σ_i) receive the largest weights. A weighted sum is then formed to detect the faulted condition. The weights are useful indicators of the relative importance of specific frequencies as indicators of a specific problem.

The method of obtaining estimates of P_D and P_{FA} given estimates of the mean and standard deviation of L over good (baseline) and over bad (faulted) experiments (μ_B, σ_B, and $\mu_F\sigma_F$) is described in Section 2.3.10.

2.3.2 Modified Likelihood Ratio Weights

For very small samples of faulted versus good machines, it is often reasonable to select the clearly dominant likelihood ratio weights and set all other values to zero. Selected weights may then be used to analyze the increased/decreased detectability due to selected tones or

tone groups. Key frequencies (fundamental, bearing tones, and others) may be analyzed separately, and each set of weights may be stored and used independently.

2.3.3 Single Frequency Signature Analysis

Single frequency signature analysis was quantified by defining a set of weights so that a single selected frequency bin was assigned a value of 1.0 and all other weights were assigned values of 0.0. Thus, the power level at a single bin became the detection statistic. The procedure for weighted sum processing is described in Section 2.3.1.

2.3.4 Multiple Frequency Signature Analysis

Multiple frequency signature analysis was quantified by assigning weights of 1.0 to selected bins and values of 0.0 to all remaining bins. The weighted sum analysis procedure described in Section 2.3.1 was then implemented.

2.3.5 Spectral Continuum Analysis

Some problem types result in spectral continuum features rather than tonal increases. Examples include operation at elevated temperature and particle contamination (see section 3.0 of this report). Detection performance for algorithms designed to detect these continuum effects were examined by applying a weighting function that omits all tones ($W_i = 0$ at each tone) and accepts spectral data in local frequency regions ($W_i = 1.0$). The weighted sum analysis technique is described in Section 2.3.1.

2.3.6 Cepstrum Analysis

Reported advantages of cepstrum analysis are that single cepstral lines indicate average "activity" of families of uniformly spaced sidebands and harmonics and can be easily monitored. Another is that the log operation results in the ability to separate or deconvolve multiplicative effects.

The power cepstrum used for this study is defined as;

$$C_p(\tau) = \int [\log G_\chi(f)] e^{j2\pi f\tau} \, df$$

where

$C_p(\tau)$ = power cepstrum,

τ = quefrequency (seconds), and

$G_\chi(f)$ = power spectrum of the time signal $\chi(t)$, defined as

$$G_\chi(f) = 2 \left| \int \chi(t) e^{-j2\pi ft} dt \right|^2$$

A second type of cepstrum termed the complex cepstrum is defined as;

$$C_c(\tau) = \int [\log S_\chi(f)] e^{-j2\pi ft} df$$

where

$C_c(\tau)$ = complex cepstrum, and

$$S_\chi(f) = \int \chi(t) e^{-j2\pi ft} dt \quad |S_\chi(f)| e^{j\phi\chi(f)}$$

Thus,

$$\log S_\chi(f) = \log |S_\chi(f)| + j\phi\chi(f)$$

A general power cepstrum analysis capability was developed. To apply the power cepstrum technique, an operator observes the spectrum processed in an arbitrary band and selects a raw, normalized, or noise spectral equalized spectrum for analysis. A window width up to full band integration is selected for cepstrum analysis. The final selection is the frequency range to search for harmonic tones. Cepstrum values are then printed to the screen and another selection may be made. The operator records the values of the cepstrum at selected quefrequencies for each

measurement. The values for baseline experiments and faulted experiments are then used to compute μ and σ of the cepstrum values. The values of μ_B, σ_B, μ_F, σ_F are used to compute P_D and P_{FA} for comparison with alternate techniques as described in Section 2.3.10.

Sensitivity to spectral continuum is a problem that can arise with cepstrum analysis, as shown in Figure 2.1. Region A will result in large cepstrum values at frequency spacing Δf. The cepstrum may be interpreted as a weighted sum with sinusoidal functions as the reference weights. Therefore, the cepstrum is much more sensitive to sinusoidal continuum variations than to harmonic series. Cepstrum's original use was to detect "scalloped" spectra obtained in multipath situations. Another problem with cepstrum analysis is its inherent sensitivity to frequency span of harmonic series, as shown in Figure 2.2. If cepstrum is taken over the entire frequency band, the harmonic series shown in B may not be detectable. Modifications that were implemented to improve the performance of cepstrum analysis are:

- Equalizing the spectrum prior to cepstrum analysis to eliminate sensitivity to the continuum, and
- Local integration over selected frequency regions.

2.3.7 Automatic Frequency Clustering

A general cluster analysis capability was developed during the study. A complete description of the algorithm is provided in Appendix F. To apply the technique, an operator selects a tone threshold after observation of the spectrum for an arbitrary band. A default cluster search is then made at the machine fundamental. Clusters are identified and highlighted on a display with average Δf and average amplitude shown. The display lists all frequencies along with their amplitudes and identifies the two largest values. The operator may then select the next frequency separation and repeat the search.

After harmonic series are identified by clustering, the following quantities may be computed and displayed:

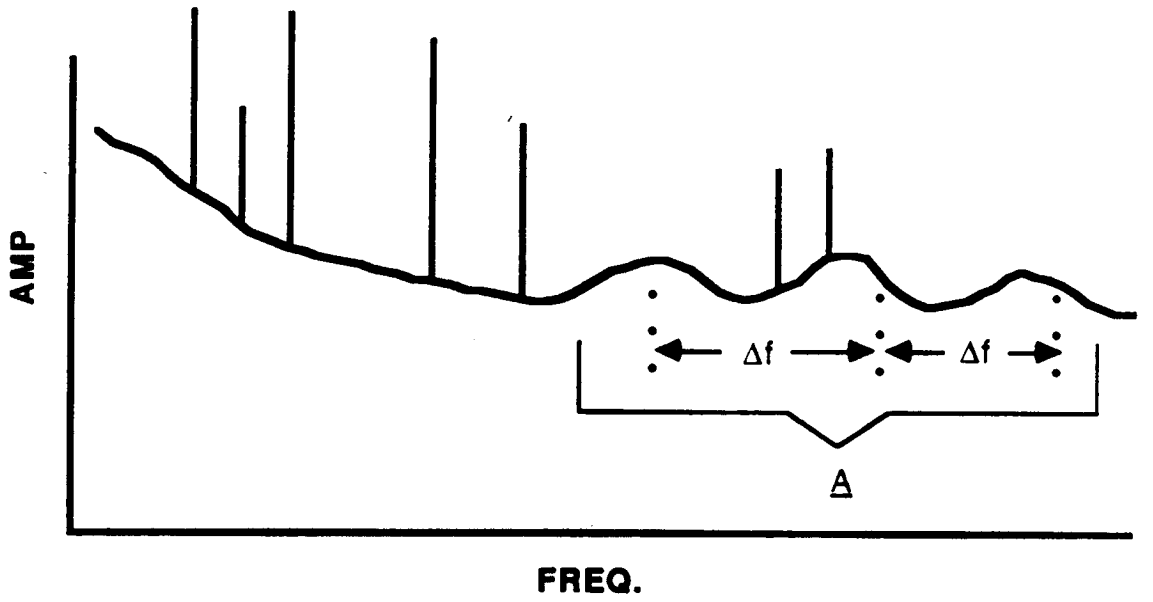

Figure 2.1 - Sensitivity of Cepstrum Analysis to Spectral Continuum

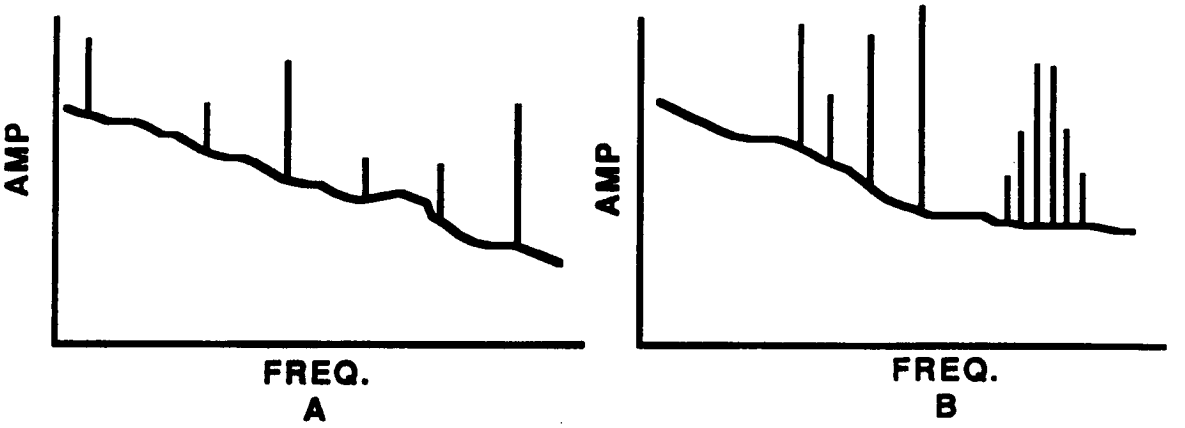

Figure 2.2 - Sensitivity of Cepstrum Analysis to Frequency Span of a Harmonic Series

1. Peak amplitude(s) of a series,
2. Average amplitude of a series,
3. Average amplitude of all series with equal spacing,
4. Number of tones in a series,
5. Average frequency spacing of a series, and
6. Frequency location of each tone in a series.

Each of these statistics may be selected for detection analysis.

The harmonic series identification algorithm developed during this study is considered to be far superior to cepstrum analysis. In effect, clustering accomplishes the aggregation of multiple tone levels to a single number (e.g. average amplitude of tones) and much more (frequency location, number of tones, asymetries, and others). Clustering also eliminates the two primary cepstrum problems noted in Section 2.3.6 of sensitivity to continuum, and localized harmonic content.

2.3.8 High Frequency Demodulation

High frequency demodulation is a technique to extract relatively low frequency information for a high frequency signal that has been amplitude modulated by a mechanical defect. The most prevalent use of the high frequency demodulation technique is in the area of bearing fault detection. Impulsive vibrations illustrated in Figure 2.3 excite resonant modes at high frequencies as illustrated in Figure 2.4 so that the vibration waveform may be modeled as an amplitude modulated carrier. The envelope signal shown in Figure 2.4 will contain discrete peaks with periodicities determined by the input rate of the defect. Spectral analysis (after effectively bandpassing the signal) of the envelope will produce a harmonic series with a fundamental frequency that is related to the bearing frequencies. A demodulation circuit was constructed as illustrated in Figure 2.5.

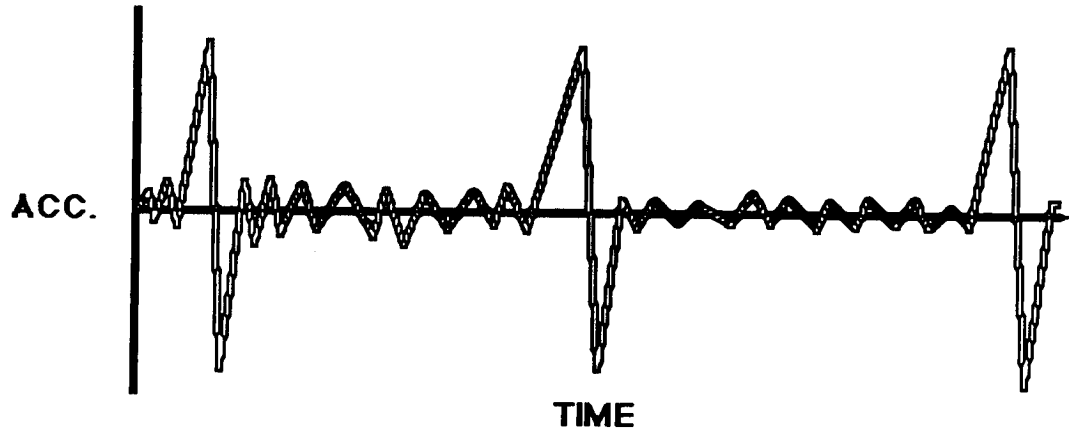

Figure 2.3 - Acceleration Waveform for Impulsive Vibrations

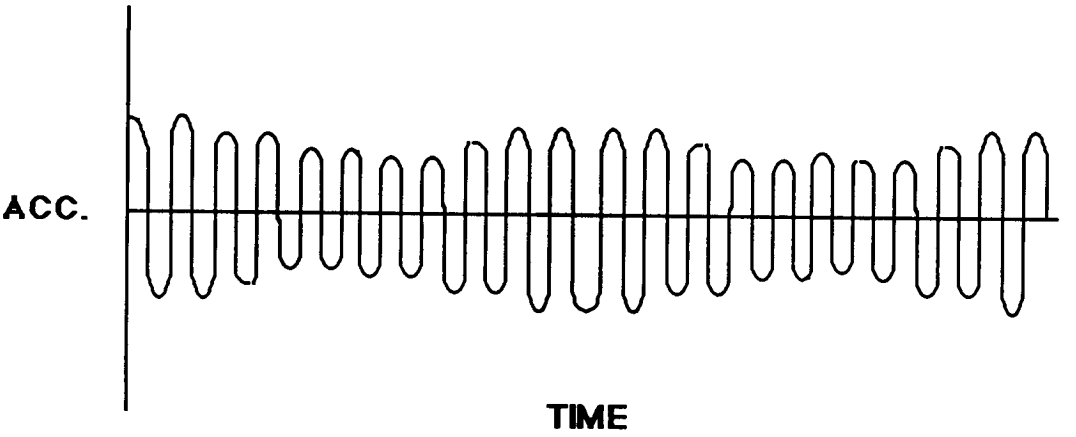

Figure 2.4 - High Frequency Resonant Mode Vibrations

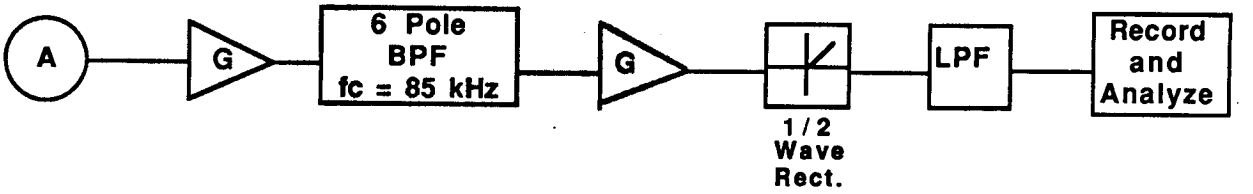

Figure 2.5 - High Frequency Demodulation Processing

Parallel data acquisition of both baseband and HFD data was implemented throughout the study. The post-processing techniques described in Sections 2.3.1 through 2.3.7 were also applied to the spectrum of the HFD data.

2.3.9 Analysis of Amplitude Statistics

Many machinery vibration studies obtain amplitude statistics or amplitude information but fail to utilize this information properly. Reference [5] discusses this in detail and provides an excellent example of the gains that may be achieved by application of classical detection theory and estimation theory. Two examples of statistical processing of amplitude samples are likelihood ratio and kurtosis. Many types of faults create distinctly different vibration amplitude distributions. For example, for a single bearing spall, the amplitude densities may appear as illustrated in Figure 2.6. The likelihood ratio

$$L(x) = P(x/Bad) / P(x/Good)$$

provides a function of x that "best" separates bad from good.

Amplitude densities are computed for baseline and faulted data as a part of the implemented processing. Likelihood ratios are then computed and used to process data.

2.3.10 Comparison of Performance

A major technical problem addressed during this study was the development of methods to compare the performance of diverse vibration monitoring techniques. The approach was to compute probabilities of detection (P_D) and probabilities of false alarm (P_{FA}) for each algorithm and each problem type. Comparison of algorithm performance as measured by P_D at fixed values of P_{FA} was used to quantify the differences in performance for each algorithm for given fault types.

In order to compute values of P_D and P_{FA}, the outputs of any algorithm were assumed to have Gaussian amplitude statistics [$G(\mu,\sigma)$] for an ensemble of experimental factors. Since these outputs are a result of the summation of numerous independent factors, a Gaussian assumption was warranted. The following procedure was then used to obtain curves of P_D versus P_{FA}:

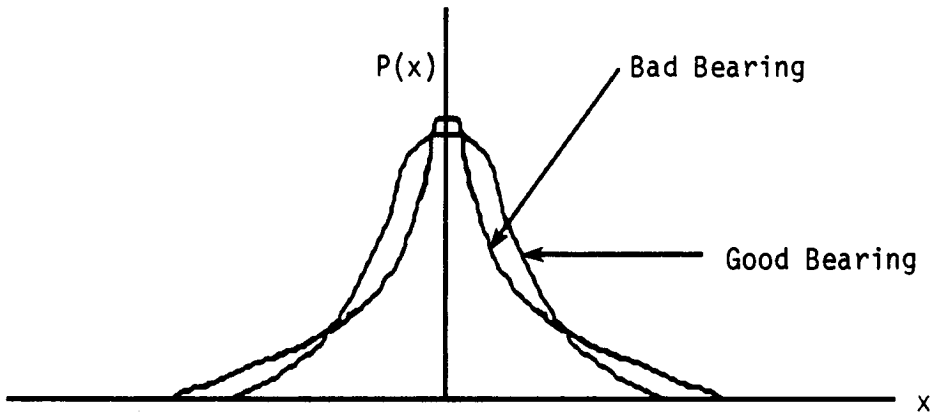

Figure 2.6 - Example Amplitude Densities

1. Measure the mean (μ) or average values of the processor output for baseline and faulted data (μ_B and μ_F).

2. Measure the standard deviation (σ) of the processor output for baseline and faulted data (σ_B and σ_F)

3. Compute P_D and P_{FA} by:

$$P_D = \int_T^\infty G(\mu_F, \sigma_F)\, dx$$

$$P_{FA} = \int_T^\infty G(\mu_B, \sigma_B)\, dx$$

Values of P_D and P_{FA} are obtained at equal values of T in order to compute P_D versus P_{FA}.

Since the values for μ and σ are estimated from a very small sample (usually four baseline experiments and four faulted experiments) a separate Monte Carlo technique was developed to quantify the uncertainty in P_D and P_{FA}. The Monte Carlo technique (see Section 2.7 of Volume II of this report) augmented the integral technique described above in those cases where relatively small differences in P_D or P_{FA} were important.

2.4 Theoretical Investigation of Microgravity Effects

A theoretical investigation of microgravity effects was conducted to assess the effects of a microgravity environment on the performance of vibration monitoring techniques. Potential gravity effects include: 1) gravitational preload on bearings induced by the rotor weight force applied axially, 2) a secondary critical speed at twice the shaft rate caused by the gravity-induced tangential component of angular acceleration associated with rotor imbalance for a horizontal rotation axis, 3) a flat-shaft secondary critical speed at twice the shaft rate caused by asymmetrical bending stiffness of a horizontal shaft, 4) nonlinearities in bearing and/or foundation stiffness which can result in slightly different spring constants with and without a weight force applied, and 5) gravitational effects on wetting, spreading, and operating characteristics of bearing lubricants.

Potential gravity effects on imbalance response of a typical spacecraft air-handling fan were assessed based on theoretical considerations. Rotor shaft bending was examined to estimate the primary critical speed. The secondary critical speed caused by imbalance in a horizontal shaft (item 2 above) occurs at a shaft rate equal to one half of this primary critical speed.

Excitation amplitude at the secondary critical speed was found to be negligible for the typical fan considered. Appendix B provides details concerning the potential microgravity effects.

2.5 Theoretical Investigation of Dissimilar Machine Effects

A theoretical investigation was performed to assess applicability of vibration monitoring techniques to machines of the same basic type that differ in size, construction detail, and operating characteristics. Machinery vibration monitoring typically requires application of a particular fault detection technique to a group of such dissimilar machines. It is natural to ask if theory, validated by laboratory tests, can provide quantitative guidance for selection and interpretation of monitoring techniques intended for application to such a group of machines. A valid assessment of vibration monitoring techniques requires investigation of enough baseline and faulted cases to support statistical comparisons. However, it is generally neither possible nor cost effective to obtain enough samples for statistically meaningful comparisons using actual machines, under controlled conditions. The following questions arise:

1. Can valid conclusions about the applicability of vibration monitoring techniques to actual machines be derived from laboratory tests performed with scale models?
2. What are the effects of size, construction differences, and operating speed?
3. What scaling laws apply?
4. What parameters must be scaled?
5. Can valid corrections for off-scale conditions be developed?

Successful resolution of these issues for a given fault type makes possible the approach shown in Figure 2.7.

Table 2.4 presents two complemetary analyses required to support valid conclusions about the applicability of vibration monitoring techniques across a range of machine sizes and operating characteristics. Equivalence of the Strouhal number was found to be critical to the analysis. A correction for off-scale conditions was developed using the dynamic model.

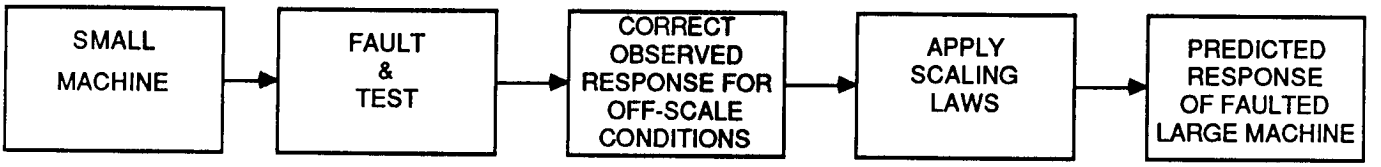

Figure 2.7 - Approach for Interpreting Small-Machine Tests to Predict Response of a Faulted Large Machine

Table 2.4 - Modeling and Analysis Required to Compare Monitoring Techniques Applied to Different Machines

Dynamic Model	Dimensional Analysis
Forces and input/output mechanics associated with specific fault type are represented.	Dimensional analysis incorporates judgement about which forces play a dominant role for the specific fault type.
A parameter study using the dynamic model supports assessment of importance of machine size, speed, and construction details.	Dynamic similarity requirement assures that ratios of dominant forces are the same for different size machines.
Validated dynamic model permits development of quantitative corrections for parameter and speed differences between machines.	Dimensional analysis based on dynamic similarity provides guidance for experimental procedures designed to compare monitoring technique performance.

Appendix C includes a comprehensive discussion of the theoretical investigations of dissimilar machine effects.

2.6 Small Machine Effects

Problem areas identified during this study include: 1) decreased vibration stability, which extended the observation periods necessary to obtain repeatable measurements, 2) increased sensitivity to machine tolerances and construction, which increased the variability of results and the difficulty of repeatable assembly, 3) increased sensitivity to minor forces and orientation changes, which were noted during experimental tests, and 4) increased sensitivity to mounting characteristics.

3.0 APPLICATION STUDY

3.1 Introduction

The purpose of the Application Study was to determine if vibration monitoring can be used to enhance advanced spacecraft reliability/maintainability through the testing of typical rotating machinery components. The technical areas to be addressed include:

1. Application and verification of vibration monitoring across varied machine types,

2. Gravitational effects,

3. Correlation of operating parameters (temperature,pressure,flow) with vibration characteristics,

4. Detection of characteristic faults by signal analysis,

5. Evaluation of multiple analysis techniques identified during the Conceptual Study, and

6. Quantification of algorithm performance by statistics.

A detailed Master Test Plan to achieve the objectives stated above was delivered and approved by the NASA Technical Monitor. The Master Test Plan is referenced as Tracor Document No. T86-01-9511-U and was DRL No. T-1951, Line Item - 5. The following sections summarize results of the Application Study.

3.2 Laboratory Demonstrator

3.2.1 Test Components

Investigations performed by Boeing and LSI during the Conceptual Study indicated clear choices for IFD test components based on the number and type of ASC rotating machinery components. The subcontactor's recommendations were incorporated into a selection process/trade study in which fault introduction, conceptual rank payoff, cost, and delivery were factors. The

final set of rotating machinery components incorporated in the Application Study is given in Table 3.1 along with their performance characteristics. The fans manufactured by ETRI were used during a special test series to demonstrate applicability of vibration monitoring to size-scaled machines. A more detailed description of these fans and their selection rationale is presented in Section 3.3.3.

Feasibility testing required that two pumps be employed. The single phase, 3600 RPM Micropump Model 120 units were used for all test conditions except for the introduction of pump motor bearing faults. The six Micropump Model 13-57-316 units, supplied by NASA, were used for the pump motor bearing tests only. The use of both pump types was necessitated by two factors: 1) lack of replacement pump head kits from Micropump on the NASA-supplied units prohibited the introduction of pump head faults and 2) the single-phase motors for the Micropump 120 units did not have replaceable motor bearings.

3.2.2 Mounting and Operation

Test setups as described in the Master Test Plan are shown in Figures 3.1 and 3.2 for the TRW fans and Micropump units respectively. It was determined during preliminary feasibility testing that several minor modifications had to be incorporated into the fans and their test setup in order to achieve repeatable results. Major factors incorporated into the feasibility tests were:

1. An additional thickness of shims were installed to obtain uniform bearing preload and repeatable data after disassembly,

2. The fans were tested with a nonducted (free-air) outlet due to the unacceptable response of the fans to the degree of tightness in the test duct mounting bracket,

3. A small 5/32" hole was drilled in the inlet hub of the fan to permit introduction of bearing faults without disassembling the unit.

All of these factors were approved by the NASA Technical Monitor and are discussed in more detail in the Monthly Progress Report dated June 11, 1986, Tracor Document No. T86-01-9513-U-8.

Table 3.1 - IFD Test Components

Manufacturer (Quantity)	Manufacturer Model Designation	Shaft Speed-Nominal (RPM)	Flow Rate (Liters/Min)	Rated Pressure (Pascals)	Motor Voltage (VAC)	Motor Freq. (Hz)	Motor Phase (No.)	Key Frequencies (Hz)
TRW-Globe Fans (4)	19A1393	10,500	600	124.6	200	400	3 DELTA	BPFI = 856 BPFO = 512 Blade Passage = 1581
ETRI Fan (1)	126LF-0182	3,150	900	Free Air	120	60	1	Rotational = 52.5 Blade Passage = 263
ETRI Fan (1)	113XN-0182	3,600	1,500	Free Air	120	60	1	Rotational = 60 Blade Passage = 360
Micropump (4)	120	3,600	0.94 1.58	4.83×10^5 6.9×10^4	120	60	1	Pumping = N x RPS Gear Mesh = 540
Micropump (6)	13-57-316	11,700	0.45	82,740*	200	400	3 WYE	BPFI = 775 BPFO = 401 Gear Mesh = 1764

*Differential Pressure

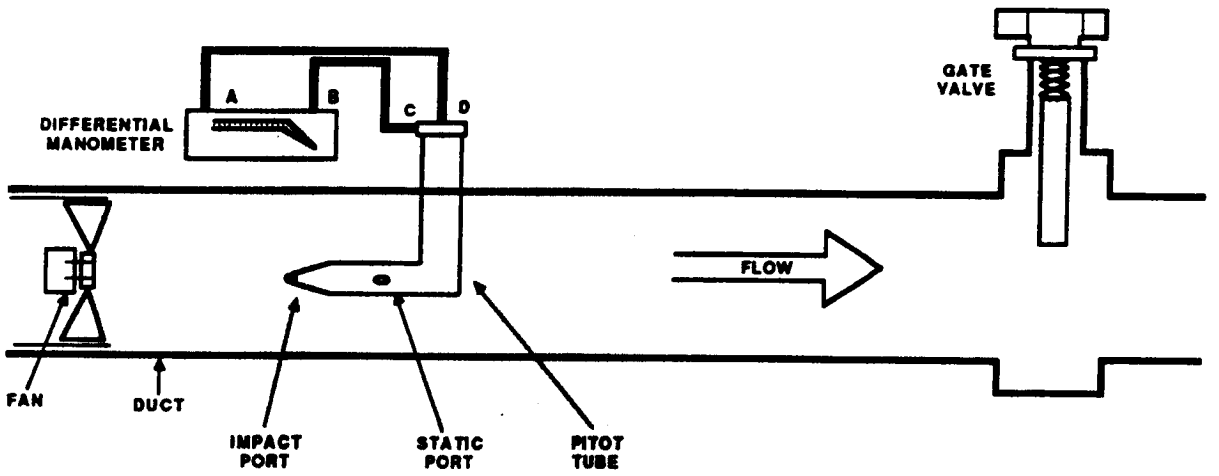

Figure 3.1 - Open Loop Fan Test

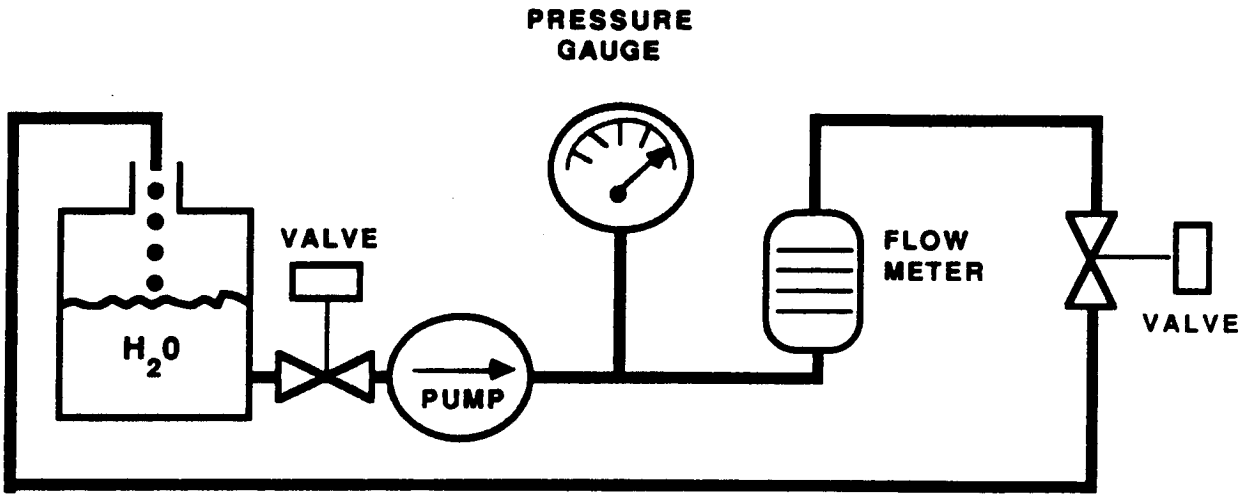

Figure 3.2 - Pump Regenerative Test Loop

3.2.3 Test Equipment

A list of the equipment used in the the feasibility testing is given in Table 3.2. The vibration sensor required special considerations due to the small size of the test components. A PCB 309A accelerometer was chosen because of its acceptable acceleration sensitivity, high useable frequency range, high mounted resonant frequency, and very light weight to minimize mass-loading effects. Accelerometer performance characteristics are summarized in Table 3.3. The accelerometers were calibrated in Tracor's Metrology Department before testing began.

3.2.4 Data Acquisition

Determination of the minimum length of vibration data required to achieve data stability and repeatability was a key area of investigation in the initial data acquisition phase. A series of tests was performed on the three-phase pumps manufactured by Micropump to resolve this issue. These pumps were the least stable of the IFD components, thereby setting the minimum criteria for consistent data acquistion on all components. The tests involved acquisiton of three separate 128 second duration acceleration data records from a single three-phase pump operating under baseline conditions with the accelerometer mounted radially. Within one of these 128 second acceleration records, three data samples of shorter duration were obtained. Figures 3.3 through 3.5 illustrate the acceleration power spectra of three one-half second samples, three eight-second samples, and three 32-second samples respectively. Figure 3.6 illustrates power spectra from three separate baseline tests of 128 second duration. The variability of the acceleration of the three data sets for each sample duration is shown below:

Data Sample Duration (sec)	Mean of Standard Deviation (dB)
0.5	3.66
8.0	2.11
32.0	1.47
128.0	0.93

Table 3.2 - IFD Laboratory Test Equipment

4	ea.	PCB 309A accelerometer and power supply/amplifiers
1	ea.	Nicolet 466B spectrum analyzer
1	ea.	Hewlett-Packard 3964A 1/4" magnetic tape recorder
1	ea.	ITHACO P11 4 channel variable gain, low noise amplifier
4	ea.	Krohn-Hite Model 3202R 2 channel low/high pass, 24 dB/octave filter
1	ea.	Hewlett-Packard 241A sine wave oscillator
1	ea.	Crown M-600 power amplifier
1	ea.	Half-Wave Demodulator
1	ea.	Tektronix 475 oscilloscope
1	ea.	IBM Personal Computer
1	ea.	Dwyer model 400-5-S differential manometer w/pitot tube
1	ea.	U.S. Gauge 160 lb/in^2 pressure gauge
1	ea.	Omega model FL-2102 flow meter
1	ea.	Omega model TTC temperature sensor/converter
1	ea.	Mitutoyo 500 series, digital 6 inch caliber
1	ea.	Fluke 8050A Digital Multimeter
1	ea.	Fluke Y8101 Current Probe

Table 3.3 - PCB Model 309A Performance Characteristics

Weight	-	1 gram
Sensitivity	-	5mV/g
Range	-	± 1000 g
Resolution	-	0.2 g
Frequency Range	-	5 - 10000 Hz (± 5%)
	-	2 - 20000 Hz (± 15%)
Resonant Frequency (Mounted)	-	120 kHz
Amplitude Linearity	-	1% FS
Transverse Sensitivity	-	5% Max. Sensitivity
Strain Sensitivity	-	0.005 g/μ in/in
Temperature Coefficient	-	0.05% / F
Construction	-	Compression; Epoxy Sealed Housing
Dimension	-	0.23" Dia x 0.3" H

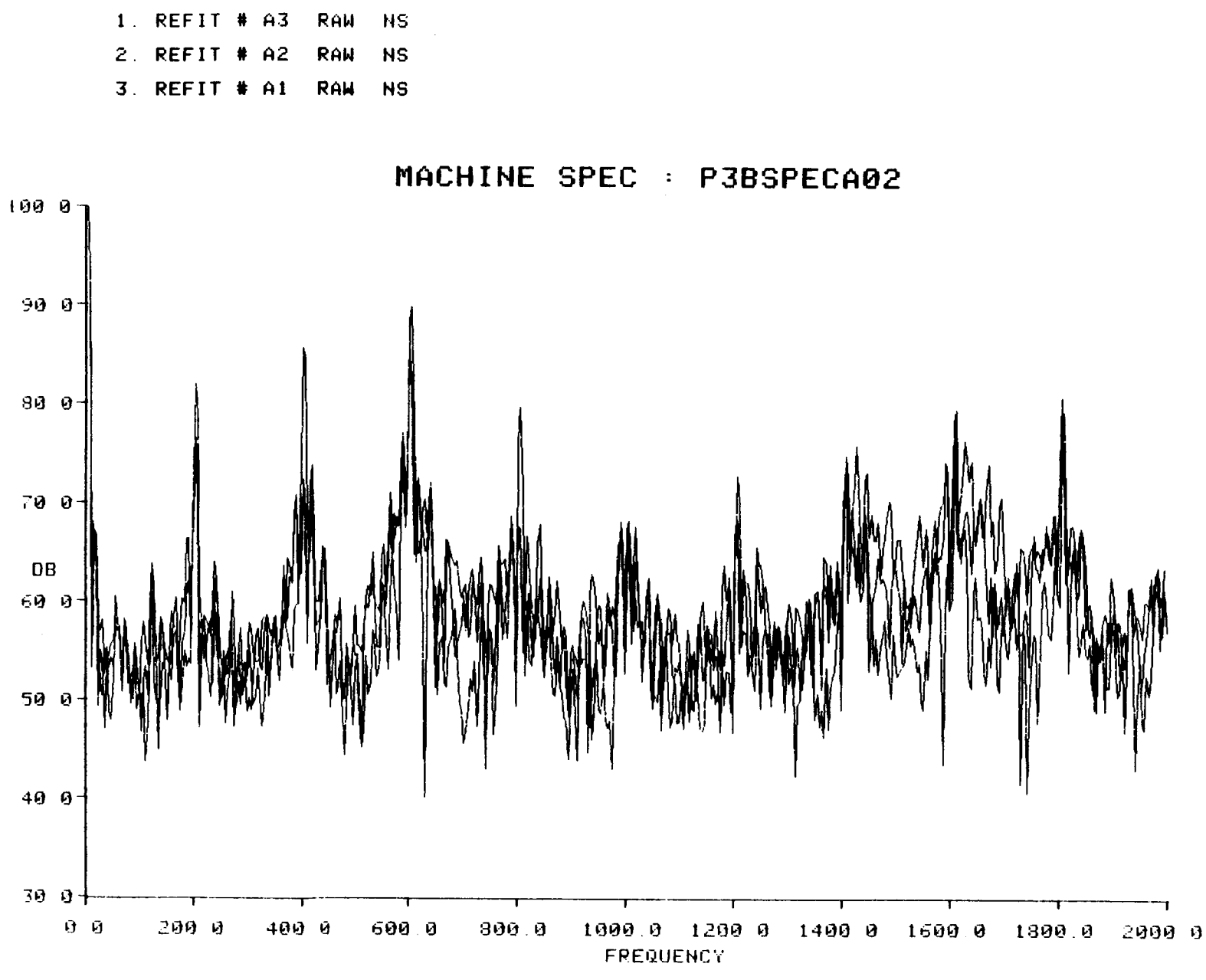

Figure 3.3 Three Phase Pump Acceleration - Three One-Half Second Samples

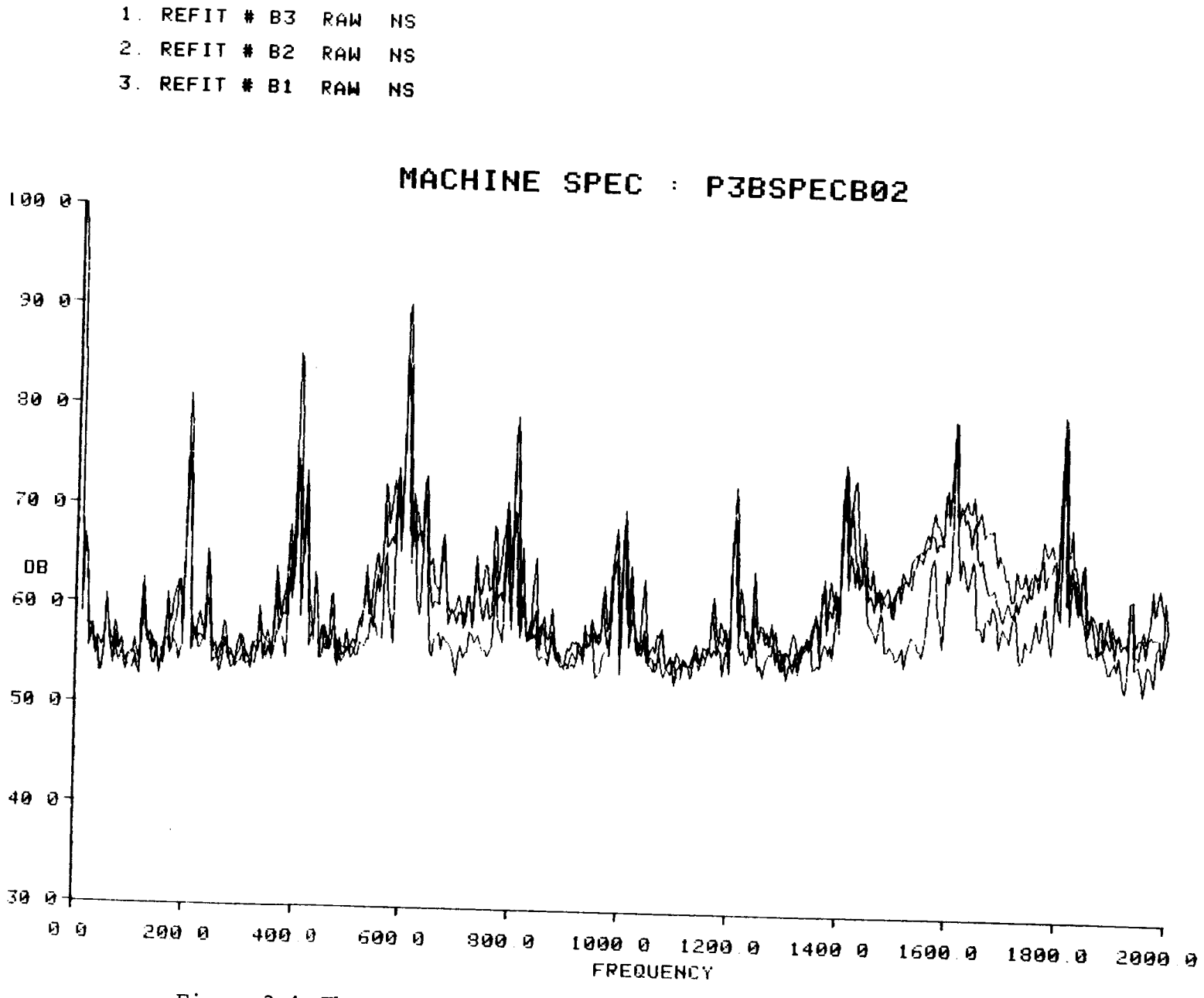

Figure 3.4 Three Phase Pump Acceleration - Three Eight Second Samples

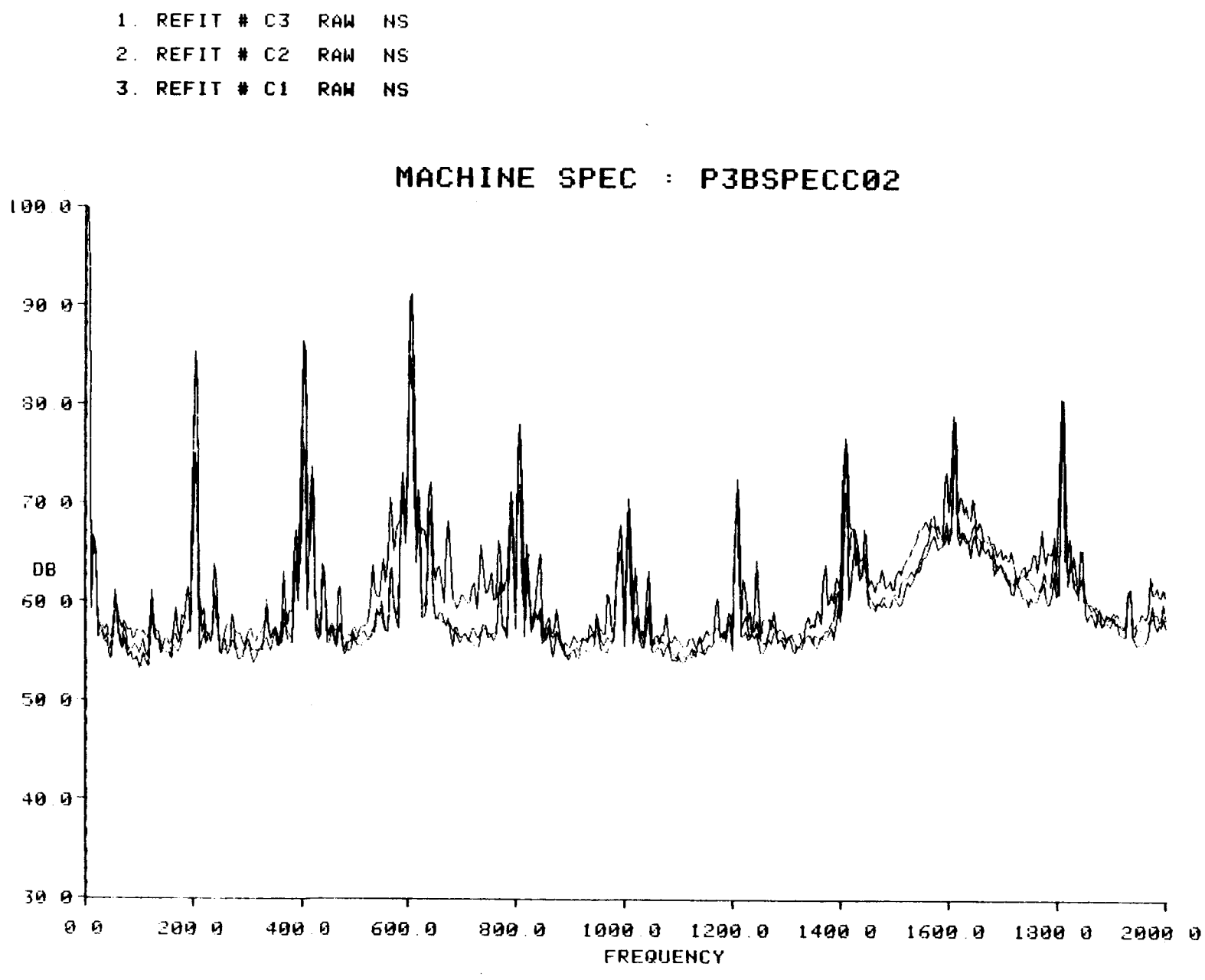

Figure 3.5 Three Phase Pump Acceleration - Three 32 Second Samples

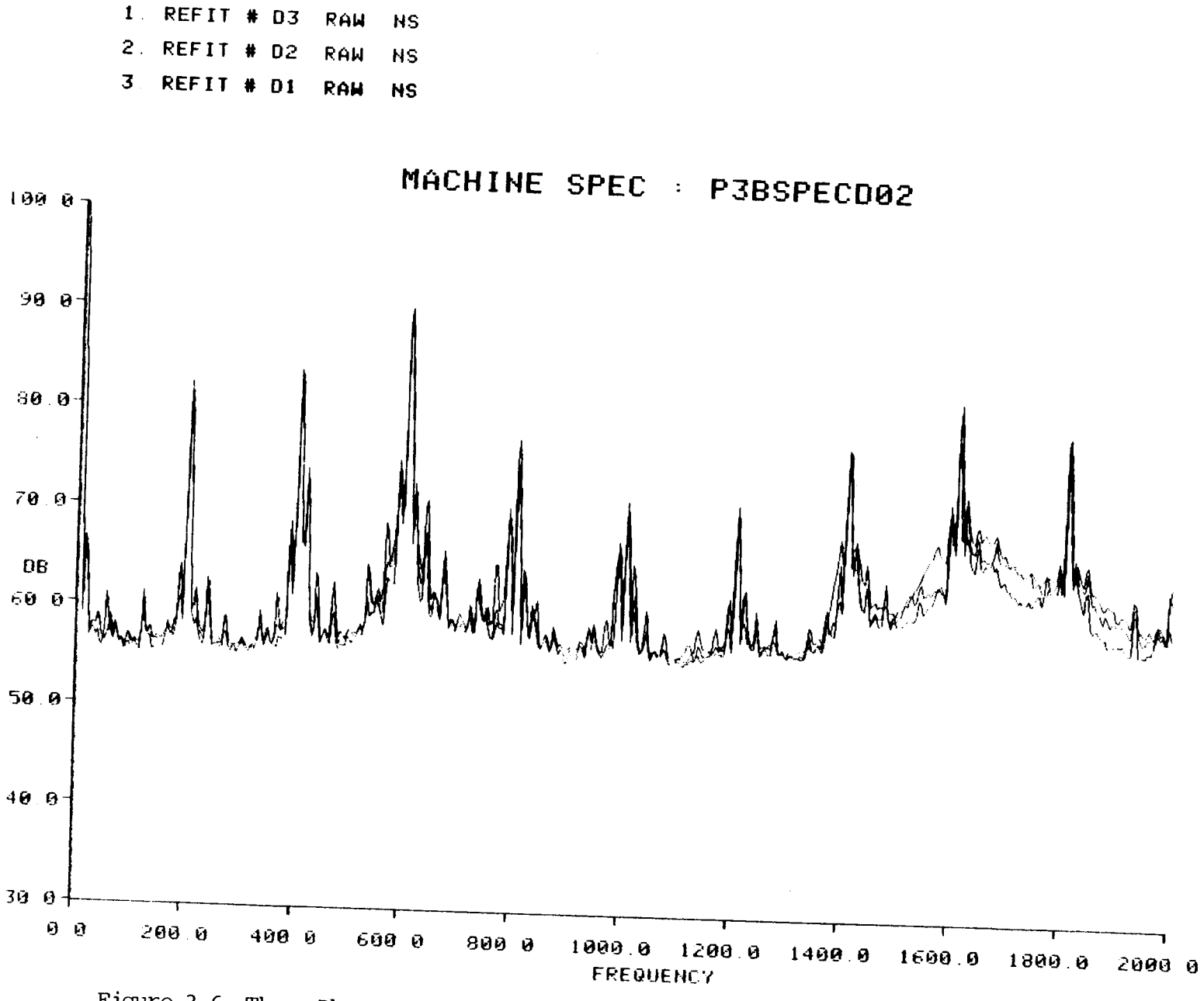

Figure 3.6 Three Phase Pump Acceleration - Three Independent 128 Second Samples

Since the mean of the standard deviation was less than 1 dB from three independent baseline data samples of 128 second duration, this minimum sample length was required for the feasibility testing of all IFD components to achieve repeatable data.

Once feasibility testing began, both baseband and HFD data were taken simultaneously to minimize the potential variance caused by separate testing. This procedure allowed more statistically significant comparisons to be made between these processing techniques. The data acquisition system designed to accomodate this testing is shown in Figure 3.7. The two Krohn-Hite lowpass filters shown before the final stage of amplification at the tape recorder in both circuits were set to the 2 kHz measurement bandwidth used during testing. The remaining Krohn-Hite filters were used in the HFD circuit and were tuned to bandpass around an 85 kHz carrier frequency. An additional stage of amplification was required before the half-wave demodulator in order to properly record the signal.

3.2.5 Data Processing

Two VAX 11/750 computers were used to process the test data acquired in the IFD laboratory. The data processing functional block diagram is shown in Figure 3.8. The data path which was predominantly used during the testing employed a CSPI MAP 300 Array Processor to digitize the analog time signal to a resolution of 12 bits. Time series processing was performed on the Number 2 VAX after the digitized time series was loaded into a database. The time series data,sampled at 8192 samples/second, was then Fourier transformed (2048 point, 512 ensemble average) and transferred by digitial tape to the Number 1 VAX for spectral processing.

Post-processing of the spectral data included the use of several processing algorithms, resident on the Number 1 VAX, that are in daily use to provide fleet maintenance support to critical rotating machinery onboard U.S. Navy submarines. The processing algorithms in software allowed the required high degree of flexibility in data analysis. After processing, the graphical data was displayed on a RAMTEK color video system, with hardcopy color output being provided by a Seiko CH-5301 Color Copier.

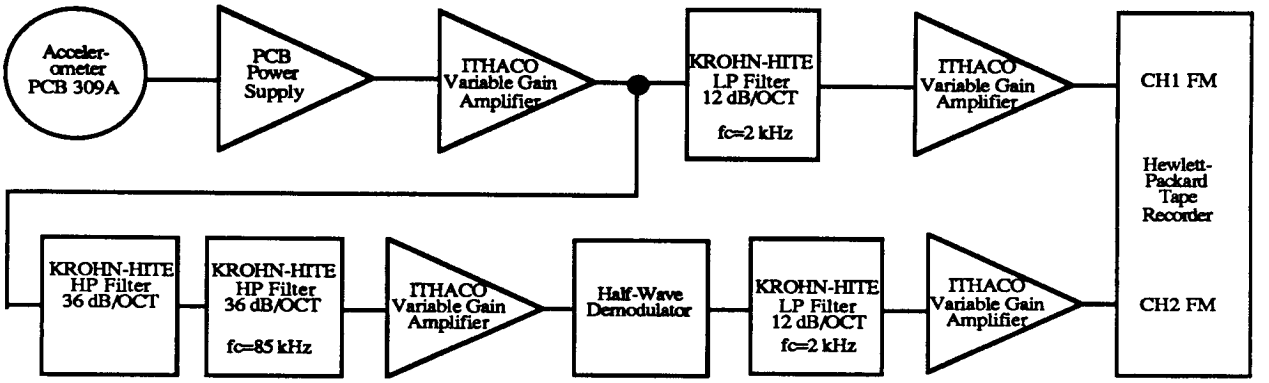

Figure 3.7 - Baseband and HFD Data Acquisition Components

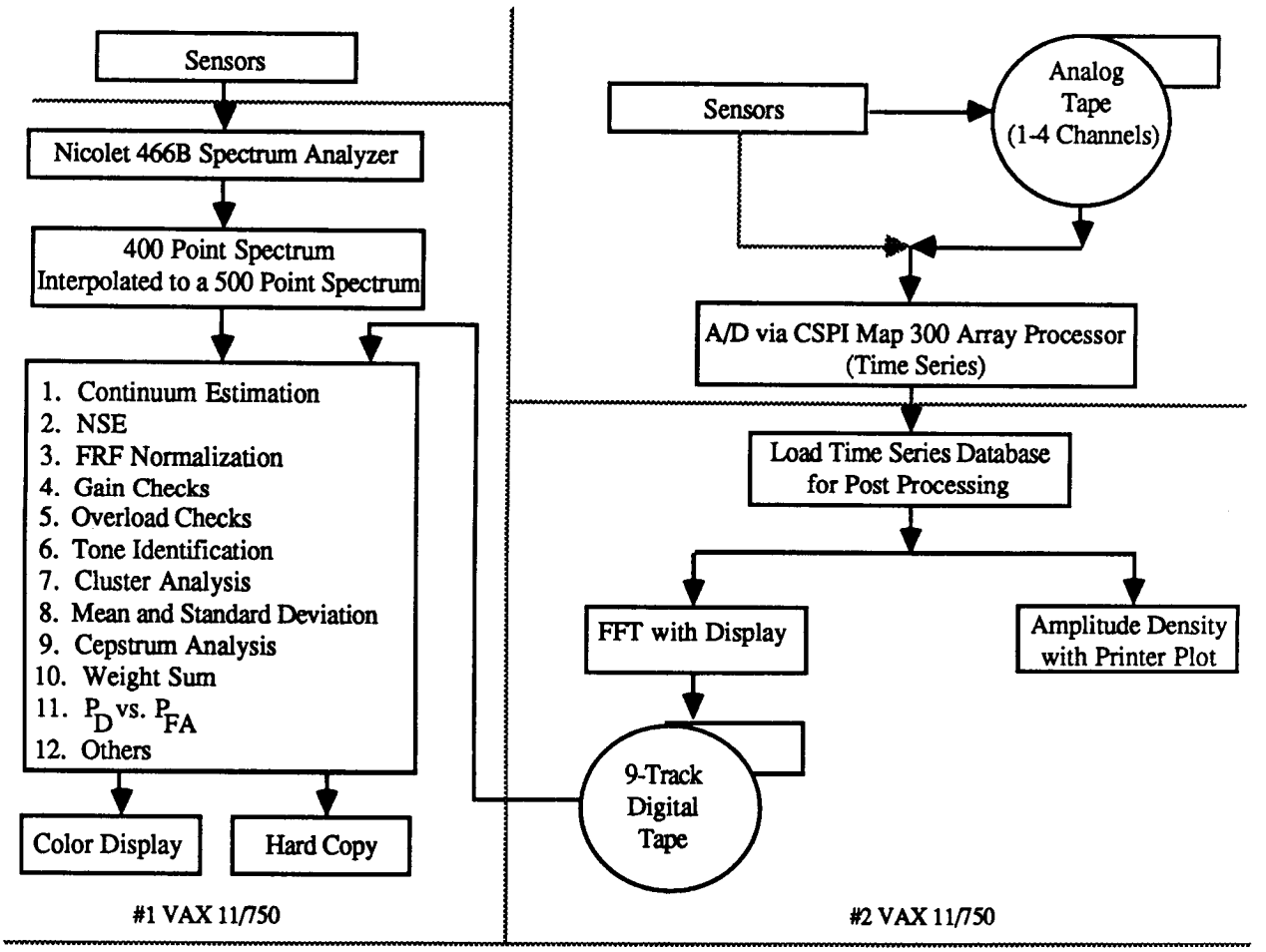

Figure 3.8 - Data Processing Functional Block Diagram

3.3 Special Laboratory Investigations

3.3.1 Introduction

Two special laboratory experiments, defined since the Master Test Plan was issued, were performed to assess the effects of microgravity and the effects of differences between machines on the performance of vibration monitoring techniques. These laboratory experiments required the purchase of additional test units and reconfiguration of some laboratory hardware. Details of the microgravity investigations are presented in Appendix B. Appendix C contains a comprehensive report on the investigation of dissimilar machine effects. The following two sections summarize the objectives, experimental approach, and results of the microgravity and dissimilar machine investigations respectively.

3.3.2 Microgravity Effects

Gravitational effects were observed by comparing response spectra of TRW fans with the shaft axis horizontal and vertical. Experimental results were obtained by performing the tests initially with multiple fans and then by repeating the same experiment on a single fan multiple times. The multiple fan experiments were performed using :

1) Four fans tested one time,

2) Simultaneous recording of both baseband and HFD data,

3) Fans with additional shims to provide axial preload on the bearings, and

4) Horizontal shaft and vertical shaft orientation.

The single-fan experiments were performed using:

1) One fan tested four times,

2) Simultaneous recording of both baseband and HFD data,

3) Fan with and without additional shims to provide axial preload on the bearings, and

4) Horizontal and vertical shaft orientation.

The results of the experiments are summarized in Figures 3.9 and 3.10. The HFD acceleration levels measured with the rotation axis horizontal exceeded those with the shaft vertical by approximately 30 dB as seen in Figure 3.9. This result is attributable to the stabilizing effect of preloading contributed by the rotor weight in a vertical orientation since the production-model TRW fan does not have axial bearing preload. Shims added to provide a slight axial preload in order to achieve repeatability were found to remove this observed gravity effect, as seen in Figure 3.10. The baseband results were relatively insensitive to orientation with or without preload.

A TRW fan with a severely imbalanced impeller (eccentricity / radius of gyration = 0.005) was also operated with the rotational axis horizontal and vertical in order to detect any effect caused by a gravity-induced tangential component of angular acceleration, but no discernable effect was identified. The observation agrees with theoretical predictions which indicate an excitation force for this effect on the order of 2×10^{-6} times the centrifugal force due to imbalance. Shaft flatness effects are not expected to be important for the short, stiff rotor assemblies typically found in spacecraft rotating machinery. No shaft flatness effects were induced during the experiments. No nonlinearity effects were observed due to the effect of machine weight on bearing and mount stiffness. No gravity effects on bearing lubricant properties were examined, since tests of this kind must be performed in an actual microgravity environment.

It is concluded that gravitational effects on bearing preload can be significant and must be taken into account. Although no gravity-induced nonlinear stiffness effects were observed in the tests, these could potentially be important for heavier machines with strongly nonlinear mounts or very flexible bearings.

3.3.3 Dissimilar Machines

The validity of applying a given monitoring technique to different machines was demonstrated in the laboratory for two axial fans differing in mass by approximately 51%. Imbalance of a fan impeller was selected as an important but readily implemented fault type to demonstrate the validity of applying a specific monitoring technique, observing amplitude change at the fundamental rotational frequency, to the two fans.

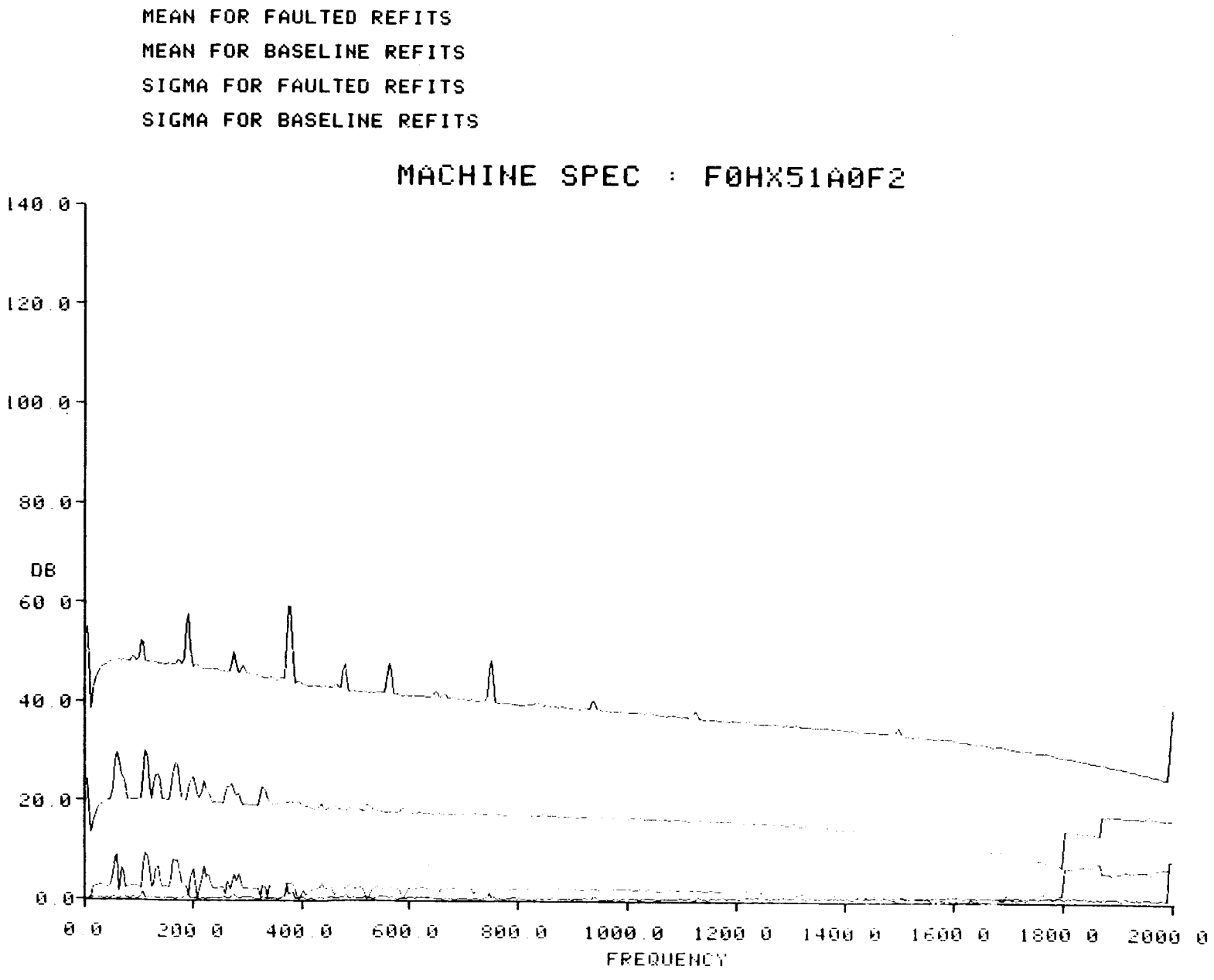

Figure 3.9 HFD Mean and Standard Deviation of Horizontal (Baseline) and Vertical (Faulted) Single Fan Tests - Without Additional Shims

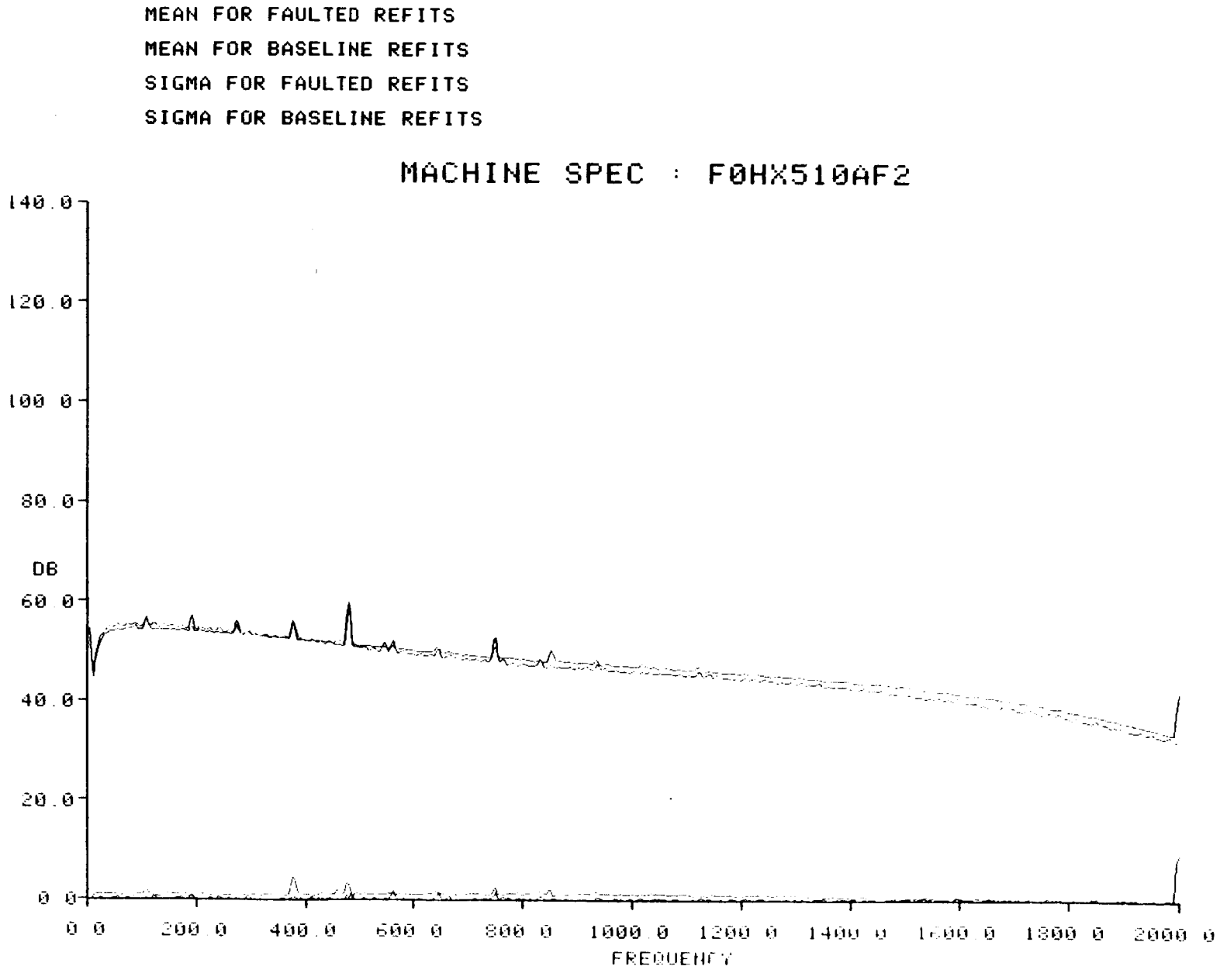

Figure 3.10 HFD Mean and Standard Deviation of Horizontal (Baseline) and Vertical (Faulted) Single Test Fan Tests - With Additional Shims

The fans selected as laboratory demonstration units approximately satisfied Strouhal-scaling criteria , which relate size, weight, and operating speed. The large and small demonstration units were ETRI Models 113XN and 126LF, respectively, as shown in Figure 3.11. The small fan is similar in construction to the large fan but not an exact replica. Both fans were mounted in a cruciform arrangement of three-sixteenths inch ID surgical tubing as shown in Figure 3.12. The shafts of both units were horizontal during the tests, with the accelerometer mounted on the top of the fan housing. The surgical tubing was attached to stiff wire brackets extending from the corners of the fan housing. This experimental arrangement was chosen to provide low mount resonance frequencies as compared with the fundamental shaft rotation frequency. Torsional restoring torque is provided by deflection of the mounts when the fan housing experiences an angular deflection about a transverse horizontal axis. Mount vertical and torsional stiffnesses were scaled by adjusting the initial unstretched tubing lengths. Imbalances were induced in each fan by attaching three different Strouhal-scaled metal weights at length-scaled positions on the impeller hubs.

It is known that viscous damping does not scale correctly with size. However, viscous effects are not considered important for machines having rolling element bearings and working fluids with sufficiently high Reynolds Numbers.

Mean square accelerometer response spectra for the large and small fans are shown in Figures 3.13 and 3.14. A shift of +6 dB must be added to the plotted spectra to obtain mean square acceleration response in dB re 10^{-6} g. A scaling-law correction of -0.6 dB must be added to the small-fan response to account for the net effect of spectrum level scaling and scaling associated with mean square acceleration response.

An additional correction for these off-scale conditions was derived and applied to the small-fan results to obtain the predicted large-fan response shown in Table 3.4. Small-fan response levels with both the scaling-law correction and the correction for off-scale conditions applied agree with large-fan levels to within 1 dB for all three imbalance conditions, thus validating the overall approach. Appendix C contains a detailed discussion.

LARGE FAN
ETRI Model 113XN

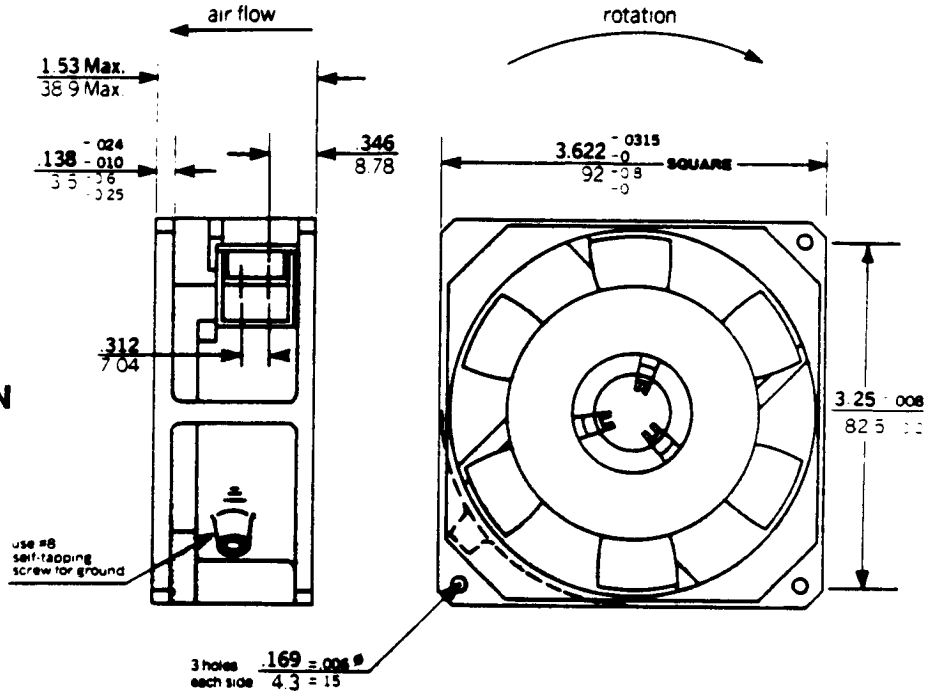

SMALL FAN
ETRI Model 126LF

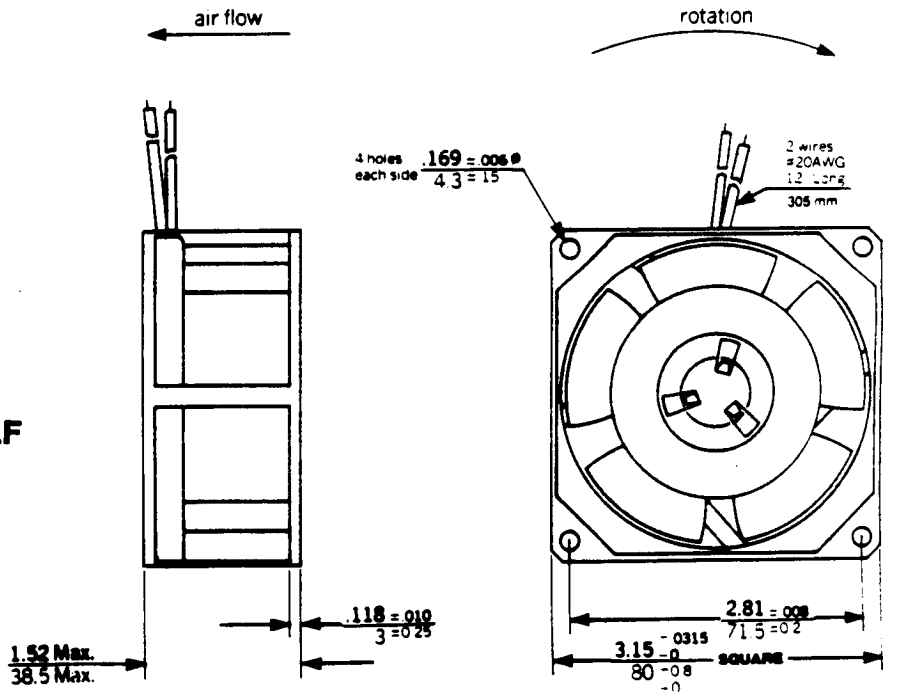

Figure 3.11 - Large and Small Demonstration Units for Dissimilar Machine Experiments

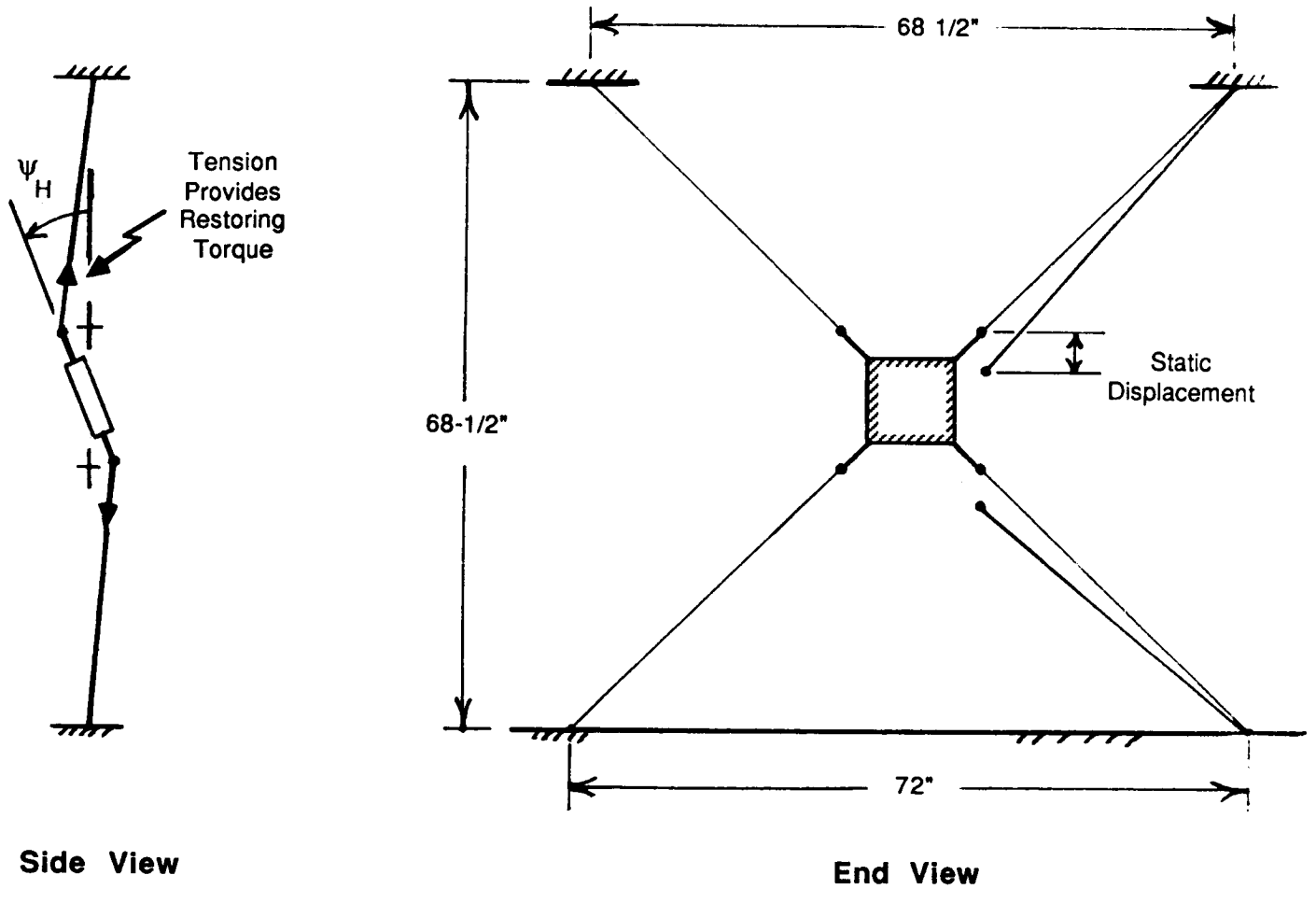

Figure 3.12 - Mounting Arrangement Used for ETRI Fans

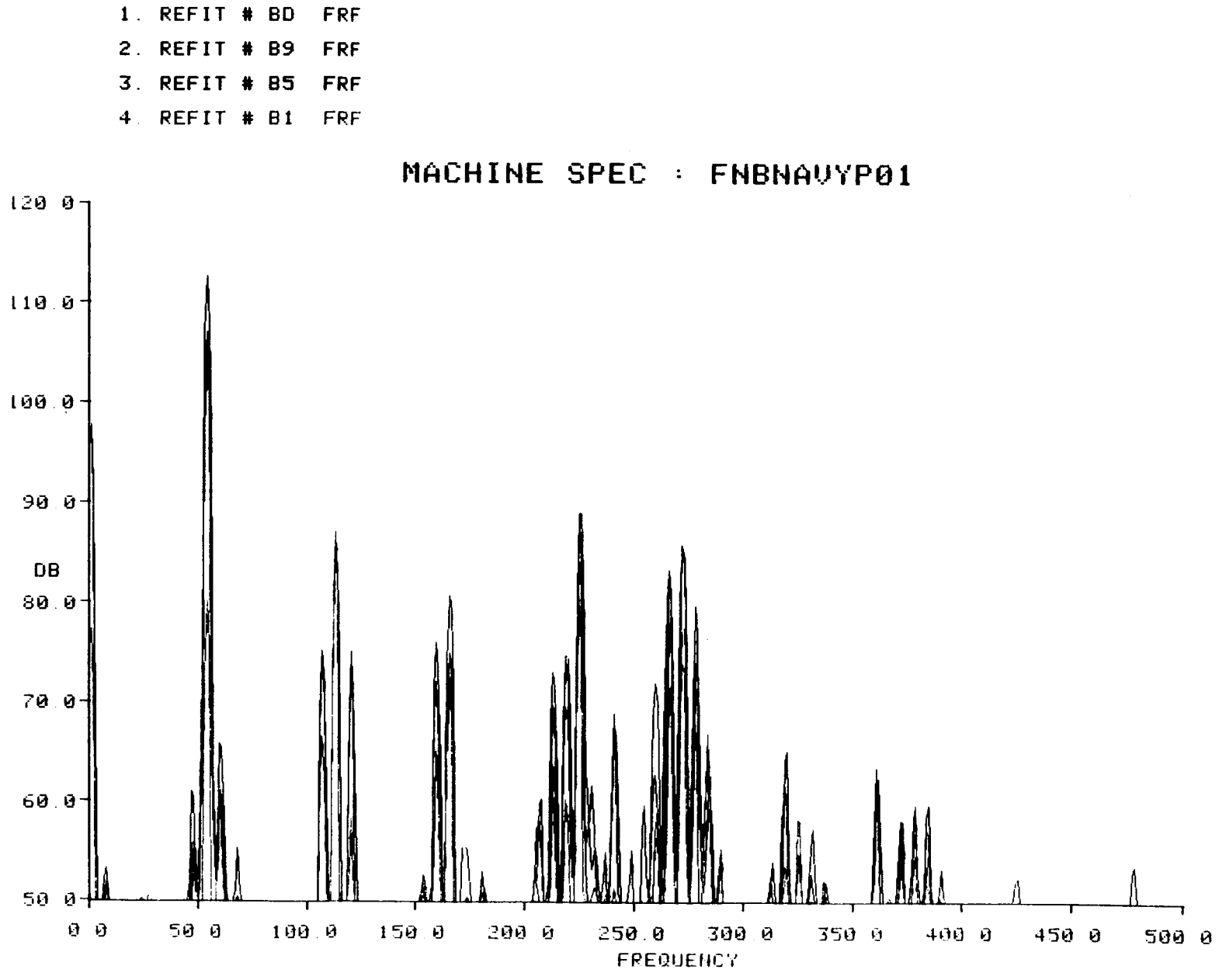

Figure 3.13 Large Fan Mean Square Accelerometer Response for Three Scaled Imbalanced Conditions

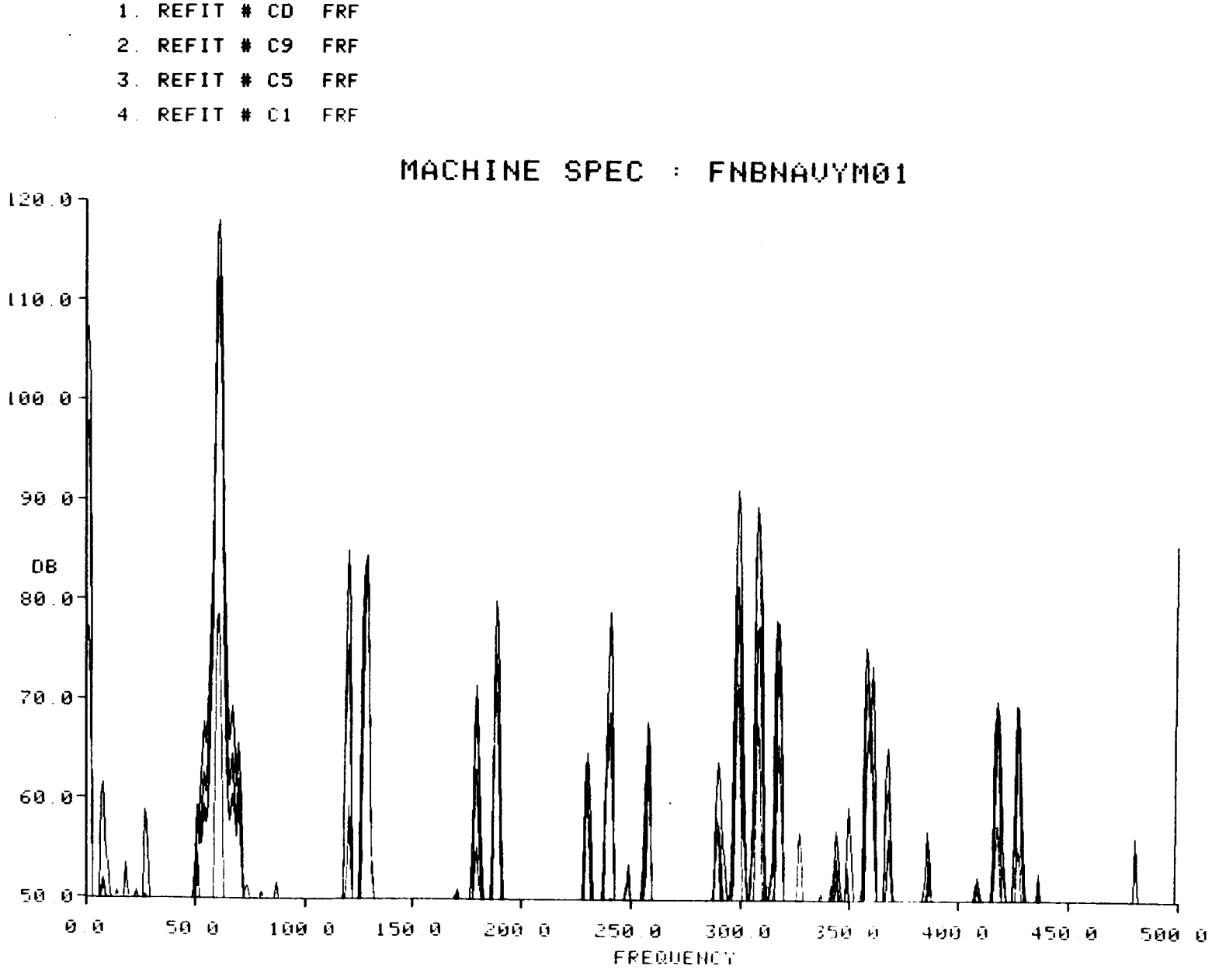

Figure 3.14 Small Fan Mean Square Accelerometer Response for Three Scaled Imbalanced Conditions

Table 3.4 - Predicted versus Measured Mean-Square Accelerometer Response for Large Fan

	Measured Small Fan Response (dB re 1 μg)	Off-Scale Correction (dB)	Measured Small Fan Response Plus Off-Scale Correction (dB re 1 μg)	Scaling-Law Correction (dB)	Predicted Large Fan Response (dB re 1 μg)	Measured Large Fan Response (dB re 1 μg)	Measured Minus Predicted LargeFan Response (dB)
Large Imbalance	123.6	-3.62	119.98	-0.6	119.38	119.0	-0.38
Medium Imbalance	118.0	-3.62	114.38	-0.6	113.78	113.6	-0.18
Small Imbalance	115.7	-3.62	112.08	-0.6	111.48	110.5	-0.98
Residual Imbalance	85.0	-3.62	81.38	-0.6	80.78	86.4	5.62

3.4 Feasibility Tests

3.4.1 General Procedure

Feasibility testing was structured as shown in Figure 3.15:

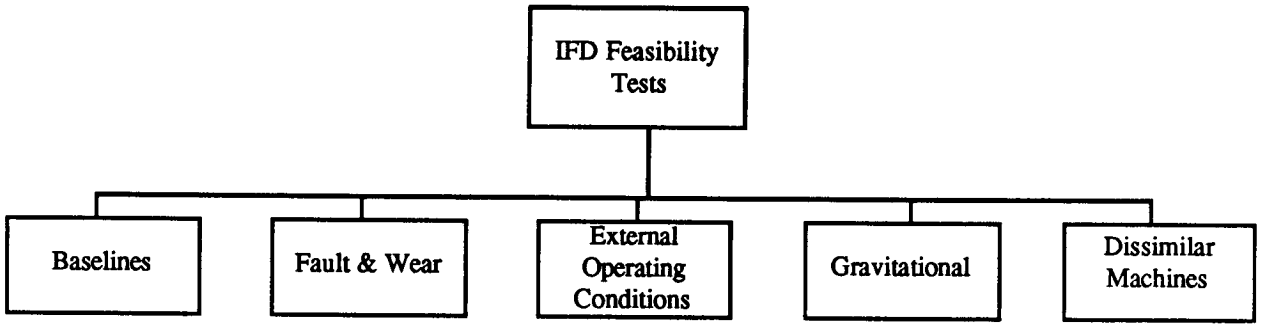

Figure 3.15 - Feasibility Testing Block Diagram

Test components were first operated normally and data were collected in the baseline condition. After baseline data were recorded, the particular fault or test condition under investigation was introduced and faulted data were obtained. Depending upon the experiment being performed, the baseline and faulted conditons were measured either globally across all test components or on a single representative component multiple times in order to develop the necessary detection statistics. The number of test components for each test is identified in the following sections. Tables 3.5 and 3.6 list specific tests performed on the fans and pumps respectively.

3.4.2 Example Results

Currently over 1200 vibration spectra are catalogued in the NASA database which is resident on the VAX 11/750. In addition, the time series data for these spectra are archived in both analogue and digitial form. Typical examples of the test results along with the test description are presented in the following sections. The purpose is to illustrate some of the computations, important procedures, and supporting evidence for selected critical analysis results. Appendix D contains a complete listing and description of the feasibility testing results.

TABLE 3.5 FANS VIBRATION TEST PLAN

- Ambient
  - Bench
  - Fan
- Accelerometer Mount/Remount Repeatability
- Accelerometer Loose Remount
- Accelerometer Mapping (4 fans)
- Fan Disassembly/Reassembly (4 fans)
- Imbalance (weight)
  - Small (0.035 gm) (4 fans)
  - Large (0.173 gm) (4 fans)
  - Large (0.173 gm) (1 fan)
- Inlet Air Restrictions (1 fan)
  - 25% Blockage
  - 75% Blockage
- Voltage Change (4 fans)
  - Under (180 V)
  - Over (220 V)
- Phase Loss (1 fan)
- Shaft Orientation
  - 4 fans
  - 1 fan
- Elevated Ambient (1 fan)
  - $22^{o}C$ --> $40^{o}C$
- Bearings - Particle Contamination (4 fans)
- Bearings - Inner Race Fault (1 fan)
- Bearings - Outer Race Fault (1 fan)
- Small/Large Fans (2 fans)

TABLE 3.6 PUMPS VIBRATION TEST PLAN

Ambient

- Bench
- Pumps (1 - 1ϕ, 1- 3ϕ)

Accelerometer Mount/Remount Repeatability (1 - 1 ϕ, 1 - 3 ϕ)

Accelerometer Loose Remount (1 - 1 ϕ, 1 - 3ϕ)

Accelerometer Mapping (1 - 1ϕ, 1 - 3ϕ)

Pump Disassembly/Reassembly (1 - 1 ϕ, 6 - 3ϕ)

Shaft Orientation (4 - 1ϕ, 6 - 3ϕ)

Phase Loss (1 - 3ϕ)

Load Conditions (1 - 1ϕ)

- Over (80 psig)
- Under (20 psig)

Voltage Change (1 - 1ϕ)

- Over Voltage (135 V)
- Under Voltage (105 V)

Coupling Imbalance (1 - 3ϕ)

- Small (0.035 gm)
- Large (0.173 gm)

Impeller Wear (4 - 1ϕ)

Impeller Fault (1 - 1ϕ)

Bearings - Loss of Lubricant (1 -3ϕ)

Bearings - Inner Race Fault (6 - 3ϕ)

Bearings - Outer Race Fault (6 - 3ϕ)

3.4.2.1 Elevated Ambient Temperature--Single Fan

Baseline data were obtained at a nominal room temperature of 22°C, after which air heating commenced. Faulted data were obtained after reaching an inlet air temperature of 40°C, which was monitored by an electronic temperature sensor. The heated air was then removed and the fan cooled to ambient temperature. A second electronic temperature sensor was attached to the stationary inlet guide vane assembly to insure consistent testing temperatures. The fan remained in operation during the entire test sequence in which four baseline and four faulted conditions were obtained.

Figures 3.16 through 3.19 illustrate, respectively, the four baseline spectra, the four faulted spectra, the mean and standard deviation of the baseline and faulted spectra, and the detection weights which were computed by subtracting the mean values at each frequency and dividing by the average of the standard deviation at each frequency. The problem manifestation is distinctive as a low frequency broadband hump repeatable with small variability. The detection weights clearly show the detectable shape.

3.4.2.2 Bearing Particle Contamination--Multiple Fans

A baseline was obtained for the TRW fan running normally, after which a small quantity of very fine steel shavings was introduced to the bearing through a 5/32" hole in the stationary inlet hub assembly over the bearing raceways. Faulted data were then obtained. The experimental procedure was performed on each of the TRW fans. Figure 3.20 illustrates acceleration versus time and shows the transient nature of the problem type. The four faulted spectra shown in Figure 3.21 indicate the high variability of the results. A plot of the mean and standard deviation of the test results, Figure 3.22, illustrates that although the contaminants increased spectrum levels by approximately 10 dB to 15 dB, the standard deviation was also 10 dB to 15 dB. The detection weights shown in Figure 3.23 are random with no distinctive patterns in response to this data variability.

3.4.2.3 Bearing Outer Race Fault--Single Fan

A series of tests was performed in which a single outer race fault was introduced into the front bearing of the fan under test. A special bearing was used with an easily removable one piece cage assembly in these tests since both the fan and the bearing had to be disassembled for

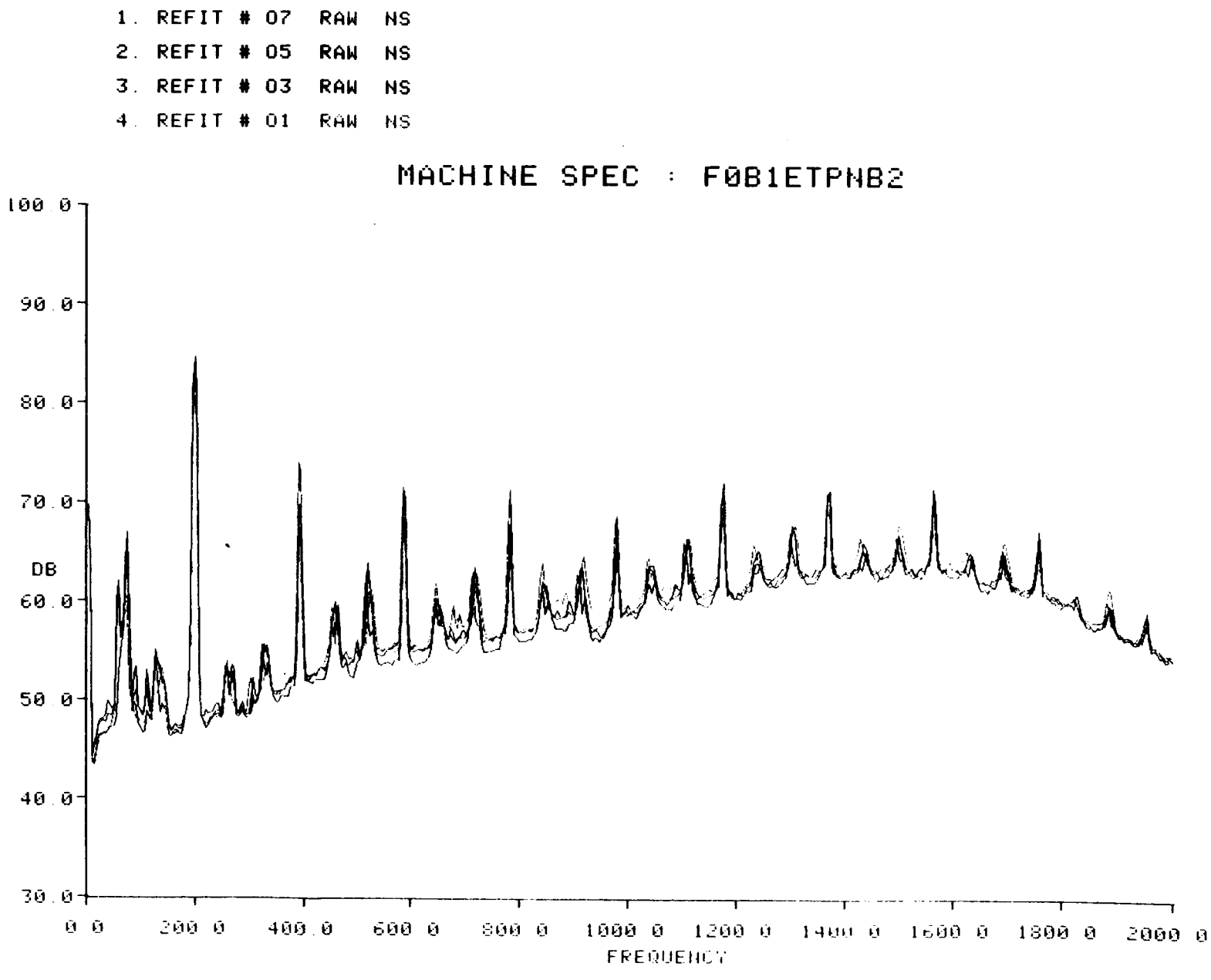

Figure 3.16 Fan Elevated Ambient Temperature - Baseline Spectra

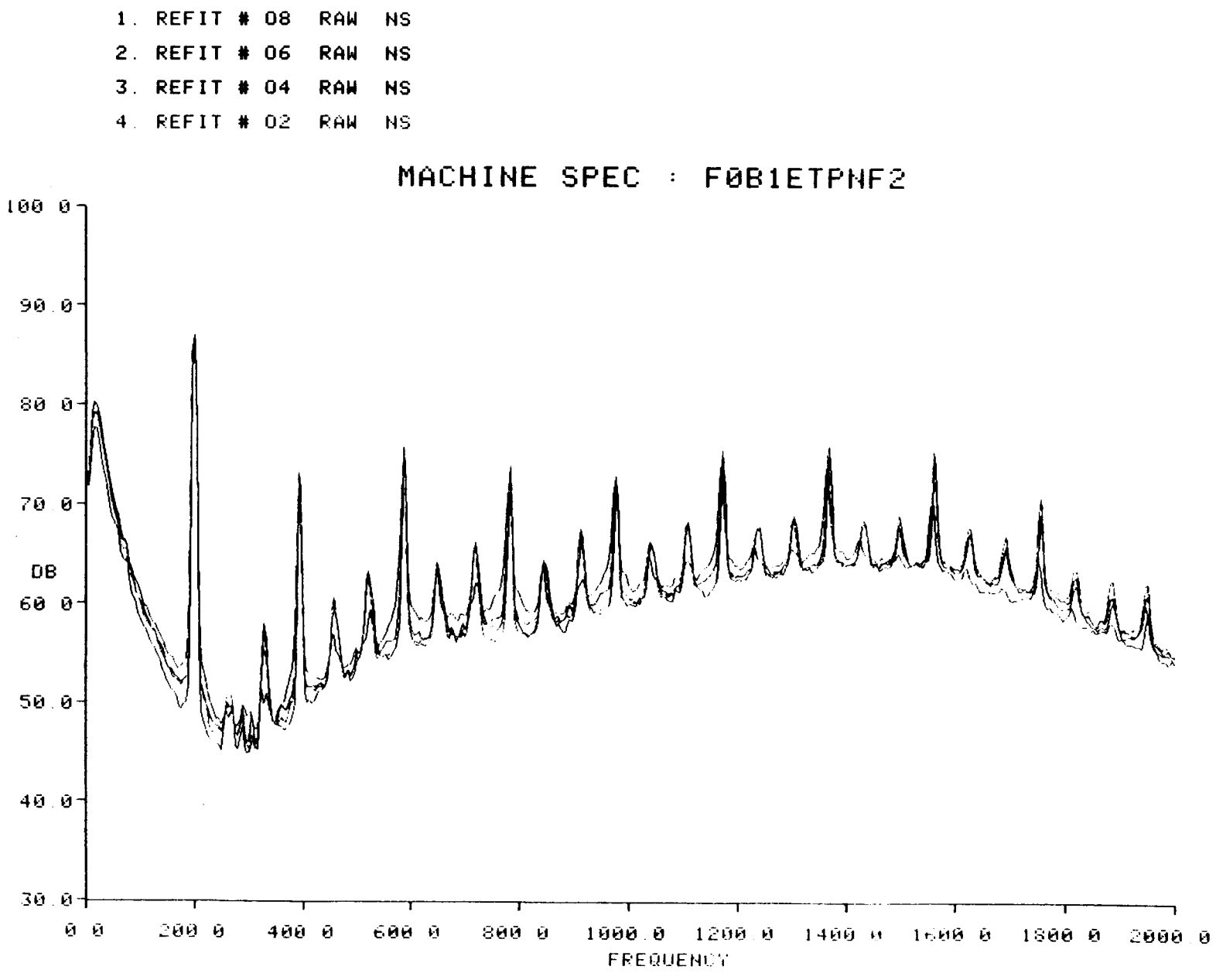

Figure 3.17 Fan Elevated Ambient Temperature - Four Faulted Spectra

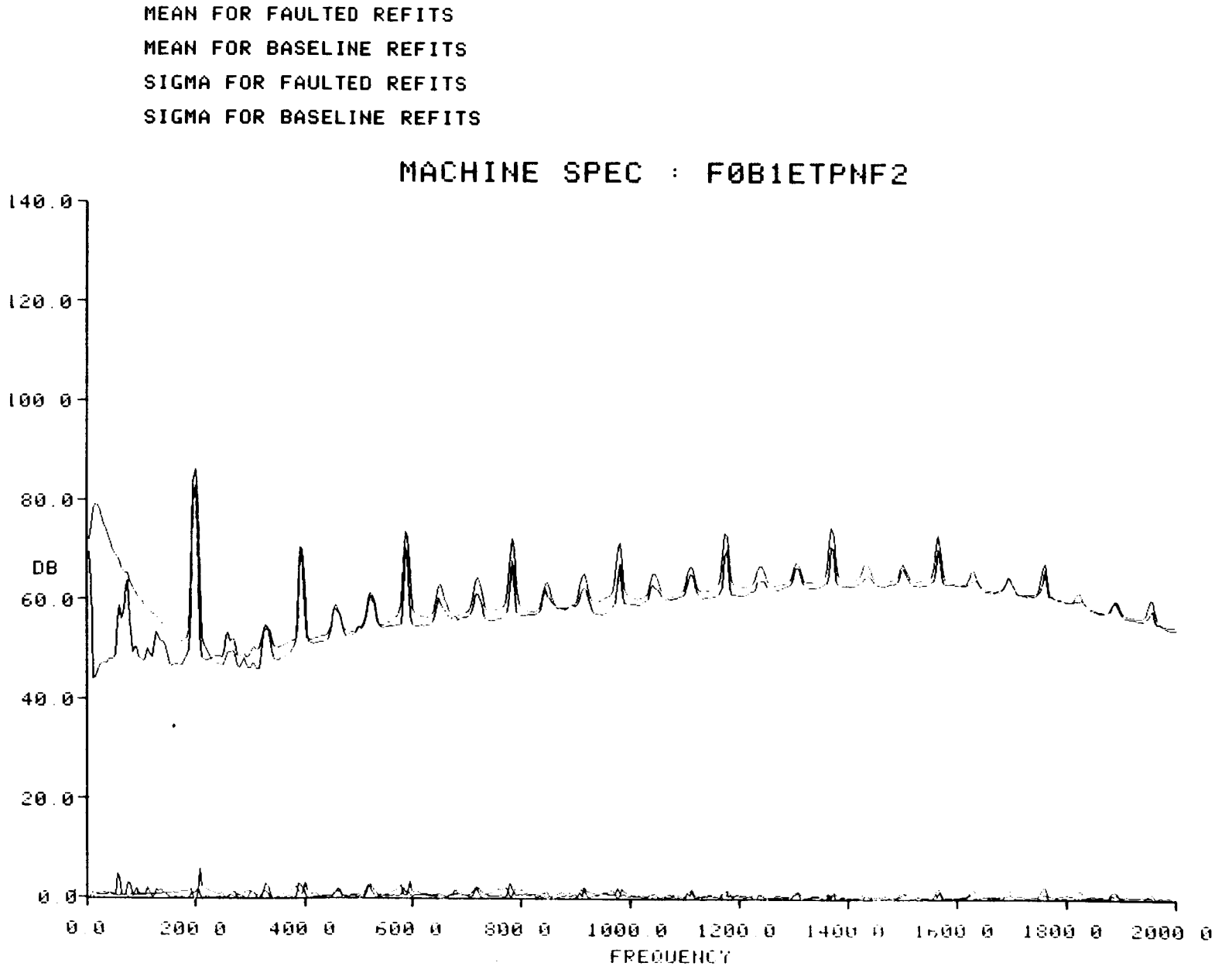

Figure 3.18 Mean and Standard Deviation for Baseline and Faulted Spectra

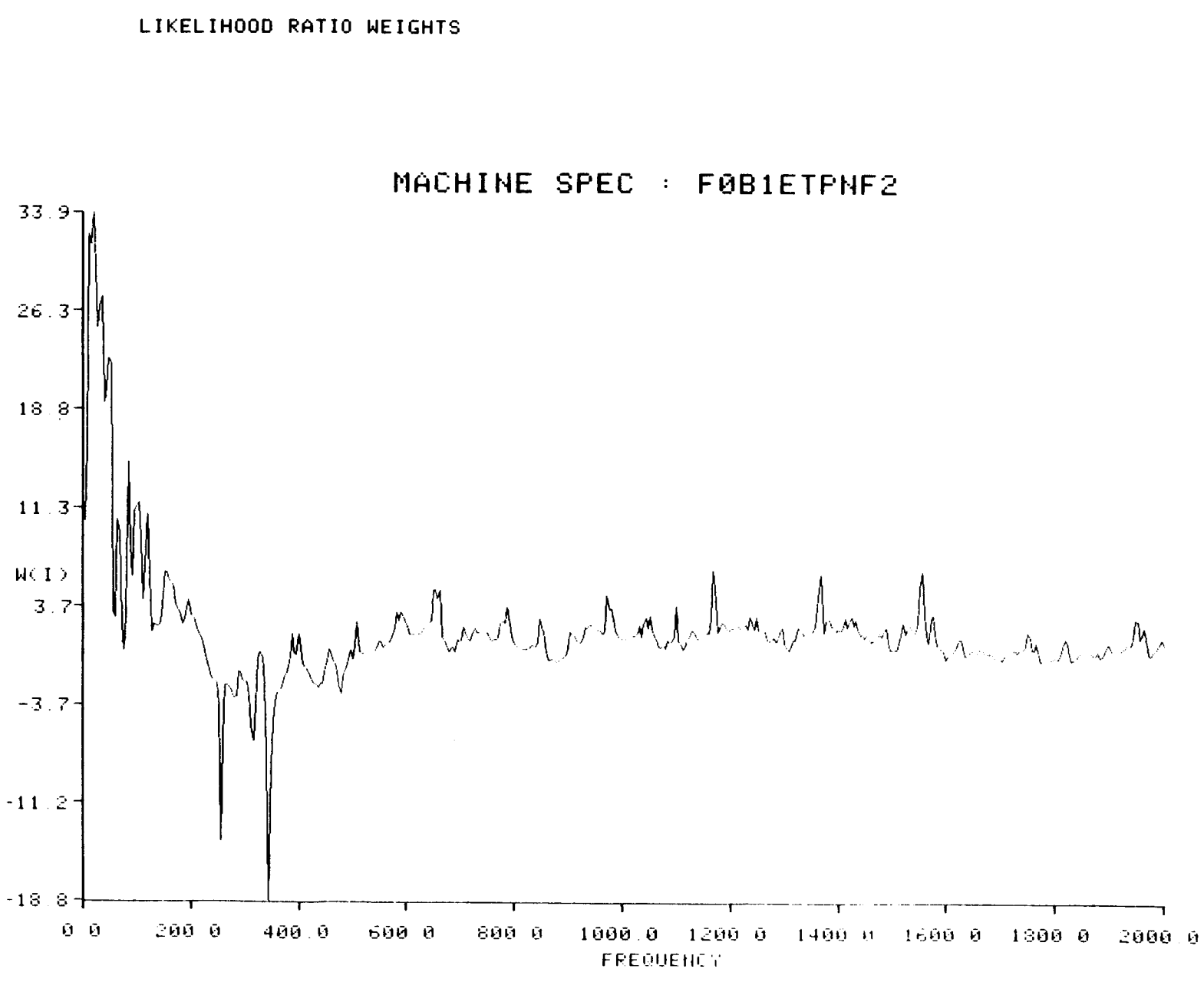

Figure 3.19 Detection Weights for Fan Elevated Ambient Temperature

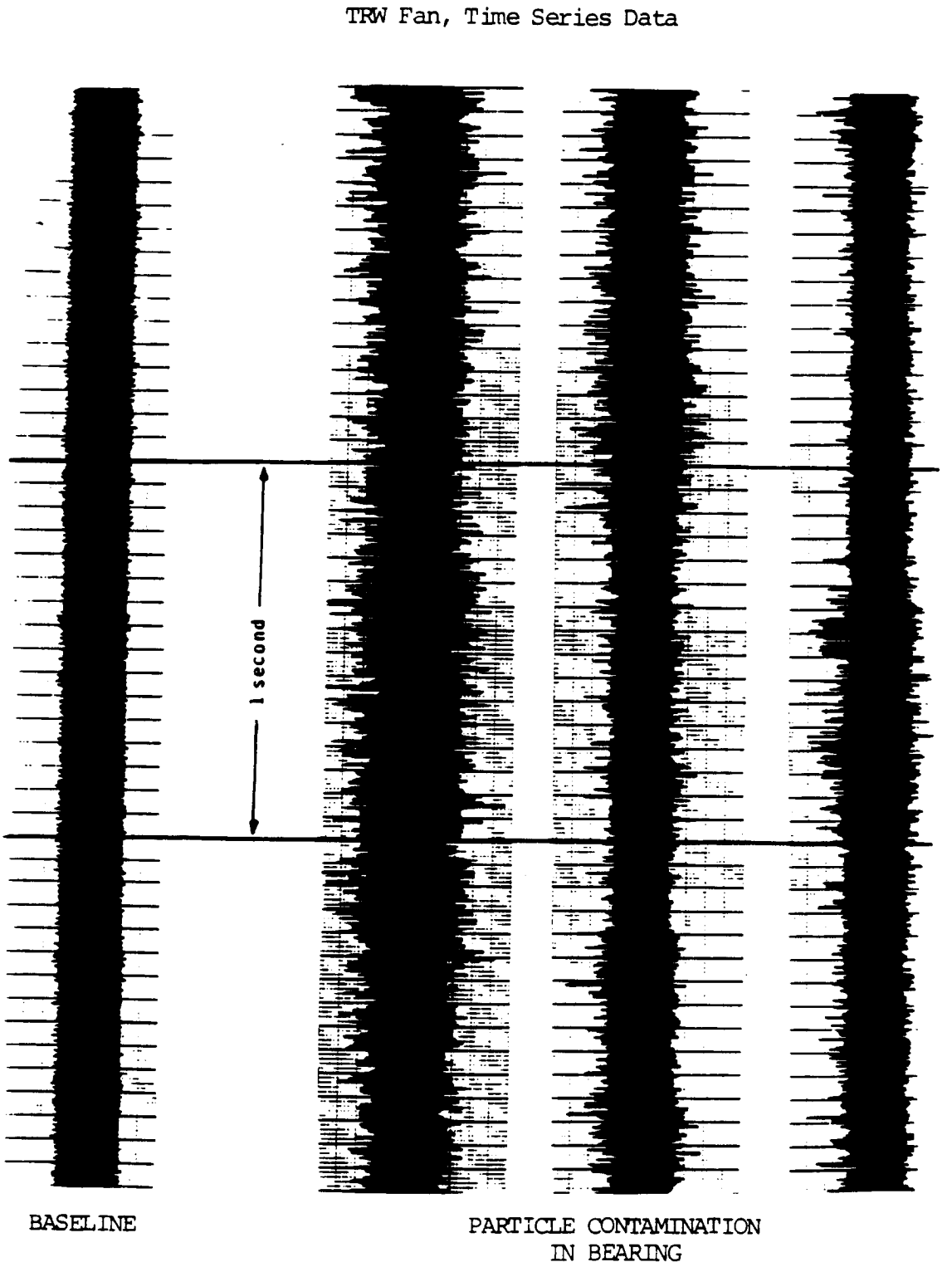

Figure 3.20 TRW Fan - Time Series Data for Particle Contamination

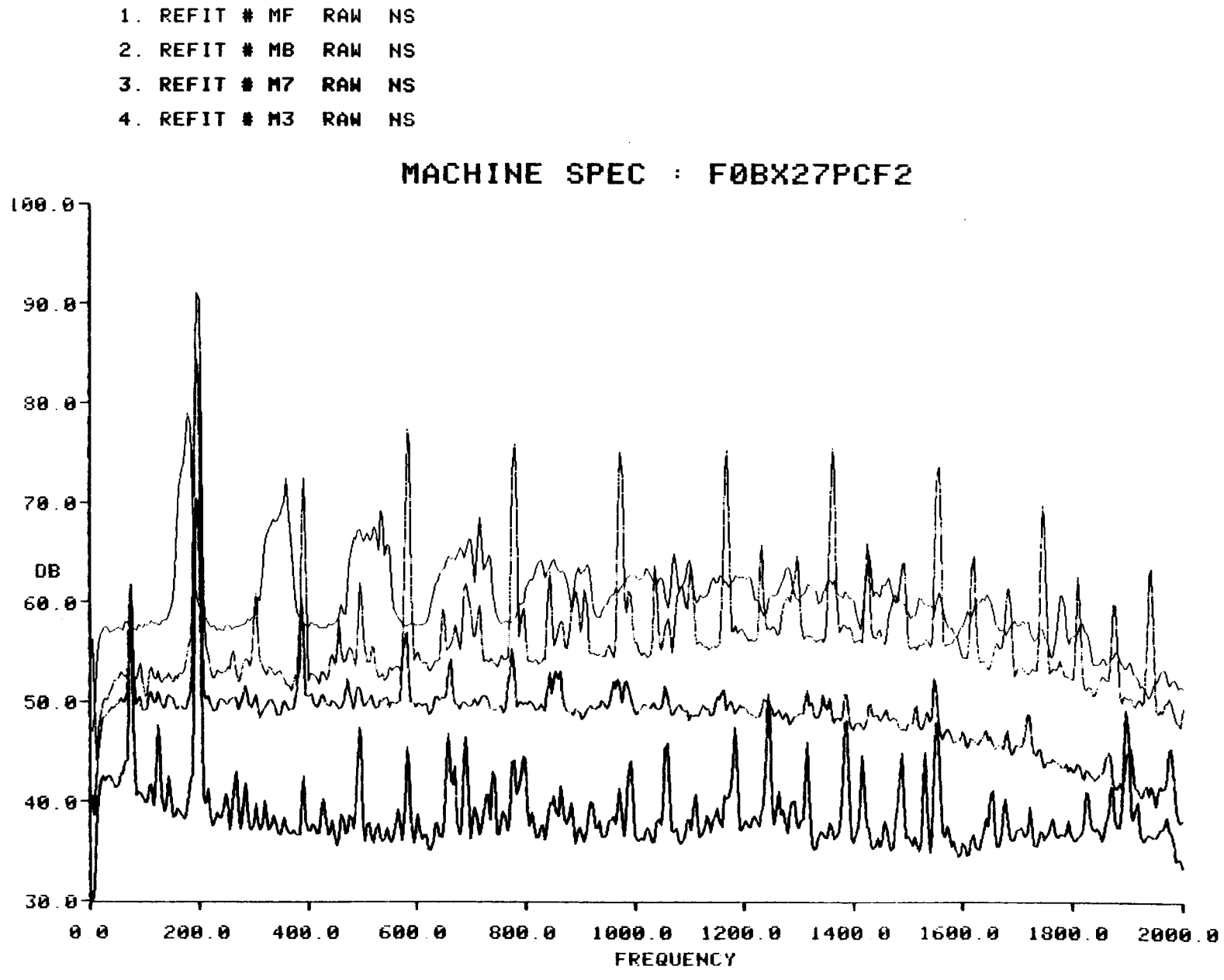

Figure 3.21 Faulted Spectra for Multiple Fan Bearing Particle Contamination

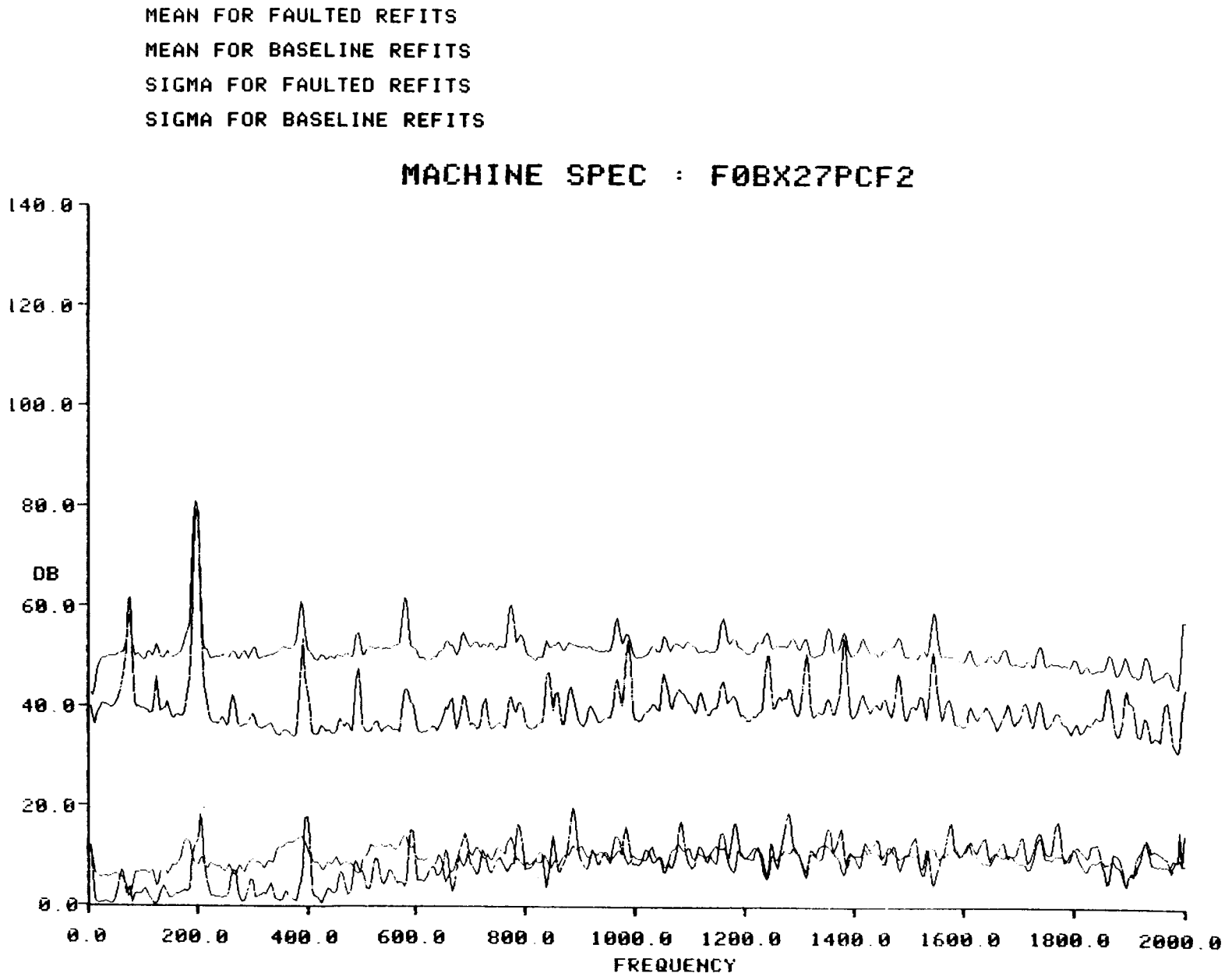

Figure 3.22 Mean and Standard Deviation for Baseline and Faulted Spectra - Bearing Particle Contamination

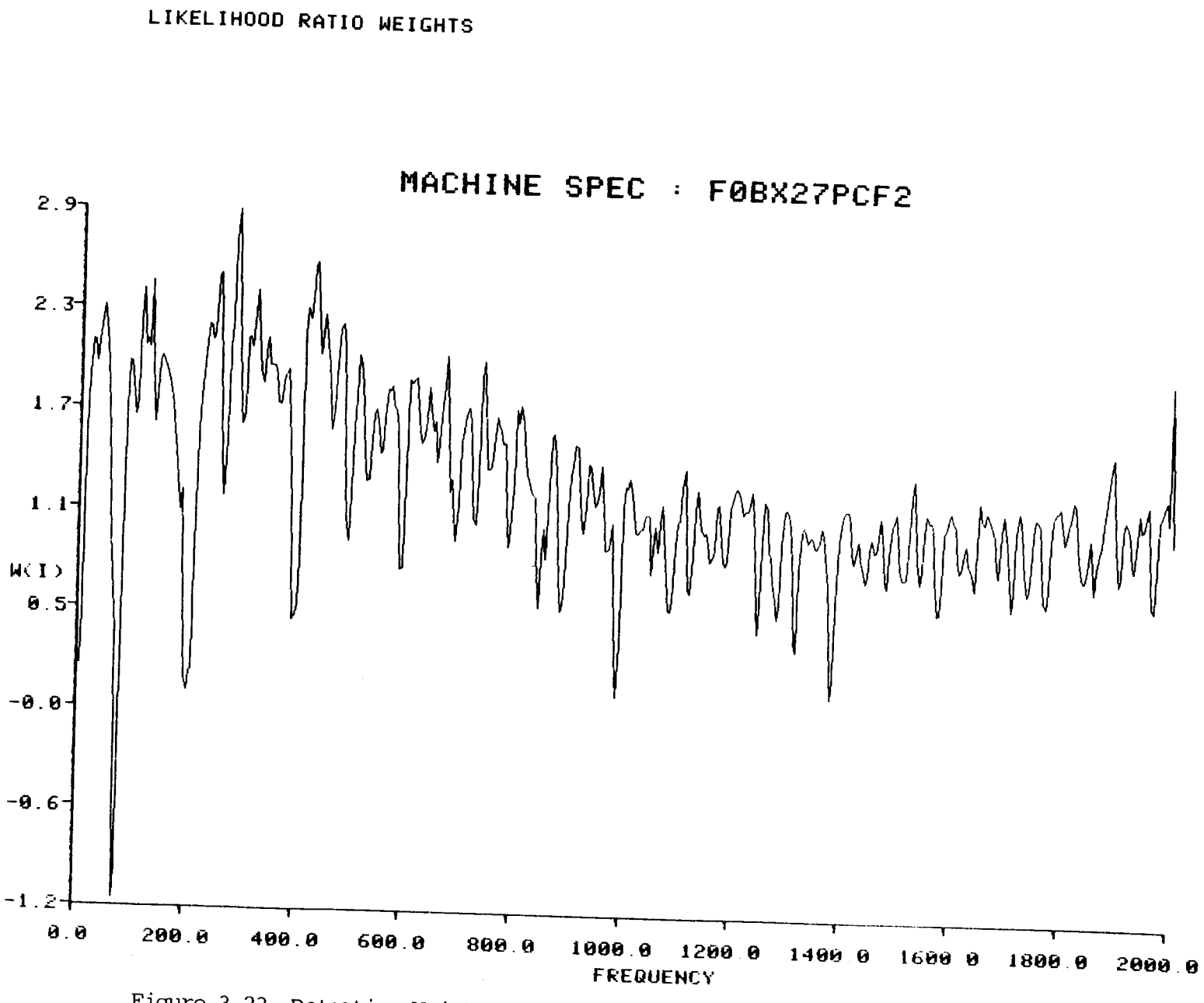

Figure 3.23 Detection Weights - Multiple Fan Bearing Particle Contamination

fault introduction. The bearings were faulted by using a "moto tool" with a carbide grinding tip to introduce a very small score across the race surface. Figure 3.24 illustrates the mean and standard deviation of the HFD baseline and faulted test results. Detection weights for these data, shown in Figure 3.25, clearly show the outer race ball passing frequency and its harmonics and demonstrate the classic HFD bearing fault detectability.

3.5 General Results

3.5.1 Probability of Detection for a Fixed Probability of False Alarm

The general results of the study are summarized in Table 3.7 for the fans and Table 3.8 for the pumps. As described in Section 2.0 of this report, the various post-processing techniques and alternate data types can be equally compared using the probability of detection values for a fixed value of probability of false alarm. This comparison is accomplished by calculating the means and standard deviations for the baseline and faulted cases using the analysis technique under investigation and then performing the detection statistics on these values. Both baseband and HFD detectability of the fault under investigation were evaluated.

The weighted sums techniques identified in Tables 3.7 and 3.8 are described below:

Signature Analysis Weighted Sums

Unmodified: The likelihood ratio weights are applied as calculated from the baseline and faulted conditions in the entire analysis bandwidth.

Modified: The likelihood ratio weights at key frequencies were retained with the calculated amplitudes while all other weights were set to zero. The modified weights were then applied to the baseline and faulted spectra to obtain the weighted sums.

Selected Frequencies BB / HFD

Continuum: Characteristic spectrum broadband shapes were used for detection by setting the likelihood ratio weights to 1.0 over this band of frequencies and zero everywhere else.

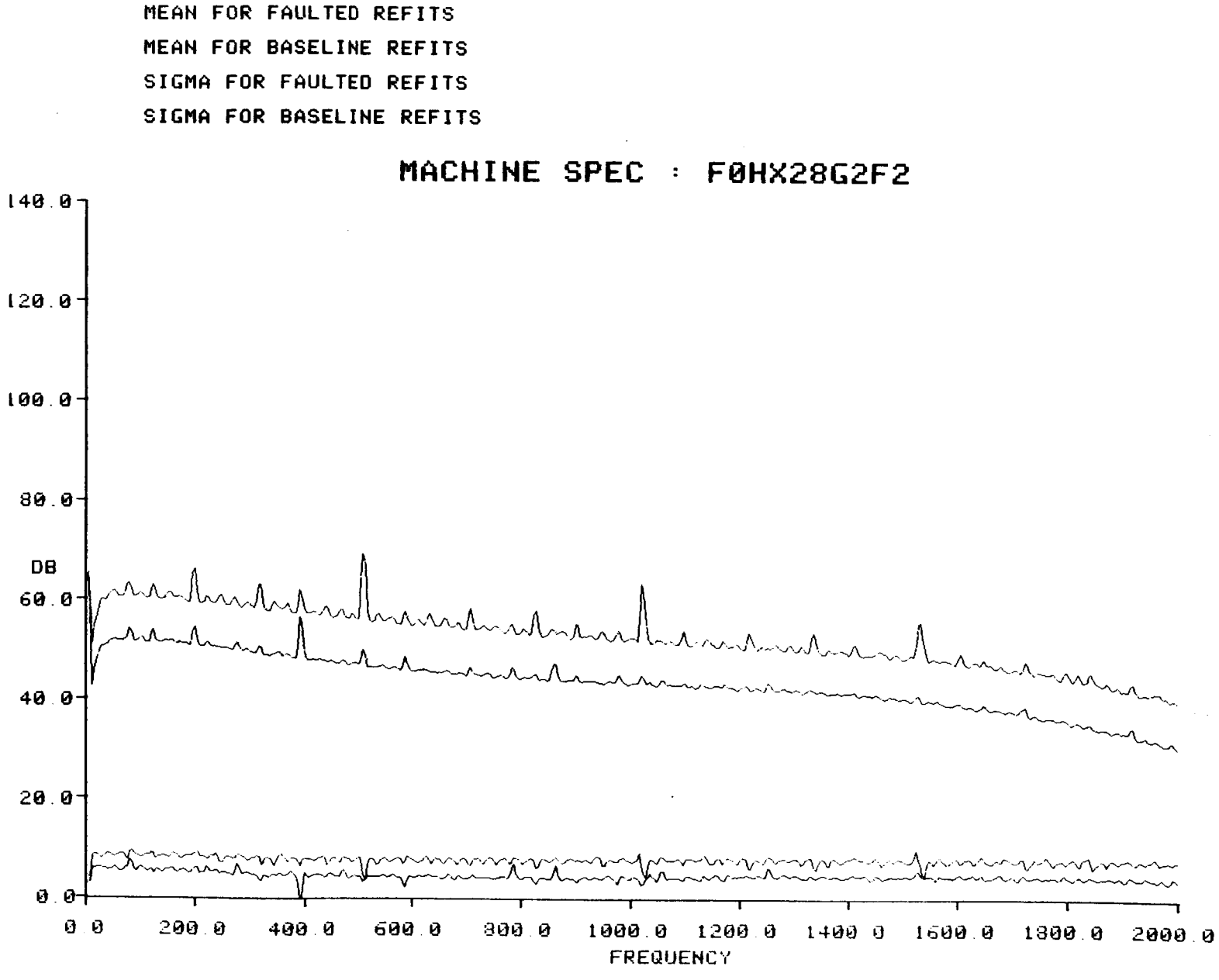

Figure 3.24 Mean and Standard Deviation of the HFD Baseline and Faulted Spectra - Bearing Outer Race Fault

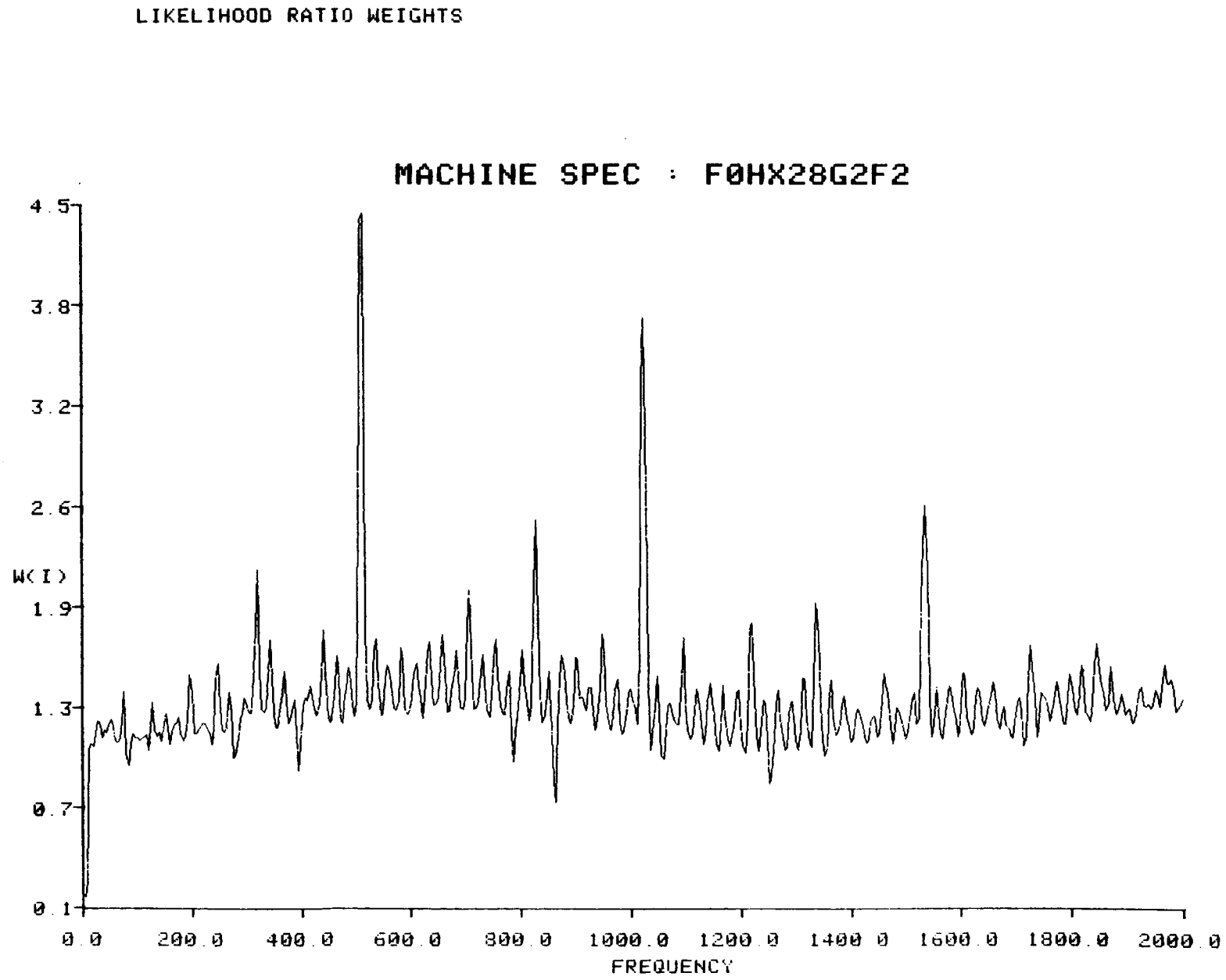

Figure 3.25 HFD Detection Weights for Bearing Outer Race Fault

TABLE 3.7
PROBABILITY OF DETECTION AT P_{FA} = 0.1 DETERMINED FOR FANS USING DIFFERENT ANALYSIS TECHNIQUES

	Selected Frequencies Baseband/HFD						Signature Analysis Weighted Sum				Time Series Weights				Cepstrum		Clustering	
	Continuum		Single Freq.		Multiple Freq.		Unmodified		Modified		Training Set		Application Set					
FANS	BB	HFD	BB	HFD	BB	HFD	BB	HFD	BB	HFD	BB	HFD	BB	HFD	BB	HFD	BB	HFD
1) Accelerometer Loose Mounting	*		*		*		.67	.99	.86	.99	*		*		*		*	
2) Imbalance																		
Small (4 fans)							.35	.14	.30	.20								
Large (4 fans)	.21	.20	.49	.34	.48	.36	.43	.25	.77	.37	.81		.04					
Large (1 fan)			1.0				1.0	.98	1.0	.99	.76		.56		1.0		.97	.96
3) Voltage Change (4 fans)	*		*		*						*		*		*		*	
Under (180 V)							.28	.17	.99	.13								
Over (220 V)	*		*		*		.22	.19	.98	.37	*		*		*		*	
4) Phase Loss (1 fan)	*		*		*		1.0	.99	1.0	.99	*		*		*		*	
5) Elevated Ambient (1 fan)	1.0		0.0	0.0	*		1.0	*	1.0	.99	1.0	.99	*		*		*	
6) Bearings (4 fans) Particle Contaminant	.58		.45		*		.65	.63	.57	.66	.72	.56	*		*		*	
7) Bearings (1 fan) Inner Race Fault	.41	.60	.35	.88	*		.60	.65	.83 [2]	.90	.87	.99	*		[1]		.50	.97
8) Bearings (1 fan) Outer Race Fault	.60	.65	.63	.93	*		.90	.67	.91	.80	.72	.86	*		[1]		.47	.99
9) Inlet Restriction (1 fan)																		
25%	*		*		*		.99	.79	.99	.80	*		*		*		*	
75%	*		*		*		1.0	.90	1.0	.90	*		*		*		*	

* - P_D values not calculated

[1] - Cepstrum analysis unsuccessful detection at key frequencies

[2] - Optimum detection on FRF; P_D = 0.45 for detection on BPFI

[3] - Selected most detectable tone (a pumping frequency)

[4] - Faulted means less than baseline means - Probability of detection not quantifiable

TABLE 3.8
PROBABILITY OF DETECTION AT P_{FA} = 0.1 DETERMINED FOR PUMPS USING DIFFERENT ANALYSIS TECHNIQUES

	Selected Frequencies Baseband/HFD				Signature Analysis Weighted Sum				Time Series Weights		Cepstrum		Clustering	
	Continuum		Single Freq.		Multiple Freq.		Unmodifed		Modified		Training Set		Application Set					
PUMPS	BB	HFD	BB	HFD	BB	HFD	BB	HFD	BB	HFD	BB	HFD	BB	HFD	BB	HFD	BB	HFD
1) Impeller Wear (4 - 1ϕ)	*		[3] .65	.30	*		.70	.48	.43	.23	*		*		[4]		[4]	
2) Impeller Fault (1-1 ϕ)	*		*		*		1.0	1.0	1.0		*		*		.97	.99	.99	
3) Bearing (1-3 ϕ) Loss of Lube	*		*		*		.99	1.0	1.0	1.0	*		*		*		*	
4) Bearings (6-3 ϕ) Inner Race Fault	*		.81	[4]	.73	[4]	.99	.47	.995	.47	*		*		*		*	
5) Bearings (6-3 ϕ) Outer Race Fault	*		.69	.17	.73	.18	.96	.05	.97	.20	*		*		*		*	
6) Phase Loss (1-3 ϕ)	*		.95		.99		1.0	.38	1.0	.59	*		*		*		*	
7) Load Conditions (80 psig) (1-1ϕ)	*		.06	.90	.97	.99	1.0	.99	1.0	.99	*		*		*		*	
8) Load Conditions (20 psig) (1-1ϕ)	*		[4]	[3] 1.0	*		.96	.99	1.0	1.0	*		*		*		*	
9) Coupling Imb. (1-3 ϕ) Small (.035 gm)	*		*		*		.76	.08	.66	.69	*		*		*		*	
Large (.173 gm)	*		*		*		.99	.19	1.0	.32	*		*		*		*	
10) Voltage Change (1-1 ϕ) Over (135V)	*		*		*		1.0	1.0	1.0	1.0	*		*		*		*	
Under (105V)	*		*		*		1.0	1.0	1.0	.97	*		*		*		*	
11) Accelerometer Loose Remount 1-1ϕ	*		*		*		.99	.96	*		*		*		*		*	
1-3ϕ	*		*		*		.99	.85	*		*		*		*		*	

* - P_D values not calculated

[1] - Cepstrum analysis unsuccessful detection at key frequencies

[2] - Optimum detection on FRF; P_D = 0.45 for detection on BPFI

[3] - Selected most detectable tone (a pumping frequency)

[4] - Faulted means less than baseline means - Probability of detection not quantifiable

Single Frequency: The likelihood ratio weight at a characteristic frequency, such as the fundamental for the imbalance tests, was set to a value of 1.0 while all other weights were set to zero.

Multiple Frequency: Similar to single frequency detection only a variable number of frequencies were set to 1.0.

Time Series Weights

Training Set: The likelihood ratio processing of the time series in the full analysis bandwidth for both baseline and faulted conditions. The set of weights derived for a particular test condition were applied to the same baseline and faulted conditions to obtain a set of weighted sums.

Application Set: The likelihood ratio weights developed on one set of time series data were applied to another series of data developed in a separate test. For example, the set of weights developed for the multiple fan -- large imbalance tests were applied to the single fan -- large imbalance test data.

3.5.2 Selection of Techniques

The general results presented in Tables 3.7 and 3.8 can be used to determine which vibration analysis techniques provide the best detectability for a given problem type. Table 3.9 ranks problem detectability and shows the highest value for the probability of detection, along with the technique which produced this value. These results demonstrate that a majority of the problem types are readily detectable ($P_D > 0.90$ and $P_{FA} < 0.1$) . In addition, severe problem types (impeller fault, large imbalance, loss of bearing lubricant, bearing race faults, and elevated temperature) are detectable at very low values of P_{FA} which would allow frequent sampling of a number of machines. Other important conclusions are:

1. The most promising technique is clearly the weighted sum [W(I)] of the baseband vibration power spectrum. These weights often identify features that are not readily observable by inspection.

TABLE 3.9
RANKING OF PROBLEM DETECTABILITY (P_D)

	PROBLEM	P_D @ P_{FA} = 0.1	P_D @ P_{FA} = 10^{-6}	ANALYSIS TECHNIQUE
1.	Pump Impeller Chip	1.0	1.0	Baseband W(I) or HFD
2.	Fan Phase Loss	1.0	1.0	Baseband W(I)
3.	Large Imbalance Single Fan	1.0	1.0	Baseband W(I)
4.	Inlet Restriction - 75%	1.0	1.0	Baseband W(I)
5.	1ϕ Pump Under Voltage	1.0	1.0	Baseband W(I)
6.	1ϕ Pump Over Voltage	1.0	1.0	Baseband W(I) or HFD
7.	Elevated Fan Ambient	1.0	.999998	Baseband W(I)
8.	3ϕ Pump Phase Loss	1.0	.87	Baseband W(I)
9.	1ϕ Pump Over Pressure (80 psig)	1.0	.39	Baseband W(I)
10.	1ϕ Pump Under Pressure (20 psig)	1.0	.14	Baseband W(I)
11.	3ϕ Pump Large Coupling Imbalance	1.0	.01	Baseband W(I)
12.	Pump Loss of Lubricant	0.99		Baseband W(I) or HFD
13.	Fan Under Voltage	0.99		Baseband W(I)
14.	Pump Inner Race Spall	0.99		Baseband W(I)
15.	Inlet Restriction - 25%	0.99		Baseband W(I)
16.	Accelerometer Loose Mounting - 1ϕ Pump	0.99		Baseband W(I)
17.	Accelerometer Loose Mounting - 3ϕ Pump	0.99		Baseband W(I)
18.	Fan Over Voltage	0.98		Baseband W(I)
19.	Pump Outer Race Spall	0.97		Baseband W(I)
20.	Fan Outer Race Spall	0.90 or 0.99 Clustering HFD		Baseband W(I) or HFD Clustering
21.	Accelerometer Loose Mounting - Fan	0.86 (0.99 with HFD)		HFD
22.	Fan Inner Race Spall	0.83 (0.90 HFD)		HFD
23.	Large Imbalance (4 Fans)	0.77		Baseband W(I)
24.	3ϕ Pump Small Coupling Imbalance	0.76		Baseband W(I)
25.	Fan Bearing Particle Contamination	0.57 (0.72-Time Series) (0.68-Continuum)		Baseband Continuum Analysis
26.	Pump Impeller Wear	0.43		Baseband W(I)
27.	Fan Small Imbalance (4 Fans)	0.35		Baseband W(I)

2. The use of reference baseline data is very important. The fan imbalance results were obtained for two cases:1) one fan repeated four times and 2) four fans tested separately. The second case corresponds to the detection of imbalance with the same algorithm of a group of fans rather than using individual references for each fan. The value of $P_D = 1.0$ at $P_{FA} < 10^{-8}$ for a single fan and $P_D = 0.77$ at $P_{FA} = 0.1$ for multiple fans.

3. Cepstrum analysis provided no significiant problem detection enhancement for the problem types investigated.

4. Amplitude processing of the time series provided limited detection capability. The likehood ratio processing only provided a significantly increased detection capability for the bearing inner race problem type. This processing should be equivalent to, or better than, most amplitude processing including peak detection and kurtosis analysis.

3.5.3 Classification Analysis

While the primary focus of this study has been on problem detection, or good versus faulted data, actual machinery monitoring applications involve good versus multiple faults. To address this application, faulted data for several problem types investigated for the IFD components were combined and the results for the weighted sum processing of baseband and HFD data were analyzed. If any or all sets yielded sums in excess of pre-set thresholds, a machine problem was identified as detected. The outputs from the classification processor were then examined to select the largest value as an indicator of the specific problem diagnosis.

Gaussian amplitude densities were assumed and measured values of the mean and standard deviation for each weight set applied to a group of faulted spectra were used to compute the relative probabilities that each weight set produced the largest output for a given problem type. Tables 3.10 and 3.11 present results of the analysis performed for several of the problem types investigated on the TRW fans using baseband and HFD data, respectively. The probability of correct classification for each problem type is given by the diagonal values in the matrix.

Table 3.10 - Classification Probabilities for Modified Weighted Sums of Baseband Vibration Spectra for Fan Data

PROBLEM K \ WEIGHTS (W_K) FOR PROBLEM K		W1	W2	W3	W4	W5	W6	W7	W8	W9	W10
1	Accelerometer Loose Mount	.08	.11	.19	.06	.01	.04	.04	.13	.16	.17
2	Small Imbalance	.06	.08	.16	.09	.003	.21	.06	.10	.10	.14
3	Large Imbalance Multiple Fans	.04	.05	(.25)	.32	.05	.0008	.04	.07	.09	.07
4	Large Imbalance Single Fan	.0000	.0000	.0000	(.9999)	.0000	.0000	.0000	.0000	.0000	.0000
5	Under Voltage	.02	.06	.13	.015	.18	.19	.06	.10	.12	.13
6	Phase Loss	.0000	.0000	.0000	.0000	.27	(.73)	.0000	.0000	.0000	.0000
7	Elevated Inlet Temperature	.0008	.0000	.0000	.014	.0000	.0000	(.98)	.0000	.0000	.0000
8	Bearing Particle Contaminant	.10	.12	.13	.09	.003	.027	.080	.13	.18	.14
9	Bearing (IR) Fault	.11	.10	.07	.07	.05	.04	.05	.09	(.31)	.09
10	Bearing (OR) Fault	.09	.11	.12	.07	.17	.04	.05	.13	.07	(.13)

Table 3.11 - Classification Probabilities for Modified Weighted Sums of HFD Vibration Spectra for Fan Data

PROBLEM K \ WEIGHTS (W_K) FOR PROBLEM K		W1	W2	W3	W4	W5	W6	W7	W8	W9	W10
1	Accelerometer Loose Mount	.16	.20	.16	.0001	.16	.16	.16	.0001	.0001	.0001
2	Small Imbalance	.12	.04	.13	.09	.09	.15	.11	.09	.08	.10
3	Large Imbalance Multiple Fans	.09	.09	.11	.12	.09	.09	.09	.11	.10	.10
4	Large Imbalance Single Fan	.09	.09	.11	.12	.09	.09	.09	.11	.10	.10
5	Under Voltage	.10	.13	.10	.08	.10	.09	.10	.09	.09	.09
6	Phase Loss	.11	.01	.27	.0002	.025	(.48)	.09	.0002	.0002	.0003
7	Elevated Inlet Temperature	.12	.31	.08	.0000	.29	.04	.16	.0000	.0000	.0000
8	Bearing Particle Contaminant	.01	.02	.01	.21	.02	.01	.01	.22	.25	.23
9	Bearing (IR) Fault	.02	.03	.01	.17	.02	.01	.02	.17	(.42)	.12
10	Bearing (OR) Fault	.04	.05	.05	.18	.04	.05	.05	.18	.17	(.20)

The values in Table 3.10 indicate that the problems readily diagnosed by baseband weighted sum processing are: large imbalance, phase loss, elevated inlet temperature, and (less reliably), bearing race faults. The HFD weighted sum processing given in Table 3.11, correctly identified fewer problem types--bearing race faults and phase loss.

Tables 3.12 and 3.13 present results of the classification analysis for the single-phase and three-phase pumps, respectively. Both baseband and HFD weighted sum processing correctly diagnosed the smaller set of problem types chosen for the single-phase pump analysis. The three-phase pump problem set resulted in smaller relative probabilities for both data types, with the baseband modified weighted sum correctly classifying three of the four problems.

Important conclusions are:

1. A processor was developed which demonstrates a significant capability to correctly classify a problem type in a representative ECLSS machine. It is important to note that the weighted sum processing or linear discriminant approach is a detection scheme and is not specifically designed for pattern classification. Further investigation and development of algorithms based on the joint distribution of frequency cells for faulted and baseline data could be used to significantly improve classification performance.

2. It is important to include only the most relavent and probable fault or problem types in the analysis in order to improve the relative probability of correct classification. Alternately, problems that occur very infrequently should not be afforded the same weight in the classification process as those that occur on a much more frequent basis. The smaller number of faults investigated for the single phase pumps, for example, generally resulted in much higher relative probabilities than the much larger group of problems utilized in the fan classification analysis.

TABLE 3.12 CLASSIFICATION PROBABILITIES
PUMP (1φ)

BASEBAND				
W(k) for Prob. k / Problem k	W1	W2	W3	W4
Impeller Wear	(.86)	.04	.03	.06
Impeller Fault	.29	(.65)	.06	.0001
Load - 80 psig	.002	.0000	(.998)	.0000
Load - 20 psig	.03	.02	.15	(.79)
HFD				
Impeller Wear	(.32)	.14	.27	.27
Impeller Fault	.00004	(998)	.0009	.001
Load - 80 psig	.10	.03	(.80)	.07
Load - 20 psig	.18	.05	.10	(.68)

TABLE 3.13 CLASSIFICATION PROBABILITIES
PUMP (3φ)

BASEBAND				
W(k) for Prob. k / Problem k	W1	W2	W3	W4
Loss of Lube	.24	.12	.36	.28
Inner Race Fault	.06	(.77)	.07	.10
Outer Race Fault	.18	.26	(.37)	.19
Phase Loss	.0000	.0004	.0006	(.999)
HFD				
Loss of Lube	.35	.36	.29	.0000
InnerRaceFault	.18	.29	.18	.35
Outer Race Fault	.26	.24	(.46)	.04
Phase Loss	.19	.17	.21	(.43)

4.0 PRELIMINARY MONITORING SYSTEM DESIGN AND IMPLEMENTATION PLAN

The purpose of this section is to describe and justify a proposed vibration monitoring system for general applications to rotating machinery used on advanced spacecraft. A discussion of maintenance philosophy factors affecting the proposed design is presented first, followed by a general description of the processing functions of the proposed design. The final subsection addresses the problems and recommended techniques for implementation of the design.

4.1 Maintenance Philosophy

4.1.1 Primary Purpose

Current spacecraft maintenance philosophy is to implement fault tolerance by use of redundant components and elimination of single-point failure pathways. Vibration monitoring and analysis capability is viewed as an extension of existing design philosophy to the machinery sub-component level. The goal is to achieve fault detection and diagnosis and then initiate appropriate corrective action prior to component failure.

4.1.2 Standardization

Results obtained during this study and described in Section 3.5 of this report have clearly demonstrated the performance advantages of standardization of equipment. The classification or diagnostic capabilities are significantly improved if a limited set of known faults may be defined. Furthermore, the weighted sum analysis of vibration spectra (see Section 3.5) is dependent on measurements of the vibration spectra of specific units and specific problems. The advantages of standardization in regard to reliability and maintainability include: 1) the performance of general performance monitoring techniques (including vibration monitoring) would be significantly improved, 2) a group of highest probability fault types could be determined through failure testing, which would facilitate diagnosis and repair, 3) training for repair and maintenance would be minimized, and 4) cost of equipment would be minimized.

4.1.3 Unit Replacement

In man-tended modes of operation and initial stages of manned operation, maintenance of advanced spacecraft should be accomplished by unit replacement to minimize required crew time. Ultimately, maintenance functions are to be performed on orbit. Two elements

of the basic rationale supporting on-orbit maintenance are 1) the need to take full advantage of the presence of man in space and 2) the high cost of transfer of components from a ground based facility to orbit. Therefore, it is anticipated that a workshop will ultimately be provided and outfitted with standard tools, diagnostic equipment and a spares inventory.

All rotating machinery components should be line replaceable. This will minimize down-time and facilitate repair of internal machinery components in the on-board workshop. Repaired units will be tested and returned to the spares inventory. Access by the astronauts to all rotating components should be assured to facilitate maintenance.

4.1.4 Additional Factors

Table 4.1 shows relevant maintenance philosophy factors in addition to those described in the preceding paragraphs. The impact of each factor on the preliminary design is also summarized in Table 4.1.

4.1.5 Vibration Monitoring Goals

4.1.5.1 Reliability

The reliability of the vibration monitoring system must be much greater than the reliability of the rotating components to be monitored. This goal impacts aspects of the proposed design as well as proposed future studies. The primary manifestation is in the need to have very low probability of false alarm and high probability of detection. The techniques for quantifying these performance statistics, developed and applied during this study, are described in Section 3.0 of this report.

4.1.5.2 Applicability to General Machine Types

This study has concentrated on small rotating components typical of the ECLSS. Machines and mechanical systems not investigated in this study which are of interest include: machinery with gears and or belts, reciprocating machines, very low RPM machines, and transient or impulsively operating machines. The vibration monitoring system described later in Section 4.0 of this report is believed to be applicable to these types of machines, provided the necessary experiments and data analysis are performed to optimize the design parameters.

TABLE 4.1 - MAINTENANCE PHILOSOPHY/MAINTENANCE FACTORS

Elements of Vib Mont/Analysis Program Plan ↓ / Maint. Phil. →	1) Minimum Required Crew Training	2) Minimum Unnecessary Maintenance Activity	3) Provide for Ultimate Autonomy of Spacecraft	4) Min. Orbit Transfer Weight Req. for Maint.	5) Maximum Use of Human Presence	6) Spacecraft Mach. will be Highly Reliable and Fault Tolerant	7) Maximum Probability of Correct Maintenance Decision	8) Provide Maint. Sched. Tool for Logistics Cycle (? 90 Days)	9) Multiple Machines of Different Types	10) Maint. Monit. Sys. has Limited Computer Resources
1. Standardization of Equipment	X	X		X	X		X		X	X
2. Evolution of Monitoring System from Analyst to Expert System on a Machine-to-Machine Basis as System Improves and Confidence is Achieved		X					X			
3. Provide Expert System	X	X	X		X		X			
4. Multi-Level Processing		X (Minimize PFA for Pred. Maint.)				X (Quality Assurance & Low PFA)	X Max. PD for Short Interval Checks	X Diag. & Trending	X	X (Prescreen Data to Omit Clearly Good)
5. Data Base Management Considered as Major Development Task									X	X
6. Provide "Quick Fix" Suggestions as well as Long Term Required Maintenance Scheduling					X (Allow Solutions in Crew Sched. Conflicts)		X			
7. Provide for Repair at Machine Unit Level	X	X								

4.1.5.3 Automation

To provide effective spacecraft machinery monitoring, all parameters should be automatically monitored onboard by system software. Existing methods requiring continuous manual monitoring of telemetry are incompatible with advanced spacecraft environments. It is likely that a single onboard crew member will be responsible for overall monitoring, fault recovery and maintenance. Similarly, ground monitoring of telemetry is inconsistent with the goal of autonomous operation.

Recent Space Shuttle missions have averaged 20 malfunctions for a seven day flight. In the event of a malfunction, the flight control team and crew consult written malfunction procedures. If the need to execute multiple malfunction procedures simultaneously arises, the crew must use their own judgement to decide the order of the procedures. It is clear that fault recovery and maintenance for the more complex advanced spacecraft environment will dictate an automatic system.

4.1.5.4 Autonomy

All processing should be performed on-site without the use of ground telemetry. Limitation on available spacecraft computer processing capability will require that as much pre-processing of data as possible be performed before input to the spacecraft processing system. Also detection and processing algorithms should be as simple as possible.

An autonomous fault recovery/maintenance prediction system should be in the form of signal processing to detect features followed by an expert system to complete the diagnosis and recommend actions. Malfunction/maintenance procedures lend themselves to expert system programs due to their rule-based "if-then" tree structure. An automated system could integrate monitoring information with spacecraft conditions, spare parts, system redundance design and maintenance procedures to provide swift alarms as well as detailed messages containing diagnosis, severity, and action information. The system would also be interactive so that the operator could prompt for additional information. A comprehensive automated system would minimize the number of malfunctions needing immediate attention and maximize on-board crew efficiency.

4.2 Functional Design

4.2.1 Vibration Monitoring Functions

During the Conceptual Study, six specific vibration monitoring functions were defined. The following list (taken from the Final Conceptual Study Report) provides a brief description of these monitoring functions.

1. Continuous Protection Against Catastrophic Failure - The goal of this function is to detect an impending failure with very high probability of detection (P_D) and very low probability of false alarm (P_{FA}). The amount of advanced warning, the ability to obtain detailed diagnostics, and the ability to assess categories of severity could all be sacrificed, if necessary, in order to achieve high P_D and low P_{FA}. The purpose of this function is to allow switching to redundant capability.

2. Early Detection of Machine Abnormalities - This function would provide detection of generic machine abnormalities with lead times that are greater than 48 hours and are ideally as long as possible. This function would require high P_D and low P_{FA}. The ability to assess level of severity and provide detailed diagnostics could be sacrificed in order to achieve accurate detections with long lead time. The purposes of this function are:

   - Provide trigger signals for the acquisition of additional data,
   - Minimize cost of repair by preventing propagation of early faults to more advanced stages of failures with higher cost of repair,
   - Prevent degradations in performance as a result of propagating faults, and
   - Allow convenient scheduling of maintenance rather than emergency maintenance.

3. Accurate Diagnosis of Problem/Given a Detected Machine Abnormality - For a given machine and monitoring system, a detected abnormality has a class of potential sources or specific problems (e.g. balance, bearing, looseness, blocked filter). The goal of this function would be to select the specific problem or problems with highest probability and, if necessary, to rank the possible problems according to their a posteriori probability. Bayesian estimation techniques are examples of the candidate processing approaches for this function. An important

problem category will be sensor problems. This function must accurately separate sensor problems (or other data acquisition problems) from true machine problems. The two purposes of the diagnosis function are: 1) to provide information to the level of severity function (item 4), and 2) to minimize repair cost and time.

4. Assessment of Level of Severity/Given a Detected Machine Abnormality - This function would operate in concert with the algorithms described in items 2 and 3. The goal of this function would be to estimate the level of severity of a problem or detected abnormality. For example, five classes of severity might be the following:

- Class 1 - No action required.
- Class 2 - Additional data collection and close monitoring required.
- Class 3 - Simple quick fixes (lubrication) or changes in operating condition (cut back flow rate) are required.
- Class 4 - Maintenance should be scheduled within a specified time interval.
- Class 5 - Immediate maintenance should be scheduled.

5. Accurate Prediction of Future Machine Condition Versus Time (Including Time to Failure)/Given a Detected Machine Abnormality - The goal of this function would be to provide predictions of the state of a machine versus time. The primary state of interest would be failure condition; however, it would also be of value to predict intermediate levels of degradation. There are two basic approaches that would be applicable for this function. The first approach would be "optimal" trend analysis of vibration parameters indicative of machine condition. The second approach would involve a state transition model based on engineering knowledge of the machine behavior. For example, it may be known that an inner race spall causes an outer race spall which causes bearing looseness, and finally, bearing failure. The time intervals for these transitions may be estimated. This is often referred to as defect propagation rate.

6. Provide Feedback Information for Control of Machine Operational Characteristics - It is well known that operational parameters such as temperature, pressure, and flow rate may be highly correlated with vibration, and all these parameters should be used to estimate the state of a machine. Furthermore, it is proposed that these combined parameters could be used as inputs to a knowledge based processor with rules related to the operation of the machine, and that the system could be automatically controlled in a way to maximize efficiency and longevity.

The level of importance of each of the six functions described above has been assessed for purposes of this feasibility study, and the rank in importance is given by the order of occurrence in the list; that is, protection against catastrophic failure is considered to be the most important and feedback control is considered to be least important.

The ranking of functions was based on the impact on space operations, maintenance reliability, and maintenance costs. In some instances, the rank of importance is also based on the interdependence of functions. For example, all functions except "continuous protection against failure" are dependent on "early detection of abnormalities"; therefore, "early detection of abnormalities" is ranked second. The third through fifth functions are very interdependent and their level of importance is considered approximately equal. The feedback function is ranked last because it adds capability rather than protects against degradations in space operations.

The highest ranked function of continuous protection against catastrophic failure was not investigated in depth during this study since it will be accomplished primarily by monitoring techniques other than vibration monitoring. The functions ranked 2 through 5 were considered to be the primary areas of interest. The matched weighting processing techniques developed during this study may be used to perform each of these functions and form the basis of the processing system described in the following section.

4.2.2 Monitoring/Analysis System Schematic

A schematic of the proposed vibration monitoring system (VMS) is shown in Figure 4.1. This VMS receives and sends information (sensor and logic data) between four sources: the accelerometer outputs, the up/down link to ground control, the display and control console operated by the crew, and the spacecraft distributed data management system (DMS). The VMS is capable of performing the six vibration functions described in Section 4.1. The functional blocks of Figure 4.1 are described in the following paragraphs.

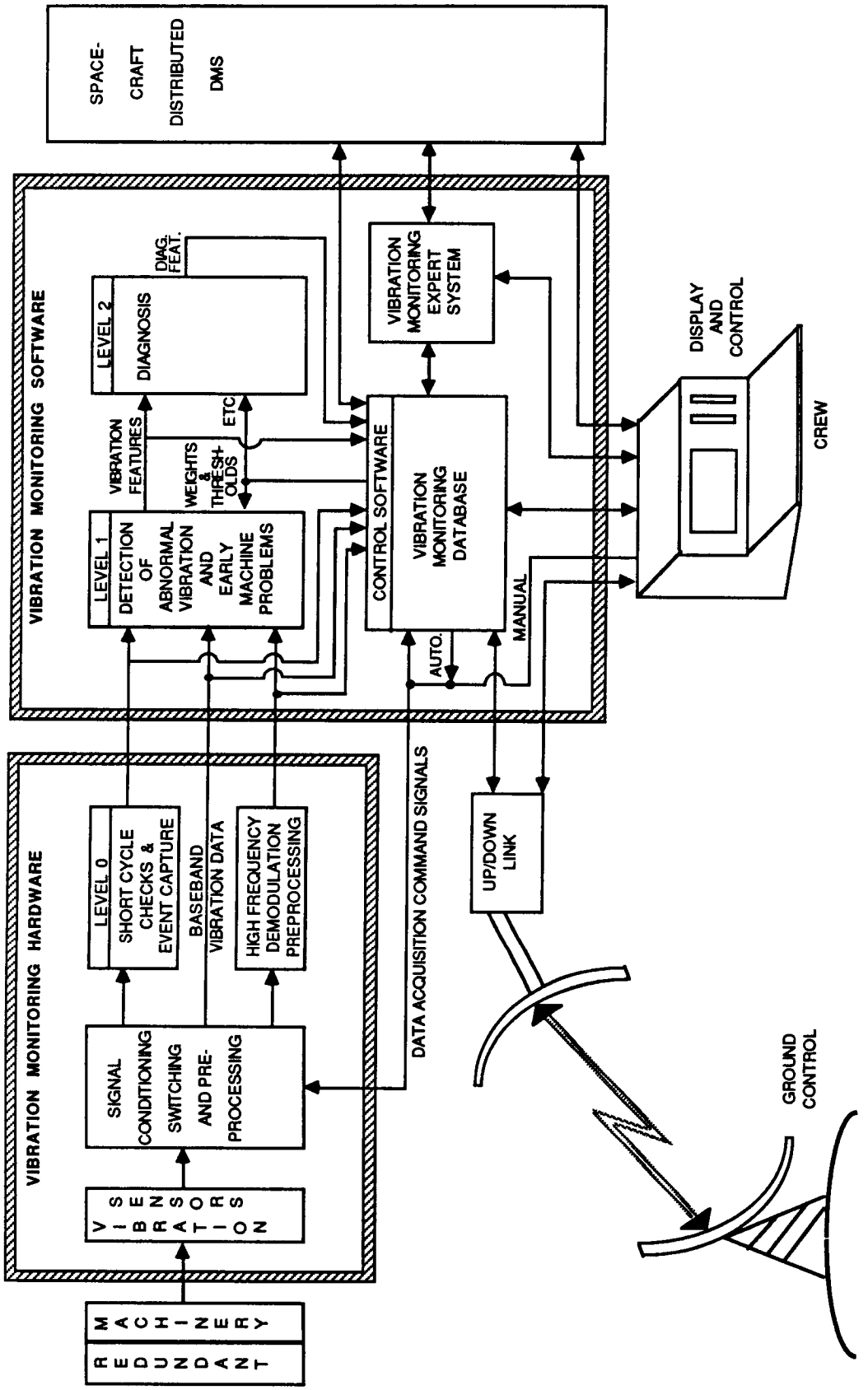

FIGURE 4.1 - VIBRATION MONITORING/ANALYSIS SYSTEM SCHEMATIC

4.2.2.1 Redundant Machinery

The machinery itself is anticipated to be doubly or triply redundant, with automatic cut-in of the spare upon failure of the primary unit. An analysis of product of failure probabilities demonstrates that the enhanced reliability resulting from vibration monitoring is significantly increased in a redundant system as compared to a non-redundant system.

4.2.2.2 Vibration Sensors

The vibration sensors (discussed in detail in Section 4.3) are equipped with local preamplifiers. The signals are sent to an analog MUX, not shown in Figure 4.1, located in the vibration monitoring system hardware cabinet (see Section 4.3).

4.2.2.3 Signal Conditioning/Switching/Preprocessing

The analog MUX passes the analog signals to an amplifier summer which allows the insertion of a calibration tone at a known stable frequency and amplitude. The calibration tone will be at a relatively high frequency and will provide a fixed reference to check gain drift and machine RPM shifts. The signals are then low pass filtered for normal baseband analysis as well as demodulated (see Section 4.3) for analysis of high frequency signals. The signals are then digitized prior to the initial vibration analysis processing.

4.2.2.4 Level Zero Short Cycle Checks and Event Capture

Protection against rapidly developing failures, such as loss of lubricant, may be detected by vibration monitoring. Experiments conducted during this study have demonstrated that severe vibration increases occur with loss of lubricant in small, high RPM pumps. Failures generally occur three hours or more after the detection of vibration increases. Continuous vibration monitoring with transient data communicated asynchronously to the computer at alarm would be required. Simple RMS power levels in selected frequency bands would be computed and compared to an alarm threshold. Threshold exceedance would cause an immediate acquisition of digitized data for detailed analysis at levels one and two.

4.2.2.5 High Frequency Demodulation

The experiments and analysis conducted during this study have indicated that HFD analysis may be valuable as a means of early detection of impulsive periodic vibration which excite resonant modes of the machine (see Section 2.0). Therefore, an HFD channel is proposed as an alternate analysis method to standard baseband analysis. Normal frequencies for HFD analysis are above 50 kHz. Therefore, demodulation and low pass filtering are performed prior to digitization to reduce the required sampling rate and corresponding implementation difficulties.

4.2.2.6 Level One--Detection of Abnormal Vibration

Vibration data are obtained and analyzed automatically at intervals defined in software. These data are processed at intervals of approximately eight to twenty-four hours.

1. Spectral Estimation - The results of the IFD study have conclusively shown that the primary method of analysis should be analysis of narrowband spectra obtained by FFT processing followed by ensemble averaging to estimate vibration power levels. Typical bandwidths and resolutions for small, high RPM machines should be :

Band 1 : 0 Hz - 2 kHz with 4 Hz resolution
Band 2 : 0 kHz - 10 kHz with 20 Hz resolution

Normally, 16 to 32 ensemble averages would be implemented, requiring four to eight seconds of data for each machine. For a nominal 50 machine group, approximately five minutes would be required. However, results obtained during this study (see Section 3.0) have shown that for small rotating machines, mechanical instabilities require that approximately two minutes of data be obtained for each machine. Therefore, approximately one to two hours may be required to acquire and process the data for an assumed 50 machine group.

2. Postprocessing of Spectral Data - As discussed in Section 3.0 of this report, analysis of vibration power spectra (both baseband and HFD) is clearly the preferred method of vibration analysis. Processing of alternate data types (e.g., likelihood ratio processing of time domain data) provided inferior problem detection capability for all problem types investigated. Therefore, it is recommended that postprocessing of vibration spectra be used as the primary method of vibration monitoring.

3. Normalization of Spectral Data - Preprocessing of the raw spectral data will be required in order to ensure repeatable data independent of machine RPM and load condition. This normalization includes adjustments for variations in machine fundamental rotation frequency (fRf) and noise spectral equalization (NSE). These normalization algorithms are described in Reference (14).

4. Weighted Sum Analysis - The postprocessing technique of most promise is the weighted sum analysis of baseband data. This analysis technique, described in detail in Section 2.3, requires a set of stored weights which are used to form a weighted sum of the spectral data. The weighted sum is then compared to a threshold, and a sum greater than threshold indicates a possible machine problem. Different sets of weights may be stored corresponding to different types of machine problems. If any or all weighted sums exceed their corresponding threshold, a machine problem is identified. The weights may be applied to either the raw spectral data or the difference between the measured spectrum and a reference spectrum. The reference spectra, weights, and thresholds are stored in the vibration monitoring database and may be modified by the crew or ground control.

5. Feature Extraction - Postprocessing of vibration data in addition to the weighted sum of spectra is performed to extract additional features. For example, estimates of the spectral continuum and specific broadband features may be used to reliably detect operation with elevated inlet temperatures (see Section 3.0).

4.2.2.7 Level Two Diagnosis

Diagnosis at level two will be initiated for all abnormal data detected at level one. The purpose of this processing is to estimate the specific problem type and level of severity. The processing technique examined during this study (described in Section 3.5.3) consists of forming weighted sums over the spectral data. The sets of weights are matched to specific problem types and levels of severity. The largest weighted sum indicates the proper diagnosis.

It should be noted that three of the vibration analysis functions listed previously in Section 4.2.1 are performed at level two by the diagnostic processing. These functions are: problem diagnosis, assessment of severity, and estimation of time to failure. It was determined during this study that the most meaningful method of estimating time to failure is to diagnose a problem and estimate the level of severity. This information is then combined with models of the machine's mechanical characteristics and failure modes to estimate time to failure. Trending information may also be required.

4.2.2.8 Vibration Monitoring Database

The vibration monitoring database will be a primary element of the VMS. Control software will interface the database to display and control inputs from the crew, the spacecraft distributed data management system, the data link to ground control, the outputs of the vibration monitoring modules, and the expert system processing. Stored information will include:

1. Reference spectra for each machine,
2. Matched weights and thresholds for detection and diagnosis,
3. Segments of vibration data for event capture of transient events,
4. Relevant historical data such as recent failures and the associated vibration features and recent maintenance recommendations,
5. Relevant platform status, crew activity, and spare parts information,
6. Information associated with data acquisition (such as duty cycle for automatic routine analysis) and transfer, and
7. Information related to display of visual aids for maintenance actions (e.g., machine schematics).

4.2.2.9 Vibration Monitoring Expert System

The expert system is required in order to provide text and visual aids regarding specific maintenance recommendations. The primary elements of a maintenance message are: 1) a binary decision to send a message (alarm), 2) identification of anomalous spectral features, 3) diagnoses of mechanical problems, 4) assessment of problem severity, and 5) a recommended maintenance action. The rules (or knowledge) required to automatically generate these maintenance message items include an extensive list of context information and man/machine interface knowledge in addition to the rules necessary to interpret the signal processing outputs. Examples of the type of rules necessary for this system are:

1. Spare parts, platform status, and crew activity and schedule,

2. The logic/decision status of the VMS for all machines,

3. Previous maintenance history for each unit,

4. Interpretation of level zero, level one, and level two data outputs including:

   - One-to-one feature to problem relationship,
   - Combination of features and problem types for a single message item,
   - Effects of message history for a given unit,
   - Correlation of events for different accelerometer positions and analysis bands,
   - Apriori probabilities of machine problems, and
   - Analysis of special features such as continuum shapes;

5. Message item text construction requiring concatenation of sentence segments,

6. Display of visual aids to assist in the implementation of the maintenance action,

7. Functional application of each machine and its criticality, and

8. Identification of problems when equal or nearly equal candidates exist.

The complete expert system consists of procedural functions developed in an appropriate language such as ADA or FORTRAN combined with symbolic reasoning functions implemented with an expert system tool such as OPS5. Higher level expert system tools such as Knowledge Engineering Environment (KEE) may not be sufficiently flexible to allow the development of the necessary hybrid (procedural and data driven) system. Forward chaining inference technique and pattern matching will be the most appropriate inferencing techniques since conclusions will be derived from a limited set of essential facts.

4.2.2.10 Display and Control

The crew member assigned to maintenance will operate and respond to the VMS through the display and control console. The operator may: acquire data in a manual mode in addition to that automatically acquired by the VMS; query the DMS for information not provided routinely by the VMS; send commands to transmit or receive ground control information and data; and query the VMS for additional advice, explanation, or back-up data. The crew operator may also redirect the VMS logic decision process, as well as modify thresholds, store new reference data, and enter additional information to initiate the system for new machines or modifications to existing machines. At each alarm and maintenance message, the five elements of a message listed in Section 4.2.2.9 and schematics, drawings, or other instructional information required to implement the maintenance action will be displayed.

4.2.2.11 Ground Control

The crew operator or the expert system can initiate transmission of data to ground or receive data from ground control via the up/down link. This would provide ground control with access to the digitized waveforms stored prior to an alarm as well as the outputs of level zero, level one, and level two signal processors and the expert system. Ground control may also initiate data acquisition and modify the VMS parameters and logic in a manner identical to the crew system control described in Section 4.2.2.10.

4.2.2.12 Spacecraft Distributed DMS

The high level VMS computer will become an integral part of the spacecraft distributed DMS. Interface will be provided through database software and the expert system. The VMS will acquire data from the DMS regarding spacecraft status, crew activity, and other platform data pertinent to the operation of the VMS. The VMS will supply information to the DMS network concerning the status of the VMS maintenance items, machinery health, and other factors required by the various subsystems that are a part of the DMS.

4.2.3 Monitoring/Analysis System Operation

Fault isolation will be at the component part level (bearing, blocked filter, etc.) where possible. Diagnostic capability is implemented where required in order to achieve very low probability of false alarm, high probability of detection, and accurate time to failure estimates. The

primary diagnostic capability at level one will be differentiation between sensor and machine faults. Detailed diagnostic capability is provided by level two processing. Level two processing may be initiated by one of three methods: 1) very long cycle computer scheduled checks (e.g. once per week), 2) automatically at each level one alarm, or 3) command from operator. The primary goal of this processing is to isolate faults to the machine component part level and accurately assess level of severity. The outputs will aid in the predictive maintenance functions and may also be used to provide quality assurance for new components or redundant units when switched to operation.

The three-level processing provides the capability to perform all anticipated vibration monitoring functions (Section 4.2.1) with efficient management of computer resources by successive screening operations. The approach also allows optimization of each functional capability.

Level zero requires no diagnostic capability, but probability of detection should be high and false alarm rate should be very low. Level one probabilities of detection are required to be moderately high but the false alarm rate should be very low to avoid the circumstance of a false alarm plus true failure situation that may result in catastrophic failure. The level two processing should have a very high probability of detection, but the false alarm rate may also be relatively high since the primary functions are to provide detailed diagnosis for level one alarms and quality assurance checks on command.

Relative thresholds for each individual machine operating in known good condition are required for functions requiring a low probability of false alarm. For those functions requiring relative thresholds, the following procedures are followed:

1. Obtain reference data (e.g., a spectrum) for the machine operating in known good condition at ground laboratories with absolute thresholds used for quality assurance (note: false alarm may be high for this function),

2. Deliver and install the machine in space and obtain a second baseline data set,

3. Verify that machine baseline data are similar to ground laboratory baseline data (a second quality assurance test), and

4. Store baseline data and set thresholds for detection of relative changes (thus obtaining a system with adequately low false alarm rate).

4.2.3.1 Decision Making Responsibility - The VMS will evolve to ultimately permit autonomous decisions by the platform commander, with alarms, diagnostics, and maintenance recommendations provided automatically by the system. The evolution will proceed from initial phases when most decisions are based on human expert analysis. The diagnoses and recommended actions of the automatic system will be compared with human analysis and improvements will be made in the system. As confidence is gained in the automatic system, it will be given increasing autonomy. This evolutionary process should begin with test bed operation and continue through initial stages of platform operation. Ground control will provide back-up technical support, signal processing capability and simulation resources as required. The platform commander will have authority to override ground control or take independent action if the communication link to ground is disrupted.

4.2.3.2 On-orbit vs. Ground Based Monitoring and Control - As described above, ultimately monitoring and control functions are to be performed on-orbit. Ground control will provide only back-up monitoring and control capability to be exercised in the event the crew is unable to perform essential functions, or when back-up technical support is required. A link from DMS to ground will be available to transmit general platform status information. An uplink can be used to activate or shut down machinery components in the event the crew is unable to take approprite action.

4.2.3.3 Degree of Fault Isolation - Level zero short-cycle checks will isolate faults to the level of the individual rotaing machinery component. Level one long-cycle checks will differentiate machinery failures from several data link failures. Close monitoring, at level two, will be capable of differentiating betweeen different failure modes of the machine with probabilities assigned to each. The decision to replace a defective unit can be based on level zero or level one output alone. Level two output provides additional diagnostic information useful for assessing the urgency of corrective action, given other current priorities. Appropriate quick fix maintenance will be recommended for situations involving intense crew activity.

4.3 Instrumentation and Implementation

The basic monitoring/analysis system concept was presented in the preceding section. In this section, the method of selecting instrumentation for the preliminary system design is discussed in detail.

Selection of instrumentation hardware is an important process to ensure the collection of reliable vibration data. Proper selection of hardware will ensure sensitivity and signal conditioning that provides adequate signal-to-noise ratios. Figure 4.2shows an expansion of the sensor/signal conditioning/processor portion of the overall VMS design.

The criteria for selecting instrumentation for the preliminary system design is driven primarily by the requirements shown in Table 4.2. A discussion of factors that affect the major hardware blocks shown in Figure 4.2 follows:

4.3.1 Sensors

The principal factors influencing transducer selection for the VMS are:

1. Frequency Response - determines bandwidth of possible analysis and ability to provide high frequency demodulated signal. The low end of the frequency response should be less than the lowest frequency to be analyzed which is approximately 5 Hz for the high RPM machines. The high end of the frequency response should be above at least the 10th harmonic of the highest frequency of interest for baseband analysis. A transducer with a high end response of 100 kHz is desireable for high frequency demodulation analysis of small, high RPM rotational machines. A flat frequency response curve is not essential as long as baseline data is taken for each different machine/transducer.

2. Weight (Mass) - The weight of the transducer should be minimized to prevent mass loading which will dampen or alter the response characteristics of the system.

3. Primary Parameter - Acceleration was selected as the most useful indicator of vibration phenomena due to the relatively good sensitivity, size, weight, and ease of use of accelerometers. Acceleration is a principal manifestation of most vibration phenomena.

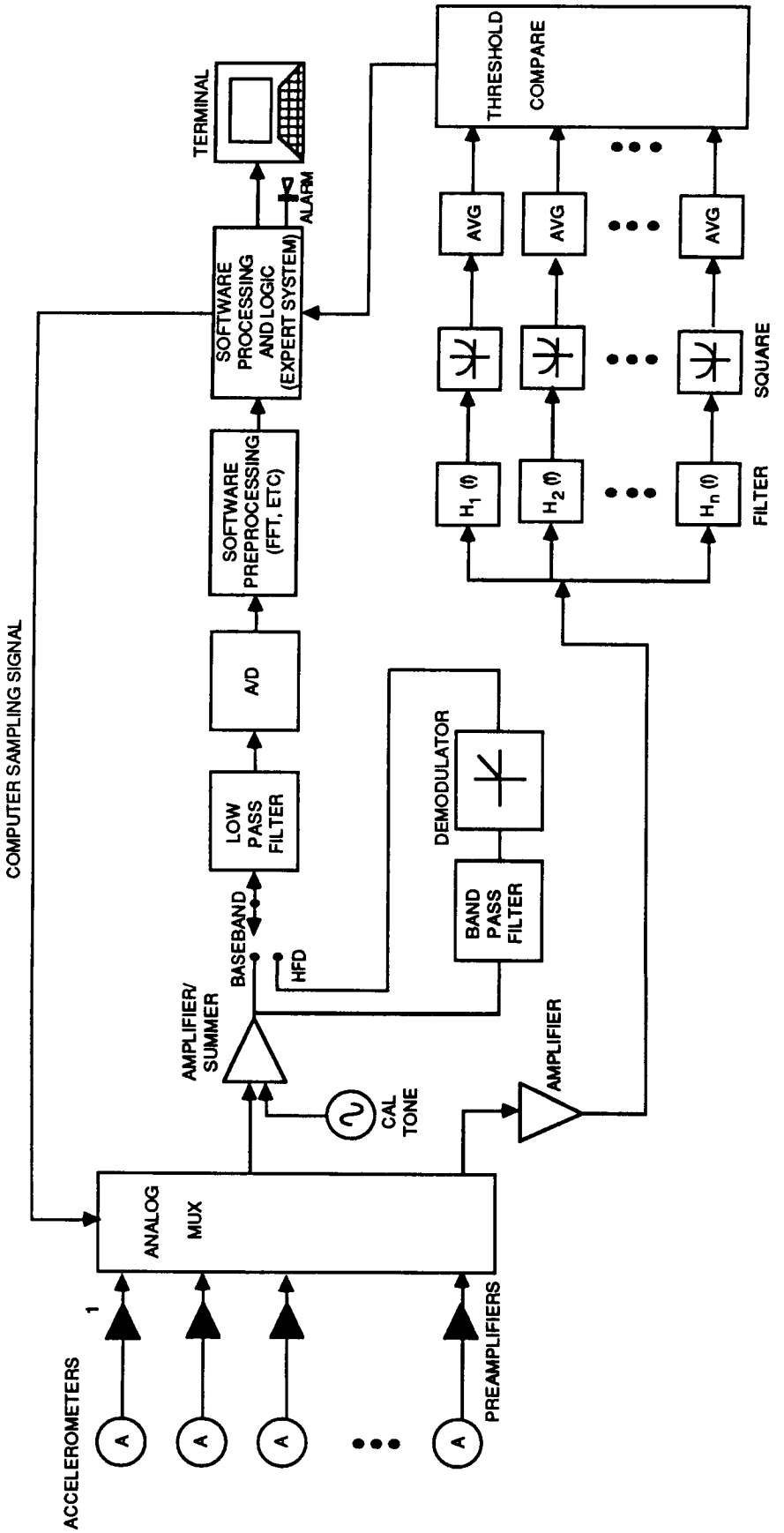

FIGURE 4.2 - MONITORING SYSTEM INSTRUMENTATION DIAGRAM

TABLE 4.2 - VIBRATION MONITORING PRELIMINARY SYSTEM REQUIREMENTS

● Sensor Performance - Sensitivity - Frequency Response - Dynamic Range - Noise Floor - Data Rate ● Space Allocation ● Weight Allocation ● Reliability (MTBF) - Automatic PM/FL - Manual PMFL ● Interface Requirements	● Processor Requirements - Memory - Computational Speed - Interface Compatibility - Expandable ● Expert System - Ease of Call-out to Procedural Language - Operation with Large Database - Inferencing Appropriate to Data Analysis ● Display Characteristics ● Growth Potential - Addition of Sensors, Preamps, etc. - Expansion of Switching Matrix - Processor • Memory Reserve • Processing Margin

4. Sensitivity - Laboratory measurements and literature research showed the acceleration range for small rotational machinery to lie in the 1 x 10^{-5} g to 1 x 10^{2} g range. Accelerometers should provide output signals from this input range that are above the noise floor of the processing electronics, and below processor clipping level at full scale input.

5. Temperature Range - The transducers must be capable of operating, without drift, over the temperaure range of the operating machinery.

6. Mounting - Transducers used in this contract were mounted using beeswax due to the necessity to mount and remove them often. The preferred permanent method is to drill and tap a hole directly in the machine structure and attach the accelerometer with a threaded stud. If the machine structure cannot be drilled, the mounting disc and stud can be welded or glued to the machine or strapdown techniques can be used.

4.3.2 Preamplifiers

The preamplifiers perform two functions: 1) they match the high output impedance of the accelerometers to the lower input impedance of processors and 2) they provide amplification prior to transmitting data signals through cables to the processor. The accelerometers are directly followed by preamplifiers which convert the high impedance, microvolt level signals from the accelerometers into a high level (0.1 to 1 volt), low impedance signal which is more immune to surrounding electromagnetic interference and compatible with further analog processing. These preamplifiers should be located within a meter of the accelerometers to avoid electromagnetic interference susceptibility.

4.3.3 Analog MUX

It is necessary to continuously monitor the machines with simple analog processing, and periodically sample for detailed analysis with digital processing. Therefore, the analog MUX shown in Figure 4.2 samples the preamplifier outputs and multiplexes the signal at two rates. The analog sampling rate would be sufficiently high to ensure power samples are obtained at a minimum of one sample per machine per hour. The sampling for digital processing would provide for a two minute record per machine at eight hour intervals.

4.3.4 Amplifier Summer

The analog MUX outputs require amplification to voltage levels compatible with the analog to digital (A/D) input levels. A calibration tone is summed with all vibration data to provide an amplitude reference to check for system drift. The stable frequency of the tone will also be used by the processing algorithms to check for variations in machine RPM.

4.3.5 High Frequency Demodulation Processing

High Frequency Demodulation processing requires the additional circuitry of a bandpass filter and a demodulator. The bandpass filter center frequency is not critical; 85 kHz was used for this study after several center frequencies were tried with little difference in processing gain. The bandwidth should be equal to or greater than the baseband analysis bandwidth. The type of demodulator used is not critical. A half wave demodulator was used in this study.

4.3.6 Continuous Monitoring

Continuous monitoring of the machinery vibration analog data is accomplished by power detection of a series of bandpass filter outputs. Bandwidths and center frequencies of the bandpass filters are selected to be most sensitive to problem types that progress rapidly to failure. For example, during this study it was determined that a band from 10 Hz to 200 Hz would effectively detect elevated temperature for small fans and a broad band from 10 Hz to 2000 Hz would be effective against loss of lubricant.

4.4 Special Considerations

In addition to the implementation and processing consideration described in Section 4.3, the following special factors must be examined in order to implement the VMS.

4.4.1 Gravity Effects

These issues are addressed in Appendix B of this report.

4.4.2 Radiation

Due to the high radiation levels in space, current MOS transistor technology is not compatible with space applications. However, technology currently exists (e.g., CMOS transistors with error correction) to radiation harden electronic components. Radiation hardening of sensors, A/D devices, and signal processing electronics is warranted due to the crucial nature of these components in the fault detection system.

4.4.3 Platform Constraints

The vibration monitoring system must be designed to accomodate advanced spacecraft power, space, weight, and hardware requirements as well as maintain immunity to potential temperature and pressure variations. The system itself must also have inherent long-term reliability and maintainability and must provide for self-testing capability.

Power, space, and weight requirements are expected to be minimal since only monitoring and signal processing functions are involved. The primary impact in this regard will be provision for cable ways, connectors, and display system.

Immunity to temperature and pressure variations is likely to be more readily achievable for the monitoring system than for the rotating machines themselves. A primary concern is temperature sensitivity of the vibrator sensors and cables. These components should remain reliable and have acceptable output under the most extreme temperature conditions anticipated.

4.4.4 Self-Testing

Self-test capability can be achieved by using at least one sensing element as an active device, transmitting a test signal, and monitoring other sensor outputs. The monitoring software can also be configured with self-test capability by incorporating a variety of simulated sensor outputs.

4.4.5 Upgrading

Future system upgrades should be implemented primarily as software changes and secondarily as computer hardware changes. The requirement for future changes in vibration sensing elements, A/D units, and data transmission cables are eliminated insofar as possible.

5.0 SUMMARY AND RECOMMENDATIONS

A detailed feasibility study to investigate the application of vibration monitoring to increased reliabiliity/maintainability of representative rotating machinery components of advanced spacecraft was completed. The study consisted of three phases: a Conceptual Study, an Application Study, and a Preliminary Monitoring System Design and Implementation Plan. A summary of the results and conclusions for each phase of the study is given below.

5.1 Conceptual Study

Rotating components of the advanced spacecraft were identified, the selection of fans and pumps as generic test items was justified, and a selection of specific fans and pumps was made.

Over 200 documents were obtained and reviewed during the literature survey to ascertain candidate concepts, vibration monitoring techniques, and fault / failure mode information of the selected components.

A systematic study to define the highest potential vibration monitoring techniques was conducted. The study included:

a) Definition and ranking of six specific vibration monitoring functions as : protection against catastrophic failure, early detection of generic abnormalities, assessment of severity, prediction of fault propagation and time to failure, diagnosis of problem, and feedback control ;

b) The identification and ranking of important fault / failure mode for each test component. Little practical information on realistic fault and failure modes was obtained from the literature survey and the rotating component manufacturers. Engineering evalutations resulted in several potential fault /failure modes to be ranked and investigated;

c) The development and ranking of a list of thirteen candidate processing techniques which had potential monitoring applications under study. The candidate techniques are described in Section 2.2.

A study was completed to define and develop methods of statistical analysis of small sample experiments that were conducted during the Application Study. Methodologies were developed which allowed valid performance comparisons of the candidate algorithms based upon concise definitions of measures of success (e.g. probability of detection, probability of false alarm, and probability of correct classification).

An investigation was conducted to assess the effects of a microgravity environment on the performance of vibration monitoring techniques. Potential gravity effects included: gravitiational preload on bearings induced by the rotor weight applied axially; nonlinearities in bearing and/or foundataion stiffness which can result in slightly different spring constants with and without a weight force applied, and the wetting, spreading and operating characteristics of bearing lubricants. An experimental investigation was defined to address microgravity effects.

A theoretical investigation was conducted to assess the applicability of vibration monitoring techniques to machines of the same type that differ in size, construction detail, and operating characteristics. A dynamic model and a dimensional analysis involving the Strouhal Number were employed during the investigation. A theoretical basis was developed to provide quantitative guidance for selection and interpretation of monitoring techniques to be applied accross a range of machines.

5.2 Application Study

A laboratory demonstrator was developed for the IFD components selected for feasibility testing. A Master Test Plan was delivered to and approved by the NASA Technical Monitor as Tracor Document T86-01-9511-U and was DRL No T-1951, Line Item - 5.

Both baseband and HFD data were taken simultaneously to allow statistically significant comparisons between these processing techniques. The time series data for the experiments were archived on analog tape and on 9-track digital tape. The test data were digitized on a CSPI MAP 300 Array Processor at a sample rate of 8192 samples per second with a resolution of 12 bits. Over 1200 vibration spectra were obtained and are resident in the VAX 11 / 750 NASA database.

Vibration analysis was demonstrated to be an effective means of early detection for a majority of the problems associated with small, high speed machines. The more severe problem types investigated (impeller fault, large imbalance, loss of bearing lubrication, bearing race faults, and elevated inlet temperature) are detectable at very low values of P_{FA} which would allow frequent sampling of numerous machines. The use of reference baselines on individual machines was also shown to significantly increase detectability . Tables 3.5 and 3.6 illustrated the problem types investigated during the feasibility testing while Tables 3.7 and 3.8 describe the general test results and analysis techniques employed.

The ranking of the diverse analysis algorithms was accomplished by utilizing the values of P_D at a fixed value of P_{FA} of 0.1 as was shown in Table 3.9. The vibration technique which has the most potential is the weighted sum of the baseband power spectrum. This technique is generic in approach but can be systematically matched to individual problems. Other conclusions that can be drawn are:

1) Processing of HFD was of marginal value for problem types other than bearing race faults. A clustering algorithm to detect harmonics combined with HFD during the analysis of the results of the fan outer race fault tests increased the value of P_D to 0.99 versus 0.90 for baseband analysis . Attempts to select "optimum" bandpass center frequencies appeared to have little effect.

2) Cepstrum analysis provided no significant problem detection for the problem types investigated in this study.

3) Likelihood ratio processing of the time series in the full analysis bandwidth provided no significant increased detection capability over spectrum analysis. This technique should be superior to most amplitude statistical processing including kurtosis and peak detection.

An effective classification capability for some problem types was demonstrated even though a primary focus of the study was problem detection. The classification capability was pursued during the study since actual machinery monitoring applications requiring level of severity assessment and time to failure predictions would require the correct fault to be diagnosed out of a set of multiple faults possibilities. The classification processor that was developed utilized the

weighted sums. It is important to note that the weighted sum processing is not specifically designed for pattern classification and that further development of alternate algorithms could be used to significantly improve classification performance. The classification analysis also demonstrated the importance of identifying the most relavent and probable fault types as candidates for classification processing.

The validity of applying a given monitoring technique to different machines was demonstrated in the laboratory for two fans of the same type, but differing approximately by 51% in mass. Imbalances were induced in each fan by attaching three different Strouhal-scaled metal weights at length-scaled positions on the impeller hubs. Mean square response of an accelerometer attached to the housing of the large fan was compared to predicitions incorporating theoretical corrections for off-scale parameter values. Predictions agreed with measurements to within less than 1 dB for the three imbalance conditions.

Gravitational effects on axial preload were observed by comparing response spectra of the production-model TRW fan with the shaft axis horizontal and vertical. The production unit used in the experiment did not have axial preload. The HFD acceleration levels measured with the rotation axis horizontal exceeded those with the shaft vertical by approximately 30 dB. This result was attributable to the stabilizing effect of preloading contributed by the rotor weight in a vertical orientation. Shims added to provide a slight axial preload in order to achieve repeatability were found to remove this observed gravity effect. The baseband results were relatively insensitive to orientation with or without preload.

5.3 Preliminary Monitoring System Design and Implementation Plan

A preliminary monitoring system and implementation plan was developed which demonstrated the feasibility of an automated vibration monitoring system (VMS) onboard the advanced spacecraft. System component design, incorporation of patterm detection/classification techniques, data base management, and expert system utilization were described which will form the basis of a final VMS. A system architecture and subsystem specifications were detailed.

Important specific design features include:

1. Analog MUX to allow continuous analog monitoring and detailed computer analyses at scheduled intervals of approximately 24 hours,

2. Three level analysis with level zero--continuous monitoring of accelerometer output power in selected bands, level one--periodic analysis of vibration spectra to detect anomalies, and level two--detailed diagnosis of vibration power spectra

3. Processing of both baseband and high frequency demodulated data ,

4. The primary method of detection and diagnosis of vibration data is a weighted sum with weights derived to "optimally" detect specific problem types , and

5. Final processing and analysis with an expert system and database management system to allow automatic generation of specific maintenance recommendations and instructional aids.

5.4 Recommendations

During the course of the IFD Feasibility Study, several different areas were deemed to require further investigation due to their importance to a final VMS onboard advanced spacecraft. These areas will be discussed below along with their recommended future action items:

Standardization of Machines

It is recommended that a conceptual plan for standardization of rotating equipment be developed and presented to key advanced spacecraft personnel. Obtaining an agreement in principle for standardization of spacecraft rotating equipment would result in the enhanced performance of an onboard fault detection system. It is also recommended that an engineering study be undertaken to define the most probable machine group for incorporating the standardization concept.

Fault / Failure Modes

The proper definiton of realistic fault and failure mode information for the advanced spacecraft rotating components is a key area of future investigation. During the course of this study, little information of practical importance was obtained from the component manufacturers or the literature concerning failure modes. As described earlier, the final number of fault / failure mode possibilities incorporated into a classification processor has a direct adverse impact on its performance. It is recommended that realistic accelerated life testing of a standard group of machines be investigated and that a failure mode set be obtained that will represent 99% of all failures.

Testing of Realistic Operation

The majority of the tests performed in the study incorporated the technique of obtaining a set of baseline data from the test components, after which the faulted condition under test was introduced. This method of fault introduction was necessary in the feasibility study. However, in a realistic vibration monitoring system, a machine may operate in a baseline condition for an extended peroid of time before a fault develops. An experimental program should be performed that incorporates :

1. Selected realistic problem types,

2. Experiments designed for obtaining data from a realistic extended baseline , which could include continuous operation over several months,

3. Development of non-intrusive, non-interrupting methods of introducing faults,

4. Fault experiments repeated at least ten times, and

5. Computation of P_D, P_{FA} for these experimental results and a comparison of results with more efficient techniques for conducting experiments (e.g. baseline samples each hour and the disassembly of machines to introduce faults).

In a area related to these experiments, it is also recommended that additional fault implementation topics be investigated. A specific program would include:

1. Definition of problem types,

2. Introduction of similar faults with slight variations (e.g. alternate imbalance locations, bearing spall characteristics, impeller chip characteristics, and others), and

3. Characterization of the detection algorithms' sensitivities to the fault implementation procedure and variations

Automated Machinery Diagnostics

The results of the application testing clearly indicated that the analysis technique based on weighted sums of the baseband power spectrum possessed the highest performance potential. This technique should be further developed and applied to a variety of evaluation data sets (sets of data from which the algorithm was not specifically derived). It is recommended that a program be performed that includes:

1. Continued development of the weighted sum approach through the investigation of normalized spectrum, both unit area and noise spectral equalization,

2. Collection of data for training algorithms (data sets that are used to develop the algorithms) and separate data for evaluation, and

3. Demonstration of the performance of the diagnostic techniques.

Advanced Tools for Vibration Power Spectra

In order to enhance an onboard VMS, continued parallel efforts in the development of advanced algorithms and techniques should be performed. As discussed previously, the weighted sums approach performs well in fault detection but is not specifically designed for pattern

classification. Further investigation and development of algorithms based on the joint distribution of frequency cells for baseline and faulted data could be used to improve classification performance. It is recommended that the following areas be investigated:

1. Jump detection algorithms and other temporal pattern recognition algorithms
2. Bayesian classification,
3. Replica correlation, and
4. Computer recognition of patterns not discernable by visual inspection (ratio of tones, simultaneous increases and decreases, and others).

Alternate Data Types

Several data types possess performance potential for satisfying the six vibration monitoring functions. Both baseband and HFD data types were examined during this feasibility study. It is recommended that investigations of the following alternate data types be undertaken:

1. Intensity Analysis,
2. Bispectrum,
3. Process Modeling, and
4. Likelihood ratio processing with training and evaluation data sets.

Microgravity Effects

The observed gravity effect on bearing preload warrants a more extensive theoretical investigation. It is recommended that this additional investigation be directed toward quantifying the performance of vibration monitoring techniques on machines designed for operation in a microgravity environment. Upon completion of the theoretical investigation, a Space Shuttle in-flight test can be designed to validate the performance of selected vibration monitoring techniques in a microgravity environment. A preliminary definition of such an in-flight experiment was developed in the Conceptual Study phase of the effort.

Dimensional Analysis

It is recommended that the analysis of sensitivity to off-scale parameters be extended to include other types of off-scale conditions. The recommended effort will determine the limits within which the approach is applicable when laboratory test units cannot be precisely Strouhal-scaled. Scaling effects already present due to size, construction and speed differences in candidate machines for advanced spacecraft service should be examined to determine whether refinements to current vibration monitoring techniques are required. It is further recommended that the approach be applied to fault types other than imbalance and measurement types other than mean-square acceleration response at the fundamental rotational frequency.

Expert System

Current expert system implementations for vibration analyses are based on traditional signature analysis, with specific vibration features assumed to be created by specific machinery faults. The weighted sum techniques developed during this study provide processor outputs that indicate problem types. Therefore, a Bayesian estimation approach might be effectively combined with the processor outputs to estimate the most likely problem types and the relative confidence in the diagnosis. Also, the expert system should be extended to provide an assessment of time to failure by combining detailed diagnosis with trend prediction. In summary, the recommended " expert system " development would consist of a hybrid of traditional procedural language processing (Bayesian estimation, trend detection, and others) combined with a rule based data driven system to incorporate operational situation factors such as spare parts, crew schedule, surrounding machinery status, and other problem context information.

REFERENCES

1. R.B. Randall, "Vibration Signature Analysis - Techniques and Instrument Systems," Noise Control and Vibration Reduction (March 1975), 6:3, p. 81.

2. M.S. Darlow and R.H. Badgley, "Applications for Early Detection of Rolling-Element Bearing Failures Using the High-Frequency Resonance Technique," ASME, 75-DET-46.

3. R.B. Randall and others, "Cepstrum Analysis", Technical Review No. 3 (1981), Bruel & Kjaer Instruments, Inc., 185 Forest Street, Marlboro, MA, 01752.

4. G.M. Milner, "Final Report - Development of an Expert System Prototype for Automatic Generation of SMMSO Vibration Monitoring Maintenance Messages," 07 November 1986, Tracor Document No. T86-01-9560-U, Tracor Applied Sciences, Analysis and Applied Research Division, 6500 Tracor Lane, Austin, TX 78725. (Unclassified)

5. G.M. Milner, "Detection of Rolling Element Bearing Damage by Statistical Vibration Analysis Revisited," DRD Report 030-01 (May 9, 1983), Tracor Applied Sciences, Analysis and Applied Research Division, 6500 Tracor Lane, Austin, TX 78725 (Unclassified).

6. S.M. Wu, "Dynamic Data System: A New Modeling Approach", Journal of Engineering for Industry (August 1977), p.709.

7. C.M. Smith, "A Description of the Hardware and Software of the Power Spectral Density Recognition (PSDREC) Continuous On-Line Reactor Surveillance System (California Distribution)," ORNL/TM-8862/VI (October 1983), Oak Ridge National Laboratory, P.O. Box X, Oak Ridge, Tennessee, 37831. (Unclassified)

8. N.L. Owsley and A.H. Quazi, "Performance of Selected Transient Signal Detectors," U.S. Navy Journal of Underwater Acoustics (July 1970), Vol. 20, No. 3, pp. 589-599.

9. S.G. Braun and B.B. Seth, "On the Extraction and Filtering of Signals Acquired from Rotating Machines," Journal of Sound and Vibration (1979), Vol. 65, pp. 37-50.

10. R.B. Coleman and T.H. Hodgson, Center for Sound and Vibration, North Carolina State University, "Single- and Multi- Channel Digital Signal Processing in Impact Machinery Noise Analysis," ASME Design Engineering Division Conference and Exhibit on Mechanical Vibration and Noise, Cincinnati, Ohio, September 10-13, 1985, Report No. 85-DET-156 (September 1985).

11. G.M. Milner and M.C. Black, "Volume I - Technical Discussion, Preliminary Conceptual Study Report for Incipient Fault Detection Study for Environmental Control and Life Support Systems," Tracor Document No. T86-01-9512-U, Contract No. NAS9-17486 (15 February 1986), Tracor Applied Sciences, Inc., 6500 Tracor Lane, Austin, TX 78725.

12. D. Choi, J. Chang, R.O. Stearman and E.J. Powers, "Bispectral Identification of Nonlinear Mode Interactions," Proceedings of the 2nd International Modal Analysis Conference, Orlando, Florida, February 1984, pp. 602-609.

13. D.H. Bell, Bruel and Kjaer, "An Enveloping Technique for Early State Detection and Diagnosis of Faults in Rolling Element Bearings," ASME Design Automation Conference, Cincinnati, Ohio, September 10-13, 1985, pp. 65-69.

14. G.M. Milner and B. Northrup, "Fundamental Rotation Frequency Estimation and Power Spectra Normalization," (10 January 1984), Tracor Applied Sciences, Inc., Analysis and Applied Research Division, 6500 Tracor Lane, Austin, TX 78725. (Unclassified)

APPENDIX A

LIST OF DELIVERABLES AND RELATED REPORTS

Contract Deliverables

1. "Program Plan for Incipient Fault Detection Feasibility Study for Environmental Control and Life Support System"
   DRL No: T - 1951
   Line Item No: 2
   DRD No: MA - 164TE

   Date: October 25, 1985

2. "Master Test Plan for Incipient Fault Detection Study for Environmental Control and Life Support System"
   DRL No: T -1951
   Line Item No: 5
   DRD No: TM - 122TA
   Tracor Document No: T86-01-9511-U

   Date: February 15, 1986

3. Monthly Progress Reports
   DRL No: T -1951
   Line Item No: 1
   DRD No: MA -182T

   Cost and Manpower Charts
   Line Item No: 3
   DRD No: MF -024TA

   Financial Management Report
   Line Item No: 4
   DRD No: MF -004TC

Reporting Dates	Tracor Document No.
1 Oct 85 - 2 Nov 85	T85-01-9531-U-1
2 Nov 85 - 30 Nov 85	T85-01-9534-U-2
30 Nov 85 - 30 Dec 85	T86-01-9505-U-3
30 Dec 85 - 1 Feb 85	T86-01-9513-U-4
1 Feb 85 - 22 Feb 86	T86-01-9513-U-5
22 Feb 85 - 29 Mar 86	T86-01-9513-U-6
29 Mar 86 - 26 Apr 86	T86-01-9513-U-7
26 Apr 86 - 24 May 86	T86-01-9513-U-8
24 May 86 - 28 Jun 86	T86-01-9513-U-9
28 Jun 86 - 26 Jul 86	T86-01-9513-U-10
27 Jul 86 - 23 Aug 86	T86-01-9513-U-11
24 Aug 86 - 27 Sep 86	T86-01-9513-U-12
28 Sep 86 - 25 Oct 86	T86-01-9513-U-13

Related Reports

- VOLUME 1 - TECHNICAL DISCUSSION
  Preliminary Conceptual Study Report for Environmental Control and Life Support Systems, Tracor Document No. T86-01-9512-U

- VOLUME 2 - APPENDICES
  Preliminary Conceptual Study Report for Incipient Fault Detection Study for Environmental Control and Life Support Systems, Tracor Document No. T86-01-9512-U

- FEASIBILITY OF VIBRATION MONITORING OF SMALL ROTATING MACHINES FOR THE ENVIRONMETAL CONTROL AND LIFE SUPPORT SYSTEMS (ECLSS) OF THE NASA SPACE STATION

G. Martin Milner, Mike Black, Mike Hovenga, and
Dr. Paul McClure (Consultant)
Tracor Applied Sciences, Inc.
6500 Tracor Lane
Austin, Texas 78725

Patrice Miller
National Aeronautics and Space Administration
Lyndon B. Johnson Space Center
Houston, Texas 77058

Presented at the 41st Meeting - Mechanical Failure Prevention Group of National Bureau of Standards, Naval Air Test Center, Patuxent River, Maryland, October 28-30, 1986.

APPENDIX B

Microgravity Effects

1.0 INTRODUCTION

A theoretical investigation and supporting laboratory tests were conducted to assess potential microgravity effects on the performance of vibration monitoring techniques. Potential microgravity effects include:

1. Gravitational preload on bearings induced by the rotor weight force applied axially. A secondary critical speed at twice the shaft rate, caused by the gravity-induced tangential component of angular acceleration associated with rotor imbalance for a horizontal rotation axis (Ref. 1).

2. A flat-shaft secondary critical speed at twice the shaft rate, caused by asymmetrical bending stiffness of a horizontal shaft (Refs. 1 & 2).

3. Non-linearties in bearing and/or foundation stiffness which can result in different spring constants with and without a weight force applied.

4. Gravitational effects on wetting, spreading and operating characteristics of bearing lubricants (Refs. 3 & 4).

Potential gravity-induced critical speed effects were examined theoretically for the TRW fan selected as a test unit and found to be negligible (Section 2.0). This conclusion was also confirmed experimentally, as discussed in Section 3.0. Gravitational preload effects were investigated experimentally and found to be

significant, as discussed in Section 3.0. Examination of the effects non-linearities on bearing and mount stiffness and consideration of gravitational effects on wetting, spreading and operating characteristics of bearing lubricants were beyond the scope of the effort.

Conclusions and recommendations are presented in Section 4.0.

2.0 GRAVITY-INDUCED CRITICAL SPEED EFFECTS

The frequency of the primary critical speed due to rotor bending is potentially important in connection with microgravity effects because a gravity can induce a secondary critical speed at one half the primary critical frequency when the shaft is horizontal. This secondary critical speed is absent when the shaft is vertical or in a microgravity environment. The rotor of the TRW fan used as a laboratory demonstration unit was subjected to a detailed bending analysis in order to estimate its primary critical frequency. The predicted primary critical frequency was found to be 18.5 kHz, well above the 200 Hz fundamental rotational frequency. This theoretical result includes the effect of impeller gyroscopic torque which provides added stiffening. A lower limiting value of 5.8 kHz for the primary critical speed was estimated by omitting gyroscopic stiffening from the analysis. The implication is that a secondary critical speed induced by gravity would be at a minimum frequency of 5.8kHz/2=2.9kHz, which is still well above the 200 Hz fundamental.

Even though the unit is designed to operate well below its primary critical speed, it may be that one of the higher-order harmonics of the fundamental is located at or near the secondary critical speed. An order-of-magnitude estimate for the amplitude of disturbing force at the secondary-critical speed was made as described in Reference 1. Imbalance causes the rotor center of mass G to be offset from the rotation axis B by an eccentricity e, as shown in Figure 2.1. If the shaft is horizontal, rotor weight W exerts a torque We $\sin\omega t$. This torque accelerates the rotor during half of its period and retards its motion during the other half.

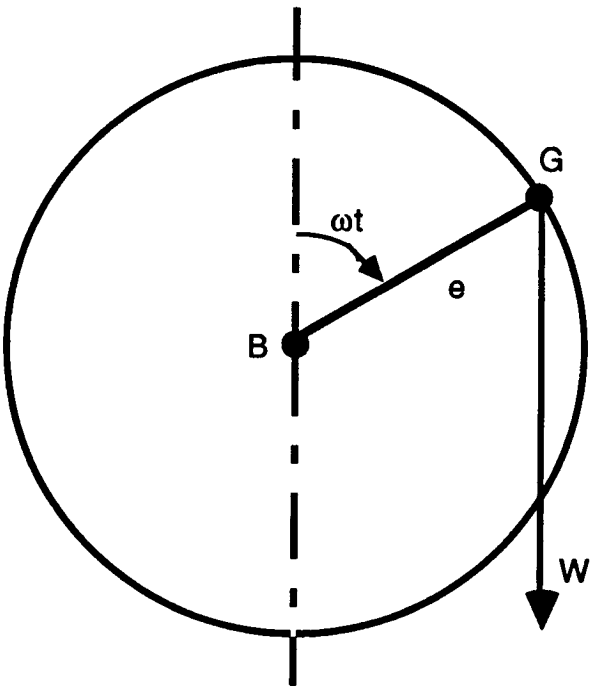

Figure 2.1
Secondary Critical Speed Caused by Unbalance and Gravity

The rotor has a moment of inertia

$$I = m\rho^2 \qquad (1)$$

where m is the mass and ρ is the radius of gyration. The shaft angular acceleration due to the gravity-induced torque is therefore

$$\alpha = \frac{We \sin\omega t}{m\rho^2} \qquad (2)$$

Point G has a tangential component of acceleration

$$a_{Gt} = e\alpha = \frac{We^2 \sin\omega t}{m\rho^2} \qquad (3)$$

which corresponds to an effective force acting on G of

$$ma_{Gt} = \frac{We^2 \sin\omega t}{\rho^2} \qquad (4)$$

The vertical component of this force is

$$ma_{Gt}\sin\omega t = \frac{We^2 \sin^2\omega t}{\rho^2} \qquad (5)$$

$$= \text{constant} - \frac{We^2}{2\rho^2}\cos 2\omega t$$

The time varying part has frequency 2ω, i.e., twice the shaft rotational frequency, and amplitude $We^2 / 2\rho^2$.

If the shaft is running at half its primary critical speed, the excitation described by Equation (5) occurs exactly at the primary critical frequency. This can excite a vibration whose level depends upon the damping present and the magnitude of the excitation.

The ratio of the secondary-critical excitation amplitude, $We^2 / 2\rho^2$, to the excitation amplitude $m\omega^2 e$ at the primary critical is

$$\frac{We^2}{2\rho^2 m\omega^2 e} = \frac{g}{2\omega^2 e}\left(\frac{e}{\rho}\right)^2 \qquad (6)$$

For the TRW fan impeller with an imbalance mass attached;

$$e = 0.0053 \text{ in} \quad (7)$$

$$\rho = 0.5854 \text{ in} \quad (8)$$

$$\omega = (2\pi)\ 200 \text{ Hz} \quad (9)$$

These correspond to

$$\frac{g}{2\omega^2 e}\left(\frac{e}{\rho}\right)^2 = 2 \times 10^{-6} \quad (10)$$

i.e., excitation due to the gravity-induced effect is six orders of magnitude below that at the primary critical. The induced eccentricity of e = 0.0053, is five to ten times the level normally encountered and therefore represents a severely imbalance rotor.

This theoretical result implies that secondary critical speed effects induced by gravity are negligible for small high-speed fans.

3.0 EXPERIMENTAL INVESTIGATION OF GRAVITY EFFECTS

The TRW fan with a severely imbalanced impeller was operated with the rotation axis horizontal and vertical in order to detect any effect caused by a gravity-induced tangential component of angular acceleration, but no discernable effect was identified. This observation confirms the theoretical prediction described in Section 2.0.

Gravitational effects on axial preload were observed by comparing response spectra with the shaft axis horizontal and vertical. The production-model TRW fan used in the experiment has no axial preload. The HFD acceleration levels measured with the rotation axis horizontal exceeded those with the shaft vertical by about 30 dB. This result is attributable to the stabilizing effect of preloading contributed by the rotor weight in a vertical orientation. Shims added to provide a slight axial preload to achieve repeatability were found to remove this observed gravity effect. The baseband results were relatively insensitive to orientation with or without preload.

4.0 CONCLUSIONS AND RECOMMENDATIONS

Conclusions are that

- Gravity effects on preload are critical to the performance of vibration monitoring techniques, and

- Other gravity effects could become important, depending upon machine design, operating characteristics and mounting.

It is recommended that the effects of gravitational preload on vibration monitoring system (VMS) performance be quantified theoretically and correlated with more extensive measurements. Machine design features, (e.g., hydrostatic, sleeve & rolling element bearing designs), operating characteristics and mounting conditions should be examined theoretically and experimentally to assess potential gravity effects on VMS performance.

References

1. J.P. Dan Hartog, "Mechanical Vibrations" Fourth Ed., McGraw-Hill, 1956, pg. 248.

2. N.F. Rieger, "Vibration of Rotating Machinery Part 1, Rotor Bearing Dynamics", The Vibration Institute, Clarendon Hills, Ill., 4th Ed., 1984, pg. 157.

3. C.H.T. Pan, A.F. Whitaker and R.L. Gauses, "Wetting, Spreading and Operating Characteristics of Bearing Lubricants in a Zero-Gravity Environment", in Spacelab Mission 1 Experiment Descriptions - 2nd Ed., NASA TM 82448, November, 1981, pg. III-17.

4. J.T. Hudson, "Design Criteria for Spacecraft Third Mechanical Systems", Presented at National Aeronautics and Space Engineering and Manufacturing Meeting, Los Angeles, CA., Oct 5-9, 1970, SAE Publication No. 700781.

Appendix C

Dissimilar Machine Effects on Applicability of Vibration Monitoring Techniques

TABLE OF CONTENTS

LIST OF ILLUSTRATIONS

LIST OF ILLUSTRATIONS

LIST OF TABLES

1.0 INTRODUCTION

Machinery vibration monitoring typically requires application of a particular fault detection technique to different machines of the same basic type that differ in size, construction detail, mount characteristics and operating speed. It is natural to ask if theory, validated by laboratory tests, can provide quantitative guidance for selection and interpretation of vibration monitoring techniques intended for application to such a group of dissimilar machines.

A valid assessment of vibration monitoring techniques requires investigation of enough baseline and faulted cases to support statistical comparisons. However, it is generally neither possible nor cost effective to obtain enough samples for statistically meaningful comparisons using actual machines, under controlled conditions. The following questions arise:

- Can valid conclusions about the applicability of vibration monitoring techniques to actual machines be derived from laboratory tests performed with scale models?
- What are the effects of size, construction differences and operating speed?
- What scaling laws apply?
- What parameters must be scaled?
- Can valid corrections for off-scale conditions be developed?

Successful resolution of these issues for a given fault type makes possible the approach shown in Figure 1.

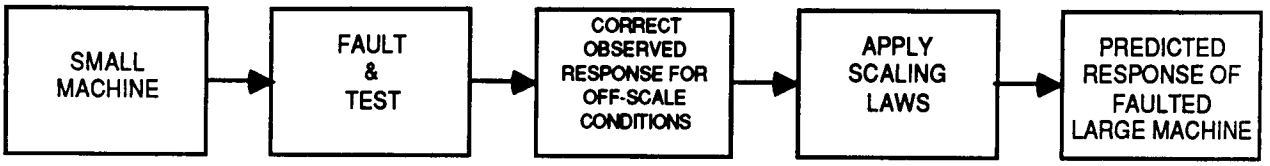

Figure 1
Approach for Predicting Response of Faulted Large Machine

Imbalance in a fan impeller was selected as an important, but readily implemented fault type to demonstrate the validity of applying a specific monitoring technique, amplitude change at the fundamental rotational frequency, to two fans of similar construction but differing by about 51% in mass. The laboratory test units are described in Section 2.0.

Two complementary analyses were performed to address the questions outlined above; a dynamic modeling analysis representing the specific fault type and a dimensional analysis incorporating the dynamic similarity requirement that ratios of dominant forces be the same for the actual machine and the laboratory model. These analyses are presented in Sections 3.0 and 4.0.

The method used to develop a correction for off-scale conditions is outlined in Section 5.0. Results, conclusions and recommendations for future work are presented in Section 6.0.

2.0 LABORATORY DEMONSTRATION UNITS

The two fans selected as laboratory demonstration units approximately satisfy scaling criteria, developed in Section 4.0, which relate size, weight and operating speed according to

$$\text{Speed} \sim (\text{Size})^{-1}, \quad (1)$$

and

$$\text{Weight} \sim (\text{Size})^{3} \quad (2)$$

The large and small demonstration units were ETRI Models 113XN and 126LF respectively (Figure 2). The small fan is similar in construction to the large fan, but not an exact replica. Nominal performance data supplied by the manufacturer are given in Table 1, taken from Reference 1.

Table 1
Nominal Performance of Demonstration Units

Model Number	Volt. (V)	Freq. (Hz)	Speed (RPM)	Maximum Del.		Locked Rotor Current (MA)	Weight		Free Air Performance (CFM)
				Power Input (watts)	Line Current (MA)		Kg.	Oz.	
Large Fan 113XN-0182	115	50/60	2850/3300	12/11	165/135	270/220	0.615	21.6	45/53
Small Fan 126LF-0182	115	50/60	2700/3200	10/8	130/100	170/140	0.400	14.0	28/32

Internal construction representative of both fans is shown schematically in Figure 3. A one eighth inch diameter steel shaft carrying the rotor is cantilevered off the housing of each fan. Preload is achieved by identical spring and spacer assemblies (not shown) installed between the bearings. R H and C denote centers of mass of the rotor, housing and assembled fan, respectively. I is the location of an imbalance mass added to simulate the fault. A is the accelerometer location.

LARGE FAN
ETRI Model 113XN

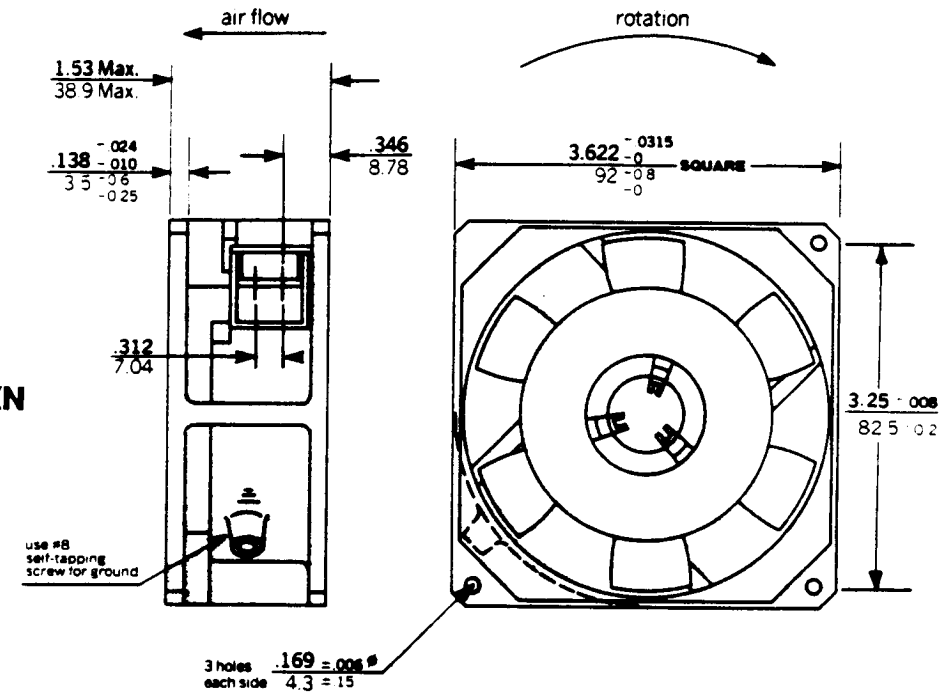

SMALL FAN
ETRI Model 126LF

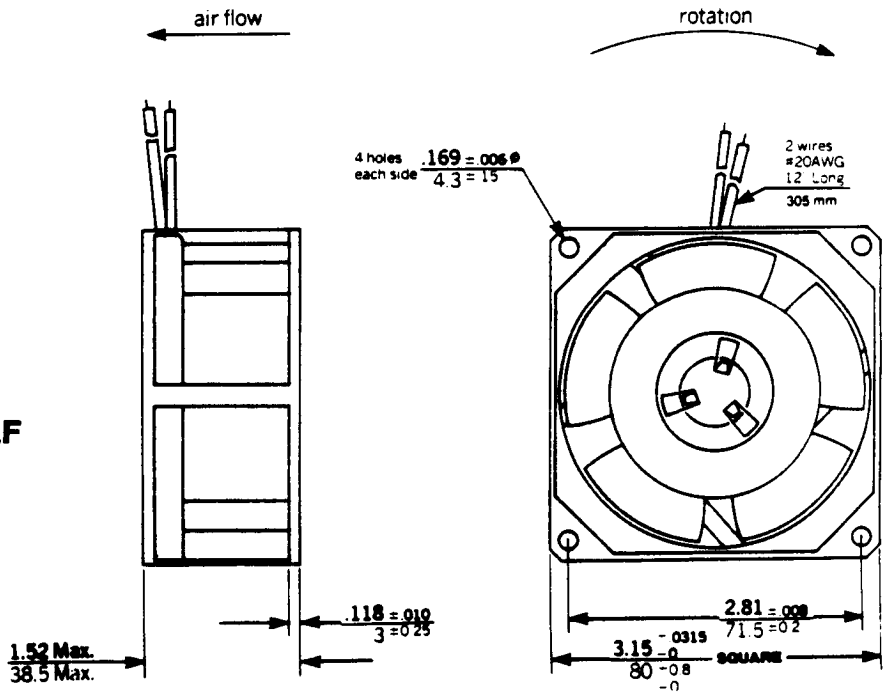

Figure 2
Laboratory Demonstration Units

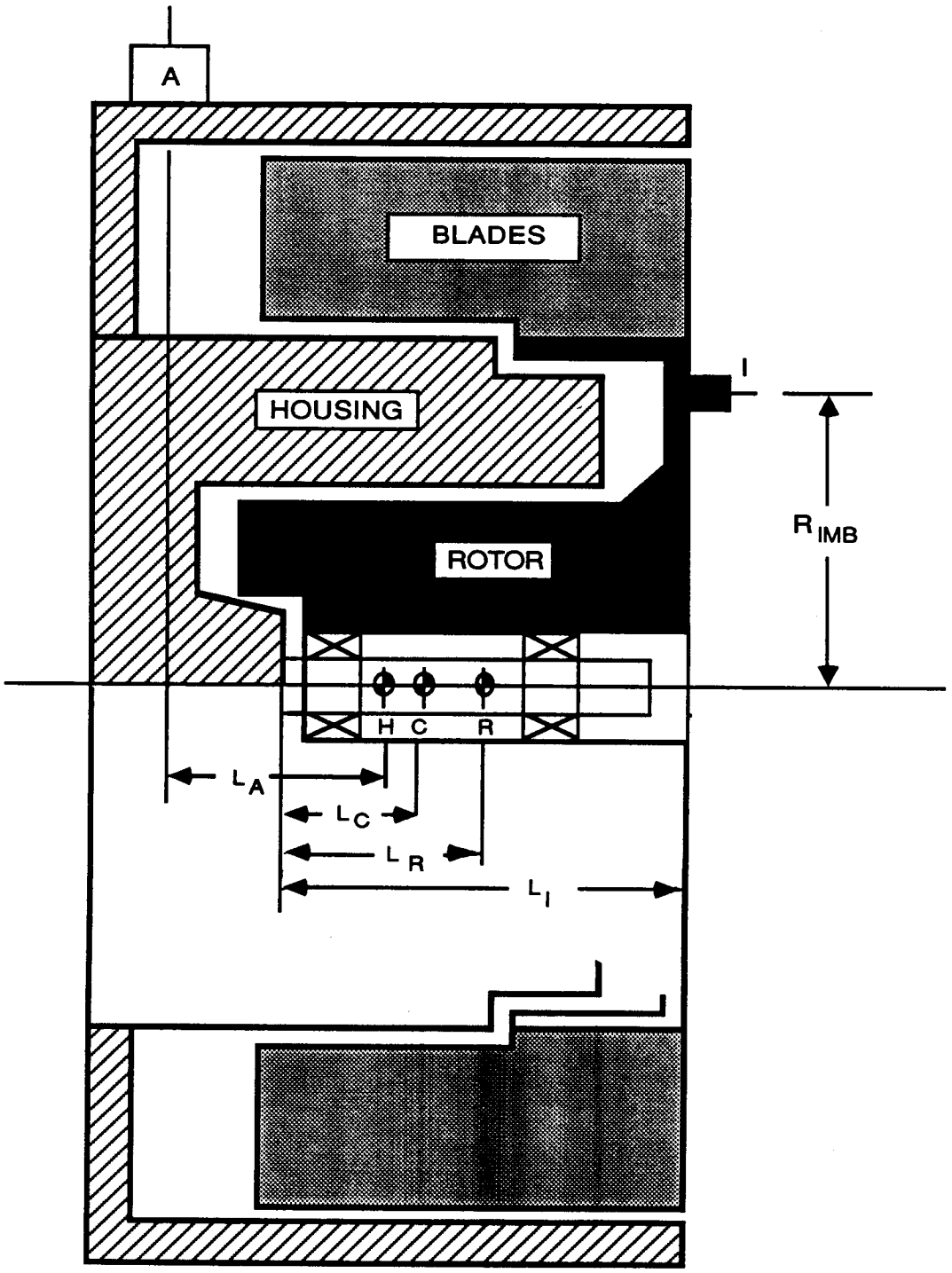

Figure 3
Schematic Showing Internal Construction of Demonstration Units

Both fans were equipped with identical sets of ABEC-3 double-shielded ball bearings. Nominal bearing parameters are shown in Figure 4.

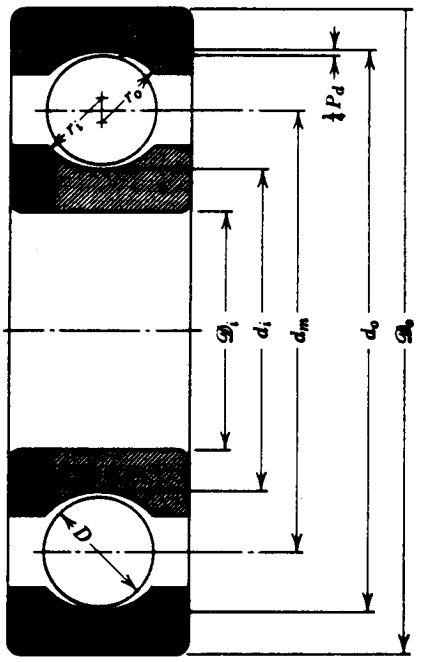

$D = 0.0620"$

$r_o = 0.0341"$

$r_i = 0.0341"$

$D_i = 0.1250"$

$d_i = 0.1560"$

$d_m = 0.2180"$

$d_o = 0.2800"$

$D_o = 0.3115"$

$P_d = 0$

Number of Balls = 6

Figure 4
Nominal Bearing Parameters

The fans were mounted on a cruciform arrangement of three-sixteenths inch I.D. surgical tubing (Figure 5). Shafts were horizontal. The tubing was attached to stiff wire brackets extending from the corners of the fan housing. This arrangement was chosen to provide a low mount resonance in vertical oscillation (~ 2 Hz) as compared with the fundamental shaft rotation frequency (50-60 Hz). Torsional restoring torque is provided by deflection of the mounts when the fan housing experiences a small angular deflection ψ_H about a transverse horizontal axis. Mount

vertical and torsional stiffness are scaled by adjusting the initial unstretched tubing lengths.

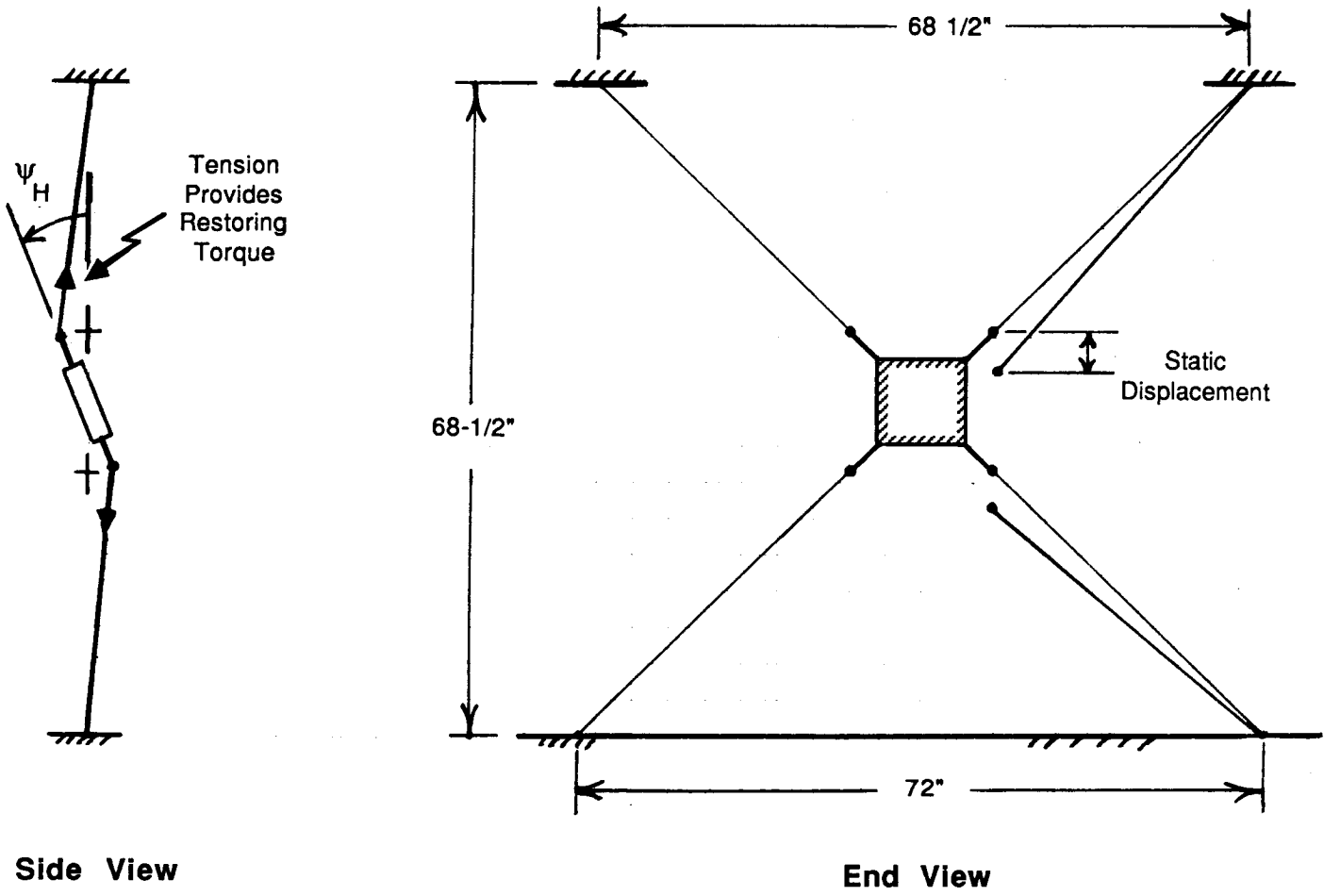

Figure 5
Mount Geometry

3.0 DYNAMIC MODEL

A dynamic model is required to quantify the input/output mechanics associated with a specific fault type. For an imbalanced rotor, the relevant parameters are inertial properties of the rotating and non-rotating components, mount and bearing stiffnesses, the imbalance mass and its location. Once validated by laboratory tests, the dynamic model facilitates quantitative corrections for parameter differences between machines.

A free-body diagram of the assembled fan is shown in Figure 6. The model incorporates three degrees of freedom; vertical housing translation y_H, housing rotation ψ_H about a transverse horizontal axis, and rotor rotation ψ_R about a horizontal transverse axis. Rotation about a vertical transverse axis is ignored because it is decoupled from the three degrees of freedom described above and produces no accelerometer response at the selected location A. Mount vertical restoring force $k_V y_C$ acts through the point C, which denotes the axial location of the assembled fan's center of mass.

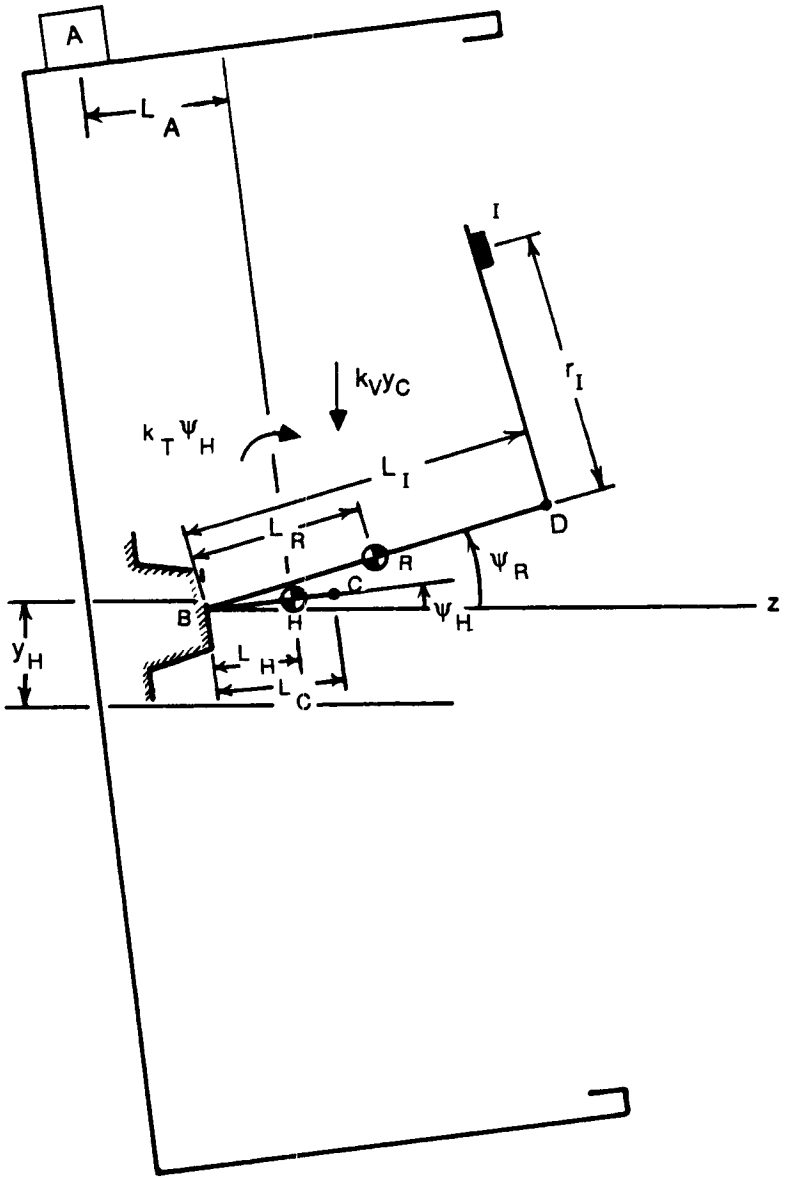

Figure 6
Free Body Diagram of Assembled Fan

The housing free-body diagram is shown in Figure 7. The rotor transmits a vertical component F_R and couple $T_R = k_R (\psi_R - \psi_H)$ about a transverse horizontal axis. F_R and T_R are applied to the housing at the base B of the shaft. Torsional stiffness k_R is a lumped parameter representing the combined effects of bearing support shaft flexure, bearing stiffness associated with Hertzian stresses at the ball-raceway contact points, and any additional flexure associated with relative angular displacement between the rotor and the housing.

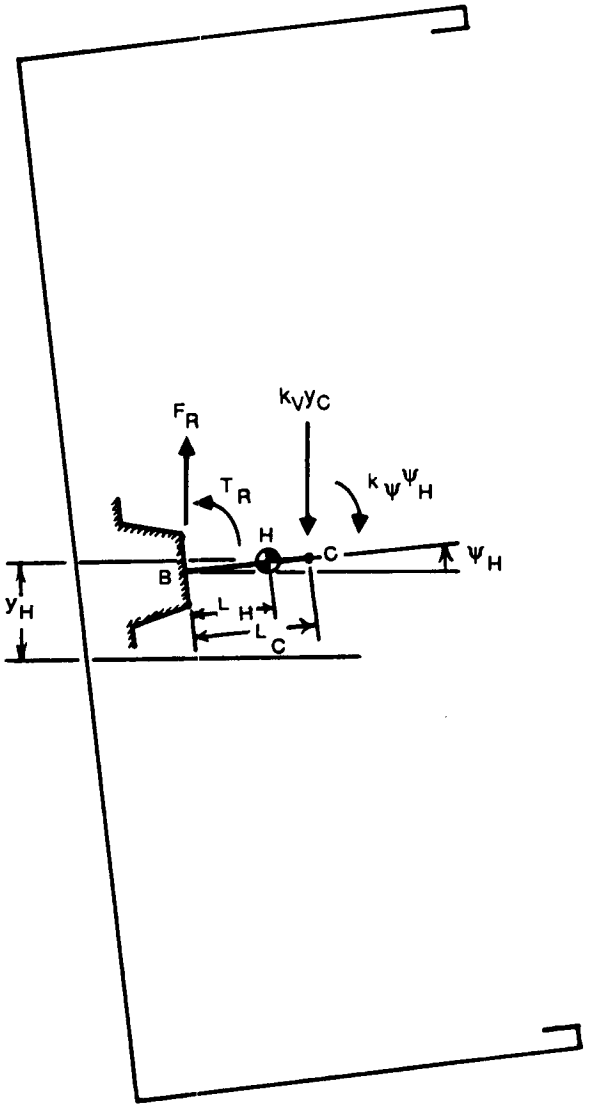

Figure 7
Housing Free-Body Diagram

Housing vertical translation y_H and housing angular deflection ψ_H about a transverse horizontal axis through H are governed by

$$m_H \ddot{y}_H + k_V y_C - F_R = 0 \qquad (3)$$

and

$$I_{TH} \ddot{\psi}_H + k_T \psi_H - T_R + k_V y_C (L_C - L_H) + F_R L_H = 0 \qquad (4)$$

The rotor free body diagram is shown in Figure 8. The gyroscopic couple $I_{PR}\omega\upsilon\psi_R$ is proportional to both the rotor rotation rate ω and the rotor whirl rate υ (References 2 & 3). I_{PR} is the rotor polar moment of inertia. The whirl angle υt is related to the rotor vertical and horizontal angular deflections ψ_R and θ_R as shown in Figure 9. The z axis is horizontal and corresponds to zero angular deflection of the rotor. The x axis is a transverse horizontal axis and the Y axis is vertical.

The gyroscopic couple provides added stiffness when υ has the same sign as ω, i.e., for a forward whirl, and reduced stiffness for a reverse whirl (Ref. 2, p. 258). The whirl rate υ is equal to ω for forced motion due to an imbalanced rotor, but must be left independent when solving for the system natural frequencies.

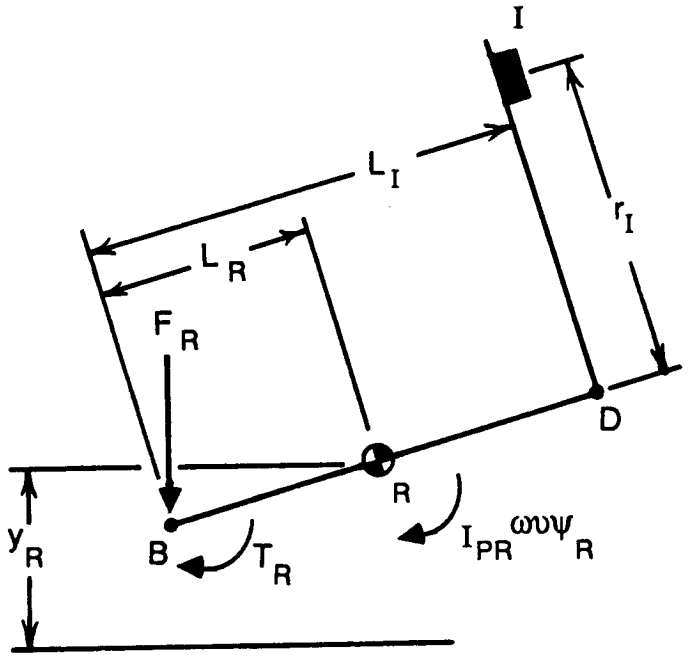

Figure 8
Rotor Free-Body Diagram

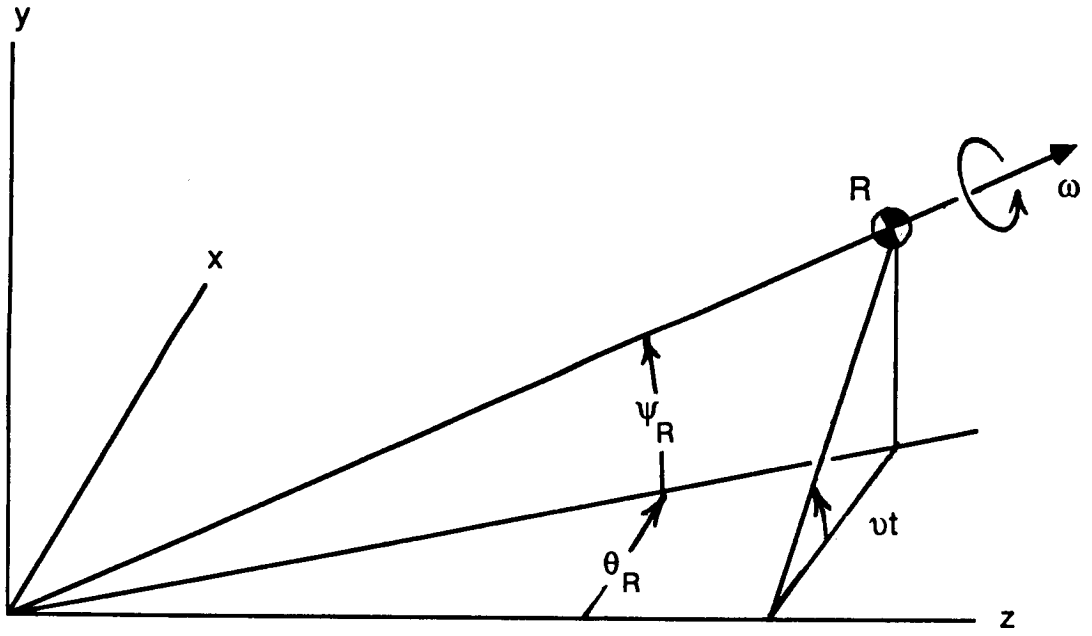

Figure 9
Geometry Defining Rotor Whirl Angle

Rotor vertical translation y_R and rotor angular deflection ψ_R about a transverse horizontal axis through R are governed by

$$m_R \ddot{y}_R + F_R + m_I \ddot{y}_I = 0 \qquad (5)$$

and

$$I_{TR} \ddot{\psi}_R + I_{PR} \omega \upsilon \psi_R + T_R - F_R L_R + m_I \ddot{y}_I (L_I - L_R) = 0 \qquad (6)$$

Kinematical constraints relating the rotor center of mass vertical displacement y_R, the imbalance mass vertical displacement y_I and the vertical mount displacement y_C of the restoring force application point are apparent from the geometry in a plane normal to the rotation axis (Figure 10). These constraints (valid for small angles) are

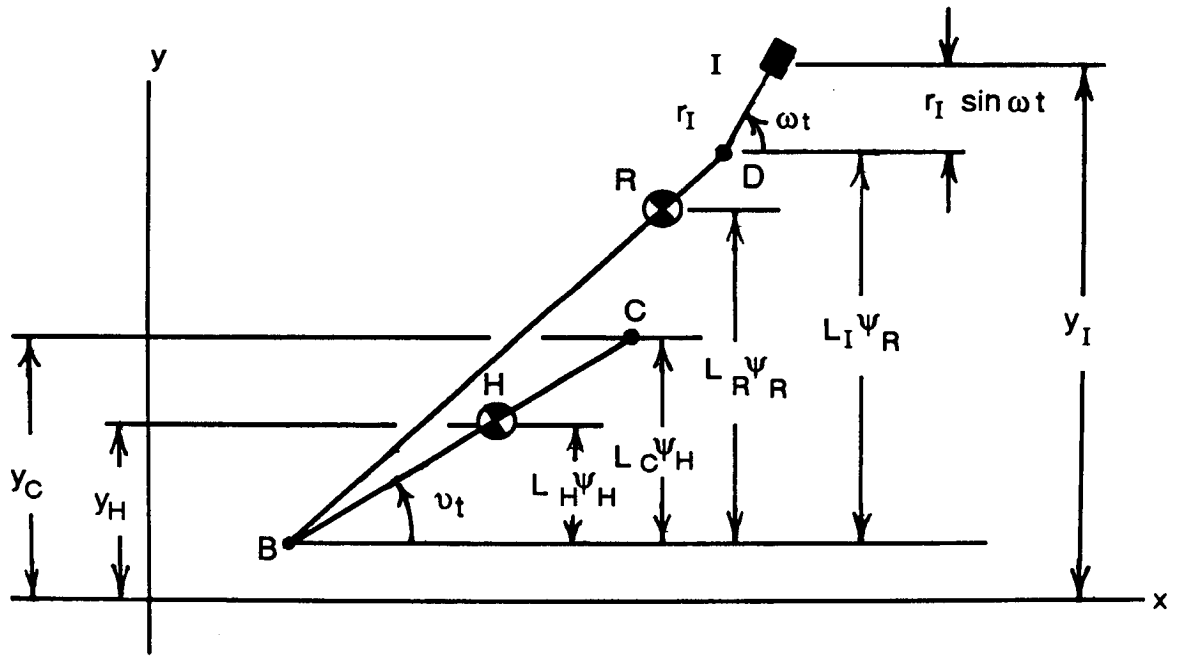

Figure 10
Geometry In A Plane Normal To The Rotation Axis

$$y_R = y_H - L_H \psi_H + L_R \psi_R \tag{7}$$

$$y_I = y_H - L_H \psi_H + L_I \psi_R + r_I \sin\omega t \tag{8}$$

$$y_C = y_H + (L_C - L_H) \psi_H \tag{9}$$

Equations (3) - (9) reduce to the three degree of freedom system represented in matrix form as equation (10). Extensive inertial and stiffness coupling exists for the selected displacement coordinates. The imbalance terms appear as sinusoidal forcing functions.

$$\begin{bmatrix} (m_H + m_R + m_I) & -(m_R + m_I) L_H & (m_R L_R + m_I L_I) \\ -(m_R + m_I) L_H & [I_{TH} + (m_R + m_I) L_H^2] & -(m_R L_R + m_I L_I) L_H \\ (m_R L_R + m_I L_I) & -(m_R L_R + m_I L_I) L_H & [I_{TR} + m_R L_R^2 + m_I L_I^2] \end{bmatrix} \begin{bmatrix} \ddot{y}_H \\ \ddot{\psi}_H \\ \ddot{\psi}_R \end{bmatrix}$$

$$+ \begin{bmatrix} k_v & k_v (L_C - L_H) & O \\ k_v (L_C - L_H) & [k_v (L_C - L_H)^2 k_\psi + k_R] & -k_R \\ O & -k_R & (k_R + I_{PR} \omega\upsilon) \end{bmatrix} \begin{bmatrix} y_H \\ \psi_H \\ \psi_R \end{bmatrix}$$

$$= \begin{bmatrix} m_I r_I \omega^2 \sin\omega t \\ - m_I r_I \omega^2 L_H \sin\omega t \\ m_I r_I \omega^2 L_I \sin\omega t \end{bmatrix} \tag{10}$$

The three critical whirl frequencies υ_i, i = 1,2,3 are found by solving the homogeneous system

$$\ddot{MX} + K(\upsilon)X = 0 \tag{11}$$

where M and K(υ) represent the mass and stiffness matrices displayed in equation (10) and

$$X = \begin{bmatrix} x_1 \\ x_2 \\ x_3 \end{bmatrix} = \begin{bmatrix} y_H \\ \psi_H \\ \psi_R \end{bmatrix} \tag{12}$$

Frequency dependence in the stiffness matrix caused by the gyroscopic coupling is indicated explicitly by the notation K(υ). The eigenvectors have the form

$$X_i = X_{Mi} \sin(\upsilon_i t + \phi_i) = \begin{bmatrix} x_{M1i} \\ x_{M2i} \\ x_{M3i} \end{bmatrix} \sin(\upsilon_i t + \phi_i) \tag{13}$$

and the modal matrix is

$$X_M = \begin{bmatrix} x_{M11} & x_{M12} & x_{M13} \\ x_{M21} & x_{M22} & x_{M23} \\ x_{M31} & x_{M32} & x_{M33} \end{bmatrix} \tag{14}$$

The eigenvalue problem,

$$[\,-M\upsilon^2 + K(\upsilon)\,]\,X_{Mi} = 0 \qquad (15)$$

leads to the characteristic equation

$$|\,-M\upsilon^2 + K(\upsilon)\,| = 0 \qquad (16)$$

which is sixth order in the whirl frequency υ but linear in the rotor frequency ω.

Parameters used in the critical whirl frequency computations are listed in Table 2. Laboratory measurements were made to determine m_H, m_R, m_I, L_H, L_R, L_I, L_C, I_{TH}, I_{TR} and I_{PR}. The mount vertical and torsional stiffnesses, k_V and k_T were adjusted to the values shown, as discussed in Section 4.0.

The rotor shaft/bearing stiffness k_R was not directly measurable with available laboratory equipment. An upper limiting value of 873 in lbf was derived based on bending of the cantilevered rotor support shaft. Additional flexibility introduced within the bearings and by rotor/bearing assembly details will significantly reduce k_R, but an extensive theoretical approach to determine these corrections was beyond the scope of the effort. Values of k_R for the large and small fans were determined empirically by performing response tests with the respective large imbalance weights attached and adjusting k_R for each fan to fit observed response at the respective operating frequencies. The values for k_R listed in Table 2 are well below the theoretical upper limit, as expected.

Table 2
Parameters Selected to Characterize Demonstration Units

Parameter	Symbol	Units	Value	
			Large Fan	Small Fan
Housing mass	m_H	lbm	1.1332	0.7420
Rotor mass	m_R	lbm	0.1961	0.1295
Imbalance mass	m_I	lbm		
Large			5.1191×10^{-3}	3.3819×10^{-3}
Medium			3.0777×10^{-3}	2.0327×10^{-3}
Small			2.0415×10^{-3}	1.3492×10^{-3}
Vertical mount stiffness	k_V	lbf in^{-1}	0.5047	0.4396
Torsional mount stiffness	k_T	lbf in	2.2981×10^{1}	8.3824
Rotor Shaft/Bearing Stiffness	k_R	lbf in	4.817×10^{1}	2.954×10^{1}
Housing Center of Mass Location	L_H	in	0.2576	0.2906
Rotor Center of Mass Location	L_R	in	0.5029	0.5756
Imbalance Mass Axial Location	L_I	in	1.1200	1.1460
Imbalance Mass Radial Location	R_I	in	0.8615	0.7505
Fan Center of Mass Location	L_C	in		
For Large Imbalance			0.2999	0.3371
For Medium Imbalance			0.2986	0.3359
For Small Imbalance			0.2980	0.3352
Accelerometer Axial Location	L_A	in	0.4126	0.4096
Housing Transverse Moment of Inertia	I_{TH}	lbf in sec^2	3.1462×10^{-3}	1.7572×10^{-3}
Rotor Transverse Moment of Inertia	I_{TR}	lbf in sec^2	1.8458×10^{-4}	9.6247×10^{-5}
Rotor Polar Moment of Inertia	I_{PR}	lbf in sec^2	2.5219×10^{-4}	1.2541×10^{-4}
Rotor Frequency	ω	Hz	52.5	60.0

Equation (16) was solved by developing a modified version of the classical iteration method described in Reference 4. The resulting critical whirl

frequencies for the large fan with large imbalance mass, are shown in Figure 11. Critical whirl frequency plots for the small fan and for the medium and small imbalance cases are similar. The critical whirl frequency plot also contains the line $\upsilon = \omega$ (i.e., whirl frequency = rotor frequency) along which the fan must operate when forced by an imbalanced rotor.

The mount resonances at 2 Hz and 13 Hz are associated with vertical bouncing and torsional motion about a transverse horizontal axis respectively. The third, higher-frequency resonance is associated with relative angular displacement between the rotor and the housing. Gyroscopic stiffening causes all of the critical whirl frequencies to increase with rotor frequency. This effect is especially pronounced for the high-frequency resonance.

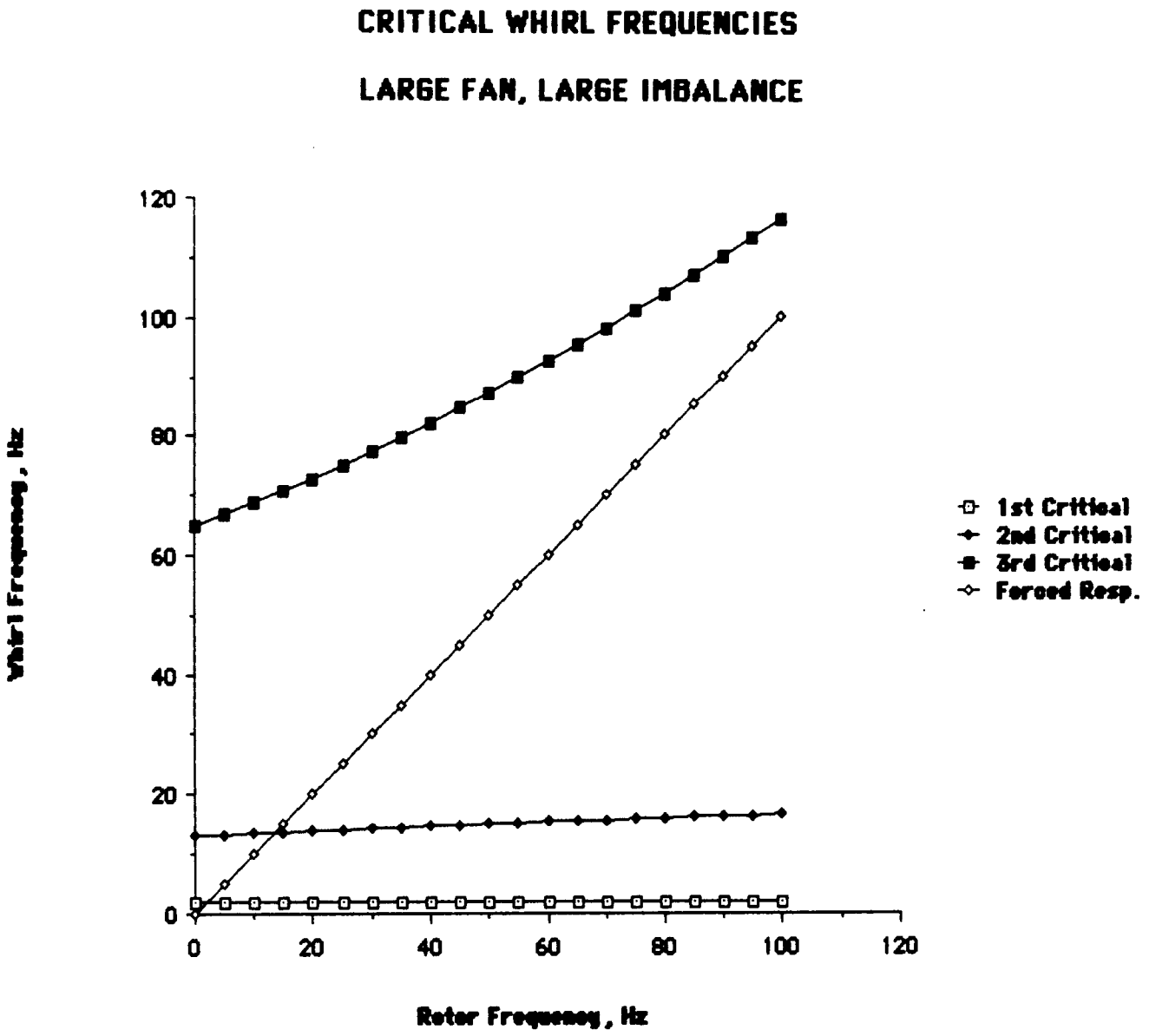

Figure 11
Critical Whirl Frequencies for Large Fan with Large Imbalance

Gyroscopic stiffening introduces modal coupling. Therefore, the forced response must be obtained by direct inversion of the system equation. Equation (10) is written

$$M\ddot{X} + K(\upsilon)\, X = Q \tag{17}$$

where

$$Q = C \sin\omega t \tag{18}$$

and

$$C = \begin{bmatrix} m_I r_I \omega^2 \\ - m_I r_I \omega^2 L_H \\ m_I r_I \omega^2 L_I \end{bmatrix} \tag{19}$$

The forced response is

$$X = B \sin\omega t \tag{20}$$

where

$$B = [-\omega^2 M + K]^{-1} C \tag{21}$$

The acceleration component normal to the housing wall at point A (Figure 6) is

$$a_A = \ddot{y}_H - L_A \ddot{\psi}_H \tag{22}$$

$$a_A = -\omega^2 (B_1 - L_A B_2) \sin\omega t \tag{23}$$

Mean square accelerometer response in dB re 10^{-6}g is given by

$$< \alpha_A^2 >_{dB\ re\ 1\mu g} = 20 \log_{10} \left[\frac{\omega^2 \left| B_1 - L_A B_2 \right|}{\sqrt{2} \times 10^{-6} g} \right] \qquad (24)$$

and plotted vs. rotor frequency in Figures 12 and 13 for the large and small fans respectively with large imbalance. The null at about 17-18 Hz occurs because the numerator of equation (24) vanishes. Its location depends upon the mounting location selected for the accelerometer.

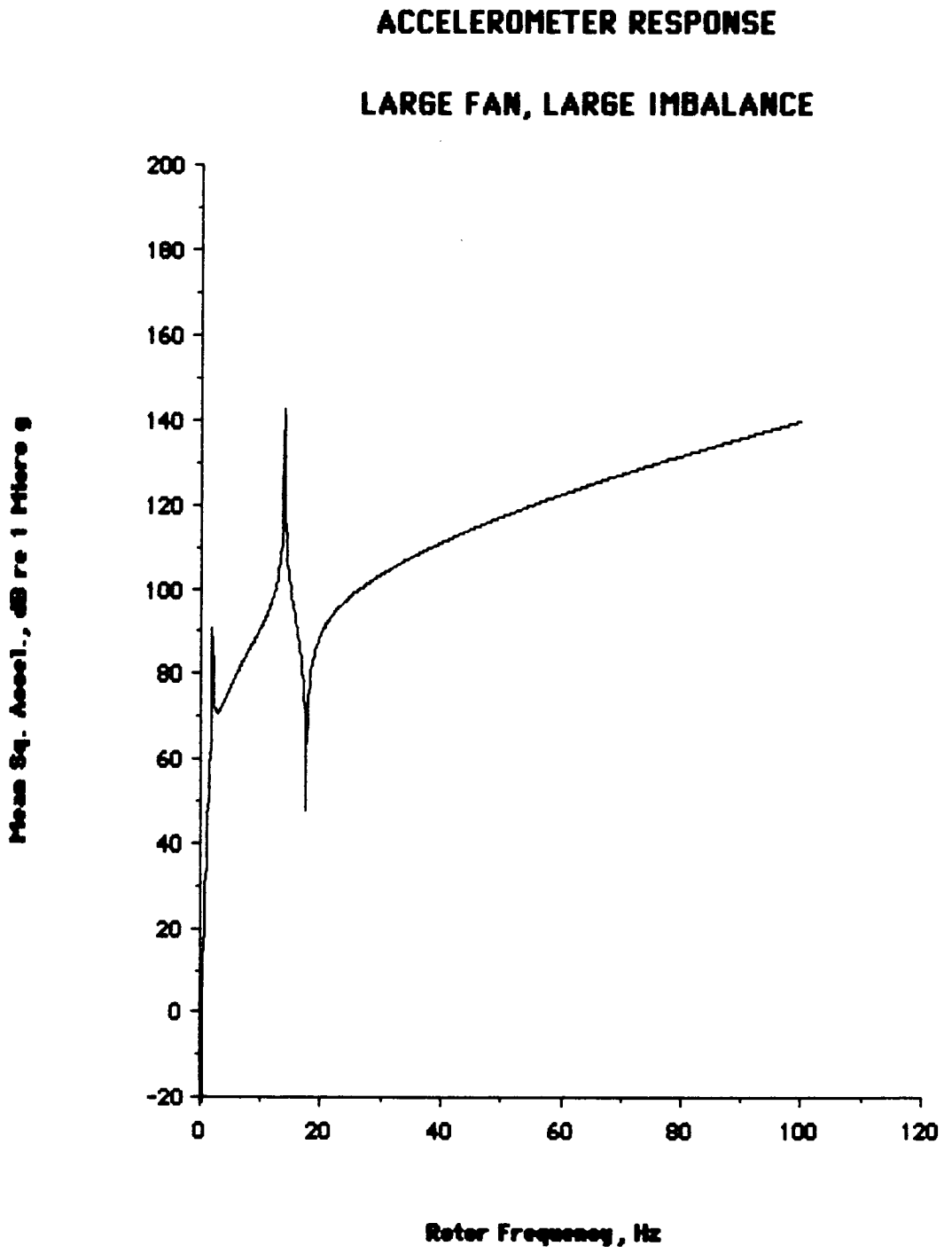

Figure 12
Accelerometer Response for Large Fan with Large Imbalance

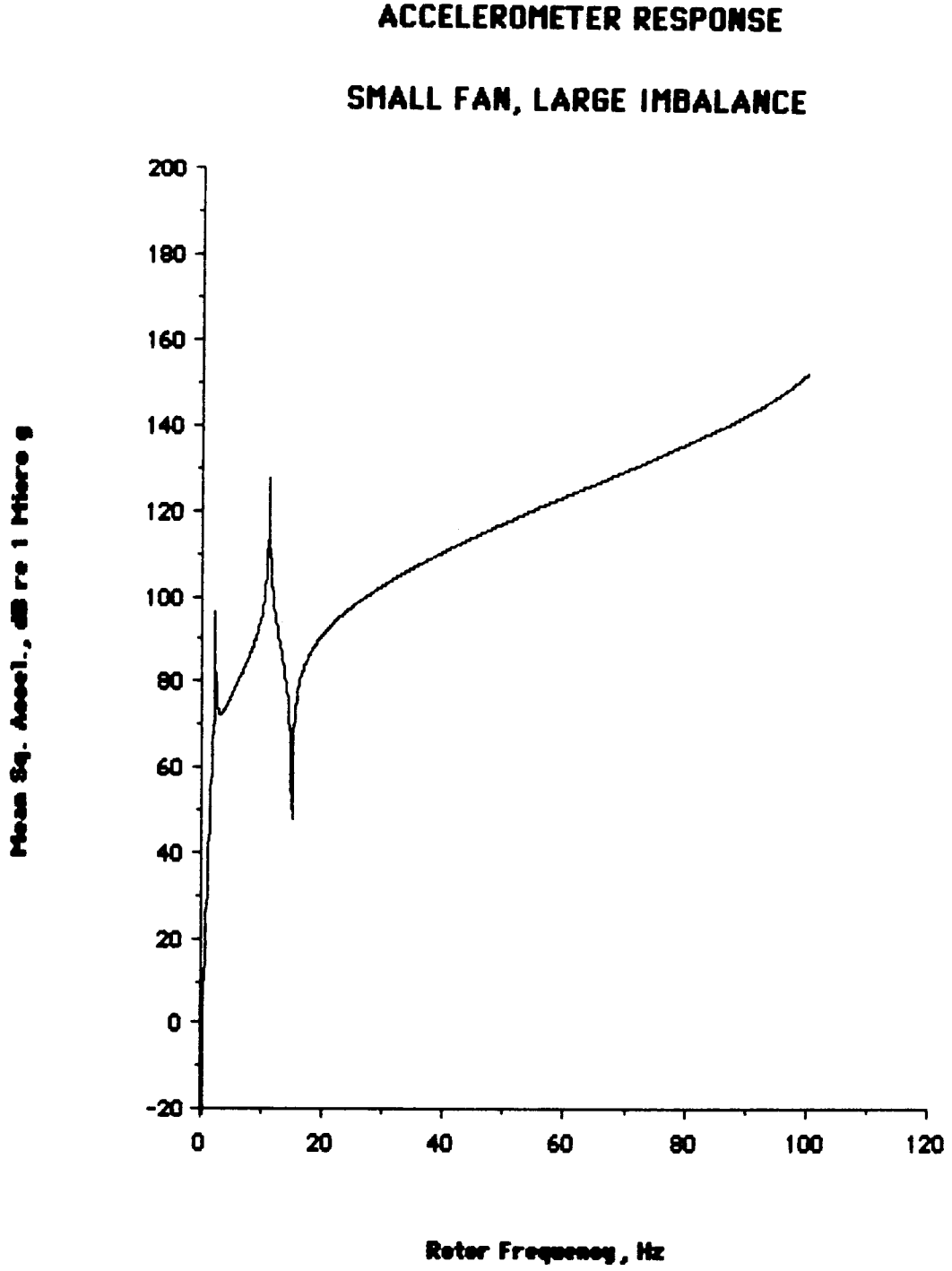

Figure 13
Accelerometer Response for Small Fan with Large Imbalance

4.0 DIMENSIONAL ANALYSIS

Dynamic similarity of machine vibrational response to an induced fault requires that the ratio of vibratory forces (proportional to mass x length x frequency squared; MLF^2) to inertial reactions (proportional to mass x length / time squared; MLT^{-2}) be the same for the small fan as for the large fan. This requires equivalence of the Strouhal Number, (LF/V), where V represents velocity. (Reference 5-8).

Strouhal Number equivalence was achieved by scaling the operating frequency of the small fan up by the same factor with which size is scaled down. Thus, velocities of rotating components at geometrically similar points in the large and small machines are ideally the same.

The types of parameters incorporated into the dynamic model are listed in Table 3 along with their scaling properties as derived from dimensional analysis. Subscripts L and S denote large and small.

Table 3
Dynamic Model Parameters & Scaling Laws

PARAMETER	SYMBOL	SCALING LAWS		
Characteristic Length	L	L_L/L_S	=	s
Frequency	f	f_L/f_S	=	s^{-1}
Velocity	V	V_L/V_S	=	1
Acceleration	A	A_L/A_S	=	s^{-1}
Force	F	F_L/F_S	=	s^2
Mass	M	M_L/M_S	=	s^3
Linear Spring Stiffness	k	k_L/k_S	=	s
Torsional Stiffness	k_{TOR}	k_{TORL}/k_{TORS}	=	s^3
Moment of Inertia	I	I_L/I_S	=	s^5
Quality Factor, Coulomb Damping	Q_C	Q_{CL}/Q_{CS}	=	1
Quality Factor, Viscous Damping	Q_V	Q_{VL}/Q_{VS}	=	s

Quality factors for Coulomb and viscous damping are included in Table 3 for reference, although damping was not included in the dynamic model. It is known that viscous damping does not scale correctly (i.e., Q_{VL} would have to equal Q_{VS} for correct scaling). Therefore, any viscous shear effects present in the small fan are too large by a factor for s. However, Viscous effects are not considered important for machines having rolling element bearings operated without slipping and working fluids with sufficiently high Reynolds Numbers (characterized by negligible boundary layer effects).

Frequency scaling requires (Ref. 8) that spectrum levels be corrected according to

$$(\text{Spectrum Level in dB})_L = 10 \log_{10} s + (\text{Spectrum Level in dB})_S \quad (25)$$

A spectrum level correction Δ_{SL} is therefore defined as

$$\Delta_{SL} = 10 \log_{10} s \quad (26)$$

Since rotor mass is critical to imbalance response, but the rotors could not be readily altered without inducing spurious imbalances, the length scale s was defined so as to make the existing rotor masses scale exactly, ie., $s = (m_{Rotor,L}/m_{Rotor,S})^{1/3} = 1.1482$. Prototype housing mass was adjusted slightly to achieve nearly exact scaling, proportional to s^3. The transverse moment of inertia of the housings and rotors and the polar moments of inertia of the rotors all satisfied the s^5 scaling requirements to within a few percent for the fans selected.

Speeds were scaled by adjusting input line frequency. Mount vertical stiffness was scaled by using different unstretched lengths of tubing for the large and small fans. Mount torsional stiffness k_{ψ}, for rotation about a horizontal axis normal to the rotation axis, could not be correctly scaled without over stressing the tubing material. As a result, mount torsional stiffness for the small fan was too low by about 45%. This was not expected to present a problem because the fans operate well above speeds that would excite mount resonances.

Small, medium and large rotor imbalances were simulated by gluing precisely scaled metal weights at length-scaled positions on each rotor (Figure 14)

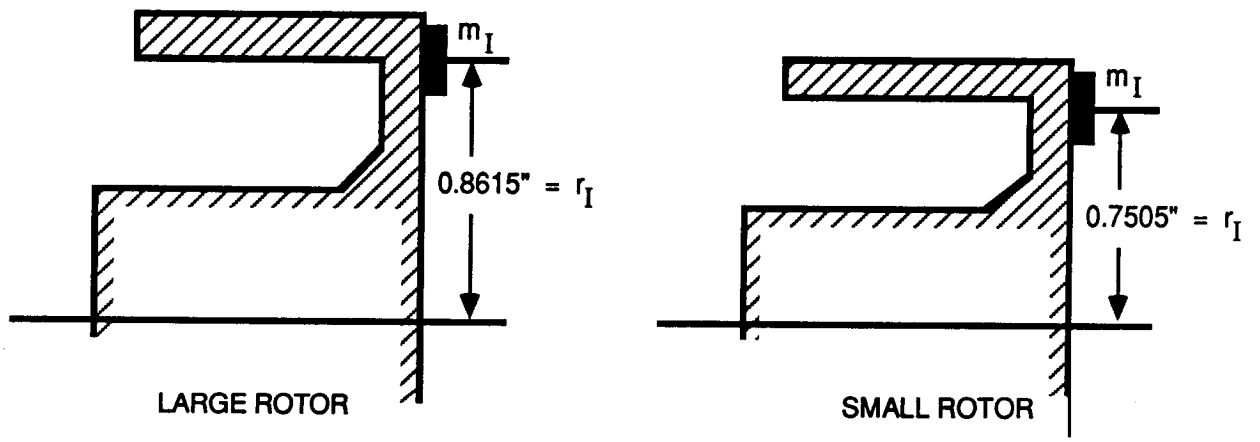

Figure 14
Imbalance Fault Scaling

5.0 CORRECTION FOR OFF-SCALE CONDITIONS

The method used to develop a correction for off-scale conditions is shown in Figure 15. Parameter sets characterizing the large and small fans are determined from manufacturer's data, direct parameter measurements and parameter identification methods as described in Section 3.0. The scaling laws developed in Section 4.0 are applied to the large-fan parameter set to obtain a scaled-fan parameter set. Comparing response predictions made using the scale-fan and small fan paramter sets provides a correction for off-scale conditions.

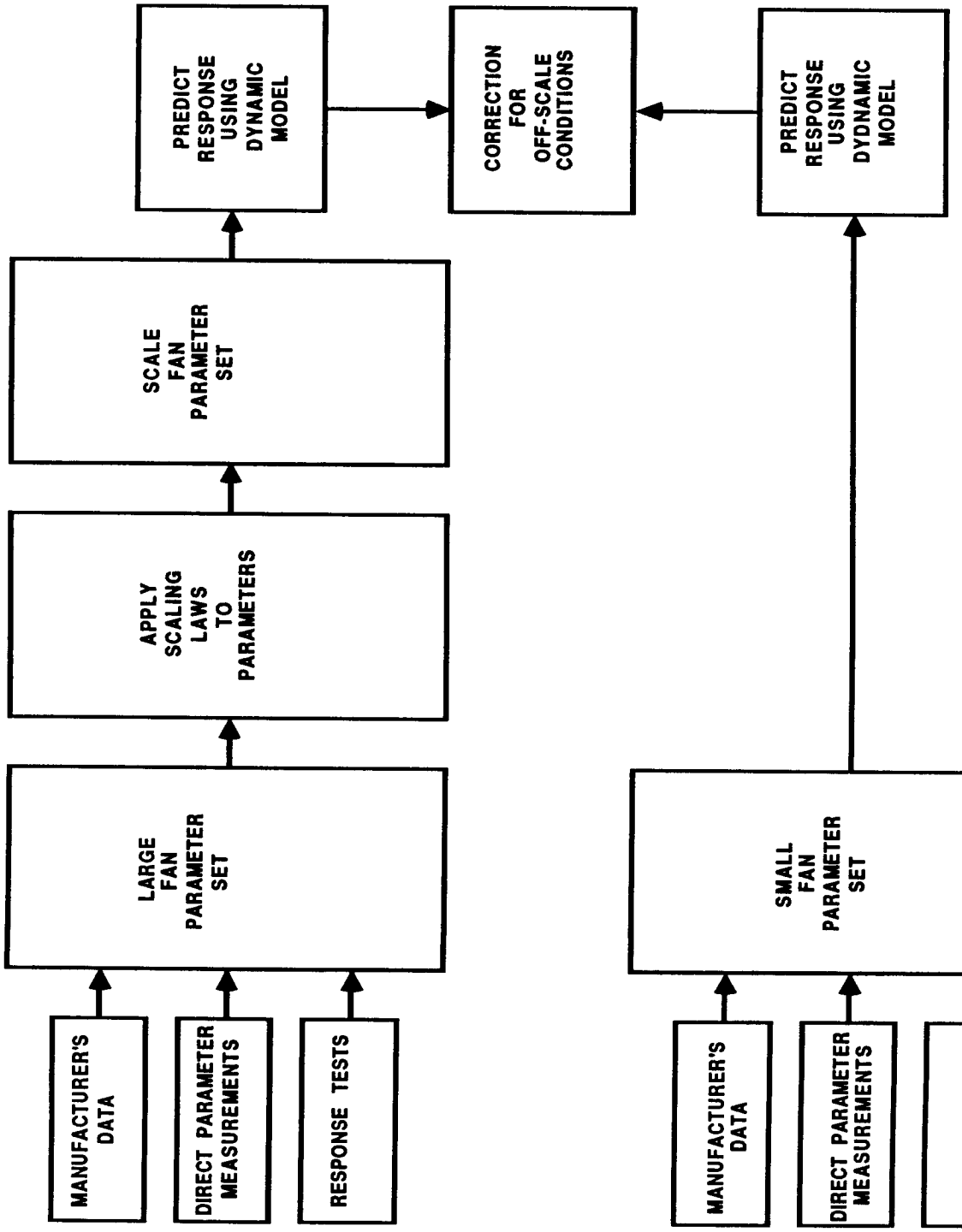

Figure 15
Method to Obtain for Off-Scale Conditions

A scale-fan parameter set derived by applying the scaling laws (Table 3) to the large-fan parameters (Table 2) is shown in Table 4.

Table 4
Scale-Fan Paramater Set

LARGE-FAN PARAMETERS	SCALING LAW (s = 1.1482)	SCALE-FAN PARAMETERS
M_H = 1.1332 lbm	s^{-3}	0.7485 lbm
M_R = 0.1961 lbm	s^{-3}	0.1295 lbm
M_I = 5.1191 x 10 lbm (large imb.)	s^{-3}	3.3814×10^{-3} lbm
= 3.0777 x 10 lbm (medium imb.)	s^{-3}	2.0330×10^{-3} lbm
= 2.0415 x 10 lbm (small imb.)	s^{-3}	1.3485×10^{-3} lbm
k_V = 0.5047 lbf in^{-1}	s^{-1}	0.4395 lbf in^{-1}
k_T = 2.2981×10^{1} lbf in	s^{-3}	1.5180×10^{1} lbf in
k_R = 4.817×10^{1} lbf in	s^{-3}	3.182×10^{1} lbf in
L_H = 0.2576 in	s^{-1}	0.2243 in
L_R = 0.5029 in	s^{-1}	0.4380 in
L_I = 1.1200 in	s^{-1}	0.9754 in
R_I = 0.8615 in		0.7505 in
L_C = 0.2999 in (for large imb.)	s^{-1}	0.2612 in
= 0.2986 in (for medium imb.)	s^{-1}	0.2601 in
= 0.2980 in (for small imb.)	s^{-1}	0.2595 in
L_A = 0.4126 in	s^{-1}	0.3593 in
I_{TH} = 3.1462×10^{-3} lbf in sec^2	s^{-5}	1.5762×10^{-3} lbf in sec^2
I_{TR} = 1.8458×10^{-4} lbf in sec^2	s^{-5}	9.2474×10^{-5} lbf in sec^2
I_{PR} = 2.5219×10^{-4} lbf in sec^2	s^{-5}	1.2635×10^{-4} lbf in sec^2
ω = 52.5 Hz	s	60 Hz

The scaling laws developed in Section 4.0 require application of a spectrum level correction, $\Delta_{SL} = 10 \log_{10} s$, as well as a correction due to the scaling relationship for acceleration (Table 3),

$$a_{AL}/a_{AS} = s^{-1} \tag{27}$$

Equation (27) implies the following relationship for mean square acceleration expressed in dB,

$$\langle a^2_{AL} \rangle_{dB \text{ re } 1\ \mu g} = \langle a^2_{AS} \rangle_{dB \text{ re } 1\ \mu g} - 20 \log_{10} s \tag{28}$$

An acceleration scale correction is defined as

$$\Delta_{AS} = -20 \log_{10} s \tag{29}$$

Figure 16 compares predicted accelerometer response for large imbalance based on the scale-fan parameter set to predicted response for large imbalance based on the small-fan parameter set. The difference, Δ_{OS}, defined as

$$\Delta_{OS} = \underbrace{\left[\langle a^2_A \rangle_{dB \text{ re } 1\mu g} \right]}_{\text{SCALE FAN}} - \underbrace{\left[\langle a^2_A \rangle_{dB \text{ re } 1\mu g} \right]}_{\text{SMALL FAN}} \tag{30}$$

is plotted in Figure 17. Figure 18 shows detailed values of Δ_{OS} near the 60 Hz operating frequency of the small fan. The quantity Δ_{OS} is the level in dB re 1 μg that

must be added to the small-fan response in order to obtain scale-fan response. The correction for off-scale conditions is virtually independent of imbalance mass, provided M_I is small compared to rotor mass M_R and housing mass M_H (Equations 10,19,21 and 24). Therefore, the same correction, Δ_{OS}, can be applied for all three imbalance conditions.

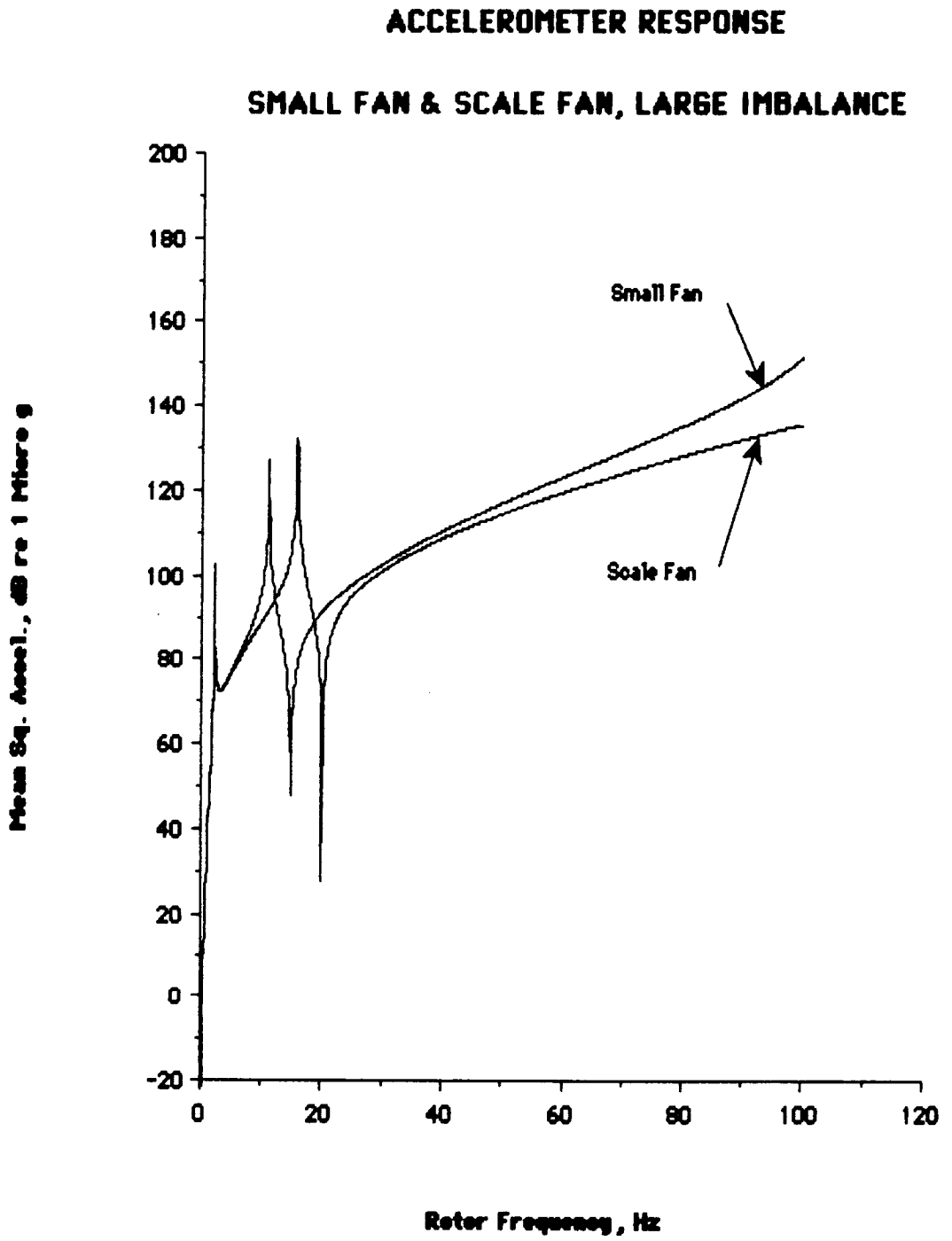

Figure 16
Accelerometer Response Comparison

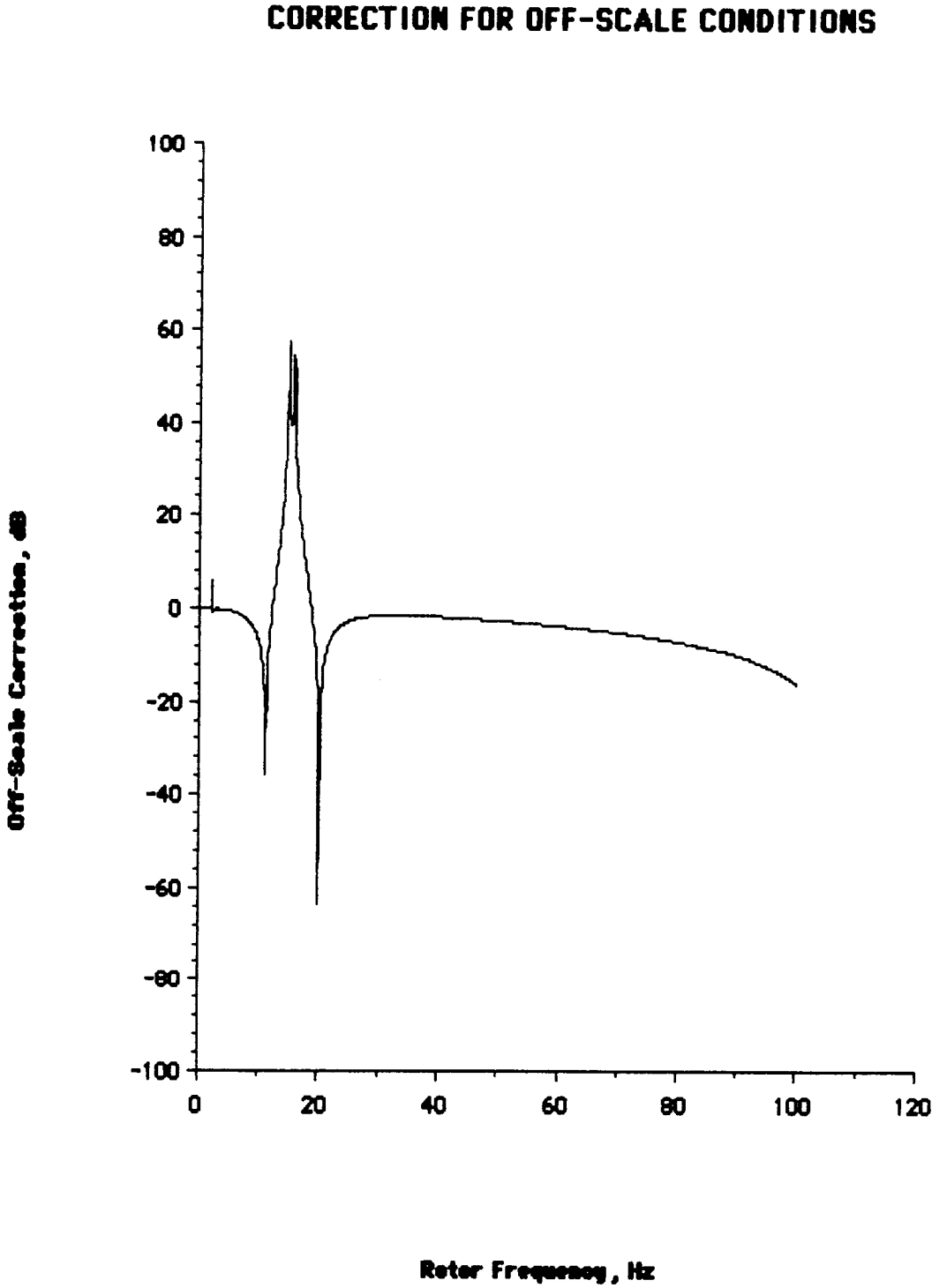

Figure 17
Correction for Off-Scale Conditions

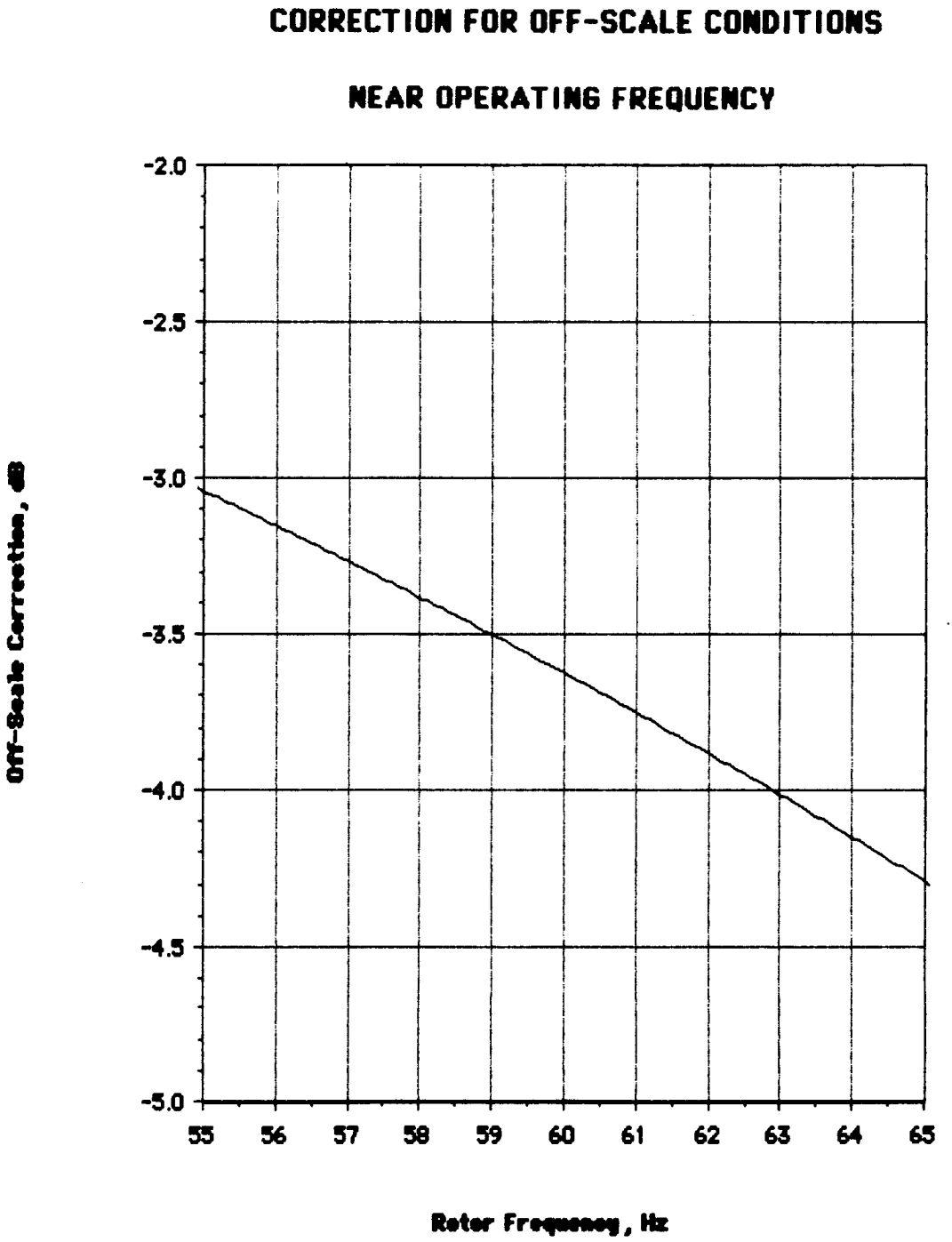

Figure 18
Correction for Off-Scale Conditions Evaluated Near 60 Hz Operating Frequency

The total scaling-law correction is

$$\begin{aligned} \Delta_{SCALING} &= \Delta_{SL} + \Delta_{AS} \\ &= 10 \log_{10} s \; -20 \log_{10} s \\ &= -10 \log_{10} (1.1482) \\ &= -0.600 \text{ dB} \end{aligned} \tag{31}$$

Predicted large-fan response is given by

$$\left[\langle a_A^2 \rangle_{dB \text{ re } 1\mu g} \right]_{\substack{\text{PREDICTED FOR} \\ \text{LARGE FAN}}} = \left[\langle a_A^2 \rangle_{dB \text{ re } 1\mu g} \right]_{\substack{\text{OBSERVED} \\ \text{FOR SMALL FAN}}} + \Delta_{OS} + \Delta_{SCALING} \tag{32}$$

A correction for operating speed variations is defined as

$$\Delta_{SV} = \left[\langle a_A^2 \rangle_{dB \text{ re } 1\mu g} \right]_{\text{SMALL FAN}} - \left[\langle a_A^2 \rangle_{dB \text{ re } 1\mu g} \right]_{\substack{\text{SMALL FAN} \\ \text{WITH SPEED} \\ \text{VARIATION}}} \tag{33}$$

The second term in Equation (33) represents dynamic model output corresponding to the small-fan parameter set with rotor frequency ω adjusted to correspond to a given shift in operating speed. Figures 19 and 20 show Δ_{SV} for a full frequency range and near the 60 Hz operating frequency respectively. The correction for speed variation is also independent of imbalance mass, provided M_I is small compared to M_R and M_H. When speed variation is present in the small-fan test unit,

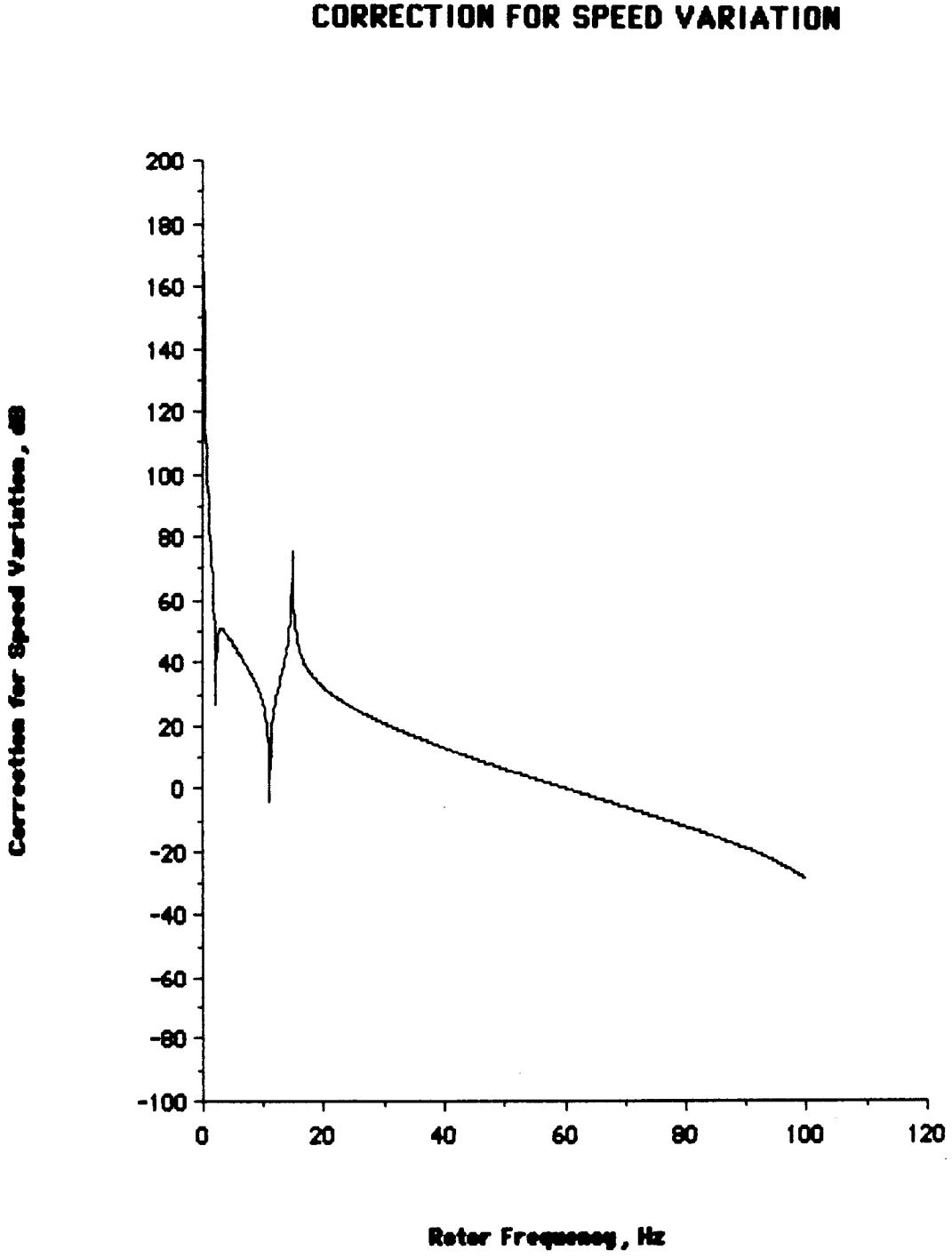

Figure 19
Correction for Speed Variation

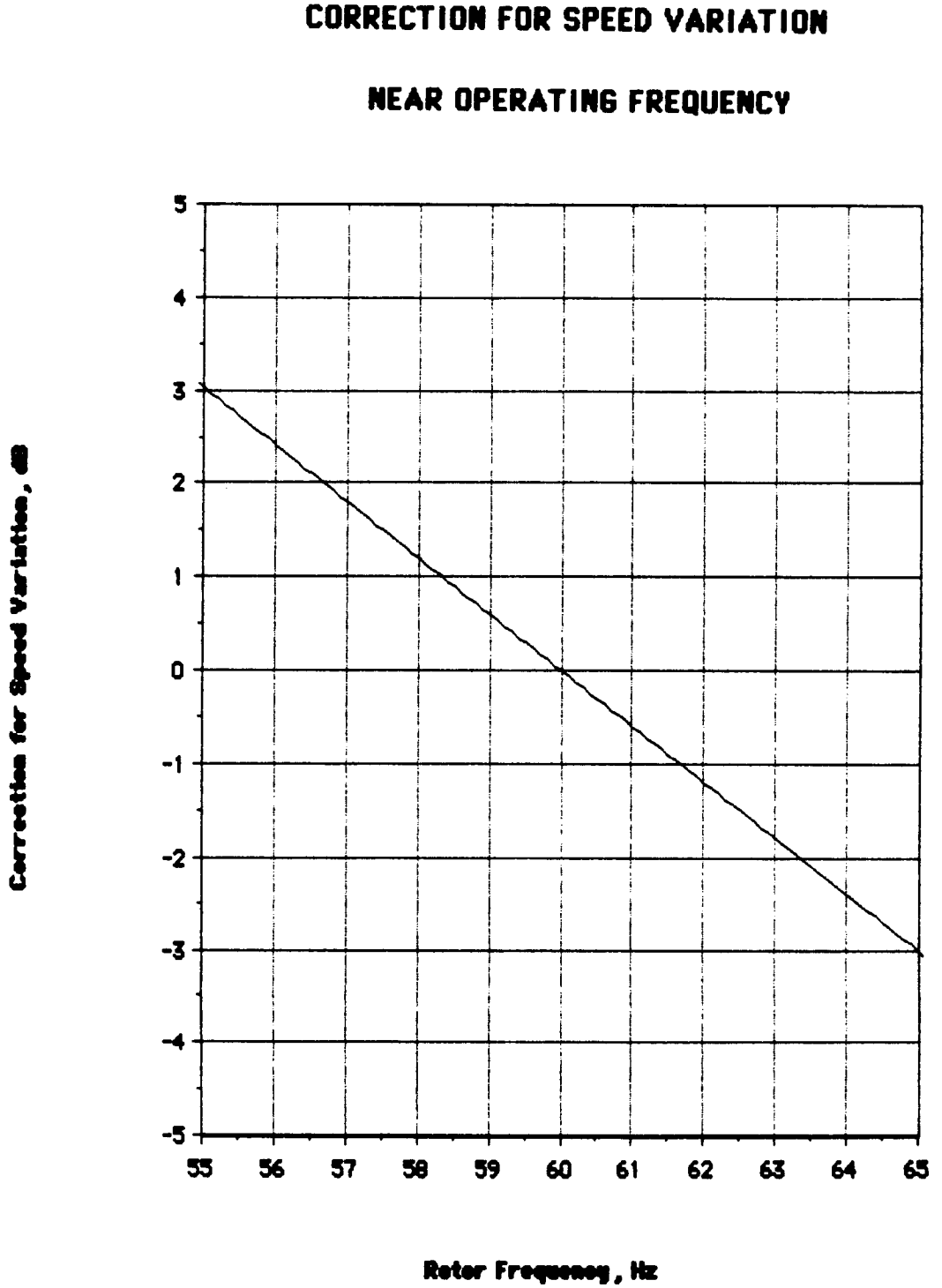

Figure 20
Correction for Speed Variation Near 60 Hz Operating Frequency

Equation (32) is replaced by

(34)

$$\left[\langle a_A^2 \rangle_{dB\ re\ 1\mu g} \right]_{\substack{\text{PREDICTED FOR} \\ \text{LARGE FAN}}} = \left[\langle a_A^2 \rangle_{dB\ re\ 1\mu g} \right]_{\substack{\text{OBSERVED} \\ \text{FOR SMALL FAN}}} + \Delta_{OS} + \Delta_{SV} + \Delta_{SCALING}$$

6.0 RESULTS, CONCLUSIONS, AND RECOMMENDATIONS

Results, conclusions, and recommendations are presented in Sections 6.1-6.3.

6.1 Results

The overall approach is validated by comparing actual and predicted response of the large fan, as shown in Figure 21.

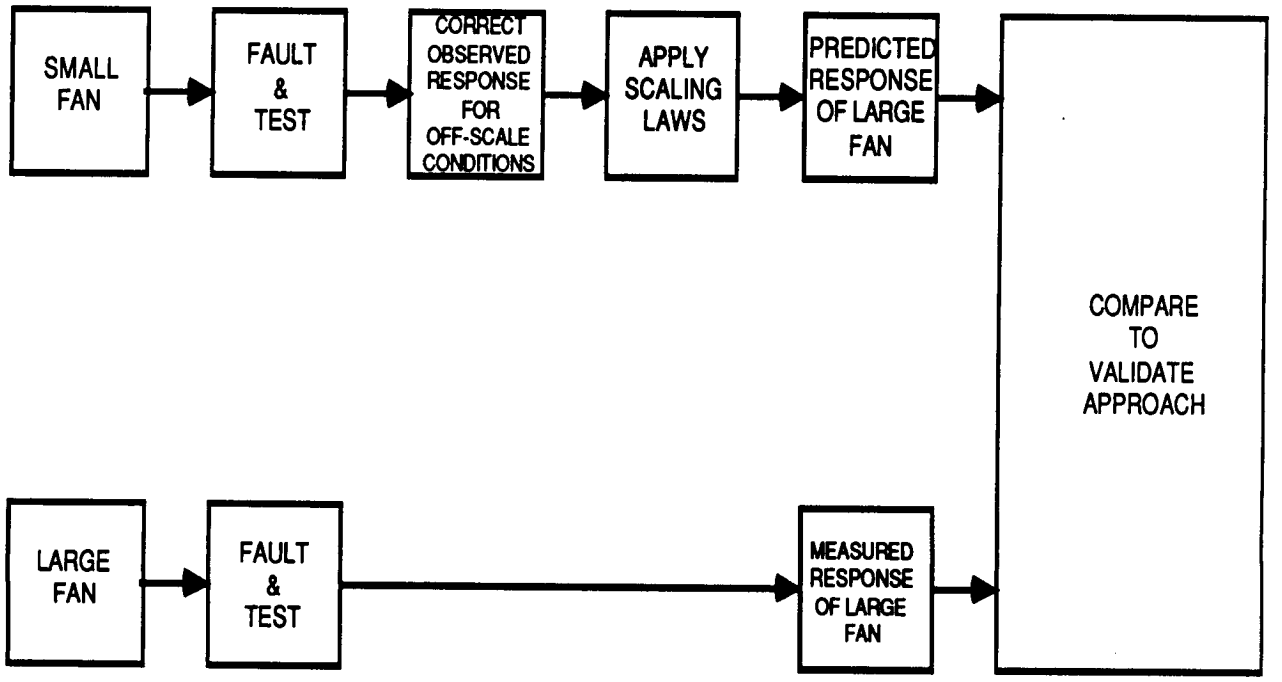

Figure 21
Method to Validate Overall Approach

Predicted large-fan response from Equation (32) is compared with measured large-fan response for large, medium and small imbalances in Table 5.

Table 5
Predicted vs. Measured Mean-Square Accelerometer Response for Large Fan

	Measured Small Fan Response (dB re 1 μ g)	Off-Scale Correction (dB)	Measured Small Fan Response Plus Off-Scale Correction (dB re 1 μ g)	Scaling-Law Correction (dB)	Predicted Large Fan Response (dB re 1 μ g)	Measured Large Fan Response (dB re 1 μ g)	Measured Minus Predicted LargeFan Response (dB)
Large Imbalance	123.6	-3.62	119.98	-0.6	119.38	119.0	-0.38
Medium Imbalance	118.0	-3.62	114.38	-0.6	113.78	113.6	-0.18
Small Imbalance	115.7	-3.62	112.08	-0.6	111.48	110.5	-0.98
Residual Imbalance	85.0	-3.62	81.38	-0.6	80.78	86.4	5.62

Predicted mean square acceleromter response levels for the large fan agree with measurements to within 1dB for all three imbalance conditions, thus validating the overall approach for the selected fault type.

6.2 Conclusions

Conclusions are that

- Techniques designed to detect rotor imbalance by responding to a change in mean square acceleration level at the fundamental can be validated using a Strouhal-scaled machine, provided critical dynamic parameters are correctly scaled; and

- Corrections for differences in construction details, mount characteristics and operating speeds can be made using a validated dynamic model that adequately represents the specific fault type.

6.3 Recommendations

Recommendations are to:

- Extend the analysis of off-scale conditions to include other types of off-scale effects as well as more severe off-scale conditions. This will determine the maximum extent to which the approach is applicable when laboratory test units can not be precisely Stouhal-scaled.

- Investigate scaling effects already present due to size and configuration differences in existing machines. This will determine whether refinements to current vibration monitoring techniques may be required because of differences in size, construction details, operating speed and mounting.

- Extend the approach to fault types other than imbalance. Bearing-related faults are of primary importance.

- Extend the approach to measurement types other than mean square acceleration response at the fundamental rotor frequency; for example, mean square acceleration at places in the spectrum associated with different faults.

- Examine sensor placement effects.

REFERENCES

1. ETRI Fans for Electronics, Catalog No. ET 121-185-20M, ETRI, Inc., P.O. Box 5006, Monroe, N.C. 28110.

2. J.P. Den Hartog, Mechanical Vibrations, Fourth Edition, McGraw-Hill (1956)

3. N.F. Rieger, Vibration of Rotating Machinery, Fourth Edition, The Vibration Institute, Clarendon Hills, Illinois (1984), Part 1.

4. Timoshenko, S., D.H. Young, and W. Weaver, Jr., "Vibration Problems in Engineering", Fourth Ed., Wiley, 1974, p. 327

5. Miguel C. Junger, The Scaling Laws Governing the Dynamic Response of a Structure to a Turbulent Boundary Layer", JUA (USN) 13, 439 (1963).

6. Wilfred E. Baker, Peter S. Westine and Franklin T. Dodge, "Similarity Methods in Engineering Dynamics", Spartan Books, 1973, p. 38.

7. H.M. Schauer and D.S. Cohen, "On the Feasibility of Model Tests for Noise Radiation Studies", JUA (USN) 10, 241 (1960).

8. David A. Bies and Peter A. Franken, "Notes on Scaling Jet and Rocket Nosie", J. Acoust. Soc. Am. 33, 1171 (1961).

APPENDIX D

VIBRATION ANALYSIS OF LABORATORY DATA

TABLE OF CONTENTS

LIST OF TABLES

1.0 INTRODUCTION

Experimental results of the feasibility testing are illustrated within this appendix. Tests performed on the IFD components are listed in Tables D-1 and D-2. The experimental results form the basis of the general Application Study results which were shown in Tables 3.7 and 3.8. Brief test descriptions are provided, followed by plots showing results which include experimental means and standard deviations, detection weights, baseline data and faulted data. Individual sections of the appendix then present the optimum signature analysis detection results for both baseband and HFD analysis.

2.0 NOMENCLATURE

A description of the nomenclature seen on the plots is given below:

1. Machine Spec : F0xxxxxxxxx -- Tracor's identification for the machine being tested, whether the data is baseband (B) or high frequency demodulation (H), and the analysis bandwidth employed.

2. Refit -- Naval terminology for a set of vibration readings obtained at a given time within a given experiment.

3. Raw -- Vibration data as was taken in the lab and which has not been corrected for speed variations which can occur between refits.

4. fRf -- Abbreviation for Tracor's Eundamental Rotational Erequency normalization algorithm which lines up all speed related tones.

3.0 CHARACTERISTIC FREQUENCIES

The key characteristic frequencies of the IFD components are shown below:

TRW Fans

Rotation	--	197.6 Hz
Bearing Frequencies	--	856 Hz BPFI
	--	512 Hz BPFO
Blade Passage	--	1581 Hz

Single Phase Pumps

Rotation	--	60 Hz
Gear Mesh (9 teeth)	--	540 Hz
Pumping Frequencies	--	Harmonics of 60 Hz

Three Phase Pumps

Rotation	--	196 Hz
Gear Mesh (9 teeth)	--	1764 Hz
Bearing Frequencies	--	401 Hz BPFO
	--	775 Hz BPFI
Pumping Frequencies	--	Harmonics of 196 Hz

TABLE D-1 FANS VIBRATION TEST PLAN

- Ambient
  - Bench
  - Fan
- Accelerometer Mount/Remount Repeatability
- Accelerometer Loose Remount
- Accelerometer Mapping (4 fans)
- Fan Disassembly/Reassembly (4 fans)
- Imbalance (weight)
  - Small (0.035 gm) (4 fans)
  - Large (0.173 gm) (4 fans)
  - Large (0.173 gm) (1 fan)
- Inlet Air Restrictions (1 fan)
  - 25% Blockage
  - 75% Blockage
- Voltage Change (4 fans)
  - Under (180 V)
  - Over (220 V)
- Phase Loss (1 fan)
- Shaft Orientation
  - 4 fans
  - 1 fan
- Elevated Ambient (1 fan)
  - $22^{o}C$ --> $40^{o}C$
- Bearings - Particle Contamination (4 fans)
- Bearings - Inner Race Fault (1 fan)
- Bearings - Outer Race Fault (1 fan)
- Small/Large Fans (2 fans)

TABLE D-2 PUMPS VIBRATION TEST PLAN

Ambient

- Bench
- Pumps (1 - 1ϕ, 1- 3ϕ)

Accelerometer Mount/Remount Repeatability (1 - 1 ϕ, 1 - 3 ϕ)

Accelerometer Loose Remount (1 - 1 ϕ, 1 - 3ϕ)

Accelerometer Mapping (1 - 1ϕ, 1 - 3ϕ)

Pump Disassembly/Reassembly (1 - 1 ϕ, 6 - 3ϕ)

Shaft Orientation (4 - 1ϕ, 6 - 3ϕ)

Phase Loss (1 - 3ϕ)

Load Conditions (1 - 1ϕ)

- Over (80 psig)
- Under (20 psig)

Voltage Change (1 - 1 ϕ)

- Over Voltage (135 V)
- Under Voltage (105 V)

Coupling Imbalance (1 - 3 ϕ)

- Small (0.035 gm)
- Large (0.173 gm)

Impeller Wear (4 - 1ϕ)

Impeller Fault (1 - 1ϕ)

Bearings - Loss of Lubricant (1 -3ϕ)

Bearings - Inner Race Fault (6 - 3 ϕ)

Bearings - Outer Race Fault (6 - 3 ϕ)

ELEVATED AMBIENT TEMPERATURE - SINGLE FAN

TEST DESCRIPTION: Elevated Ambient Temperature - Single Fan

A series of tests was performed in which the ambient temperature presented to a single fan rose from 22°C to an average temperature of 40°C by means of resistance heating. A baseline was obtained at the nominal room temperature of 22°C, after which air heating commenced. After reaching an inlet air temperature of 40°C, which was monitored by an electronic temperature sensor, the faulted data was obtained. The heated air was then removed and the fan allowed to cool down to ambient conditions. A second electronic temperature sensor was also attached to the stationary inlet guide vane assembly to ensure consistent testing temperatures. The fan remained in operation during the entire test sequence in which four baseline and four faulted conditions were obtained.

Results Presented:

Baseband

1) Collection of baseline refits - F0B1ETPB.2
2) Collection of faulted refits - F0B1ETPF.2
3) Mean and standard deviation of the baseline and faulted refits.
4) Unmodified likelihood ratio weights.

1. REFIT # 07 RAW NS
2. REFIT # 05 RAW NS
3. REFIT # 03 RAW NS
4. REFIT # 01 RAW NS

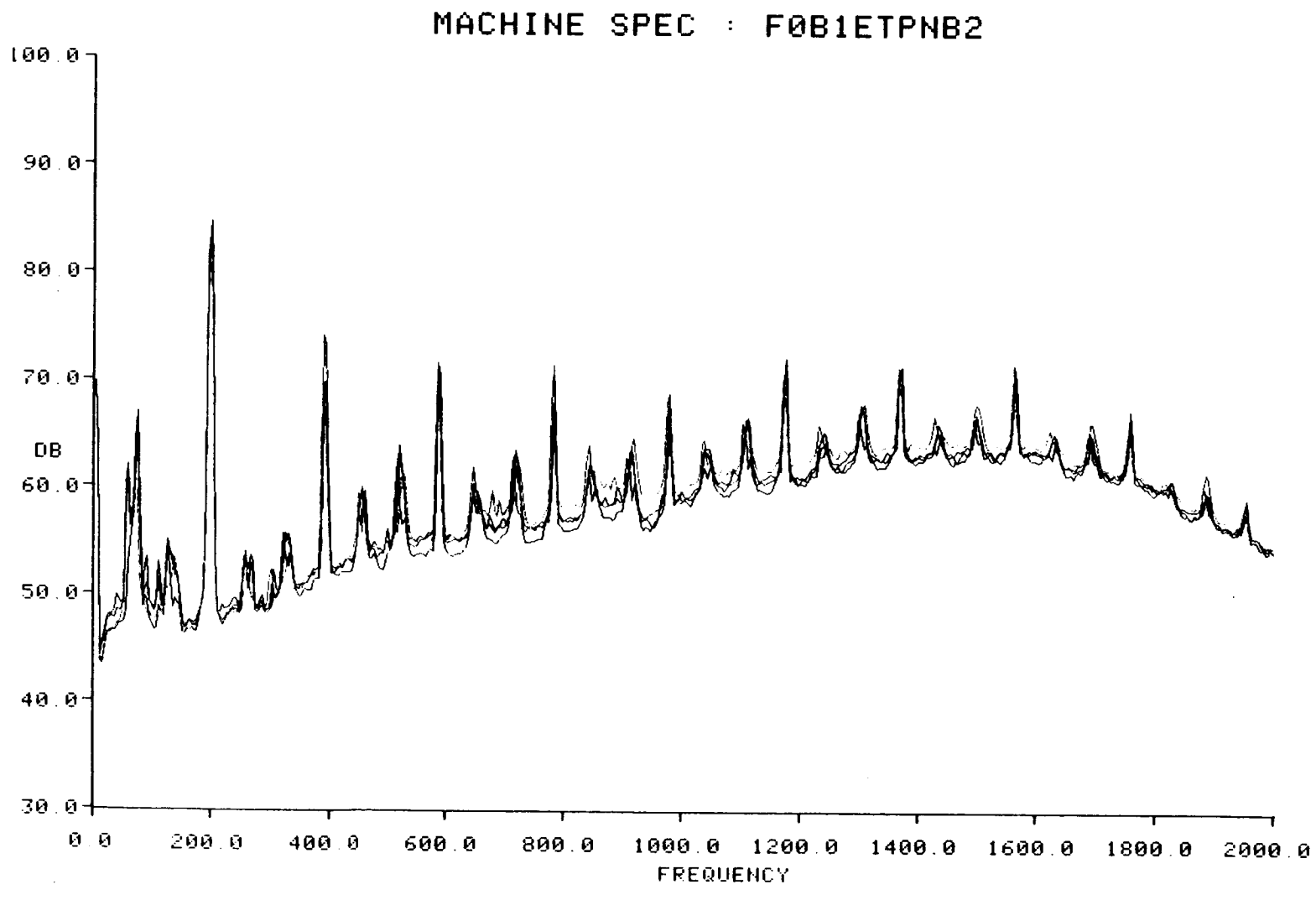

1. REFIT # 08 RAW NS
2. REFIT # 06 RAW NS
3. REFIT # 04 RAW NS
4. REFIT # 02 RAW NS

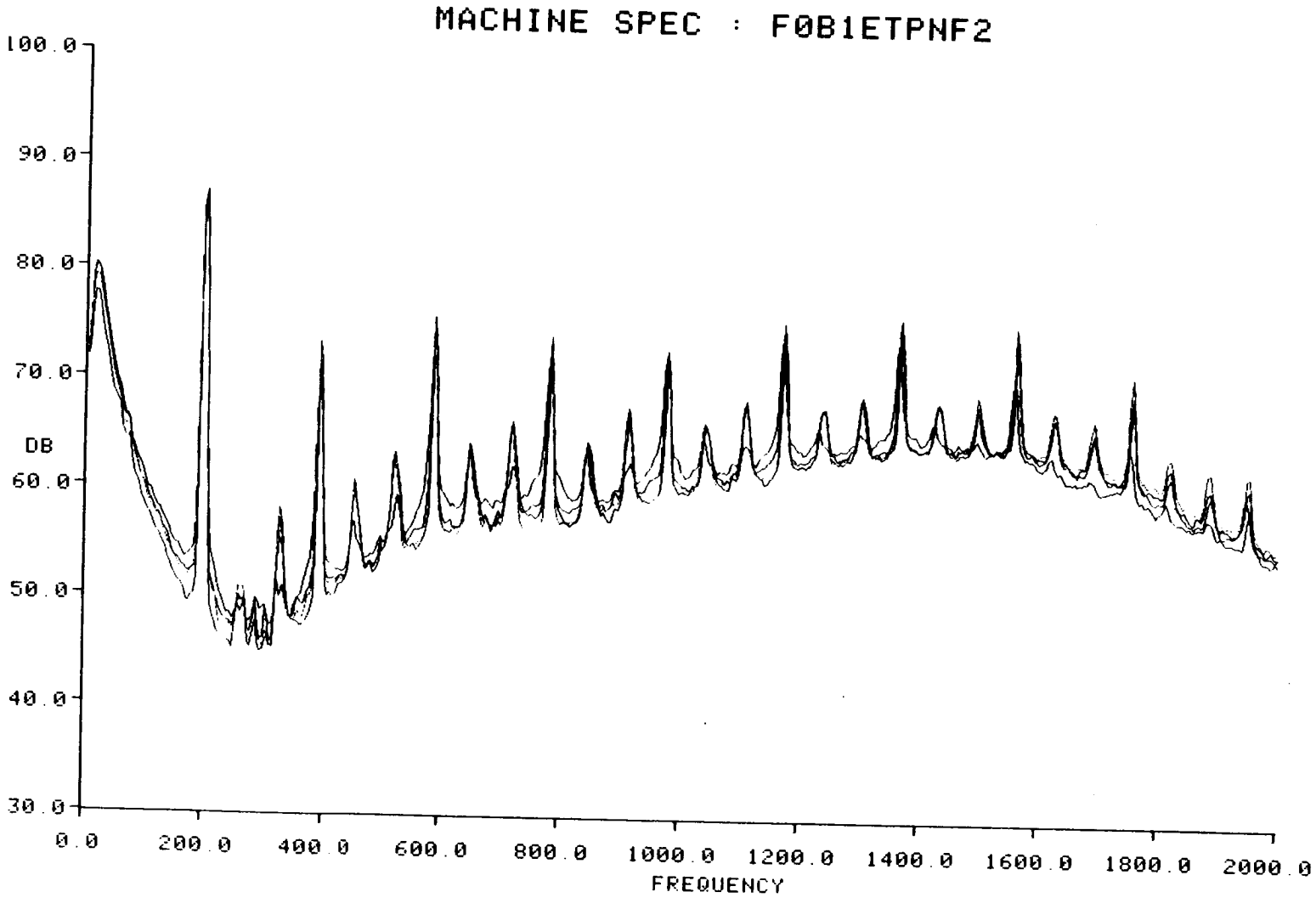

MEAN FOR FAULTED REFITS
MEAN FOR BASELINE REFITS
SIGMA FOR FAULTED REFITS
SIGMA FOR BASELINE REFITS

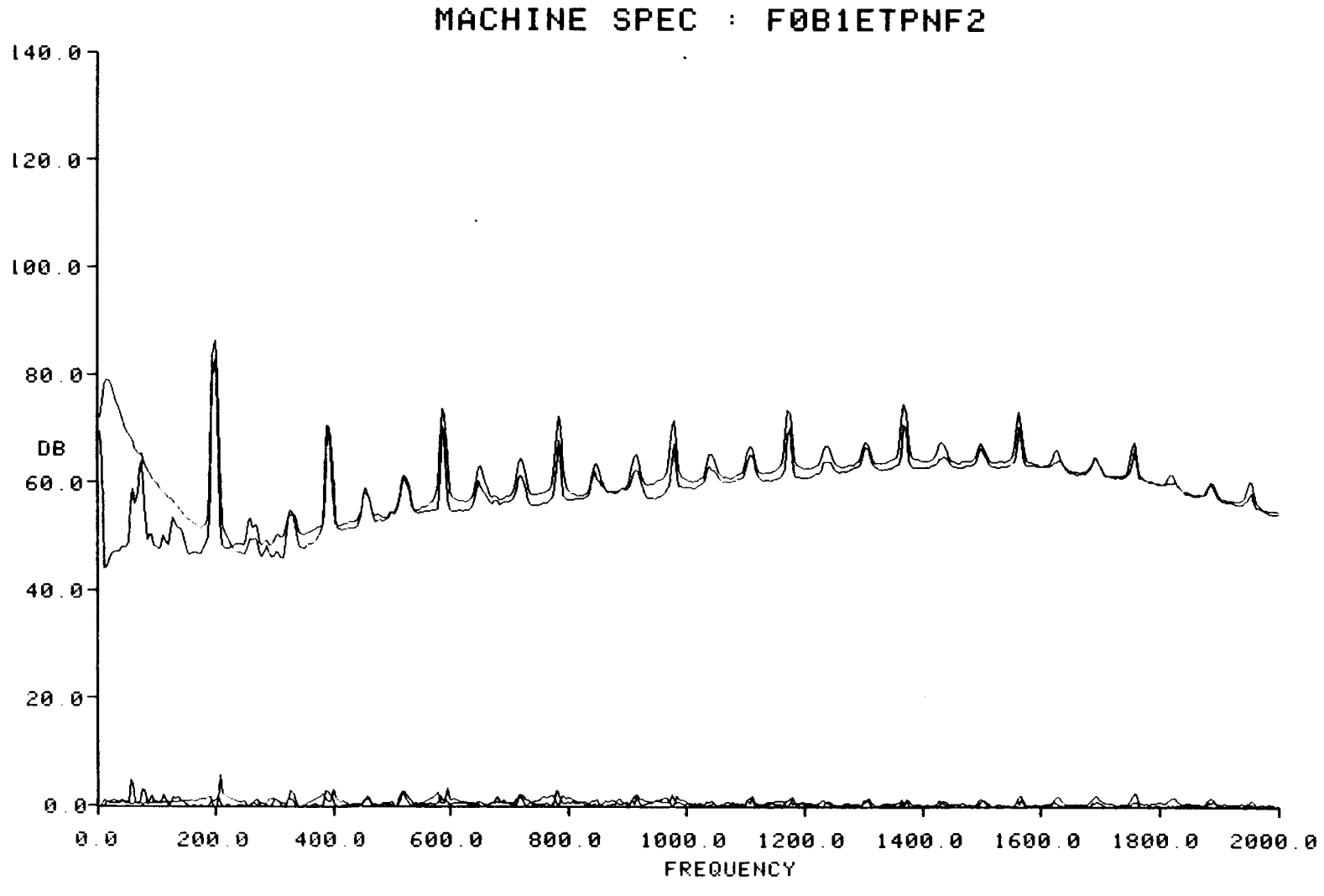

LIKELIHOOD RATIO WEIGHTS

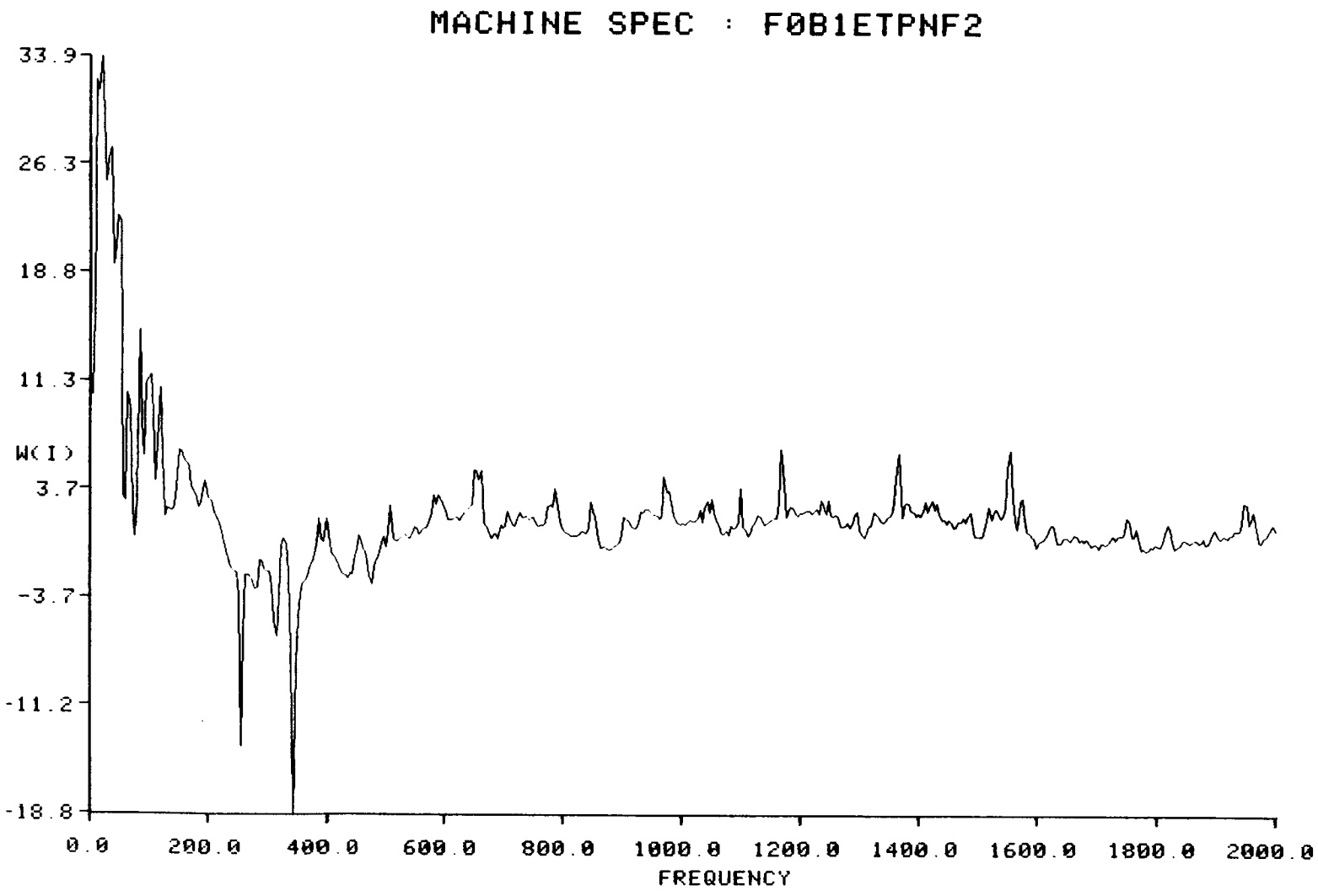

OPTIMUM SIGNATURE ANALYSIS DETECTION - Elevated Ambient - Single Fan

P_D for P_{FA} = 0.1

Baseband	HFD
1.0	0.99

BEARING PARTICLE CONTAMINATION - MULTIPLE FANS

C-3

TEST DESCRIPTION: Bearing Particle Contamination - Multiple Fans

A series of tests was performed in which the effect of bearing contaminates was evaluated in each of the four test fans. To minimize the potential test variance of having to disassemble the test fans between baseline and faulted conditions, a 5/32" hole was placed in the inlet hub of the test fans over the front bearing (with respect to the fan inlet) cage assembly. A baseline was obtained to the fan under test running normally, after which a small quantity of very fine steel shavings introduced to the bearing through the 5/32" opening. Both baseband and high frequency demodulation data was obtained simultaneously.

Results Presented:

Baseline

1) Baseline and faulted time series strip chart.
2) Collection of faulted refits - F0BX27PCF.2
3) Mean and standard deviation for the baseline and faulted refits.
4) Unmodified likelihood ratio weights.

High Frequency Demodulation - F0HX27PCF.2

5) Mean and standard deviation for the baseline and faulted refits.
6) Unmodified likelihood ratio weights.

TRW Fan, Time Series Data

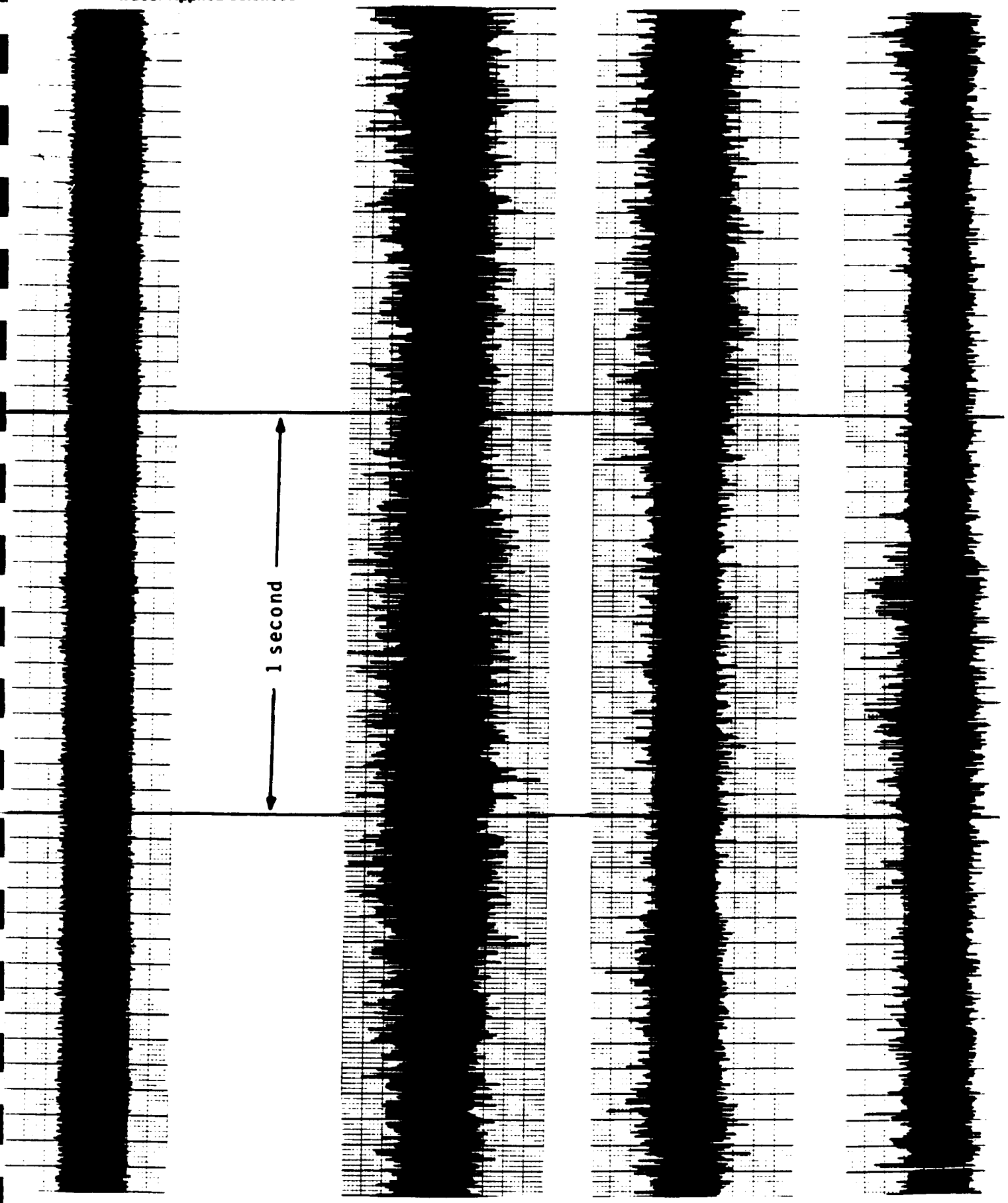

BASELINE

PARTICLE CONTAMINATION IN BEARING

ORIGINAL PAGE IS
OF POOR QUALITY

1. REFIT # MF RAW NS
2. REFIT # MB RAW NS
3. REFIT # M7 RAW NS
4. REFIT # M3 RAW NS

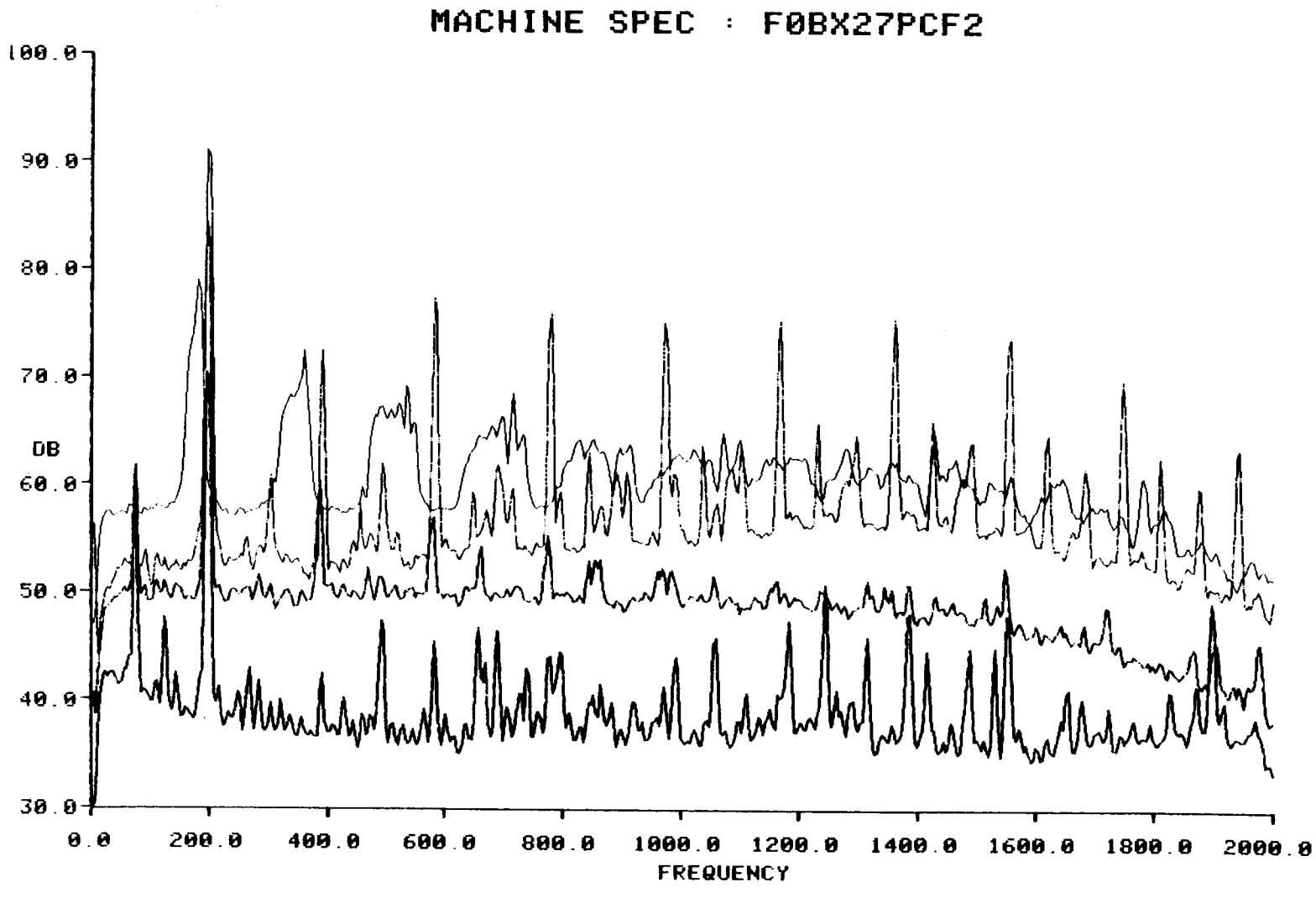

MEAN FOR FAULTED REFITS
MEAN FOR BASELINE REFITS
SIGMA FOR FAULTED REFITS
SIGMA FOR BASELINE REFITS

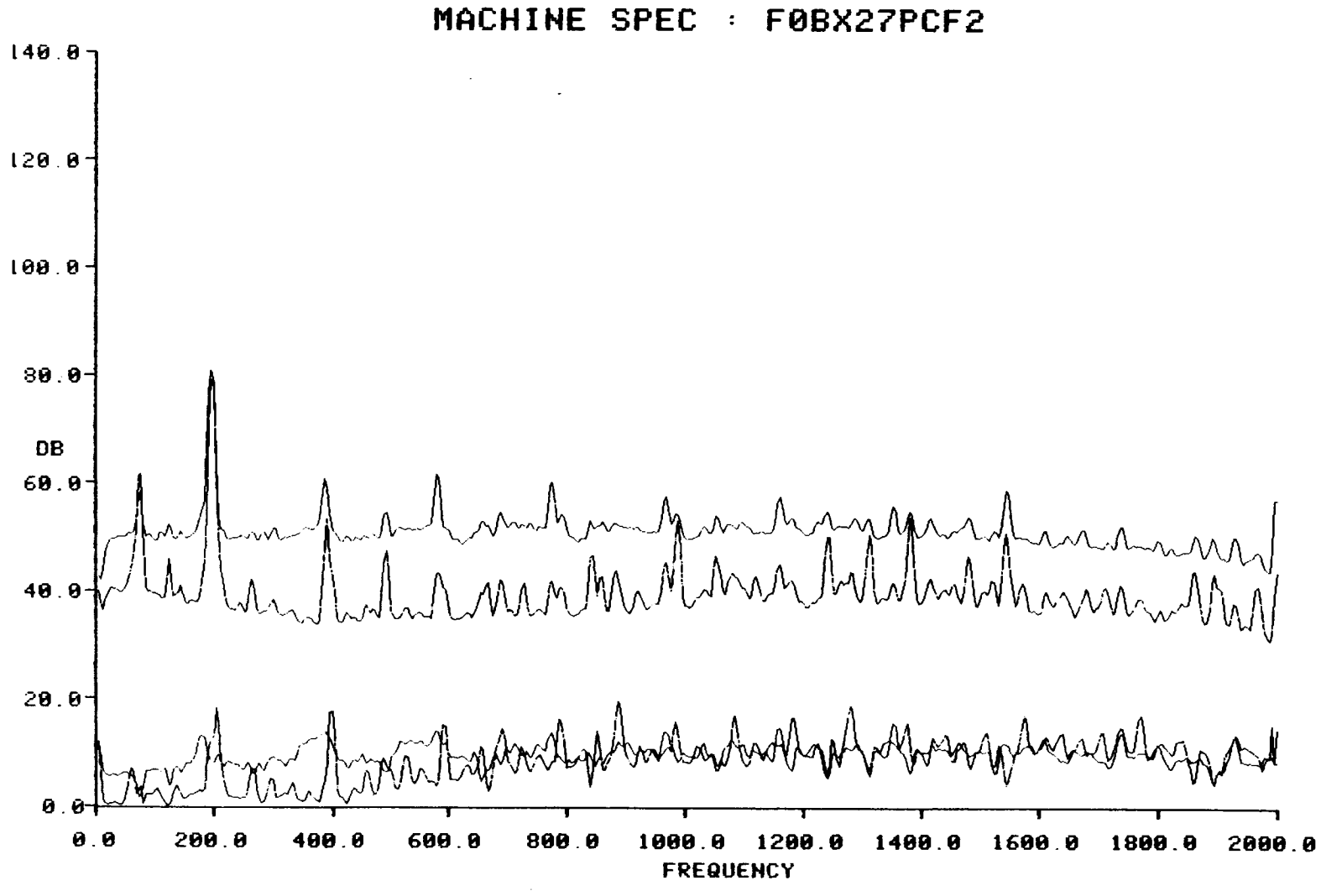

LIKELIHOOD RATIO WEIGHTS

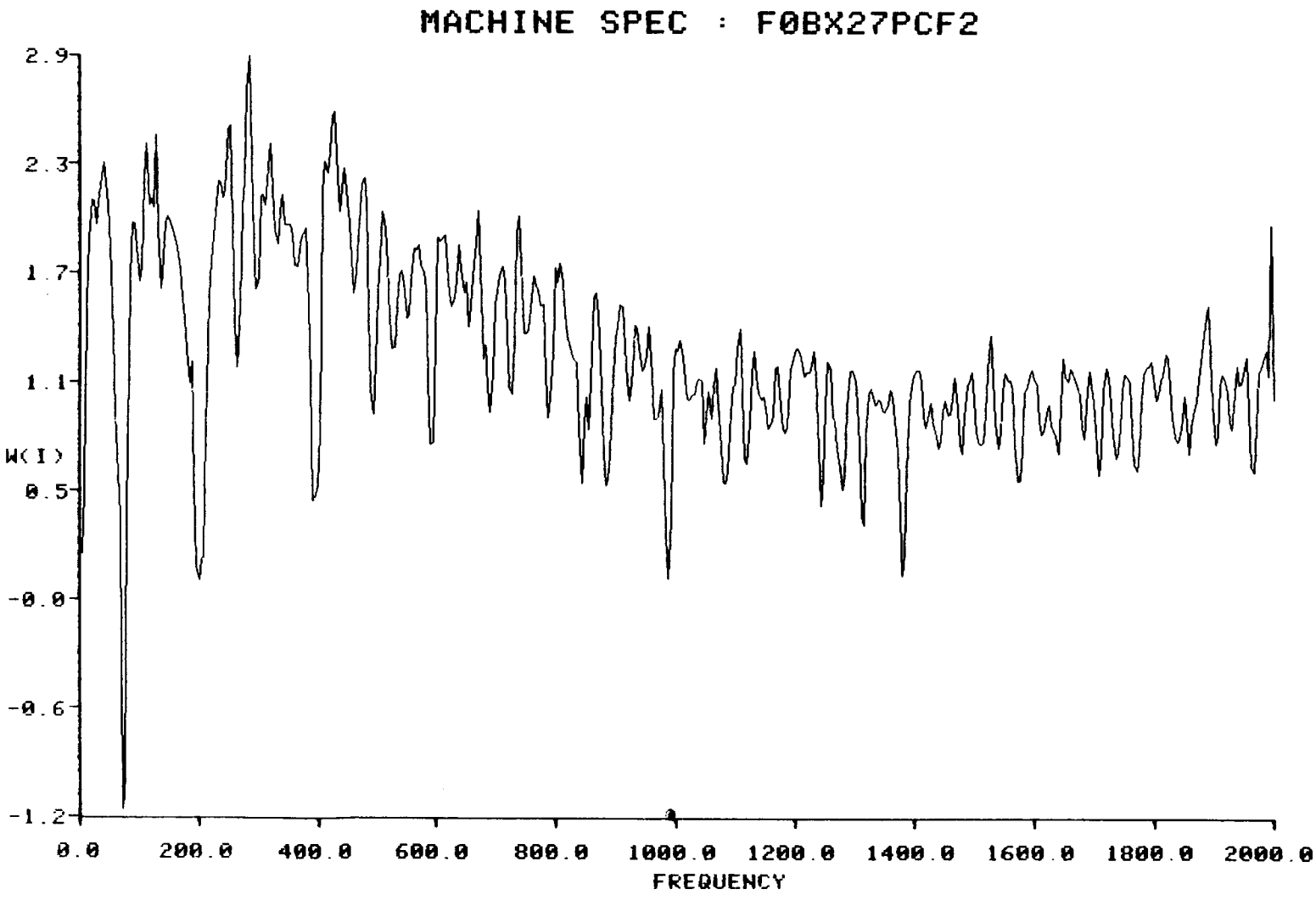

MEAN FOR FAULTED REFITS
MEAN FOR BASELINE REFITS
SIGMA FOR FAULTED REFITS
SIGMA FOR BASELINE REFITS

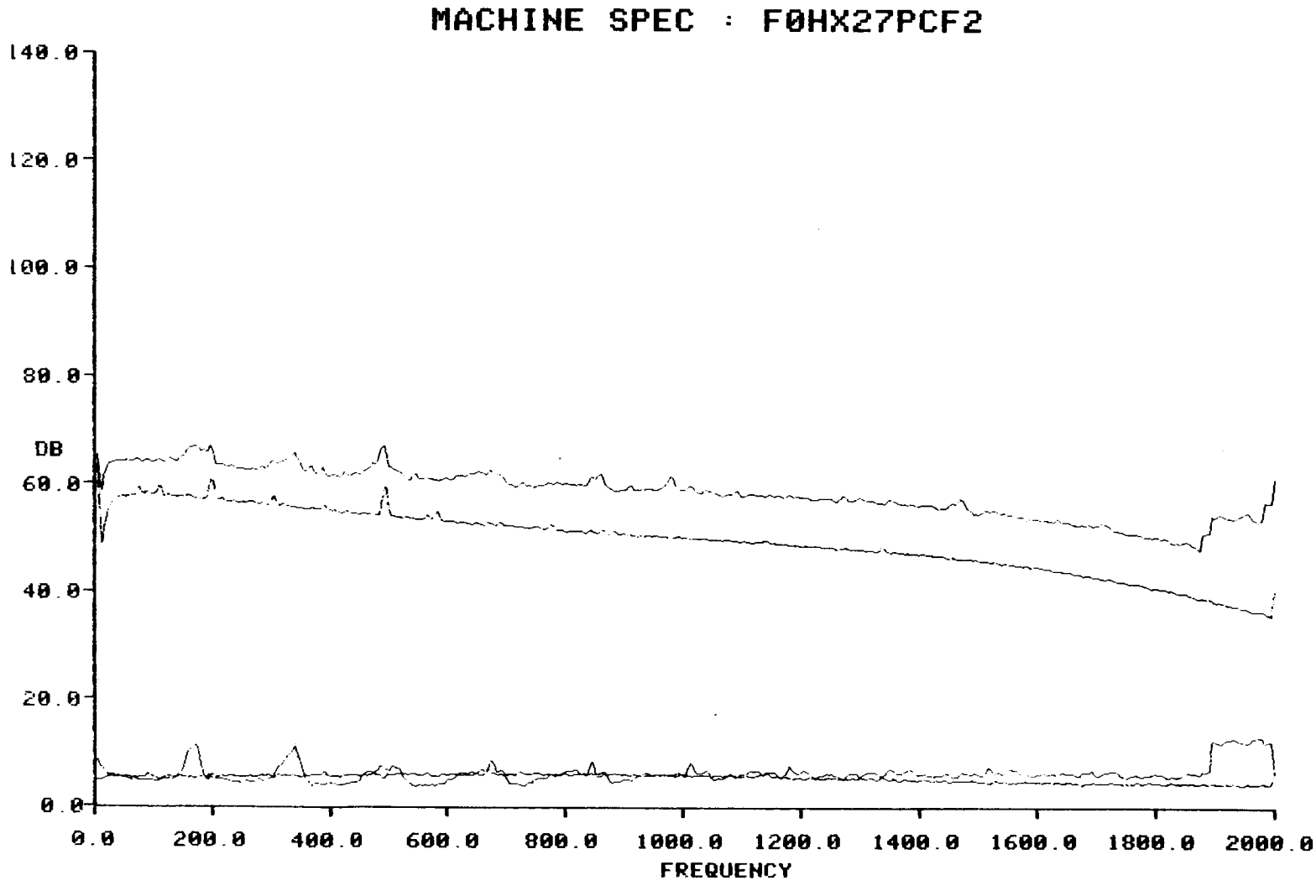

LIKELIHOOD RATIO WEIGHTS

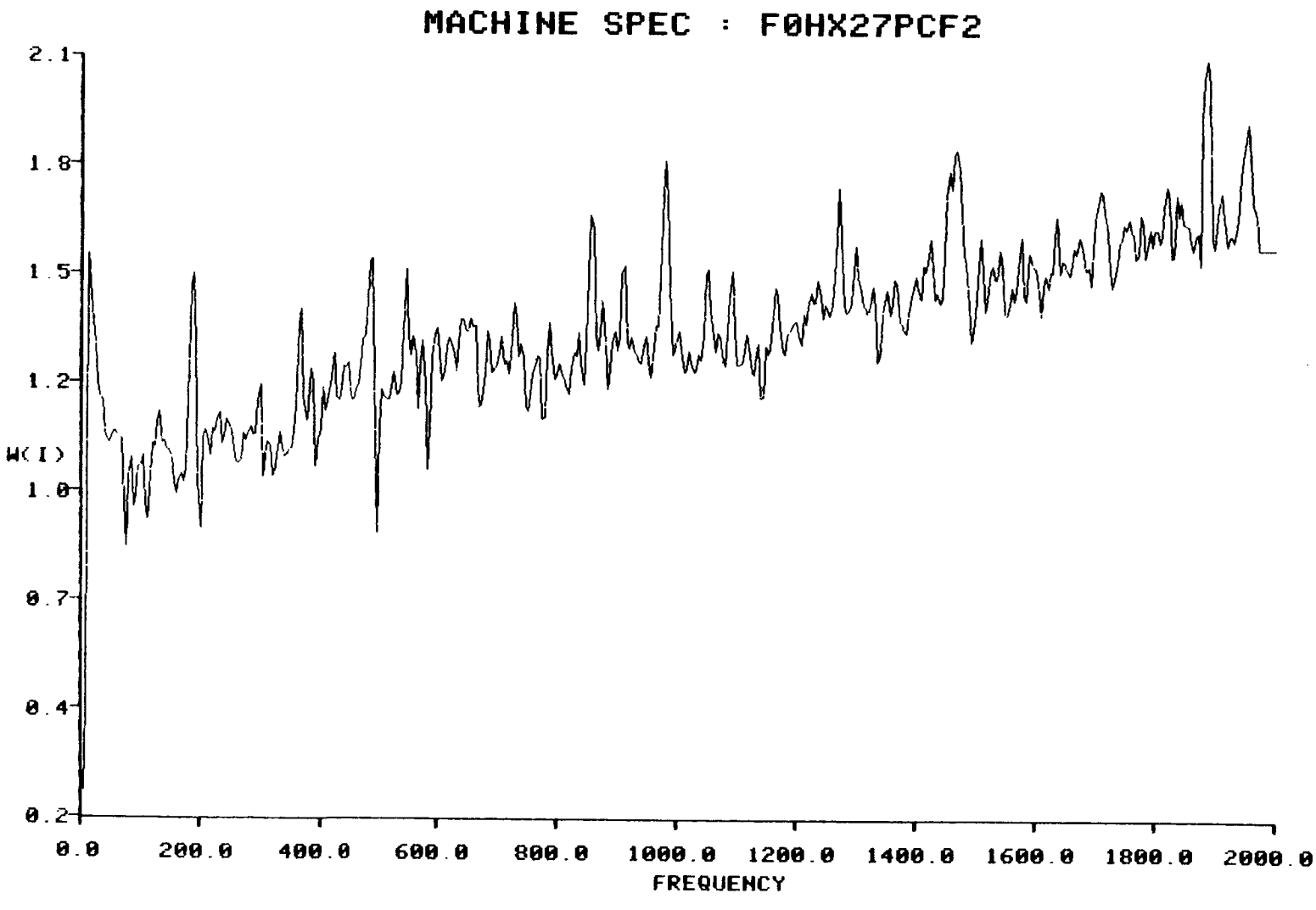

OPTIMUM SIGNATURE ANALYSIS DETECTION - Bearing Particle Contamination

P_D for P_{FA} = 0.1

Baseband	HFD
.65	.66

PHASE LOSS - SINGLE FAN

TEST DESCRIPTION: Phase Loss - Single Fan

A series of tests was performed in which the loss of a single-phase of the three-phase power to a single test fan was evaluated. A baseline was obtained with the three-phase fan running normally, after which one of the phases was removed. Three baseline and three faulted conditions were obtained. Both baseband and high frequency demodulation data were obtained simultaneously.

Results Presented:

Baseband - F0BXX200F.2

1) Mean and standard deviation of the baseline and faulted refits.
2) Unmodified likelihood ratio weights.

MEAN FOR FAULTED REFITS
MEAN FOR BASELINE REFITS
SIGMA FOR FAULTED REFITS
SIGMA FOR BASELINE REFITS

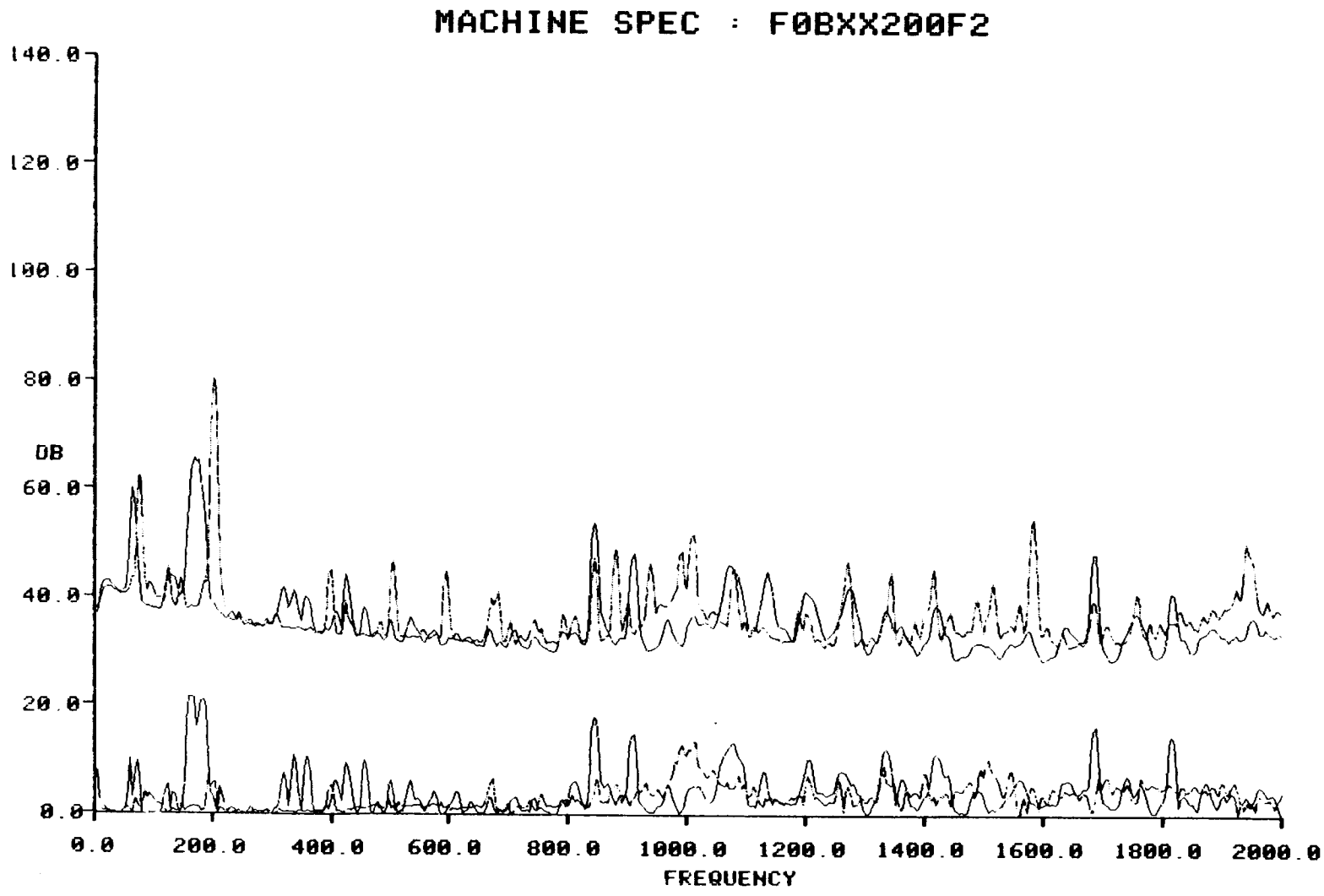

LIKELIHOOD RATIO WEIGHTS

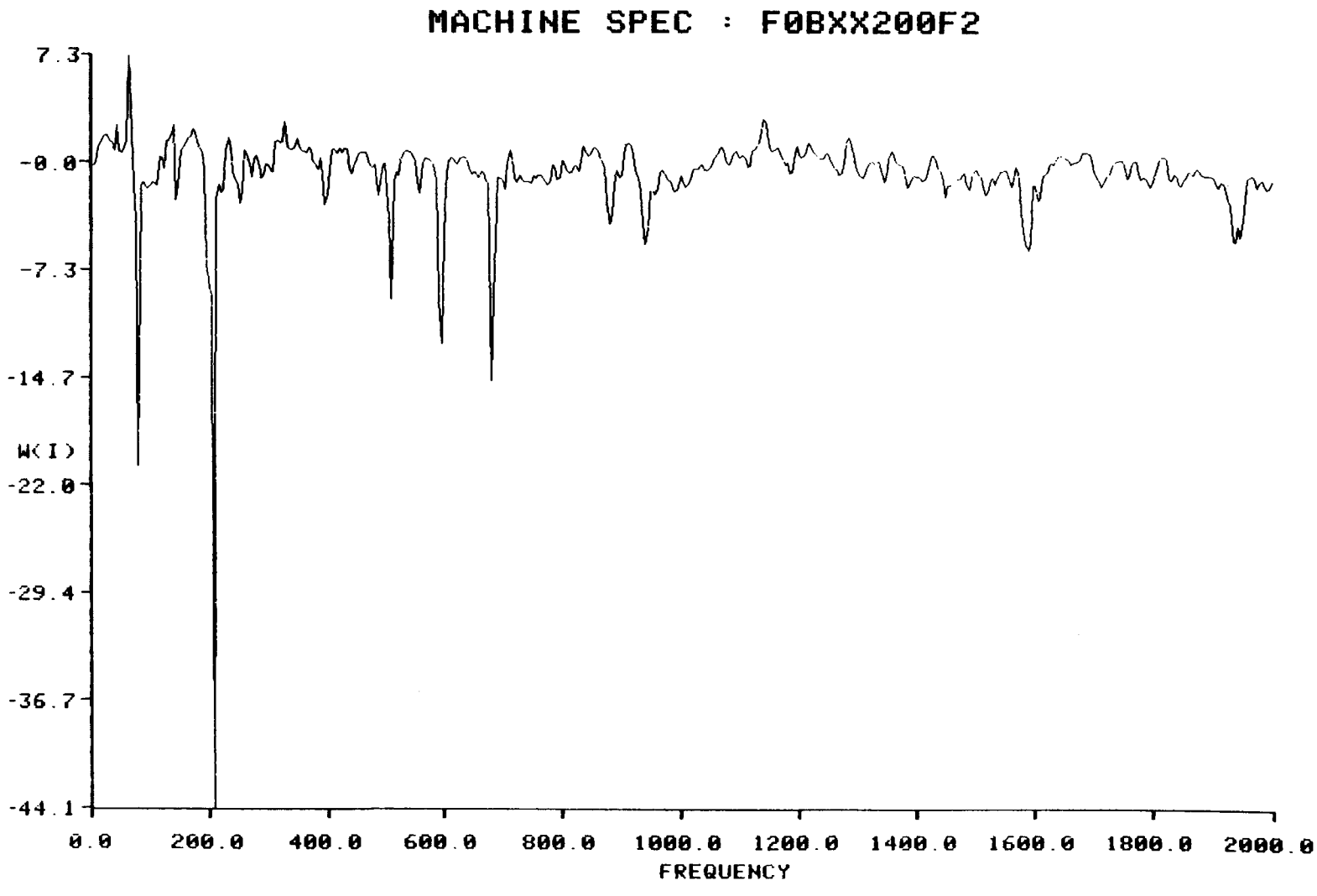

OPTIMUM SIGNATURE ANALYSIS DETECTION:
Phase Loss - Single Fan

P_D for P_{FA} = 0.1

Baseband	HFD
1.0	0.99

INNER RACE FAULTS - SINGLE FAN

TEST CONDITIONS: Inner Race Faults - Single Fan

A series of tests was performed in which a single inner race fault was introduced into the front bearing of the fan under test. This series of tests required that the fan and its bearing be disassembled and reassembled after fault introduction. A special bearing which used a easily removable one piece cage was employed during these tests. No force was required at any stage of the bearing disassembly/reassembly process.

The bearings, after disassembly, are faulted by using a "moto tool" with a carbide grinding tip to score across the inner race surface. It was not possible to accurately quantify the depth of the score. However, the faults were hard to visually identify and could best be located by lightly placing a pick on the raceway and running it around the race until a slight "roughness" was felt. The bearing faults introduced were quite small for this procedure to be used. Care was exercised in the removal of any foreign material generated during the faulting process before reassembly.

Results Presented:

Baseband - F0BX2900F.2

1) Mean and standard deviation for baseline and faulted refits.
2) Unmodified likelihood ratio weights.
3) Modified likelihood ratio weights (all weights set to zero except BPFI (856 Hz) and its harmonic).
4) Modified likelihood ratio weights (all weights set to zero except for five large positive weights which are modulations of the rotational speed).

5) Cluster analysis of a faulted refit with a search performed on rotational speed.

High Frequency Demodulation - F0HX2900F.2

6) Mean and standard deviation of the baseline and faulted refits.
7) Modified likelihood ratio weights (all weights set to zero except BPFI and its harmonic).

MEAN FOR FAULTED REFITS
MEAN FOR BASELINE REFITS
SIGMA FOR FAULTED REFITS
SIGMA FOR BASELINE REFITS

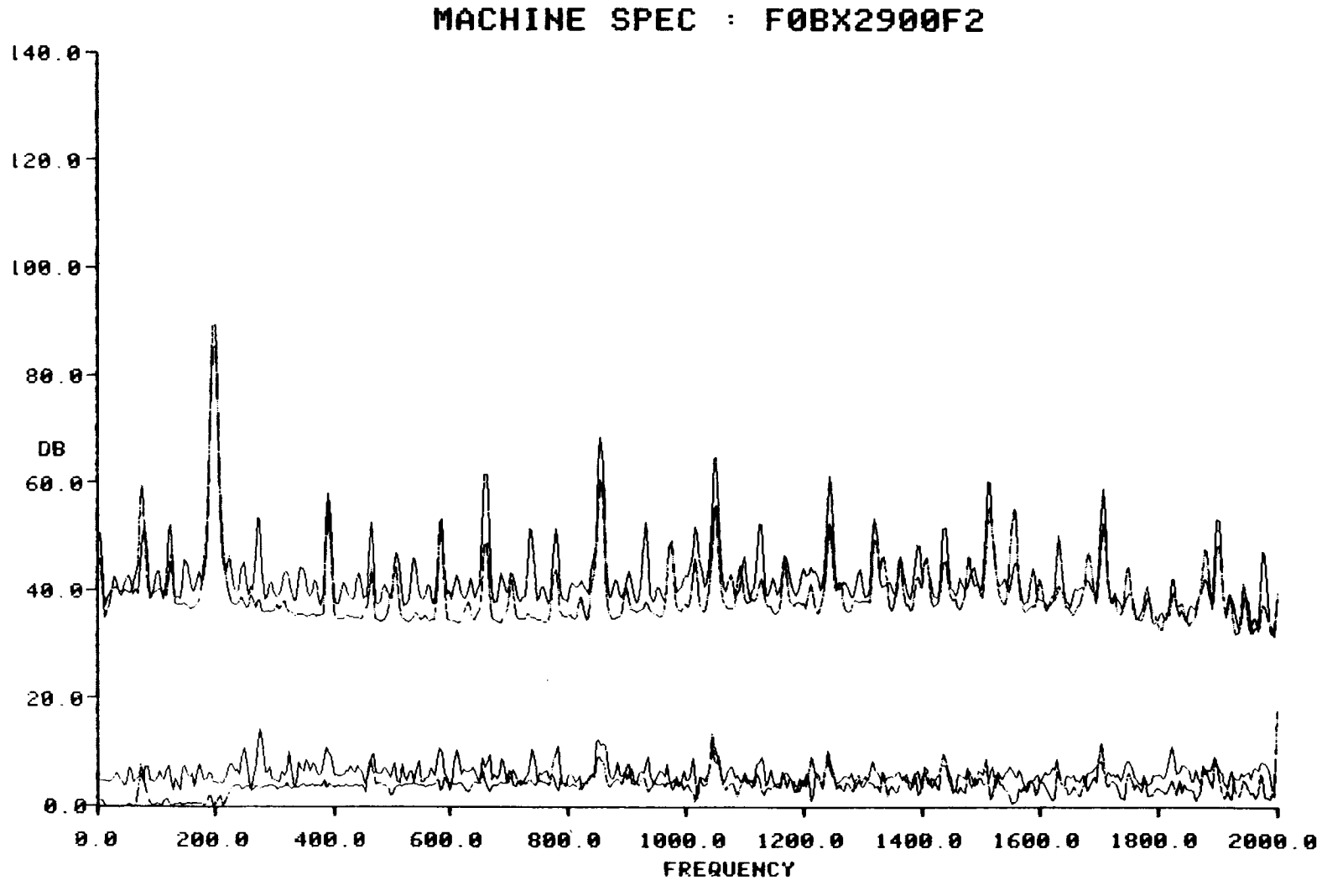

LIKELIHOOD RATIO WEIGHTS

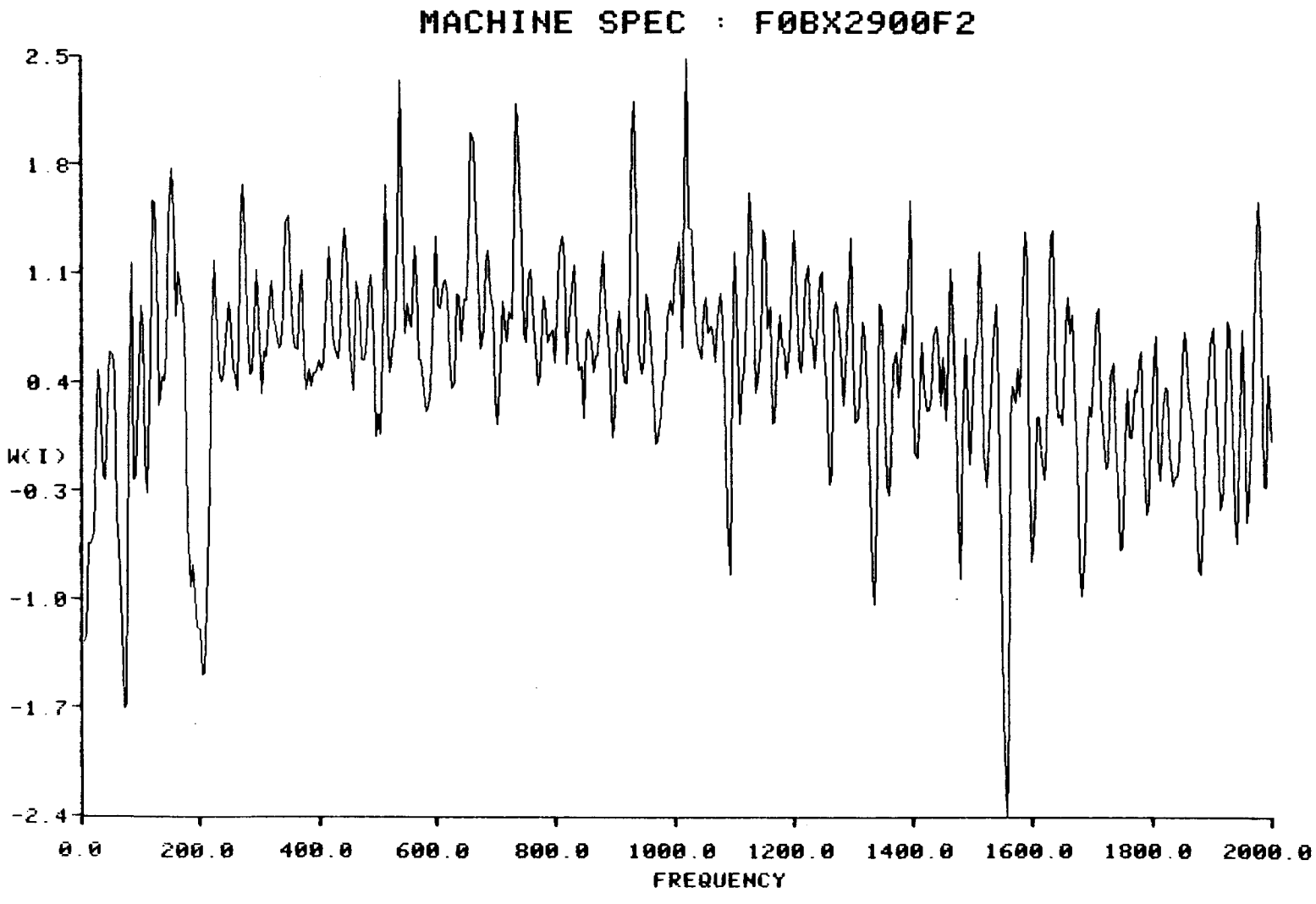

LIKELIHOOD RATIO WEIGHTS

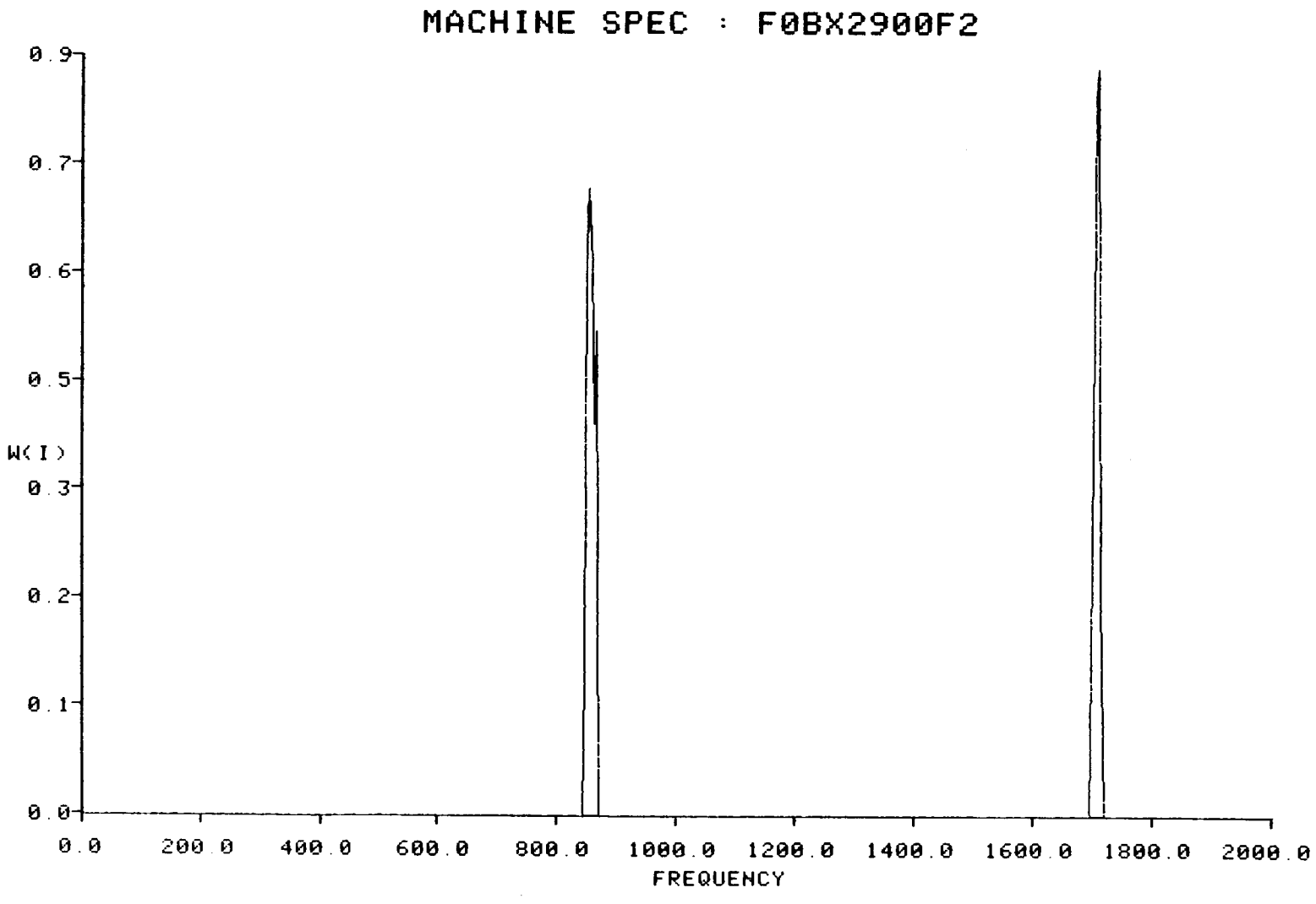

LIKELIHOOD RATIO WEIGHTS

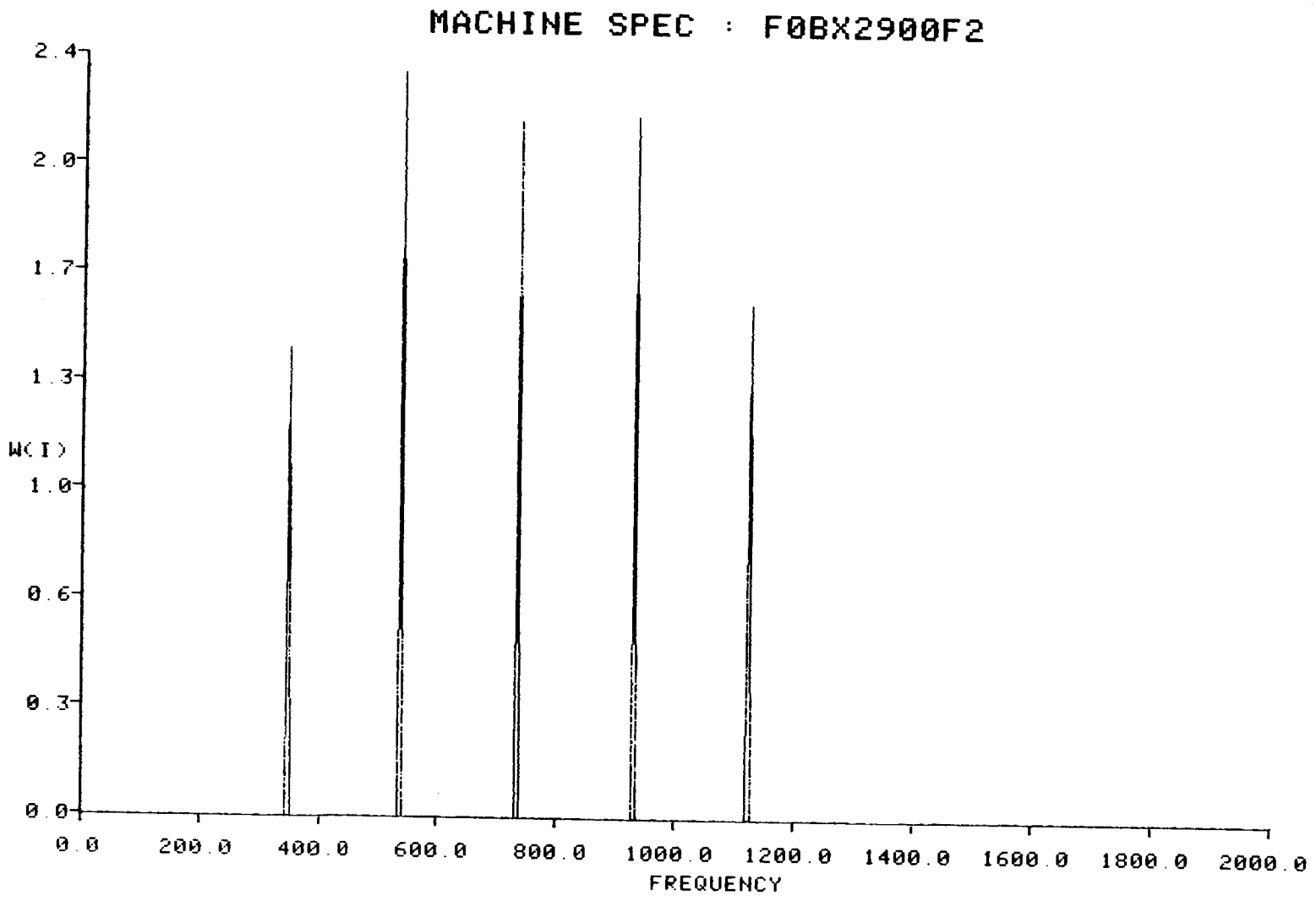

1. REFIT # L7 FRF
2. REFIT # L7 BB CONTINUUM FRF

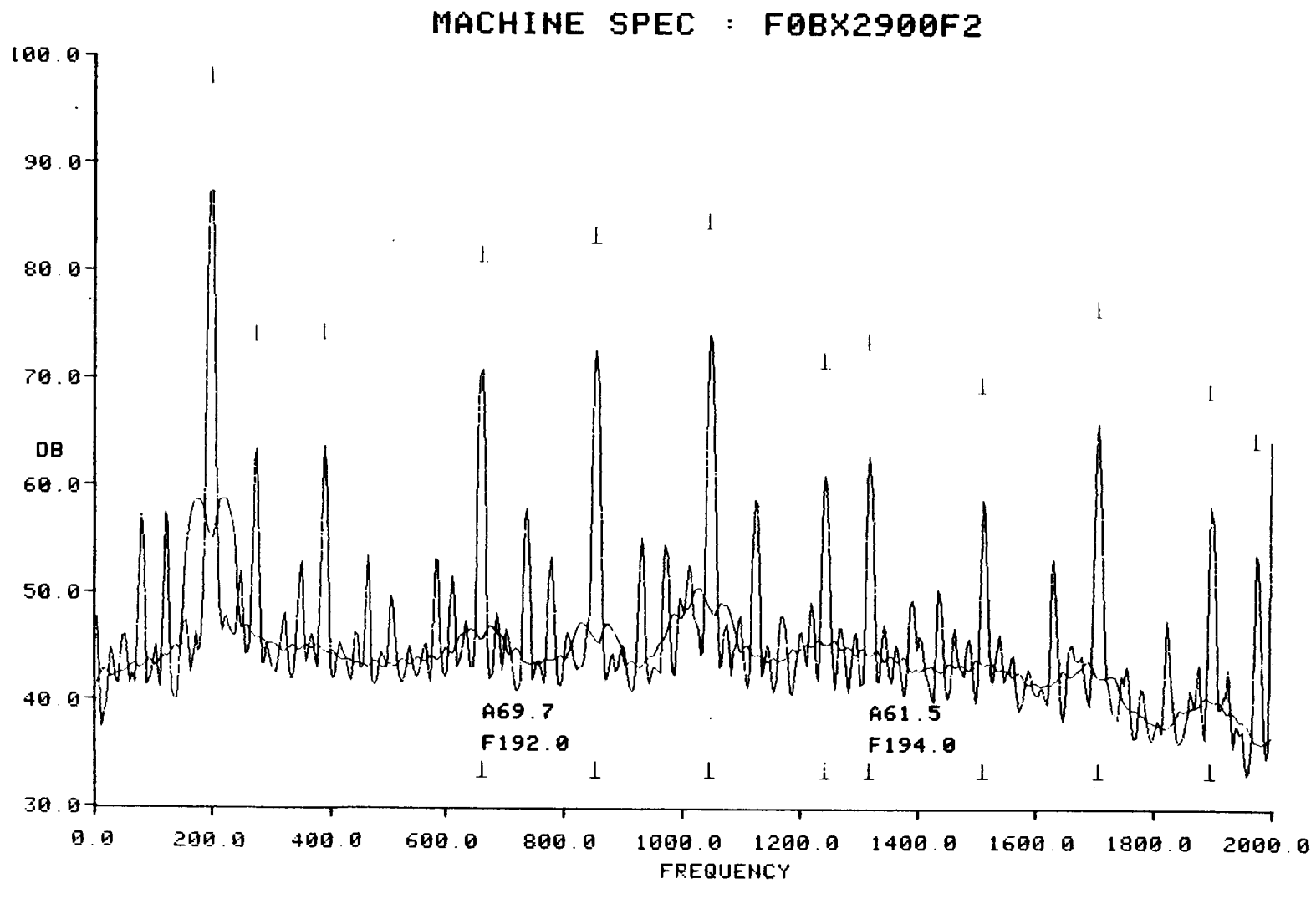

MEAN FOR FAULTED REFITS
MEAN FOR BASELINE REFITS
SIGMA FOR FAULTED REFITS
SIGMA FOR BASELINE REFITS

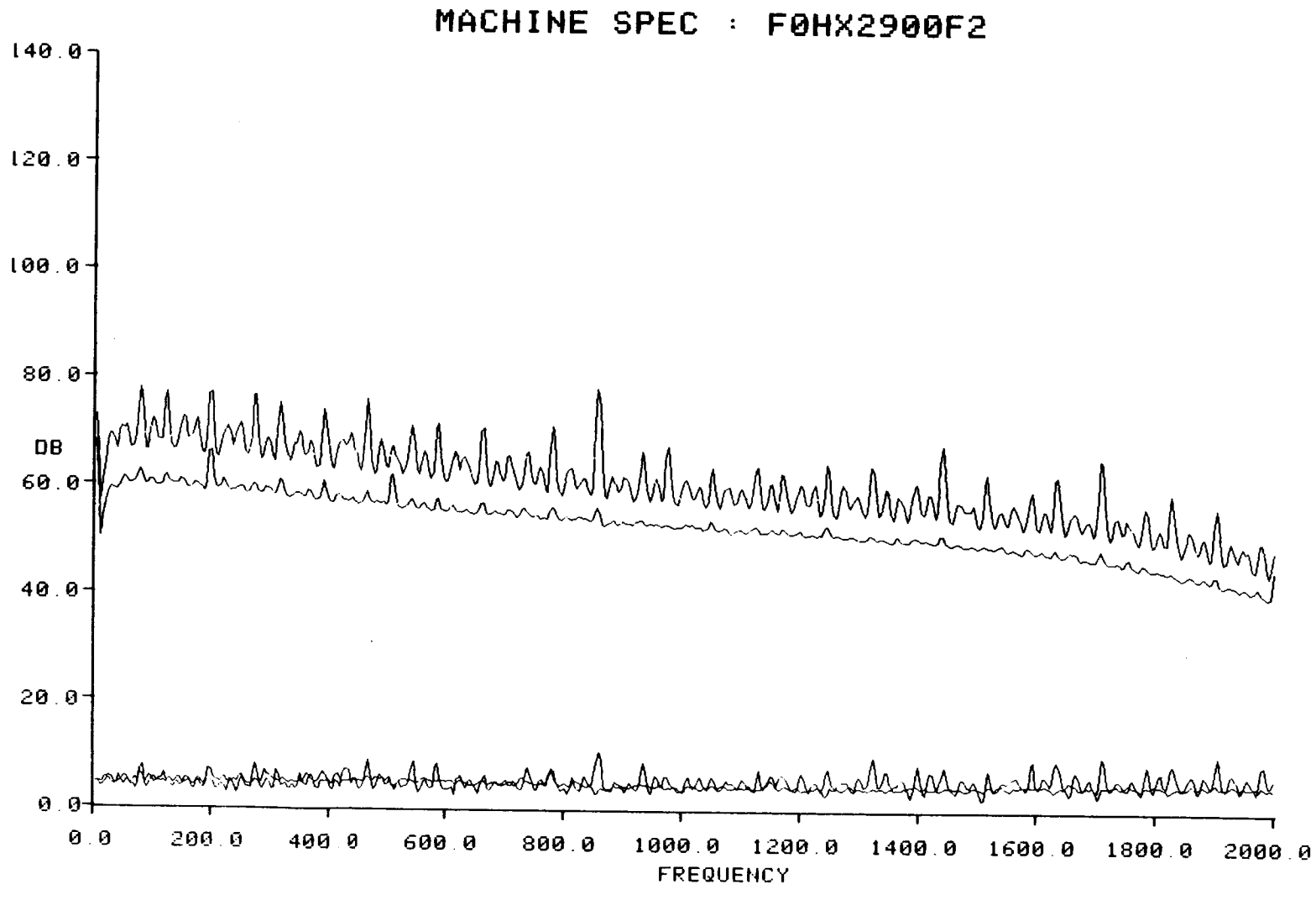

LIKELIHOOD RATIO WEIGHTS

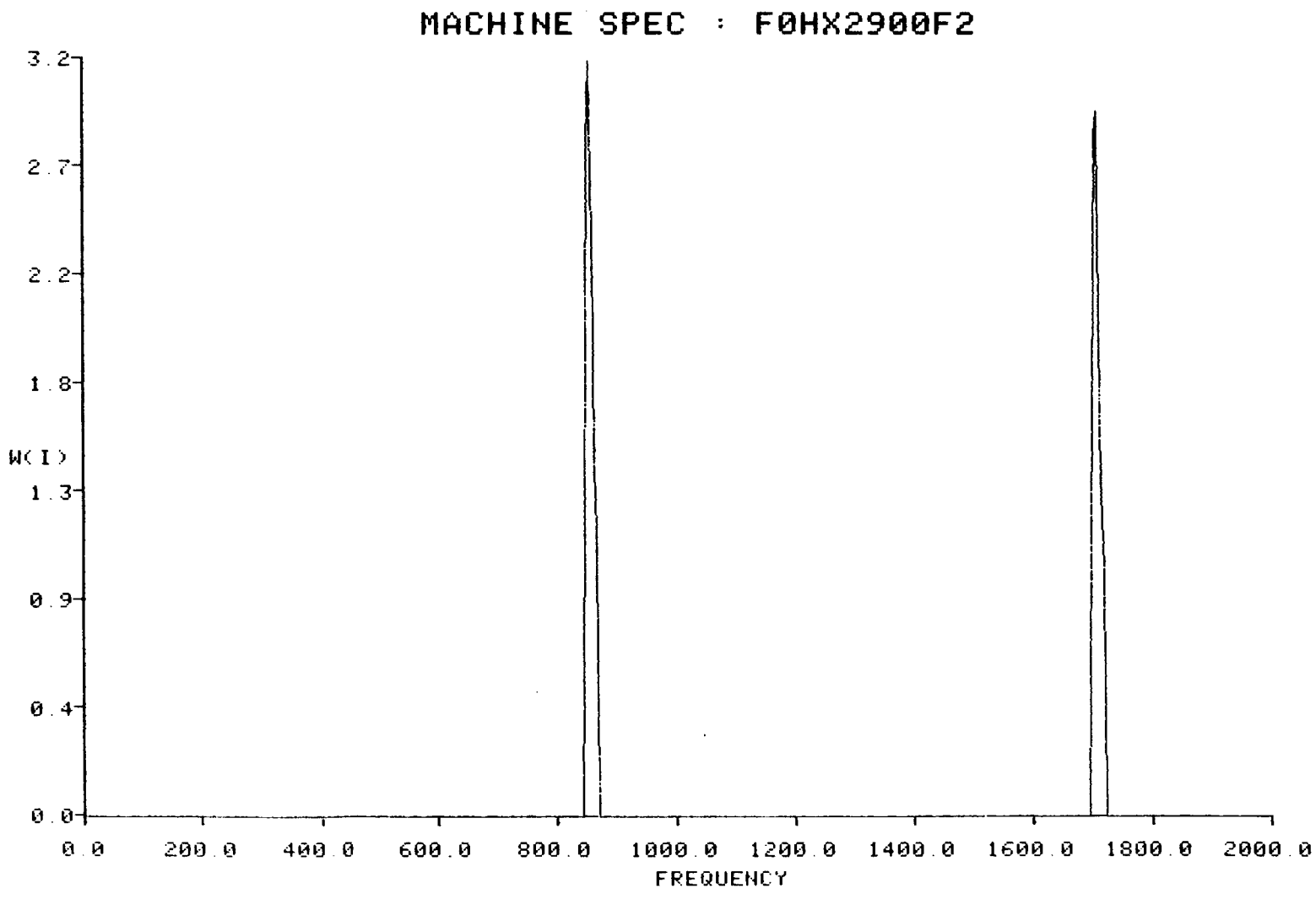

OPTIMUM SIGNATURE ANALYSIS DETECTION - Bearing Inner Race Fault - Single Fan

P_D for P_{FA} = 0.1

Baseband	HFD
0.83	0.90

OUTER RACE FAULTS - SINGLE FAN

TEST DESCRIPTION: Outer Race Fault - Single Fan

A series of tests was performed in which a single outer race fault was introduced onto the front bearing of the fan under test. The methodology of the test procedure for fault introduction was the same as was described in the inner race fault test description.

Results Presented:

Baseband - F0BX28G2F.2

1) Mean and standard deviation for the baseline and faulted refits.
2) Unmodified likelihood ratio weights.
3) Modified likelihood ratio weights (all weights set to zero except for BPFO (512 Hz) and its harmonics).

High Frequency Demodulation - F0HX28G2F.2

4) Mean and standard deviation for the baseline and faulted refits.
5) Unmodified likelihood ratio weights.
6) Modified likelihood ratio weights (all weights set to zero except for BPFO and its harmonics).

MEAN FOR FAULTED REFITS
MEAN FOR BASELINE REFITS
SIGMA FOR FAULTED REFITS
SIGMA FOR BASELINE REFITS

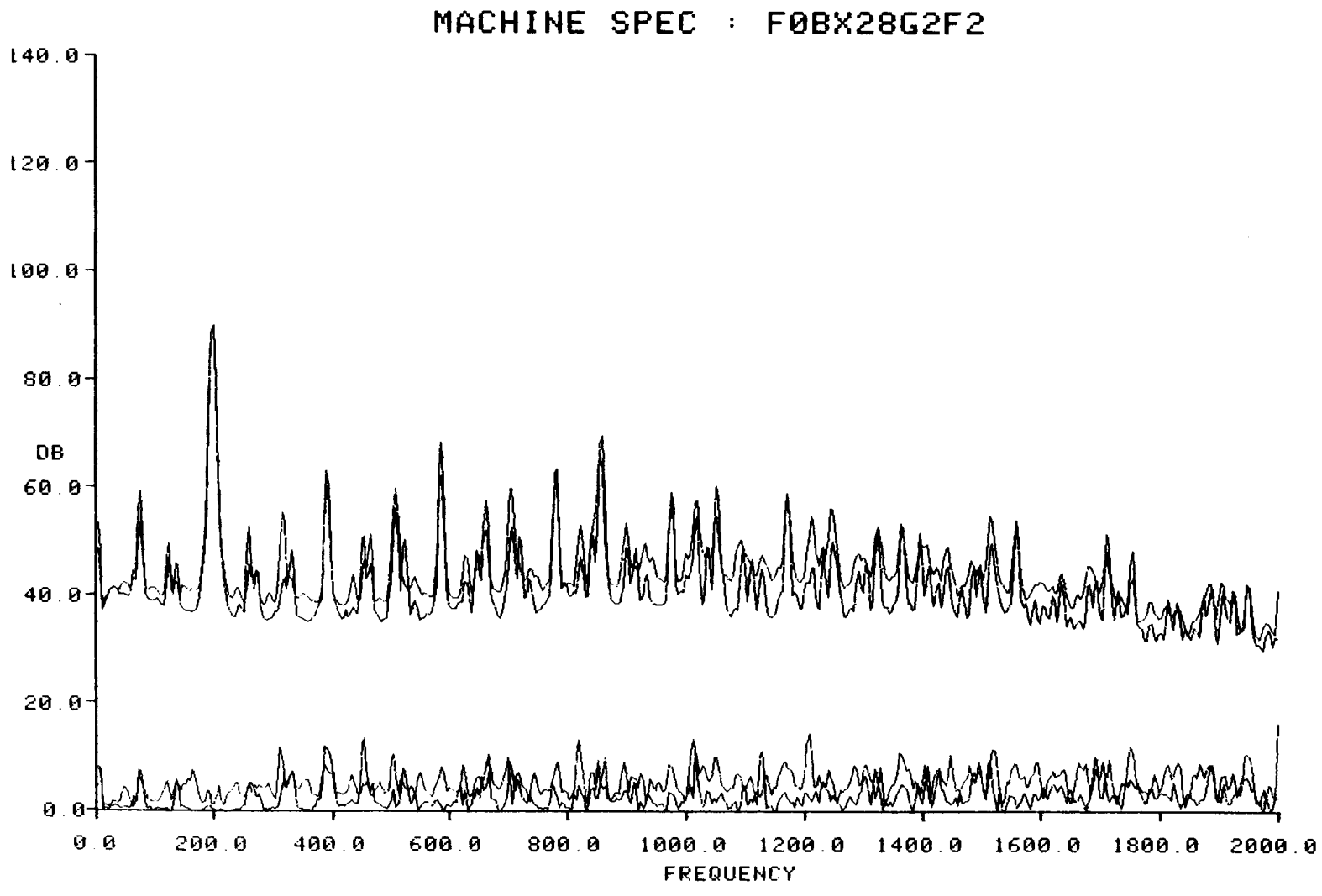

LIKELIHOOD RATIO WEIGHTS

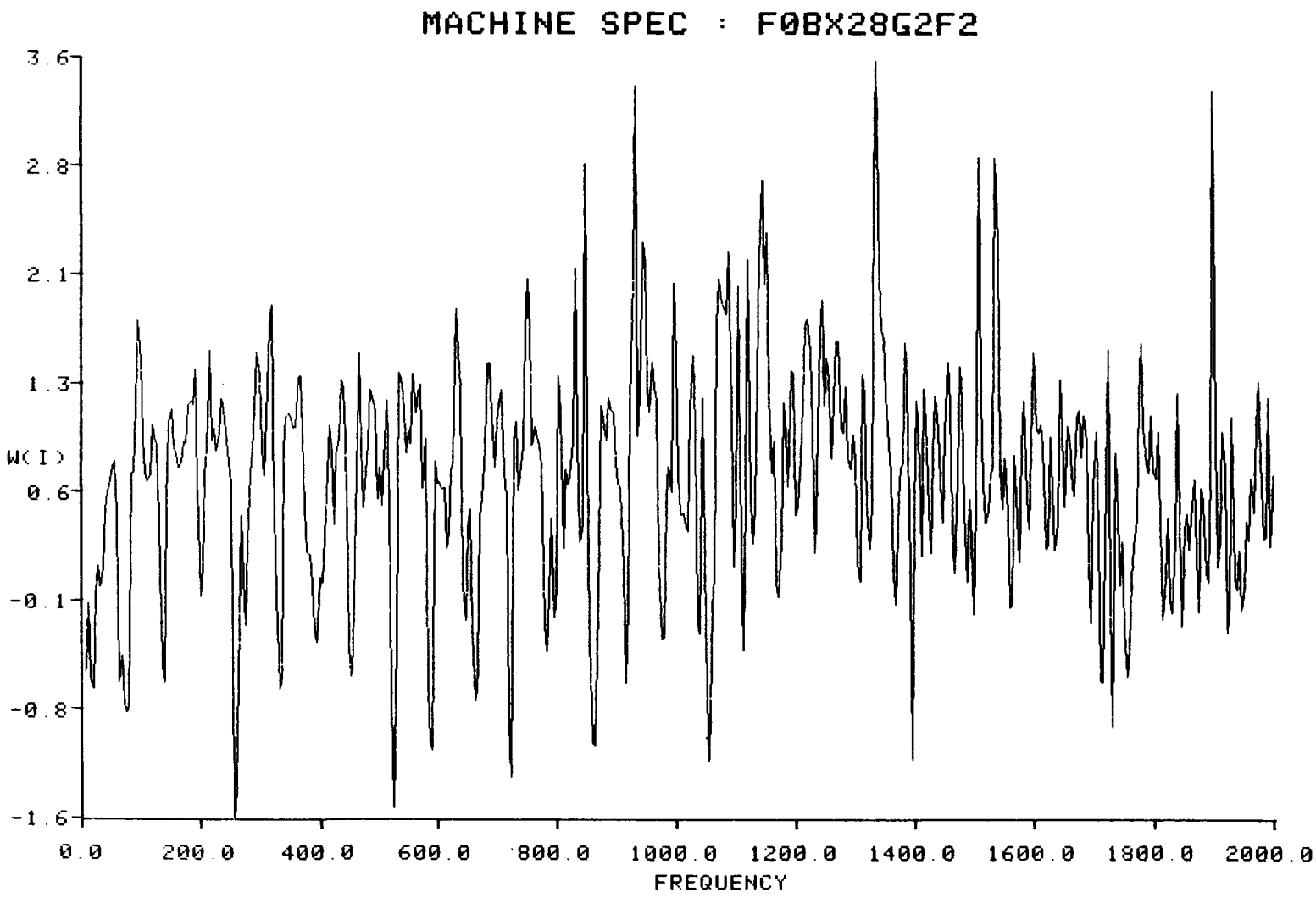

LIKELIHOOD RATIO WEIGHTS

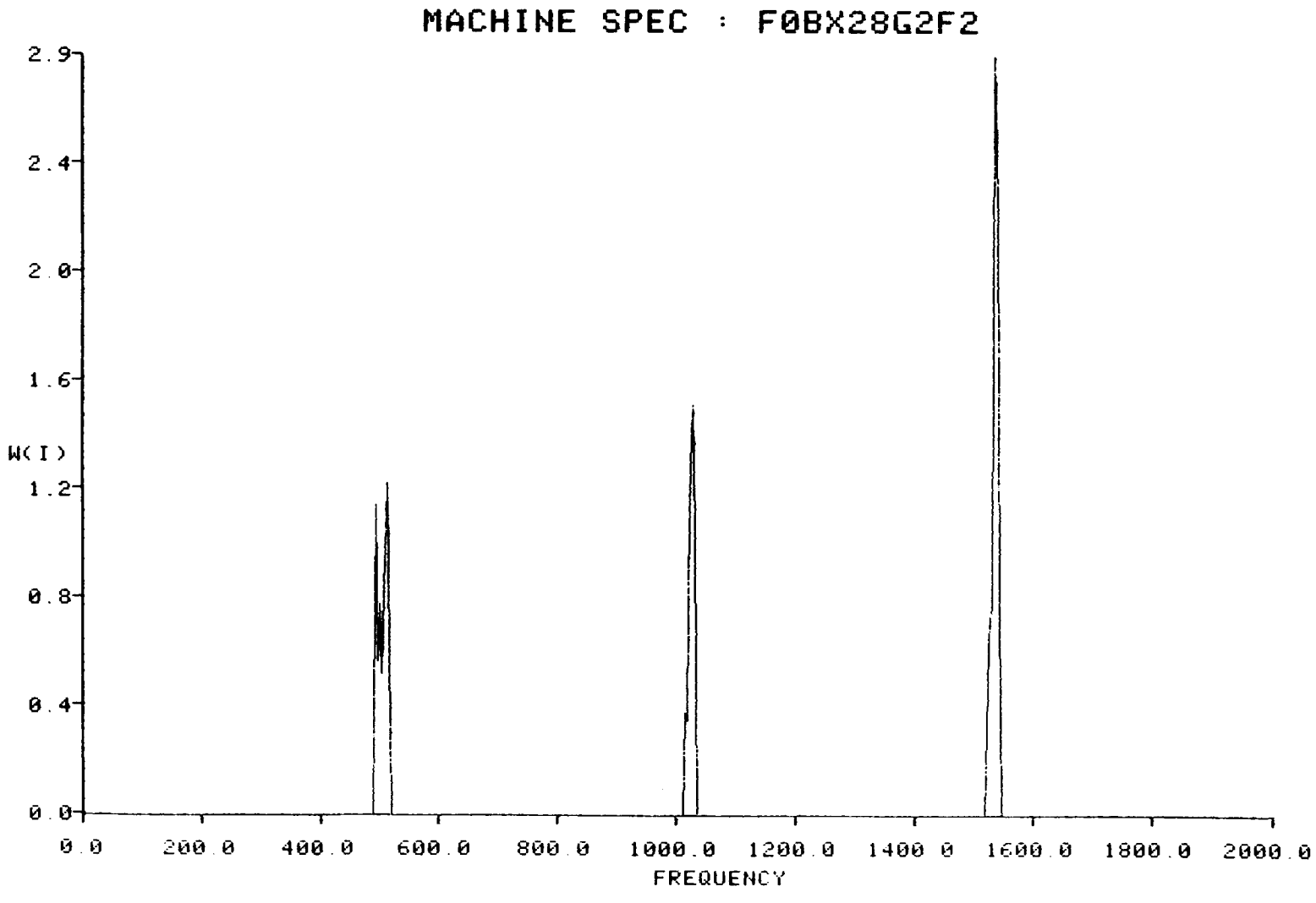

MEAN FOR FAULTED REFITS
MEAN FOR BASELINE REFITS
SIGMA FOR FAULTED REFITS
SIGMA FOR BASELINE REFITS

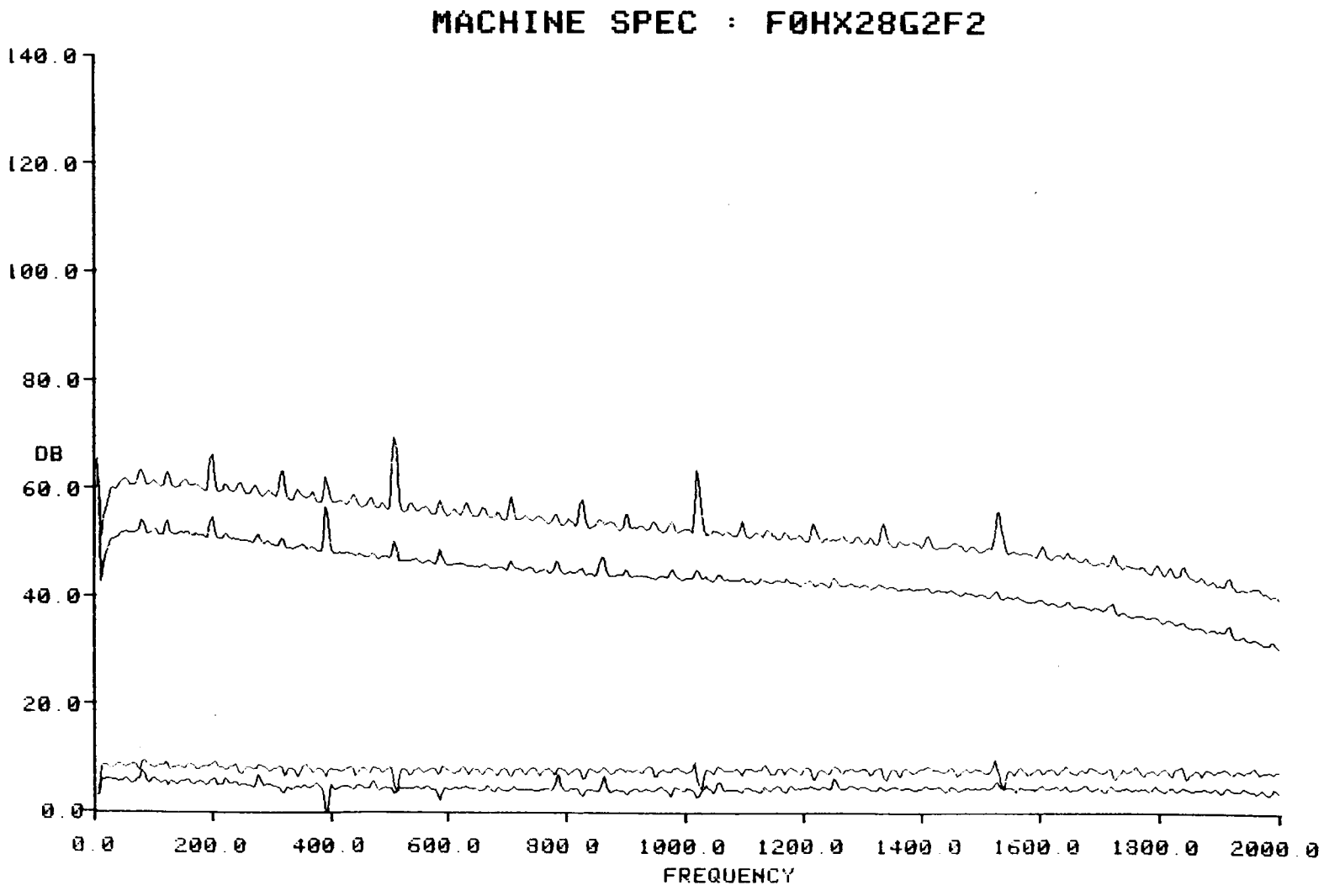

LIKELIHOOD RATIO WEIGHTS

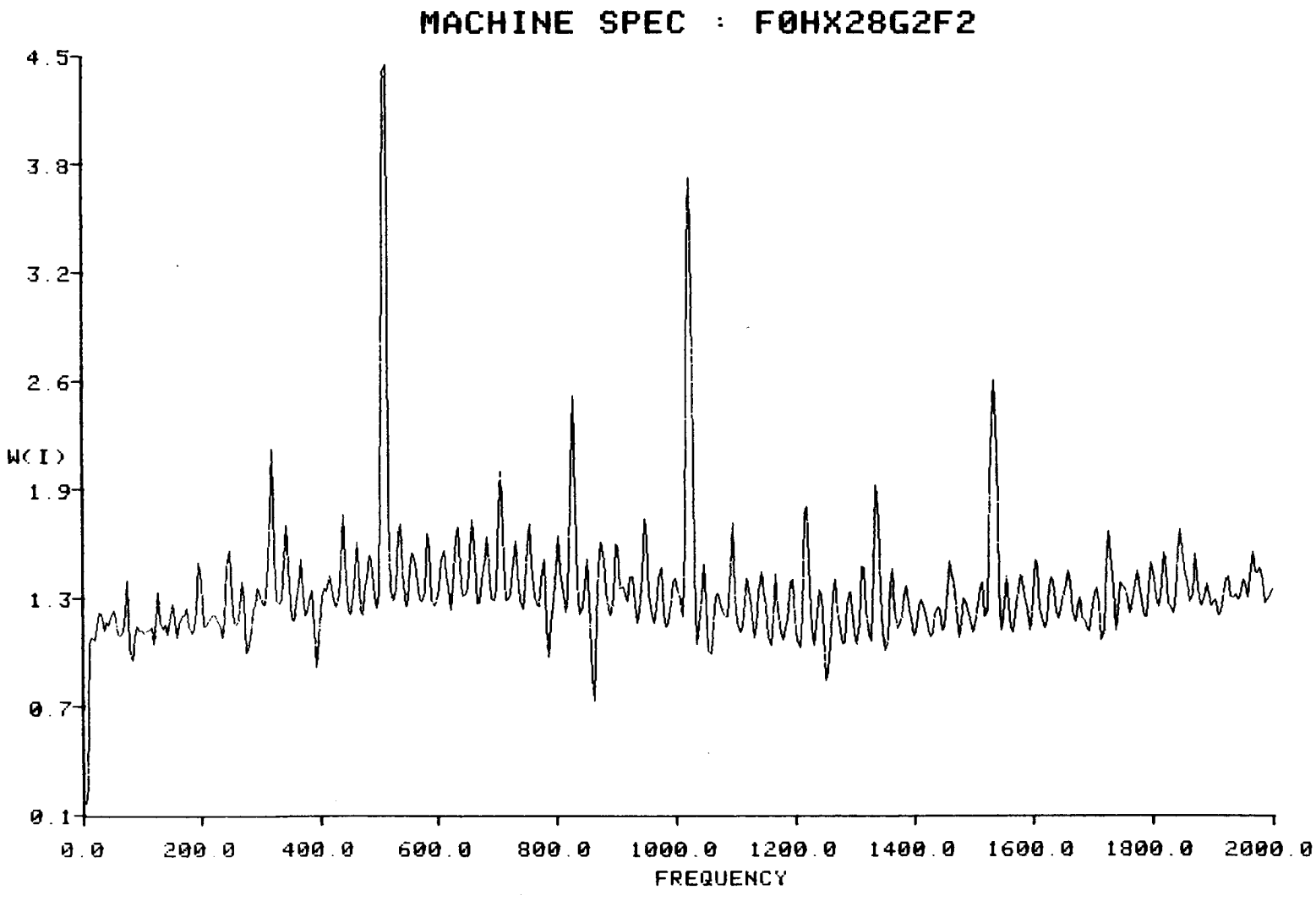

LIKELIHOOD RATIO WEIGHTS

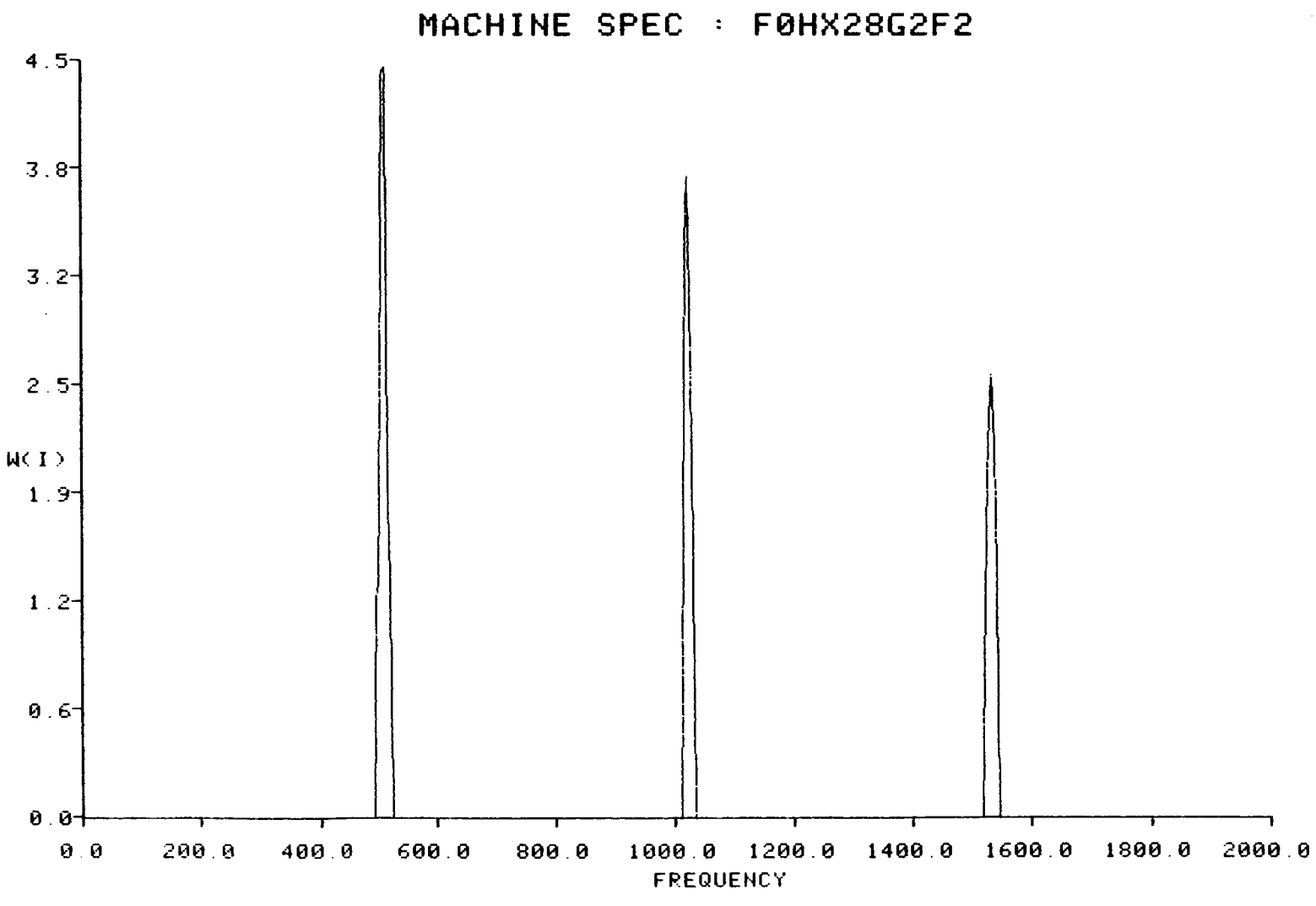

OPTIMUM SIGNATURE ANALYSIS DETECTION - Outer Race Faults - Single Fan

P_D for P_{FA} = 0.1

Baseband	HFD
0.91	0.80

IMPELLER WEAR - MULTIPLE SINGLE PHASE PUMPS

TEST DESCRIPTION: Impeller Wear - Multiple Single Phase Pumps

A series of test was performed in which the faulted condition of impeller wear on the gear teeth was evaluated on each of the four single phase test pumps. A set of baselines was collected with the pumps running normally, after which the pumping fluid was removed. The pumps were allowed to run dry an average of 16 hours. The pumping fluid was then reapplied to the pumps and a set of faulted data was obtained. Both baseband and high frequency demodulation data were obtained simultaneously.

Results Presented:

Baseband - P1BX38SPF.2

1) Mean and standard deviation for the baseline and faulted refits.
2) Unmodified likelihood ratio weights.

High Frequency Demodulation - P1HX38SPF.2

3) Mean and standard deviation for the baseline and faulted refits.
4) Unmodified likelihood ratio weights.

MEAN FOR FAULTED REFITS
MEAN FOR BASELINE REFITS
SIGMA FOR FAULTED REFITS
SIGMA FOR BASELINE REFITS

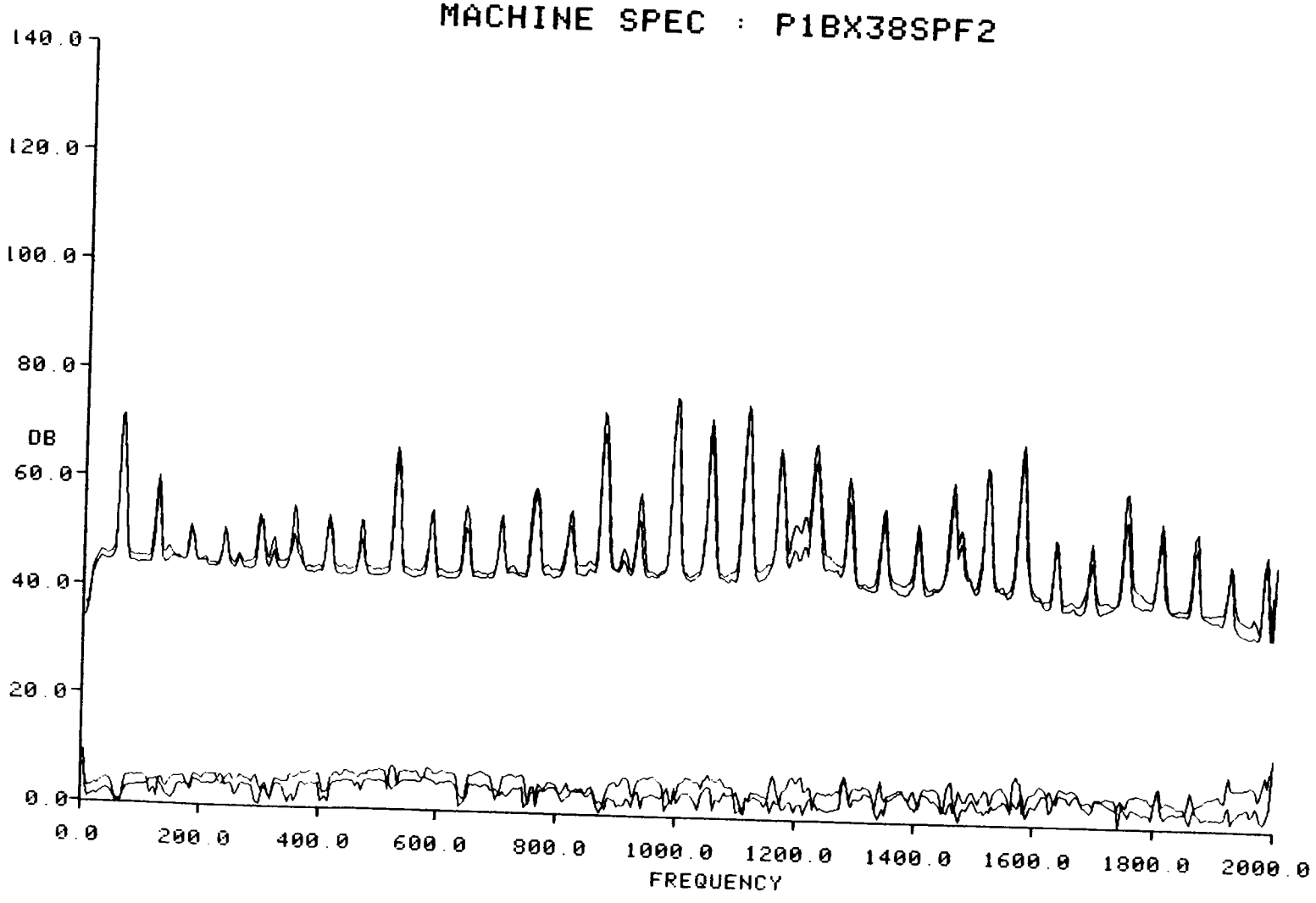

LIKELIHOOD RATIO WEIGHTS

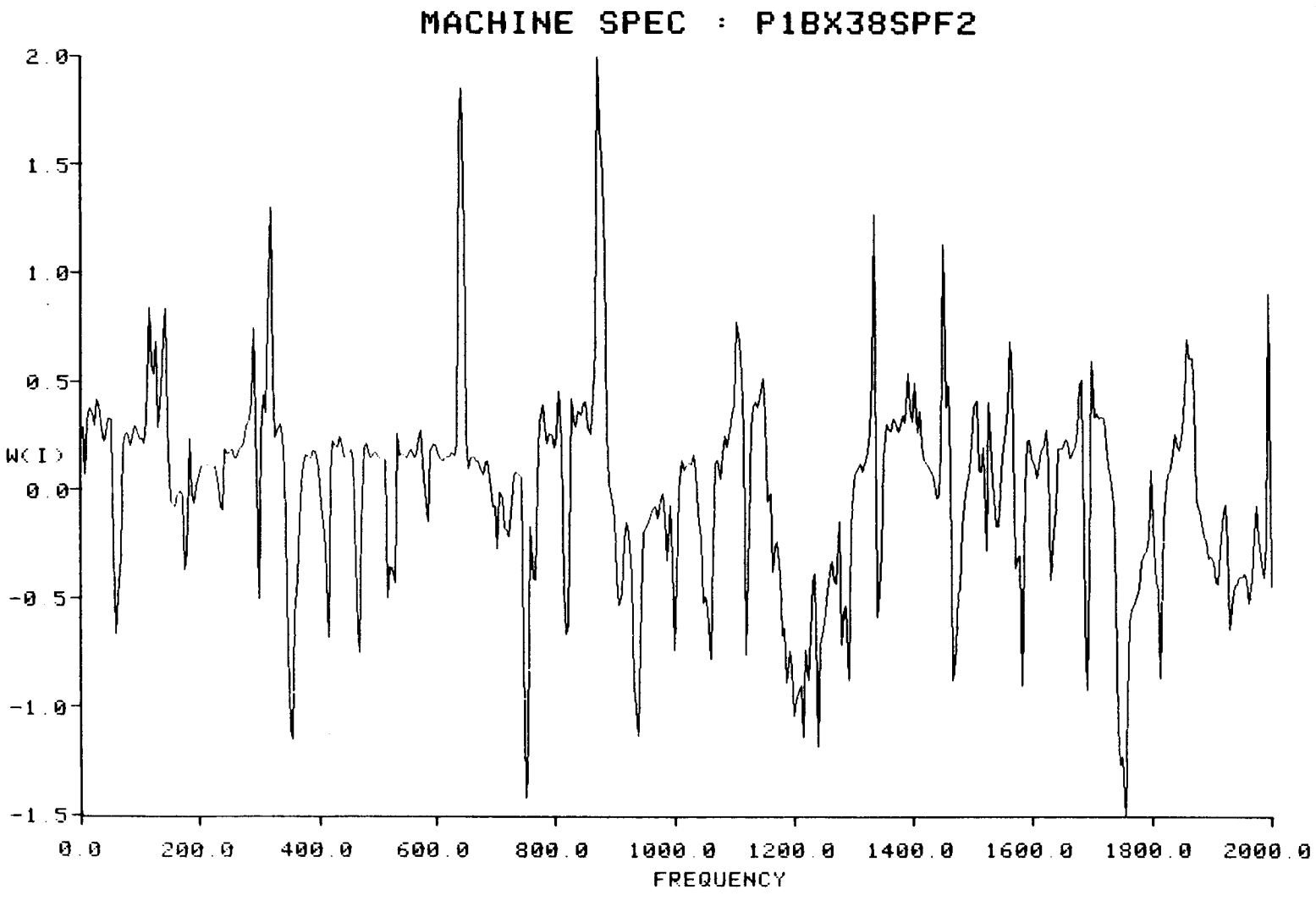

MEAN FOR FAULTED REFITS
MEAN FOR BASELINE REFITS
SIGMA FOR FAULTED REFITS
SIGMA FOR BASELINE REFITS

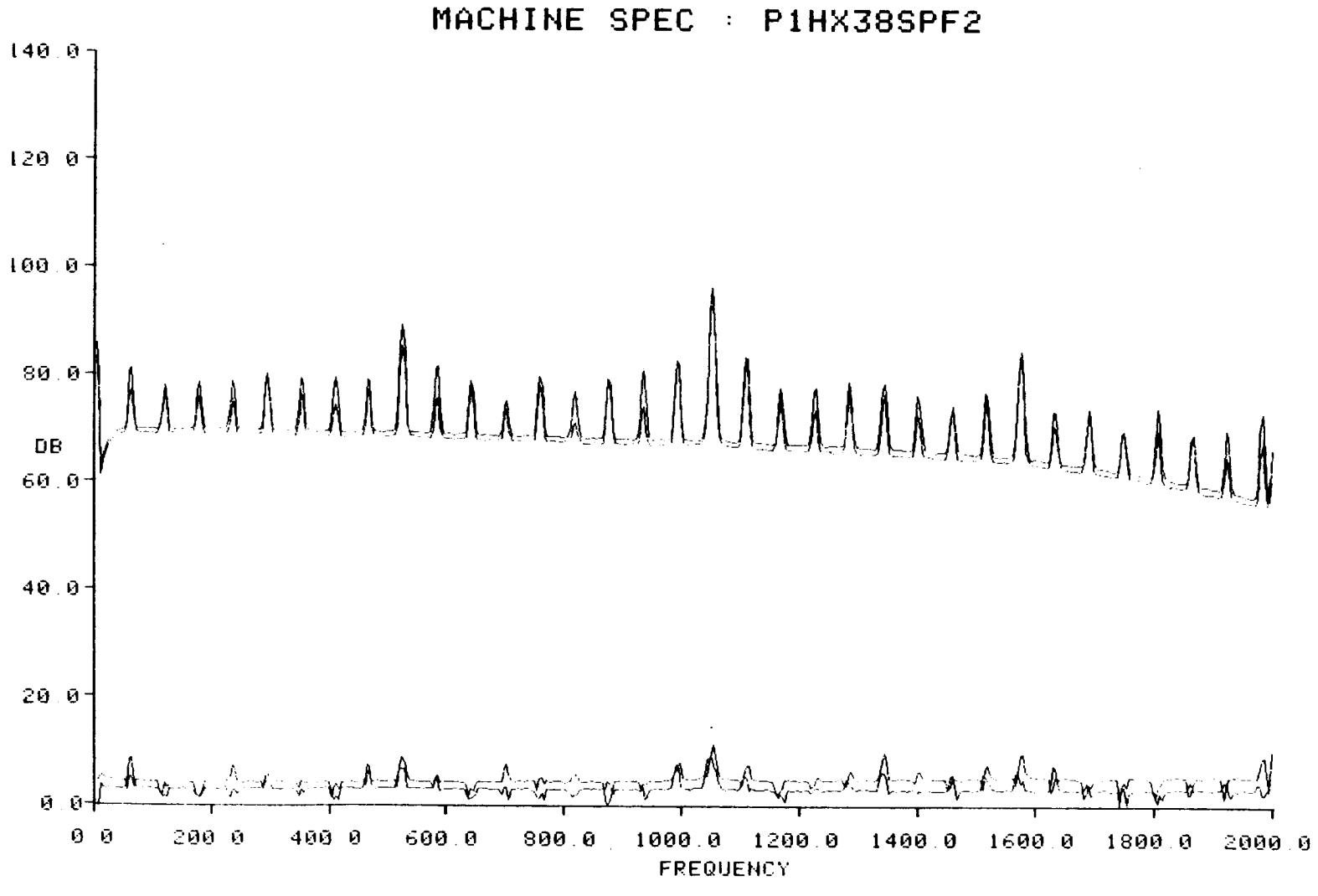

LIKELIHOOD RATIO WEIGHTS

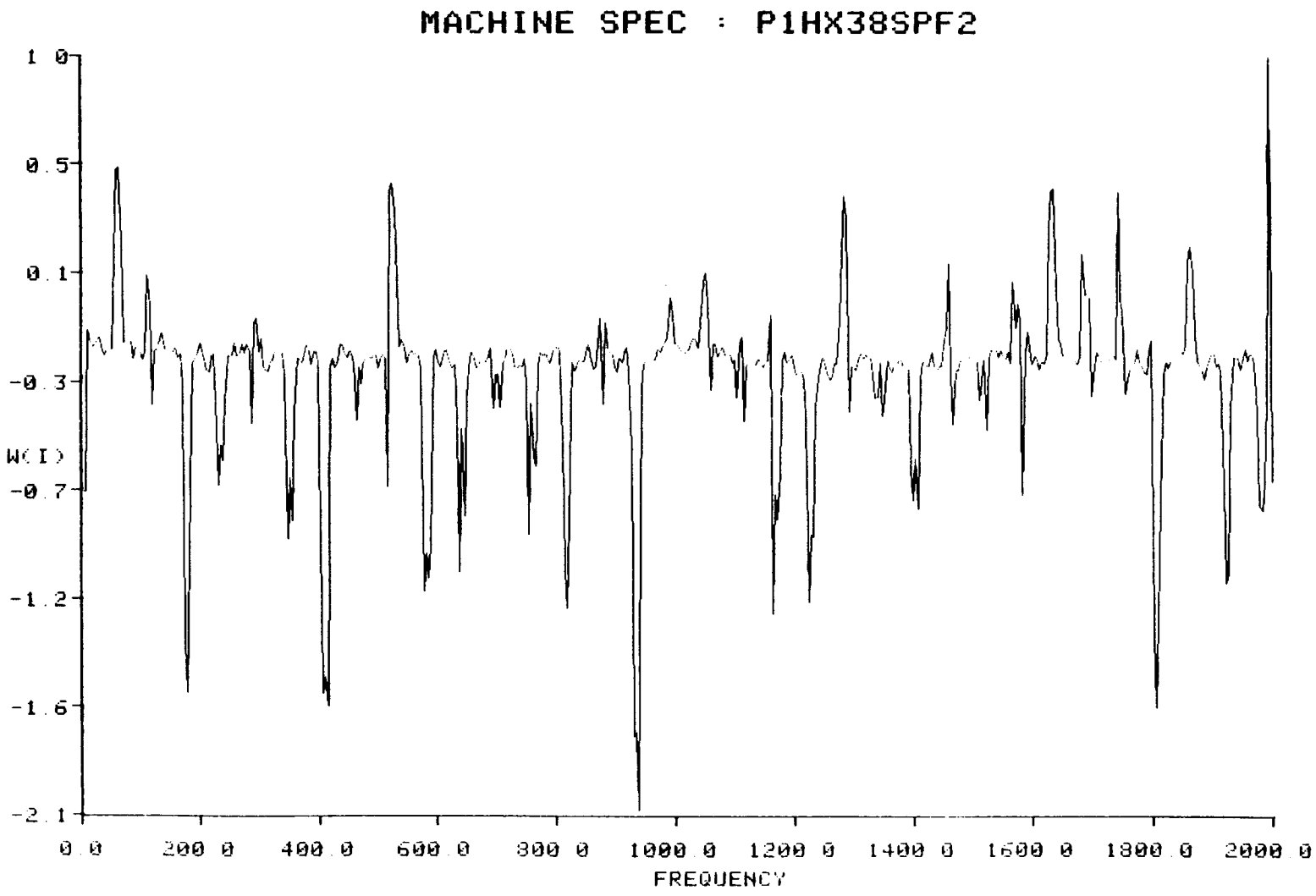

OPTIMUM SIGNATURE ANALYSIS DETECTION:
Impeller Wear - Multiple Single Phase Pumps

P_D for P_{FA} = 0.1

Baseband	HFD
0.70	0.43

BEARING LOSS OF LUBRICANT - SINGLE THREE PHASE PUMP

TEST DESCRIPTION: Bearing Loss of Lubricant - Single Three Phase Pump

In a series of ongoing tests, the condition of bearing loss of lubricant in a single three phase pump was evaluated. A series of four baseline readings were collected on a three phase pump with new motor bearings installed. The pump was then stopped, disassembled, and all the lubricant removed from the front bearing (with respect to the pump head). The automated data collection system on the VAX was then employed after the pump was restarted. The pump was allowed to run to failure.

The results presented a collection of faulted conditions from two tests. The pump failed within two hours for both test cases.

Results Presented:

Baseband - P3BX46A0F.2

1) Mean and standard deviation for the baseline and faulted refits.
2) Modified likelihood ratio weights (FRF and DC component contribution set to zero.)

Note:
1) Spurious decrease in the standard deviation at 550 Hz produces the large positive weight.
2) Minimum change at pumping frequencies when combined with the continuum increase at low frequency may be the best identifier.

MEAN FOR FAULTED REFITS
MEAN FOR BASELINE REFITS
SIGMA FOR FAULTED REFITS
SIGMA FOR BASELINE REFITS

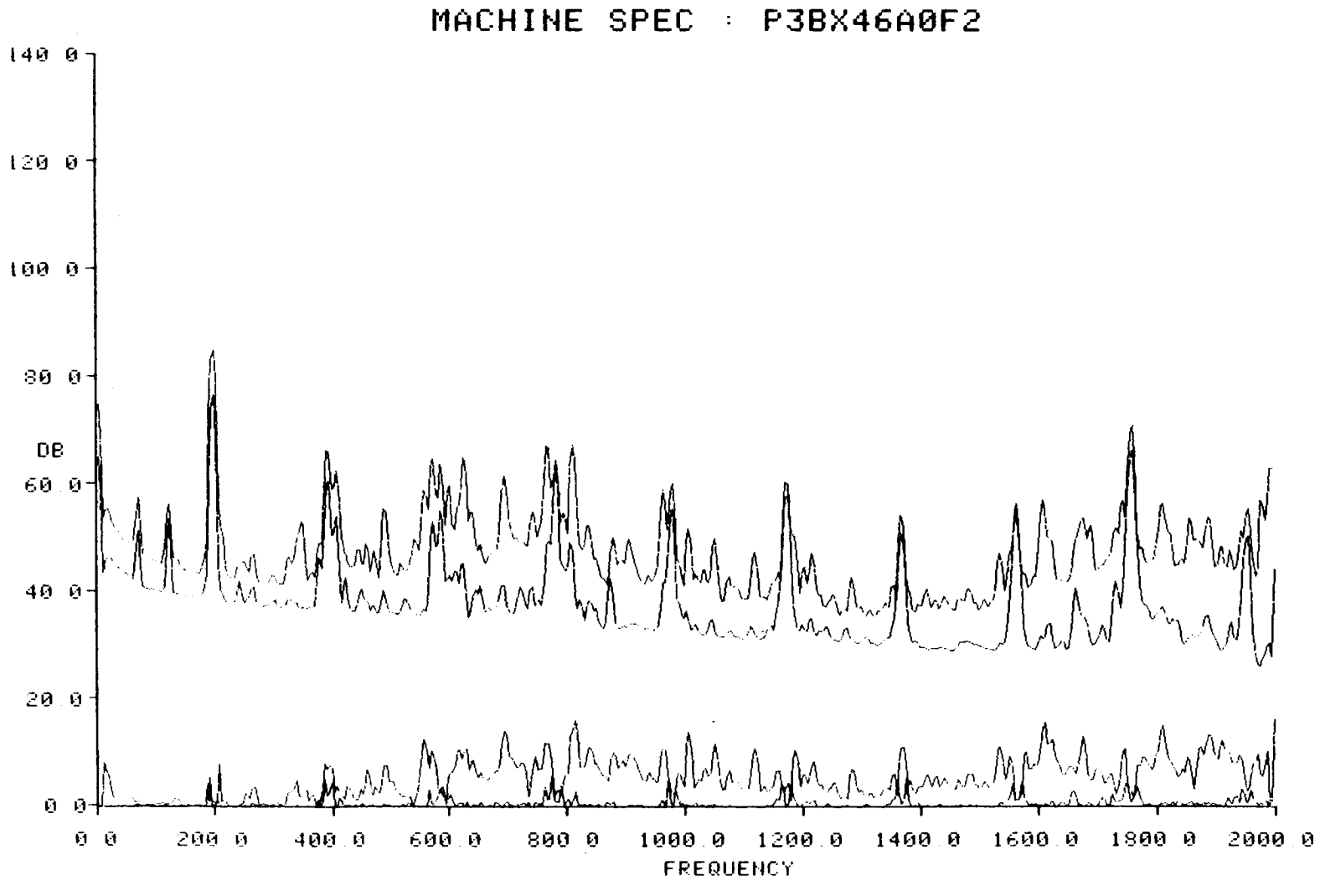

LIKELIHOOD RATIO WEIGHTS

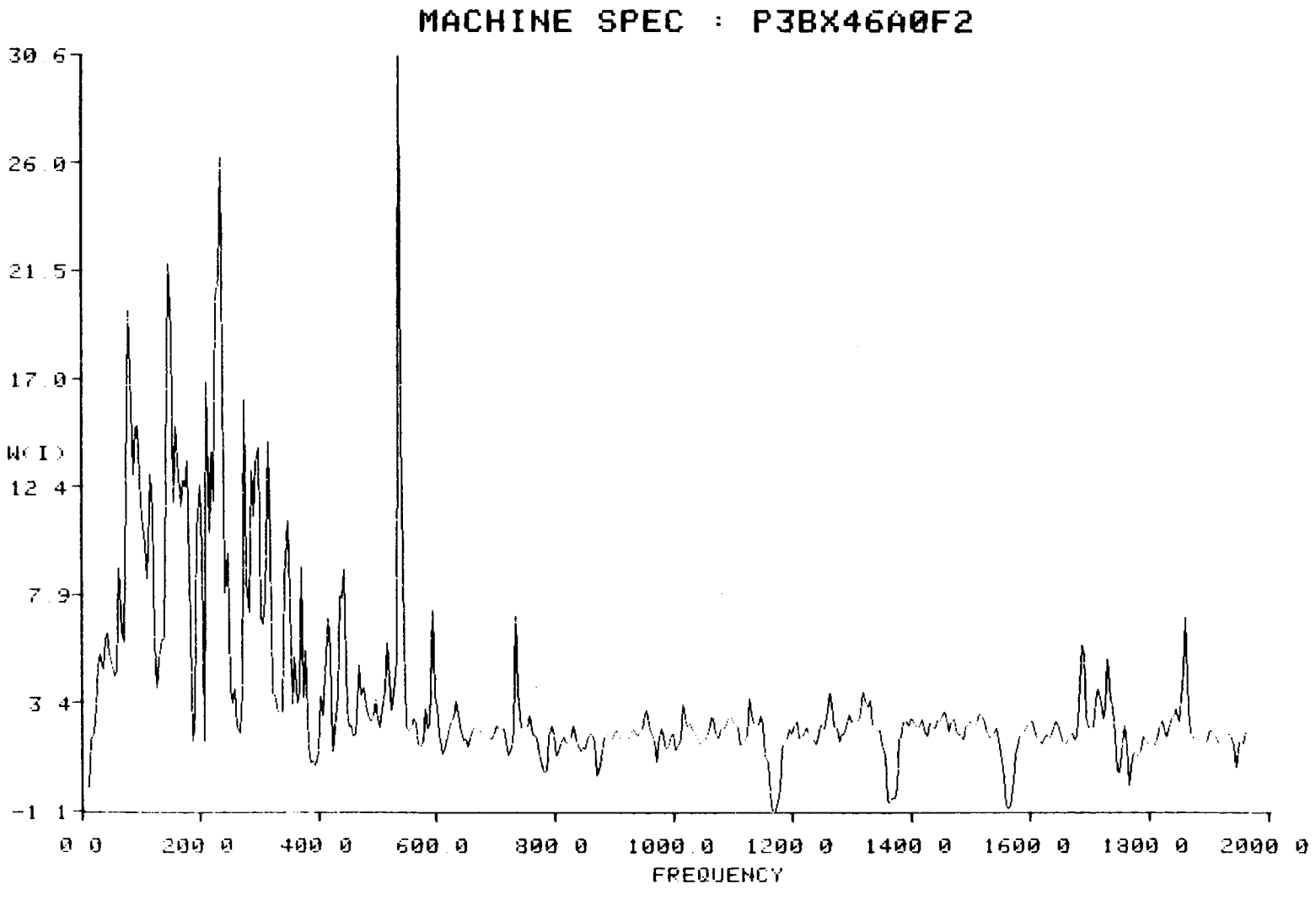

OPTIMUM SIGNATURE ANALYSIS DETECTION:
Bearing Loss of Lubricant - Single Three Phase Pump

P_D for P_{FA} = 0.1

Baseband	HFD
1.0	1.0

IMPELLER FAULT - SINGLE ONE-PHASE PUMP

TEST DESCRIPTION: Impeller Fault - Single One-Phase Pump

A series of tests was performed on a single one-phase pump in which an impeller fault was evaluated. A baseline was collected with the pump running normally. The pump was then stopped, the head disassembled, and the tip of one of the driven gear teeth was shaved across the entire width of the tooth. The pump was then reassembled and the faulted data was collected. Both baseband and high frequency demodulation data were obtained simultaneously.

Results Presented:

Baseband

1) Collection of baseline refits - P1BXX490B.2
2) Collection of faulted refits - P1BXX490F.2
3) Mean and standard deviation for the baseline and faulted refits.
4) Unmodified likelihood ratio weights.

High Frequency Demodulation

5) Collection of baseline refits - P1HXX490B.2
6) Collection of faulted refits - P1HXX490F.2
7) Mean and standard deviation for the baseline and faulted refits.
8) Unmodified likelihood ratio weights.

1. REFIT # ME RAW NS
2. REFIT # MD RAW NS
3. REFIT # MC RAW NS

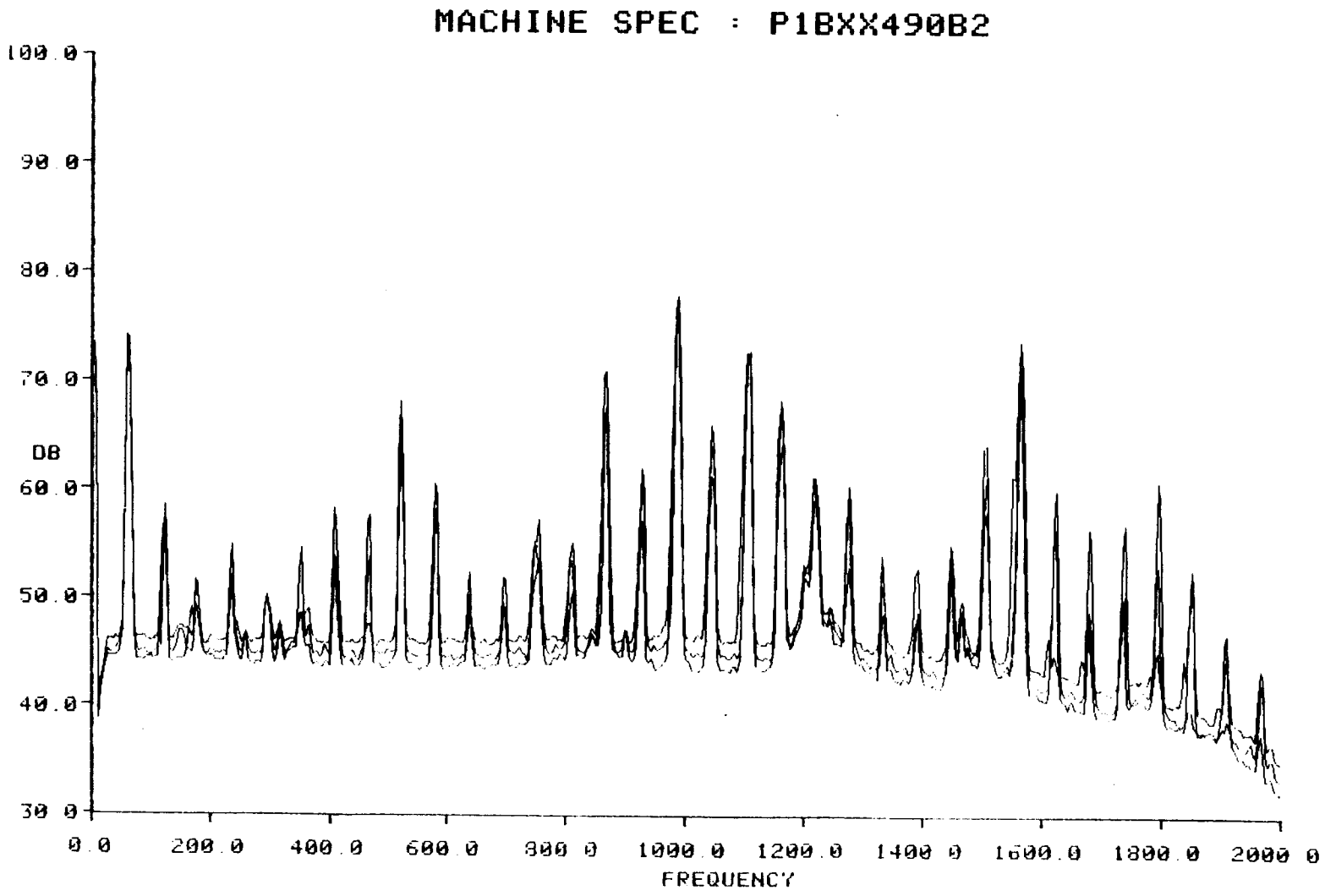

1. REFIT # MM RAW NS
2. REFIT # ML RAW NS
3. REFIT # MK RAW NS

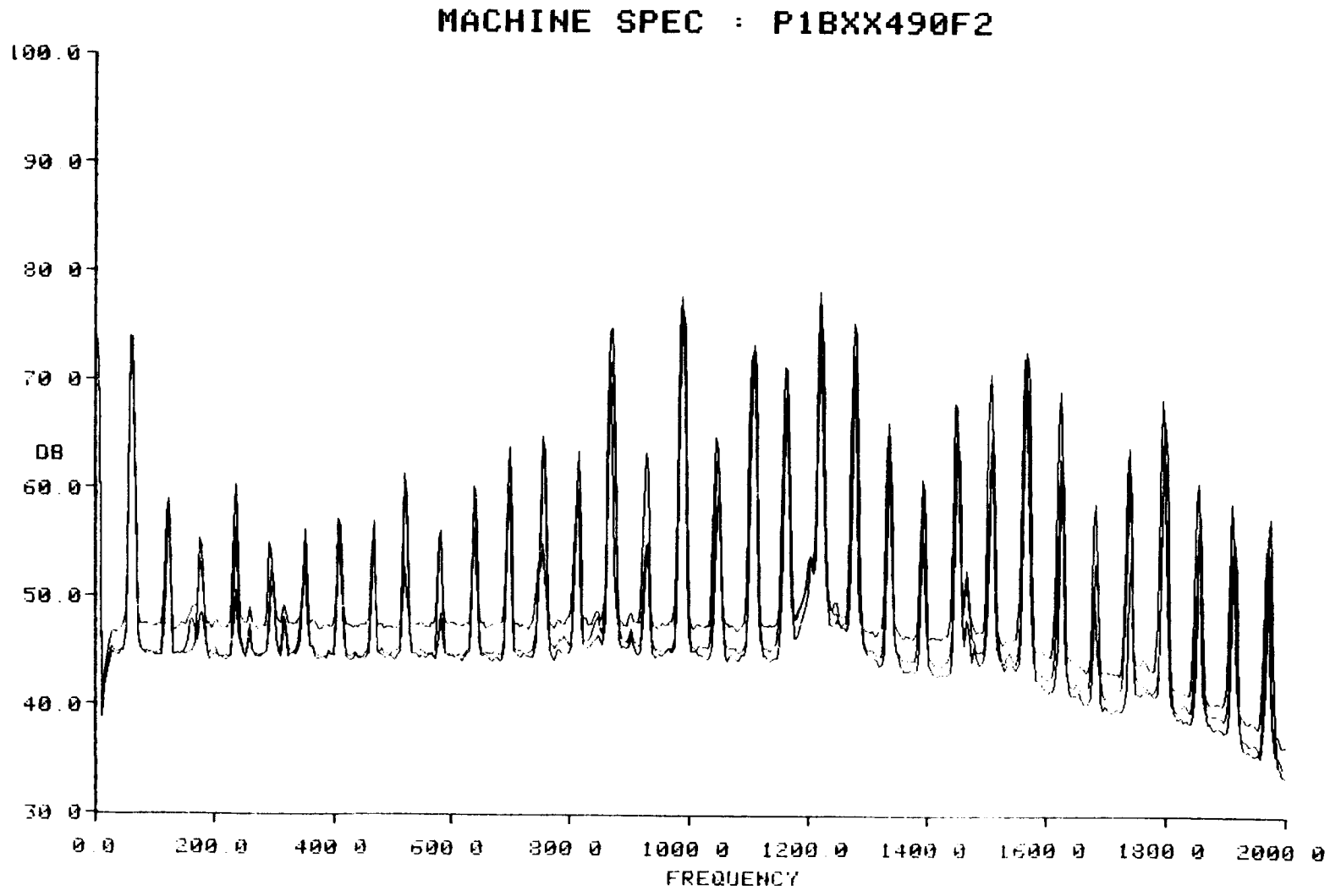

MEAN FOR FAULTED REFITS
MEAN FOR BASELINE REFITS
SIGMA FOR FAULTED REFITS
SIGMA FOR BASELINE REFITS

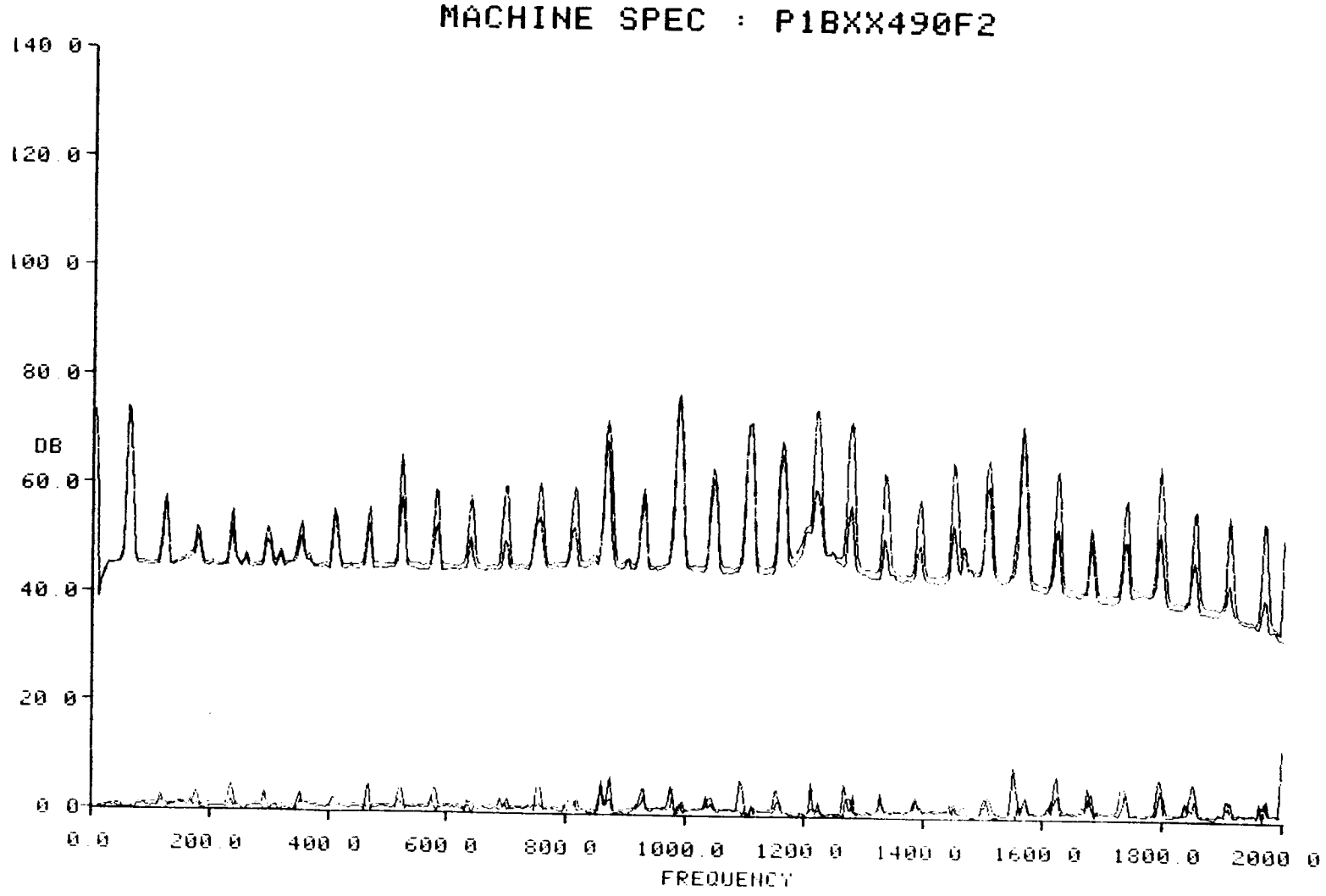

LIKELIHOOD RATIO WEIGHTS

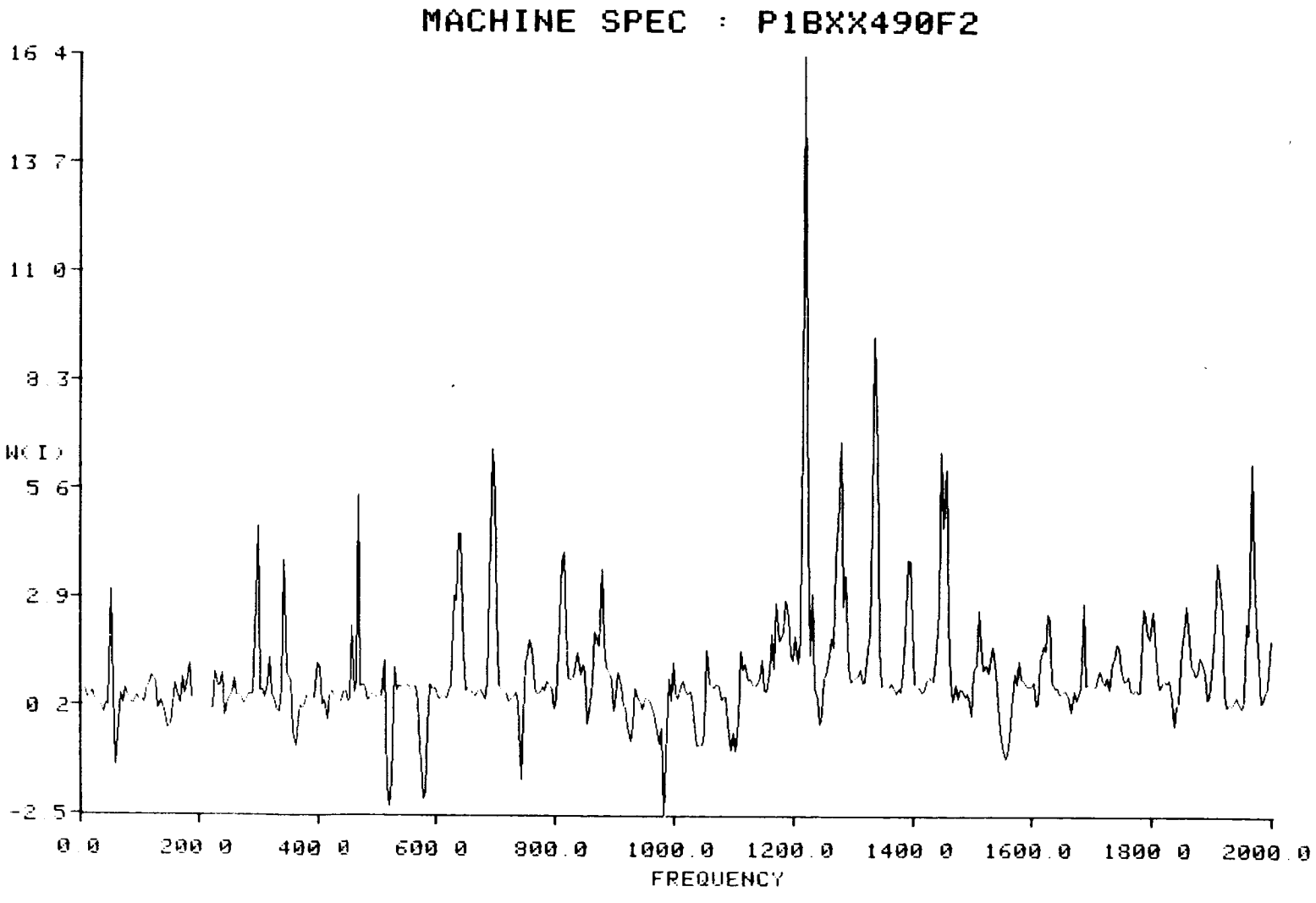

1. REFIT # MI RAW NS
2. REFIT # MH RAW NS
3. REFIT # MF RAW NS

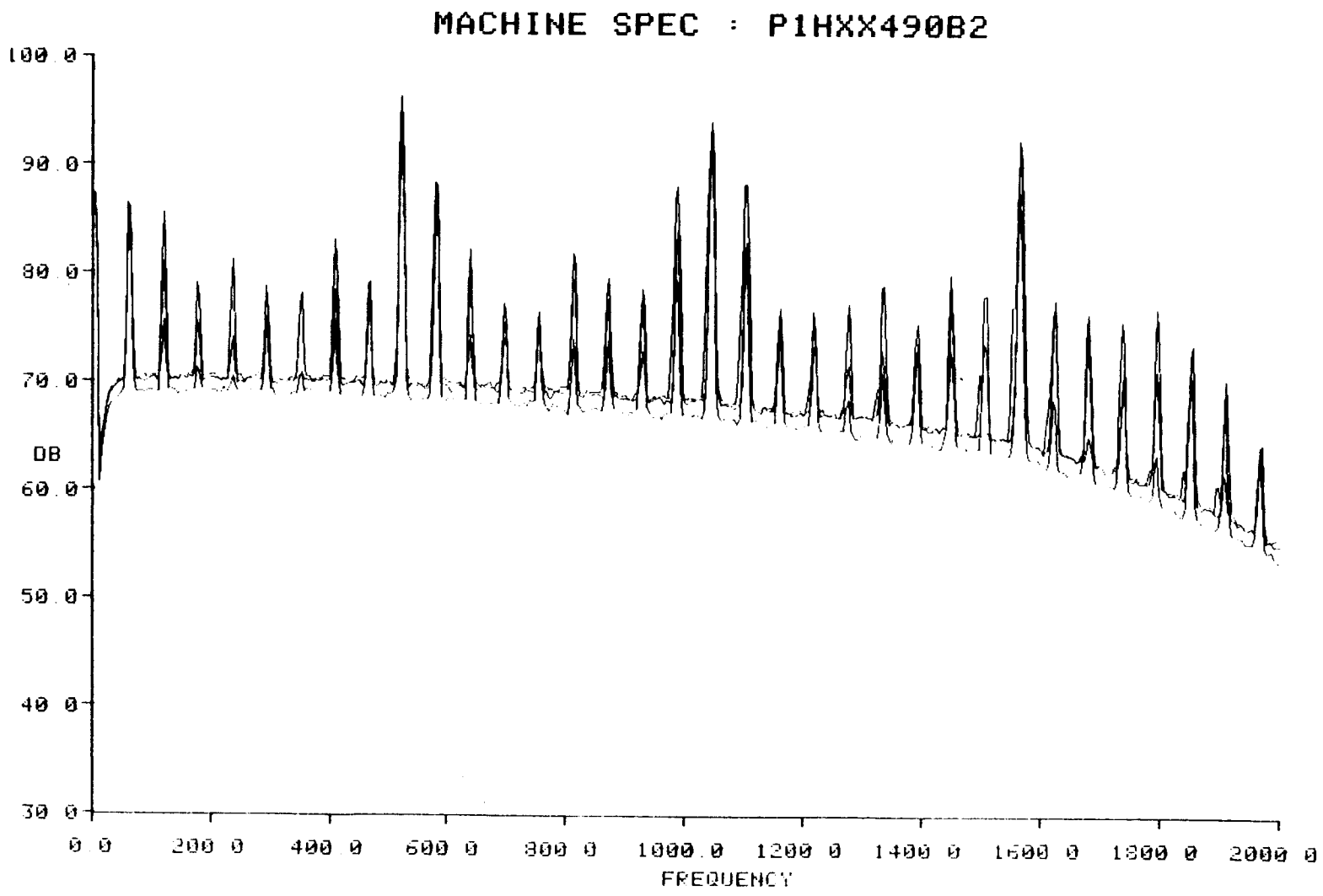

1. REFIT # MQ RAW NS
2. REFIT # MP RAW NS
3. REFIT # MO RAW NS

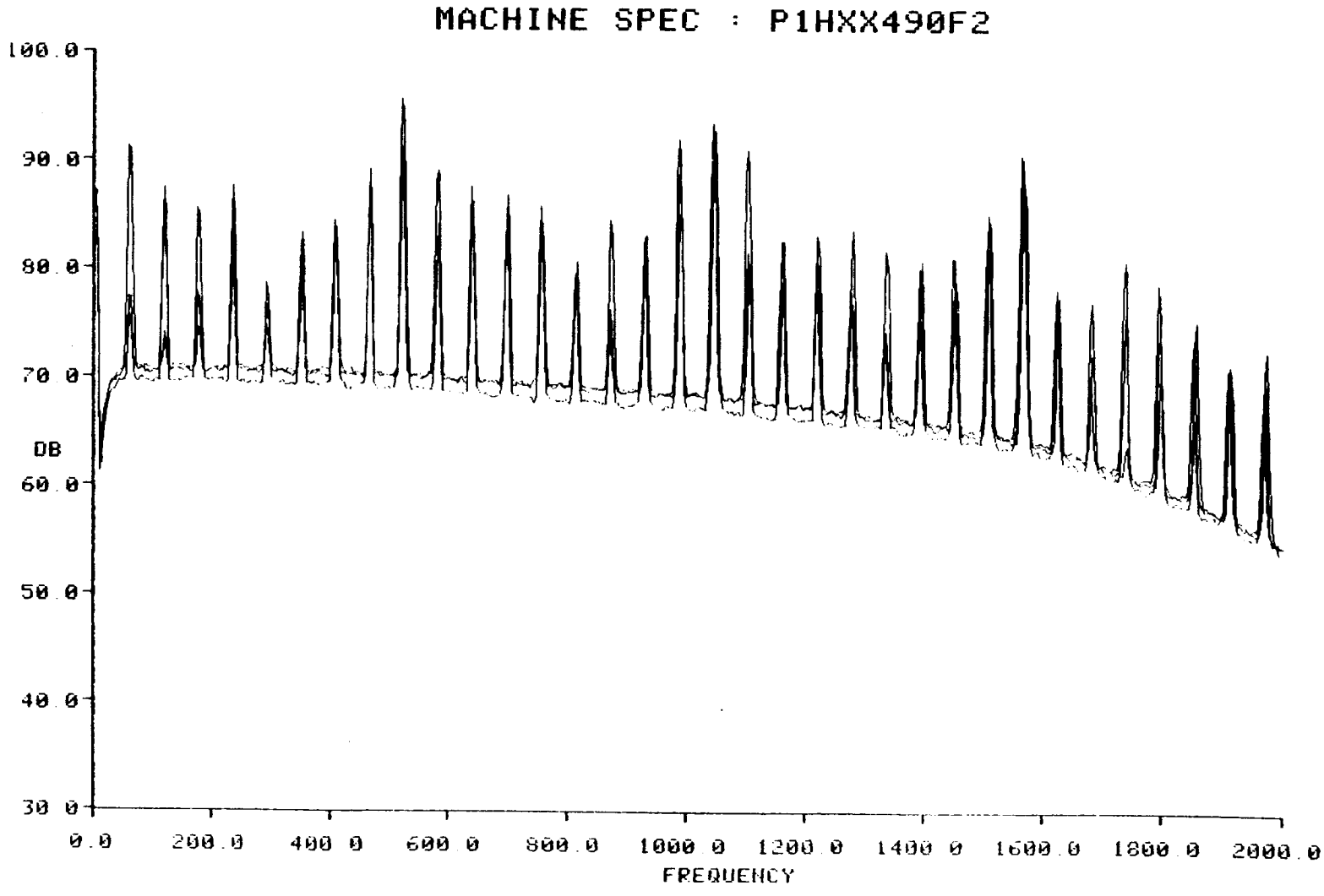

MEAN FOR FAULTED REFITS
MEAN FOR BASELINE REFITS
SIGMA FOR FAULTED REFITS
SIGMA FOR BASELINE REFITS

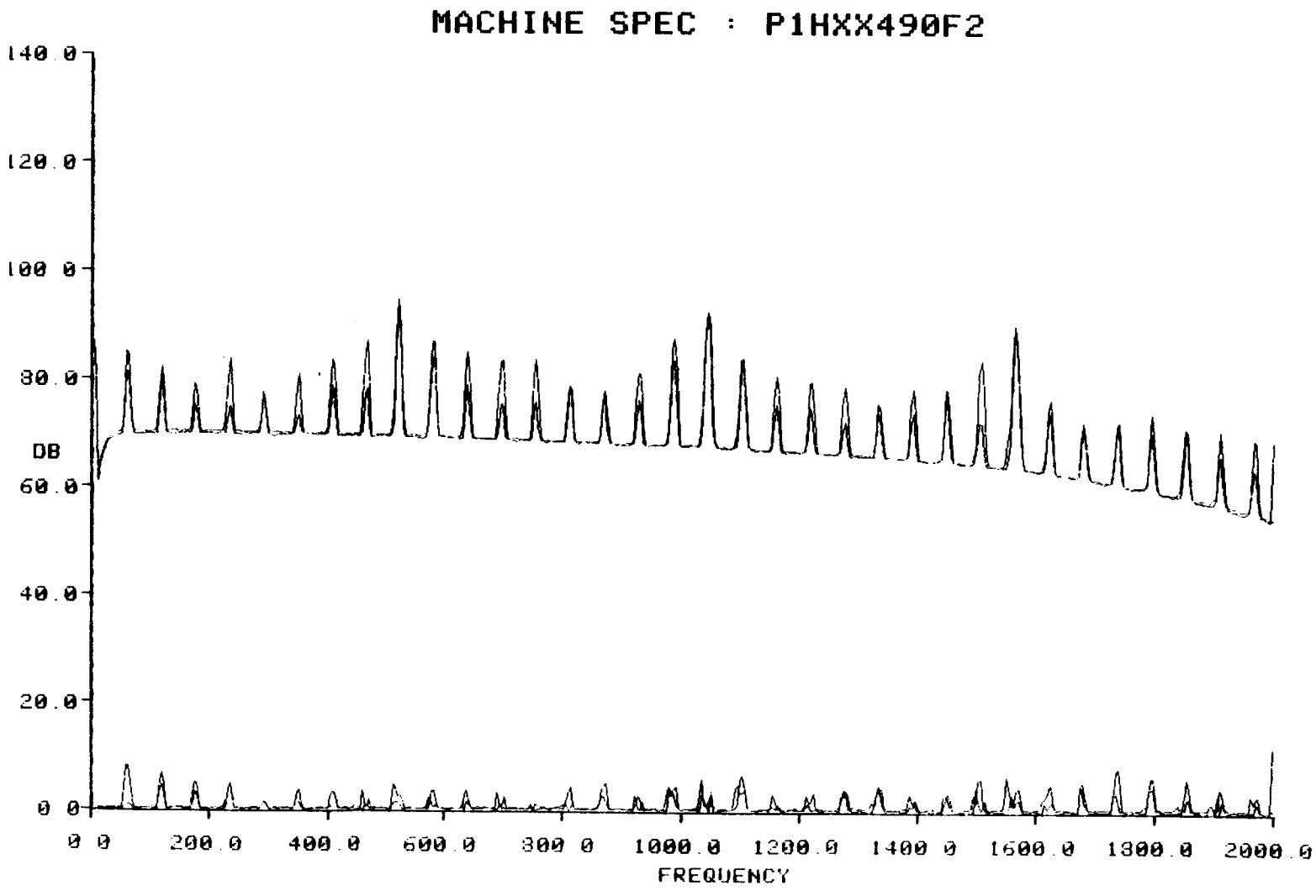

LIKELIHOOD RATIO WEIGHTS

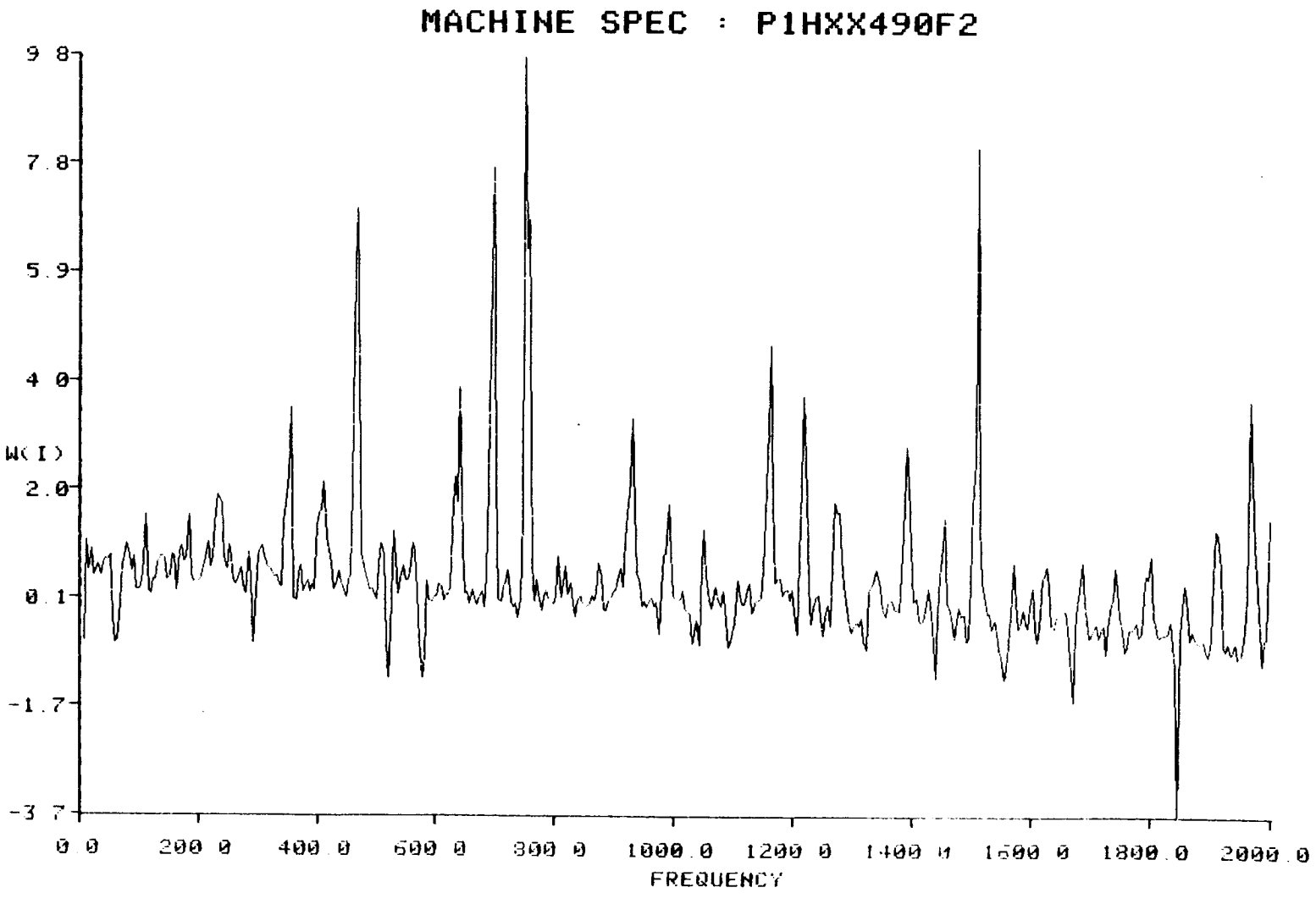

OPTIMUM SIGNATURE ANALYSIS DETECTION - Impeller Fault - Single One-Phase Pump

P_D for P_{FA} = 0.1

Baseband	HFD
1.0	1.0

LARGE IMBALANCE - SINGLE FAN

TEST DESCRIPTION: Large Imbalance - Single Fan

A series of tests was performed in which a single fan was imbalanced four separate times with a small nut weighing 172.8 mg at a radius of 10.2 mm from the shaft centerline. A baseline reading was obtained before each separate imbalance introduction. Both baseband and high frequency demodulation data were obtained simultaneously.

Results Presented:

Baseband - F0BX18SPF.2

1) Mean and standard deviation of the baseline and faulted refits.
2) Unmodified likelihood ratio weights.

High Frequency Demodulation - F0HX18G2F.2

3) Mean and standard deviation of the baseline and faulted refits.
4) Unmodified likelihood ratio weights

Note: Half-order frequencies, indicative to looseness, increase with imbalance.

MEAN FOR FAULTED REFITS
MEAN FOR BASELINE REFITS
SIGMA FOR FAULTED REFITS
SIGMA FOR BASELINE REFITS

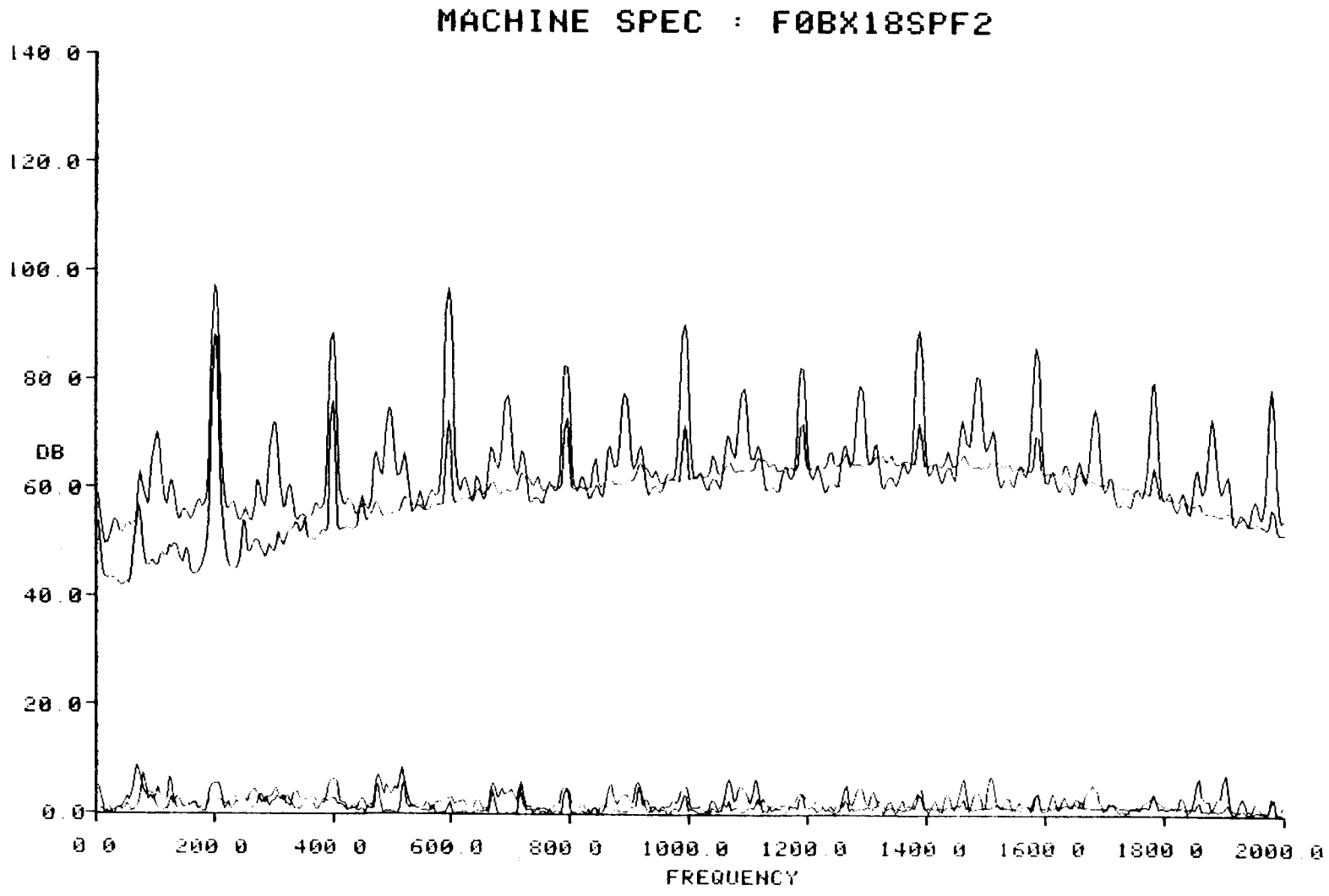

LIKELIHOOD RATIO WEIGHTS

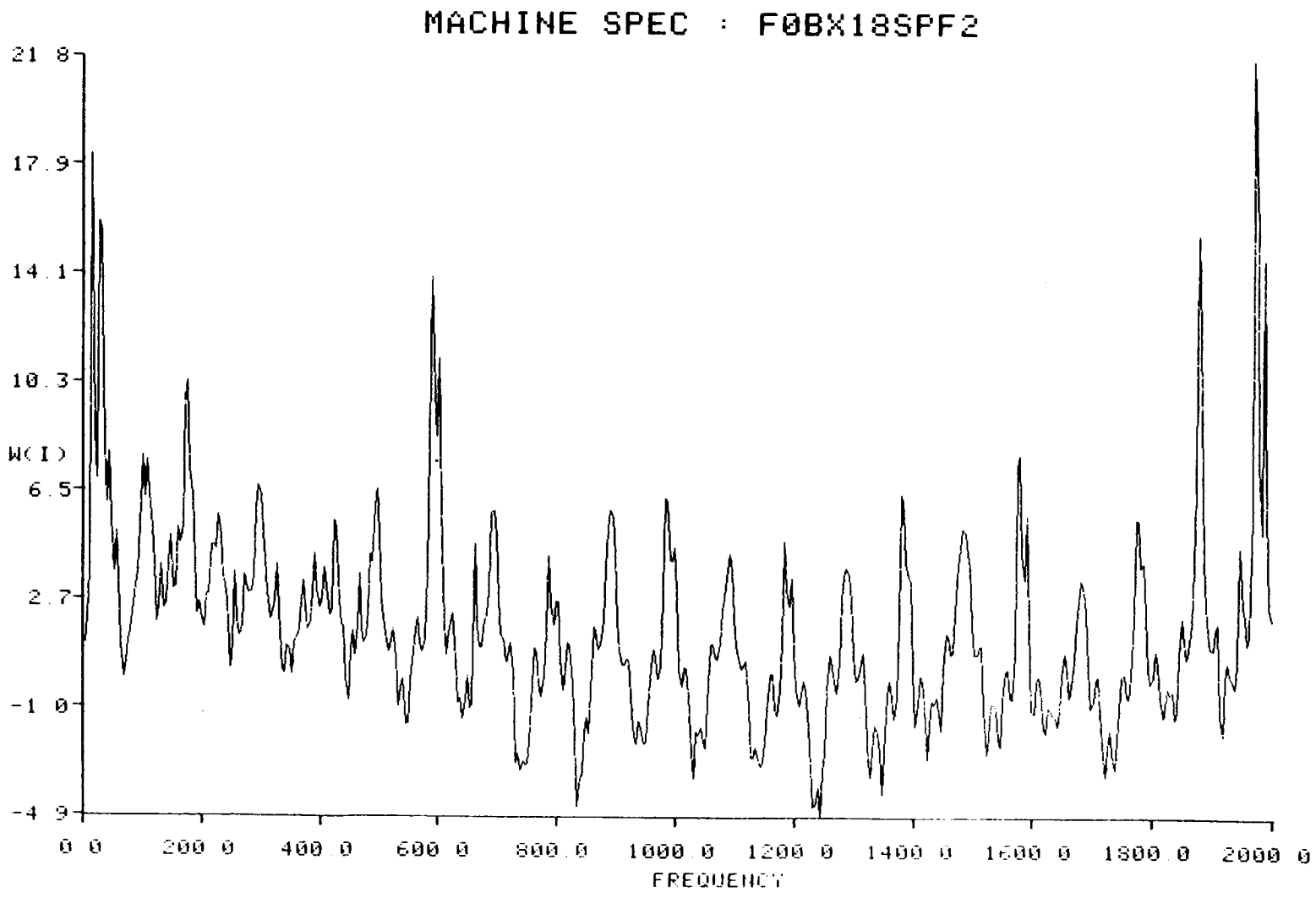

MEAN FOR FAULTED REFITS
MEAN FOR BASELINE REFITS
SIGMA FOR FAULTED REFITS
SIGMA FOR BASELINE REFITS

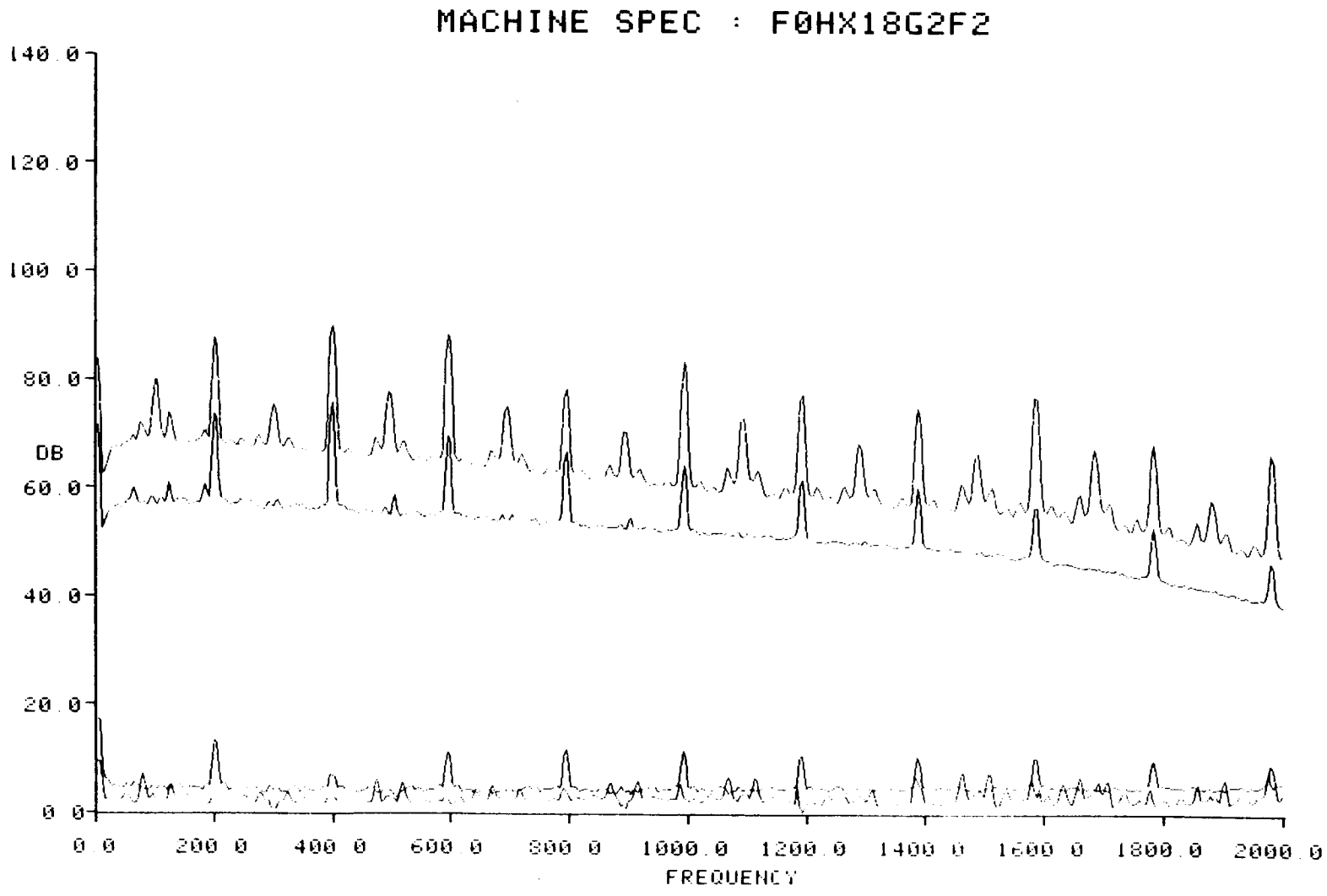

LIKELIHOOD RATIO WEIGHTS

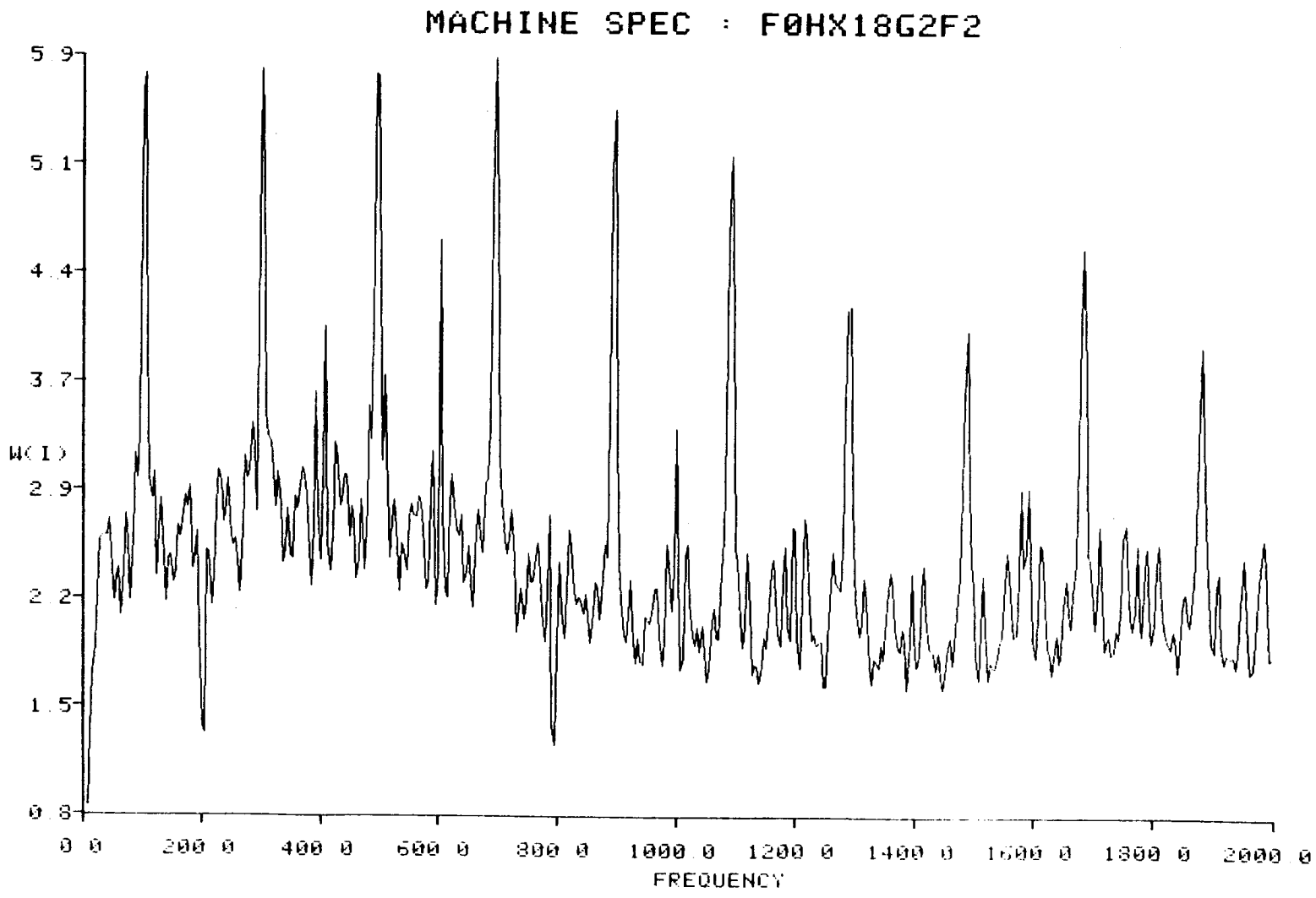

OPTIMUM SIGNATURE ANALYSIS DETECTION:
Large Imbalance Single Fan

P_D for P_{FA} = 0.1

Baseband	HFD
1.0	0.99

Voltage Change -- Multiple Fans

TEST DESCRIPTION: Voltage Change -- Multiple Fans

A series of tests were performed in which an over and under voltage condition on each of the four test fans was evaluated. A baseline was recorded at nominal operating voltage (200V) . The voltage was then reduced approximately 10% to 180V and a set of faulted data obtained. The operating voltage was then increased to 220V, approximately 10% over nominal, and a second set of faulted data obtained. The above test procedure was performed on each test fan once. Both baseband and high frequency demodulation data were obtained simultaneously.

Results Presented:

I. Under Voltage

Baseband -- F0B22BG1F.2

1) Mean and standard deviation of the baseline and faulted refits
2) Unmodified likelihood ratio weights
3) Modified likelihood ratio weights (all weights set to zero except at the large positive and negative excursion at 120Hz)

High Frequency Demodulation -- F0H22BG1F.2

4) Mean and standard deviation of the baseline and faulted refits
5) Unmodified likelihood ratio weights

II. Over Voltage

Baseband -- F0B22BG2F.2

6) Mean and standard deviation of the baseline and faulted refits
7) Modified likelihood ratio weights (all weights set to zero except at the large positive and negative excursion at 120Hz)

MEAN FOR FAULTED REFITS
MEAN FOR BASELINE REFITS
SIGMA FOR FAULTED REFITS
SIGMA FOR BASELINE REFITS

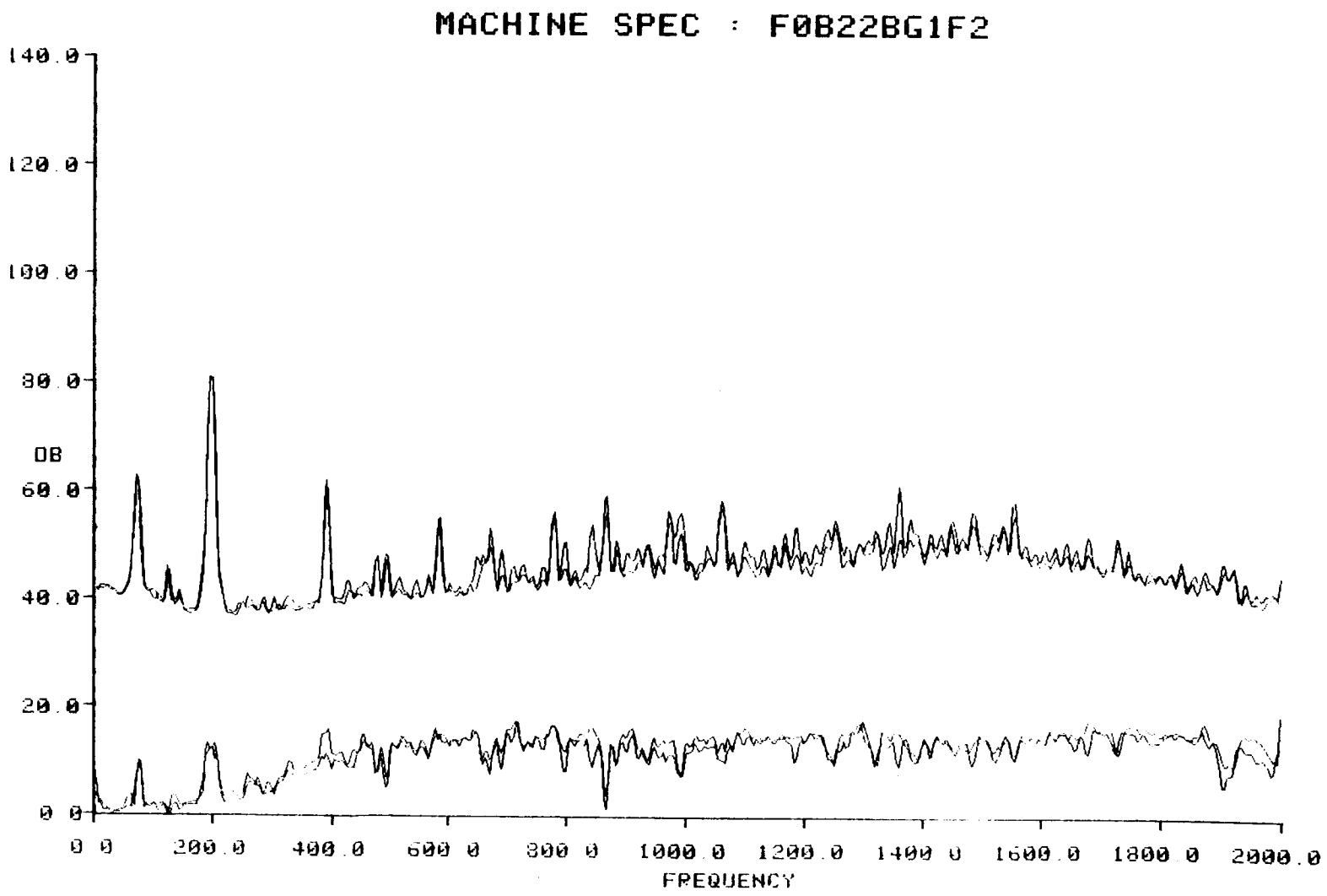

LIKELIHOOD RATIO WEIGHTS

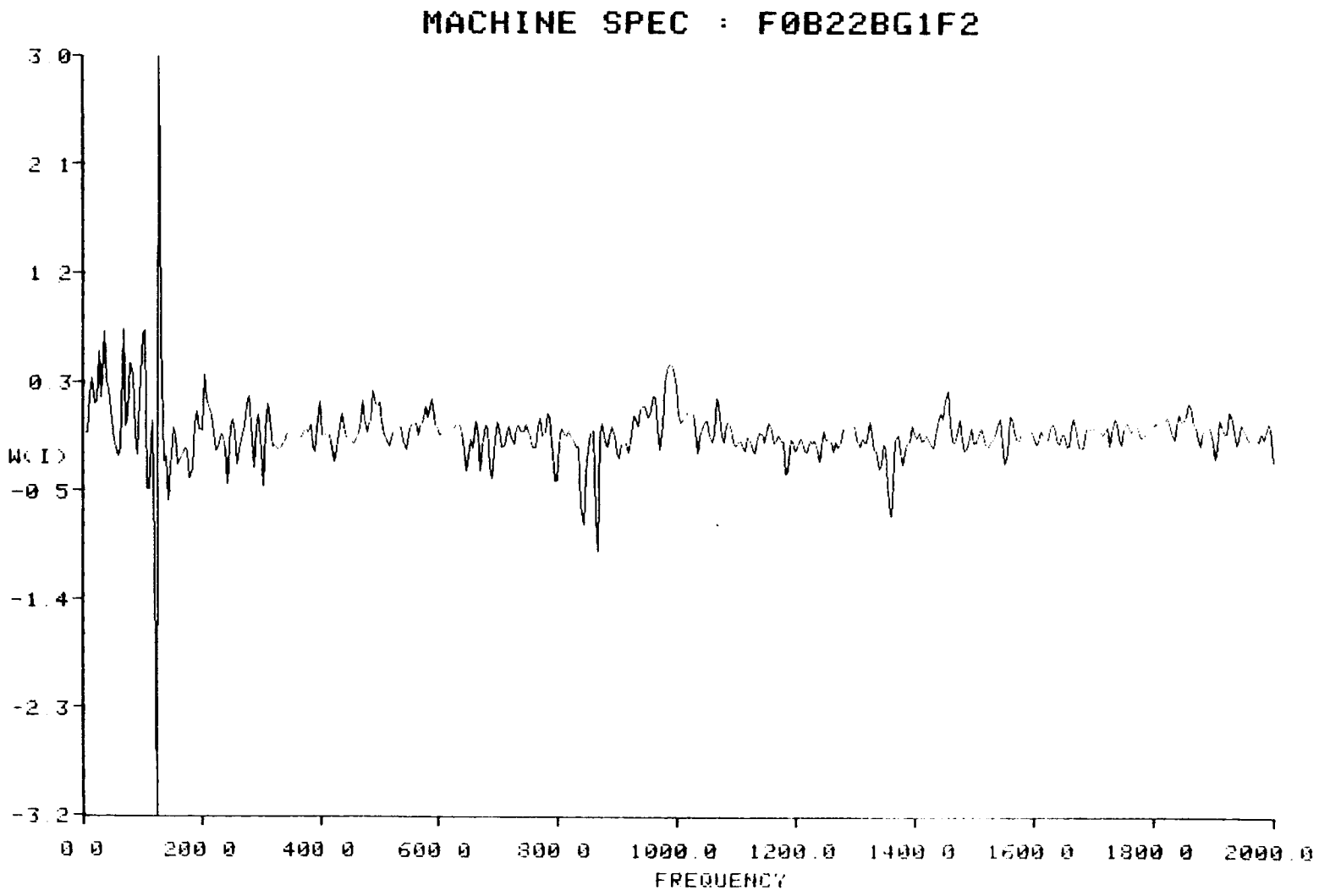

LIKELIHOOD RATIO WEIGHTS

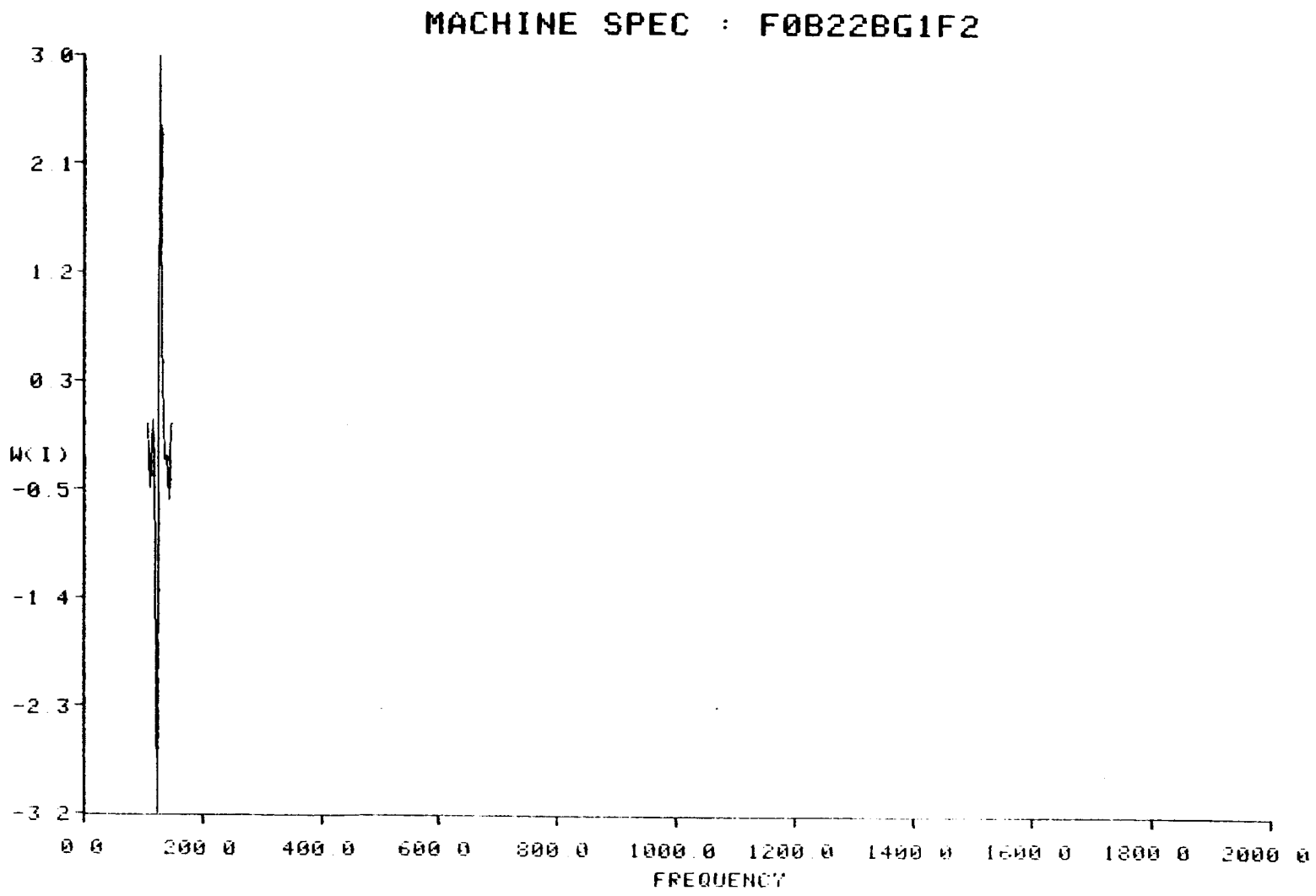

MEAN FOR FAULTED REFITS
MEAN FOR BASELINE REFITS
SIGMA FOR FAULTED REFITS
SIGMA FOR BASELINE REFITS

MACHINE SPEC : F0H22BG1F2

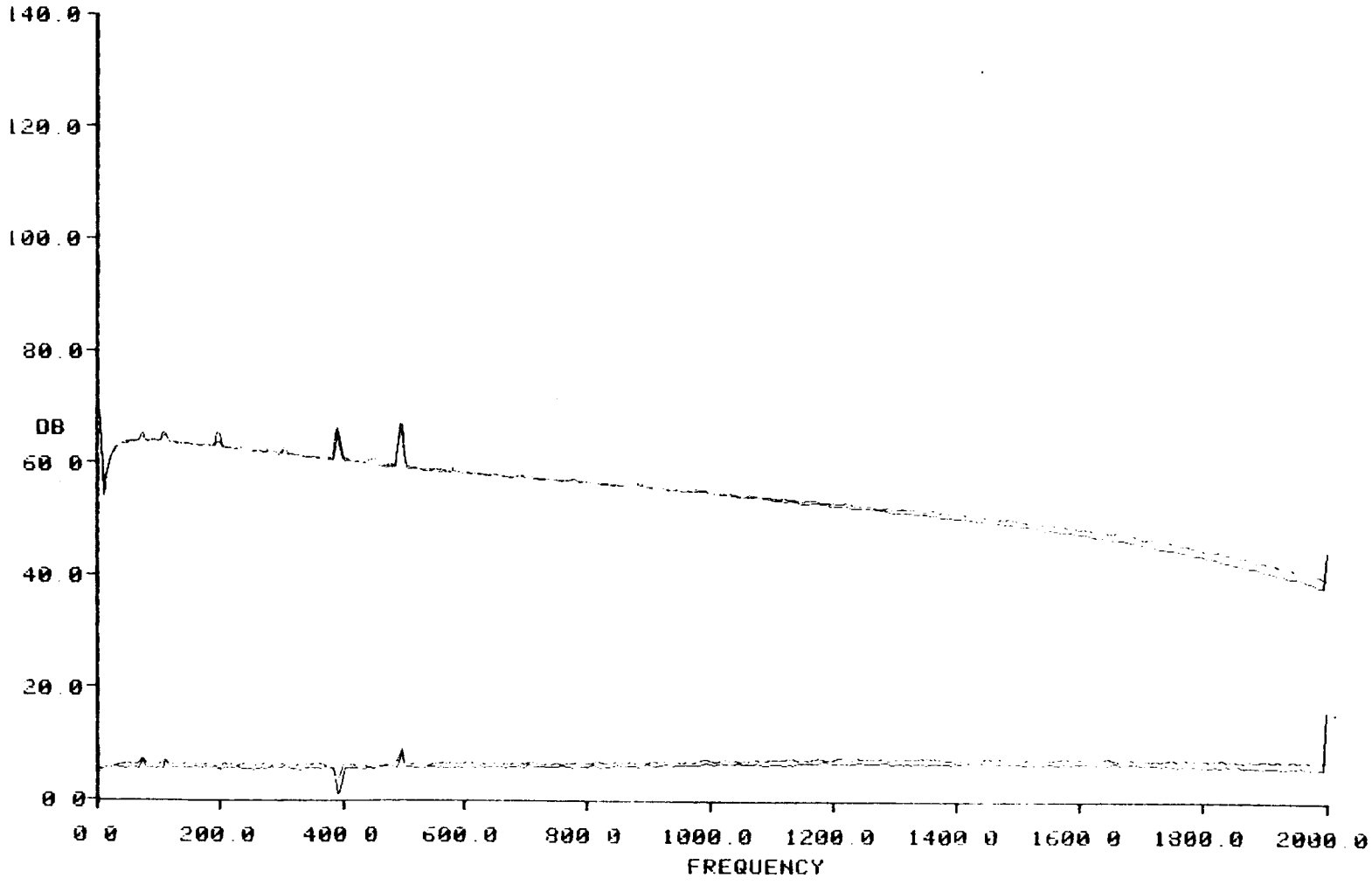

LIKELIHOOD RATIO WEIGHTS

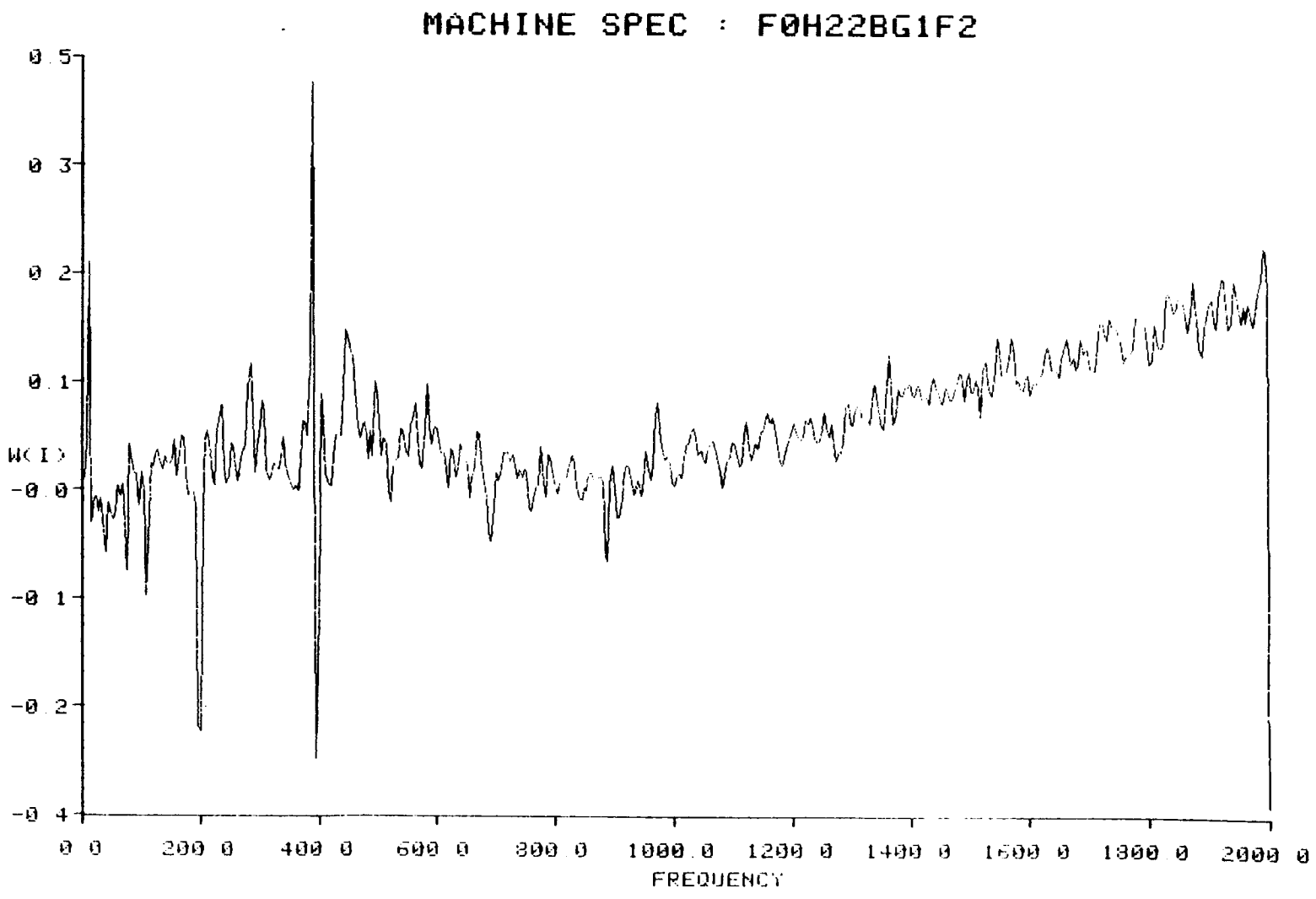

MEAN FOR FAULTED REFITS
MEAN FOR BASELINE REFITS
SIGMA FOR FAULTED REFITS
SIGMA FOR BASELINE REFITS

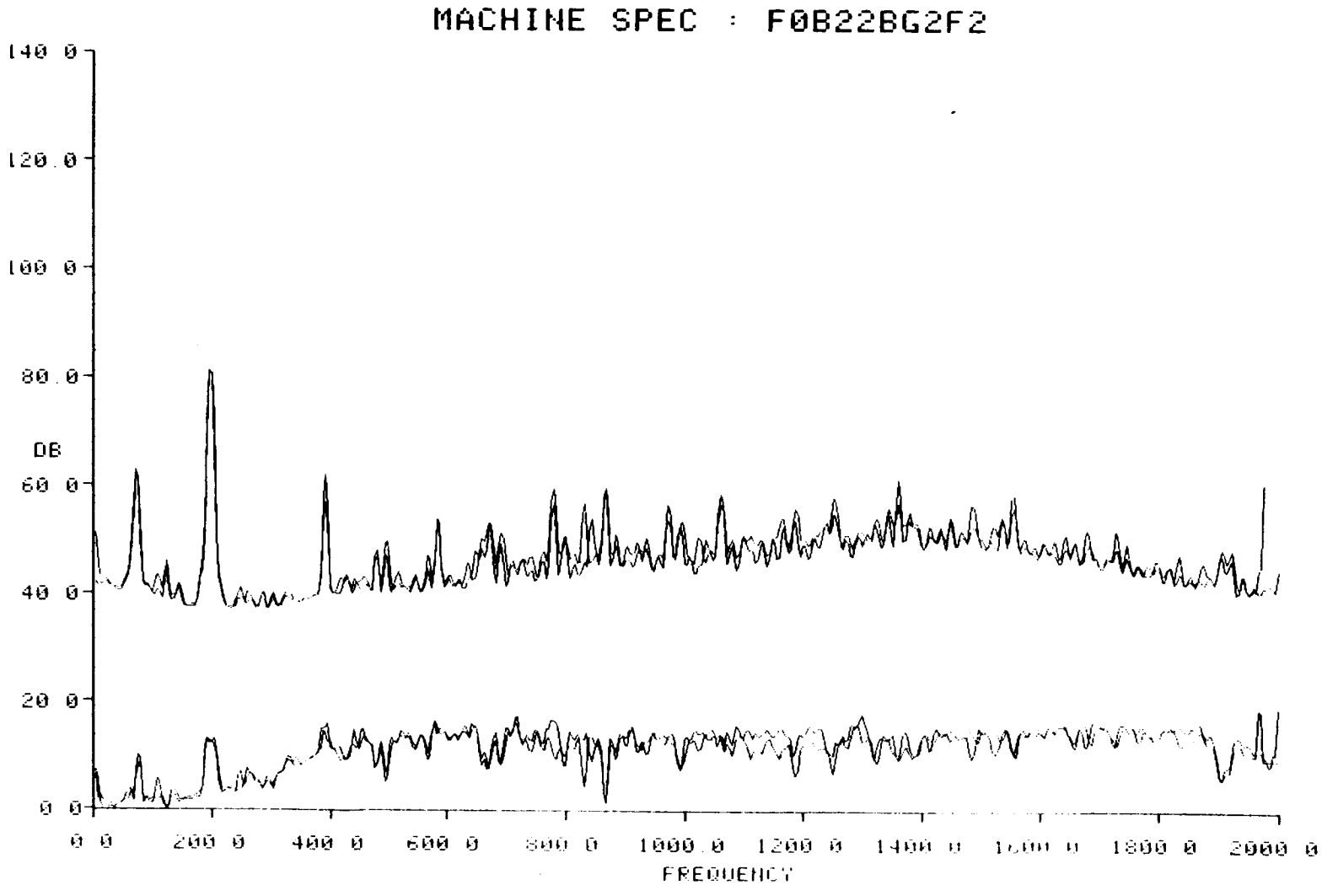

LIKELIHOOD RATIO WEIGHTS

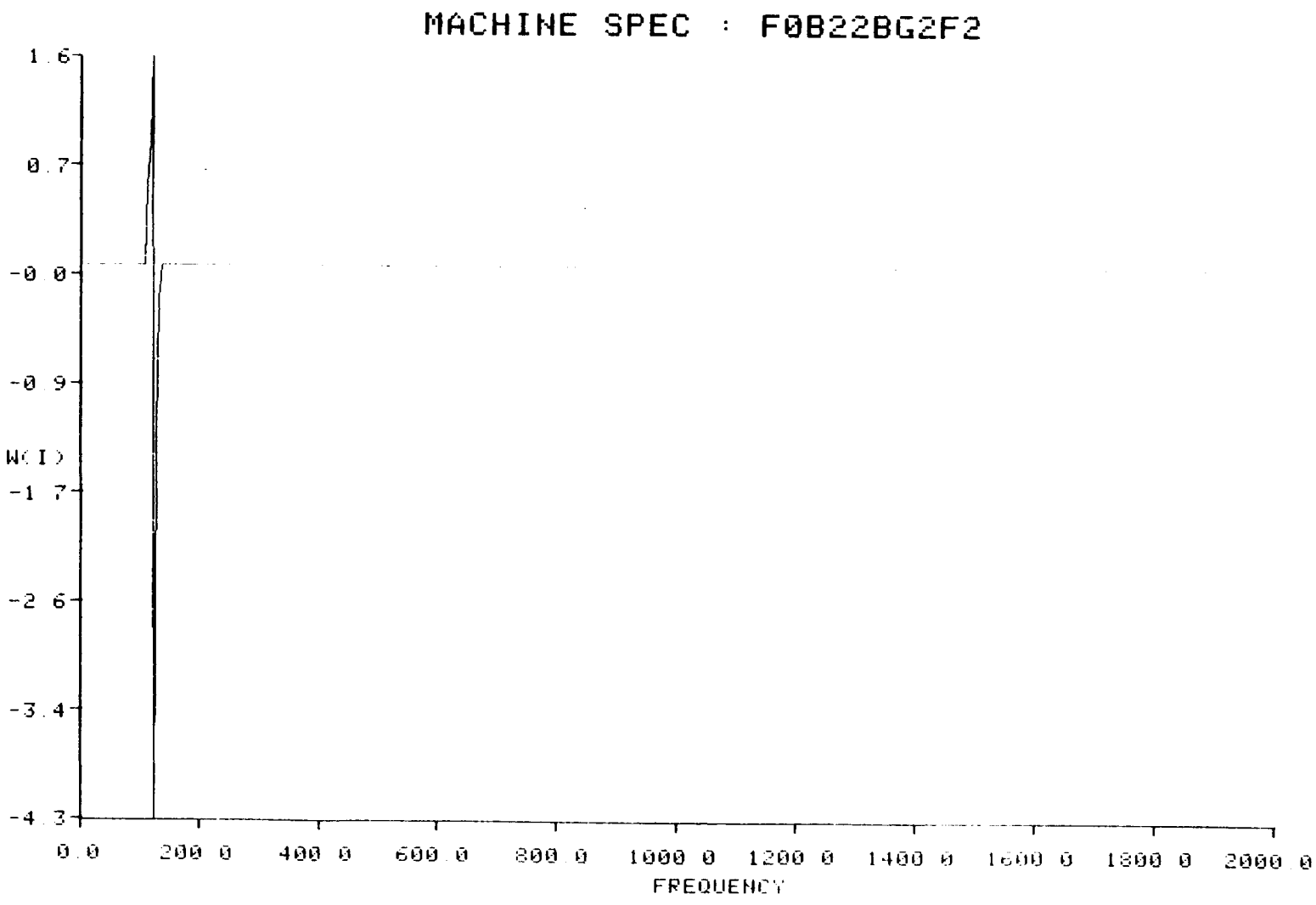

Optimum Signature Analysis Detection: Voltage Change -- Multiple Fans

P_D for $P_{FA} = 0.1$

Test Condition	Baseband	HFD
Under Voltage	0.99	0.17
Over Voltage	0.98	0.37

INNER RACE FAULT-MULTIPLE THREE PHASE PUMPS

TEST DESCRIPTION: Inner Race Fault - Multiple Three Phase Pumps

A series of tests was performed in which a single inner race fault was introduced into the front bearing of six three phase pumps. A baseline reading was obtained, after which the pump was disassembled and the bearings faulted. The bearings were faulted by using a "moto tool" with a carbide grinding tip to score across the inner race surface. It was not possible to accurately quantify the depth of the score. Care was exercised in the removal of any foreign material generated during the faulting process before reassembly and obtaining the faulted data. Both baseband and high frequency demodulation data were obtained simultaneously.

Results Presented:

Baseband - P3BX4100F.2

1) Mean and standard deviation of the baseline and faulted refits.
2) Unmodified likelihood ratio weights.
3) Modified likelihood ratio weights (all weights set to zero except at rotational frequencies).

High Frequency Demodulation - P3HX4100F.2

4) Mean and standard deviation of the baseline and faulted refits.
5) Modified likelihood ratio weights (all negative weights set to zero).

MEAN FOR FAULTED REFITS
MEAN FOR BASELINE REFITS
SIGMA FOR FAULTED REFITS
SIGMA FOR BASELINE REFITS

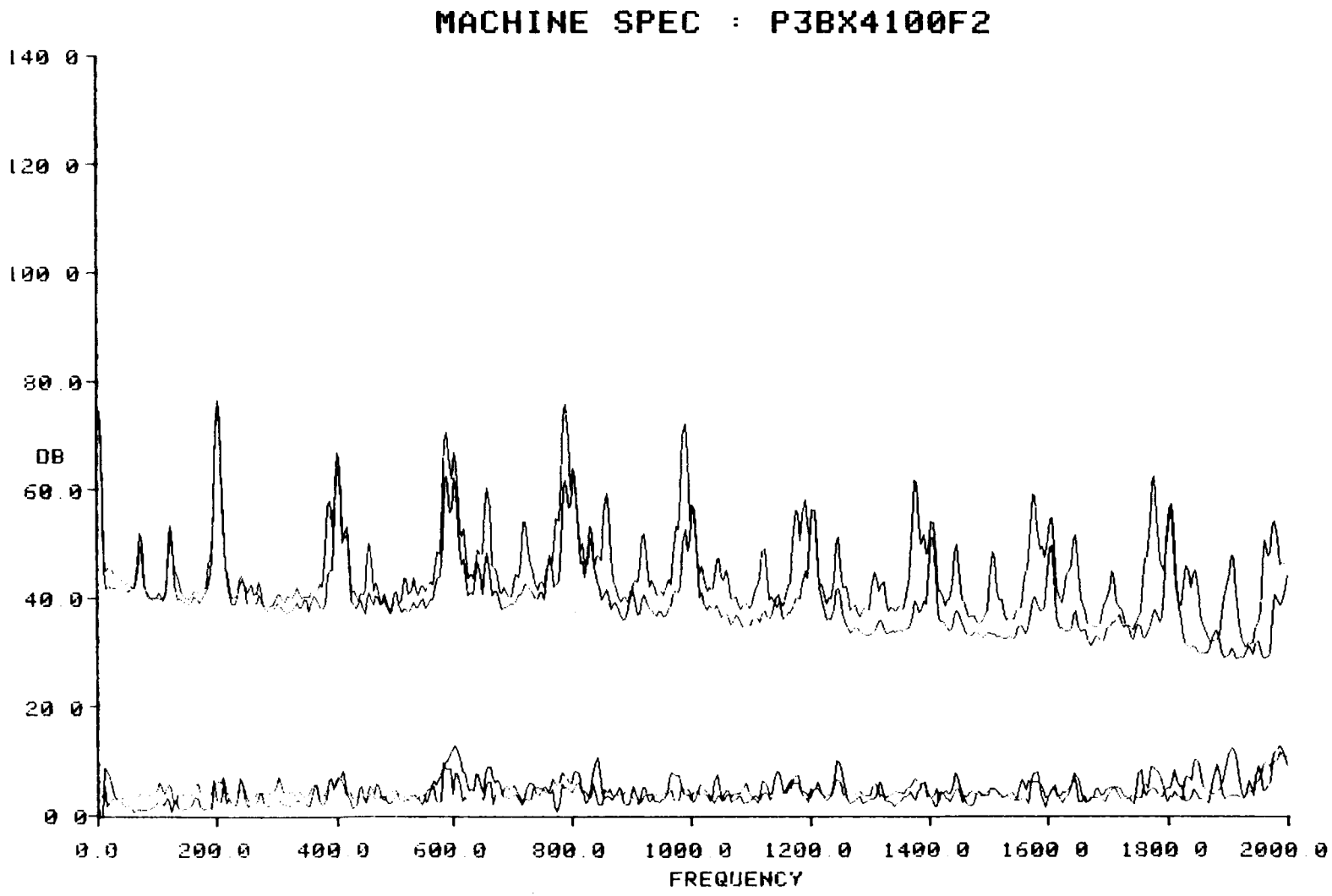

LIKELIHOOD RATIO WEIGHTS

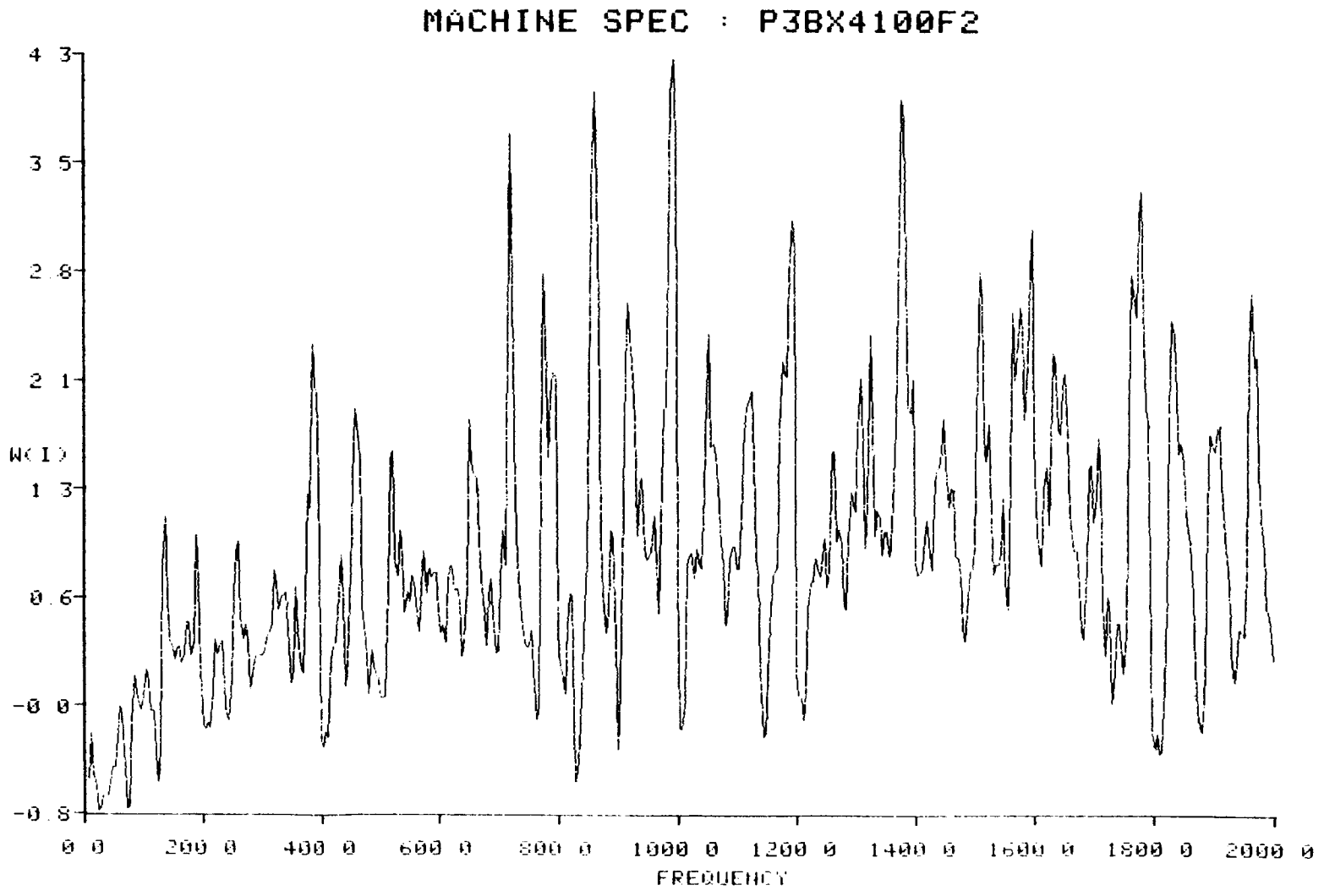

LIKELIHOOD RATIO WEIGHTS

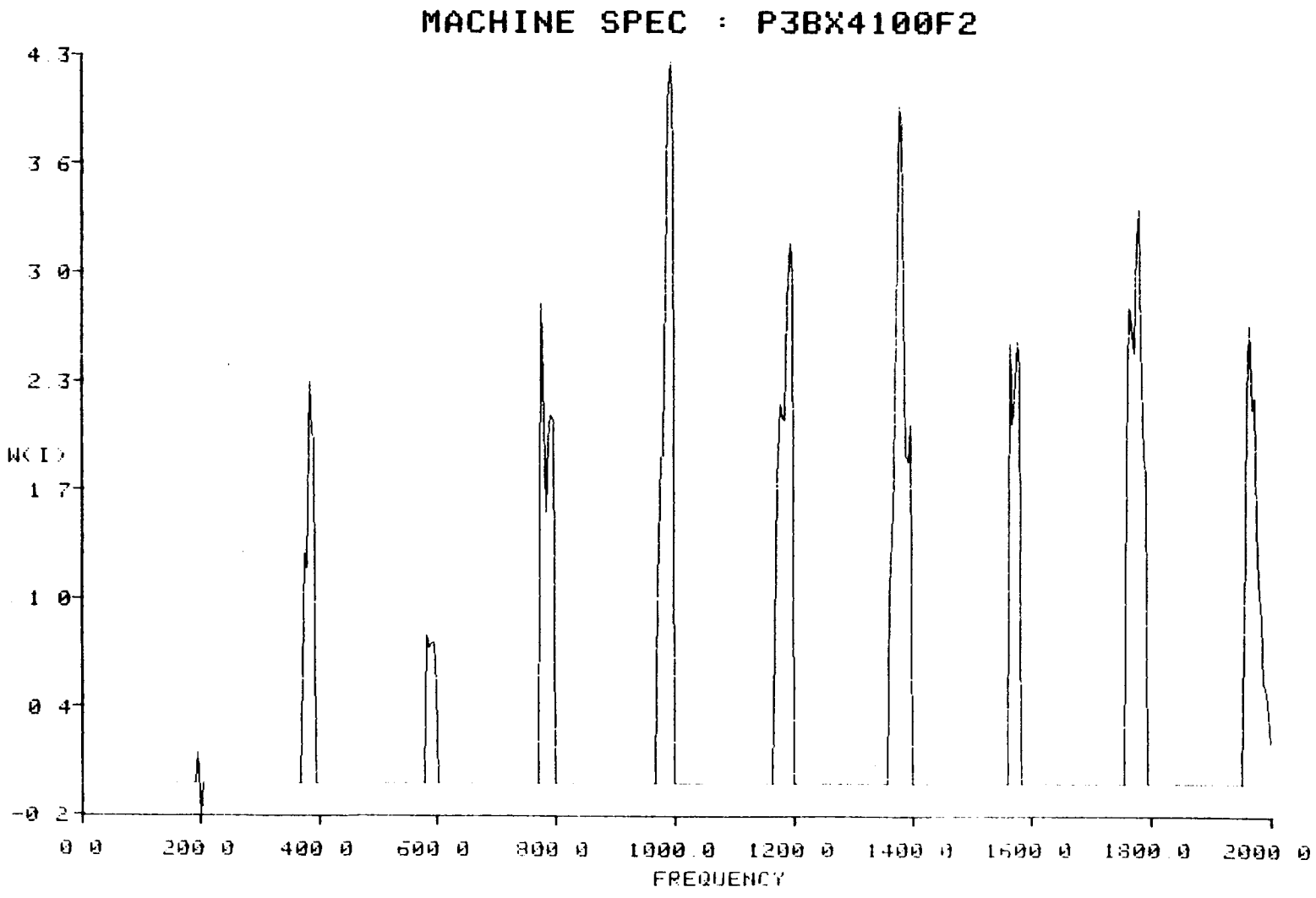

MEAN FOR FAULTED REFITS
MEAN FOR BASELINE REFITS
SIGMA FOR FAULTED REFITS
SIGMA FOR BASELINE REFITS

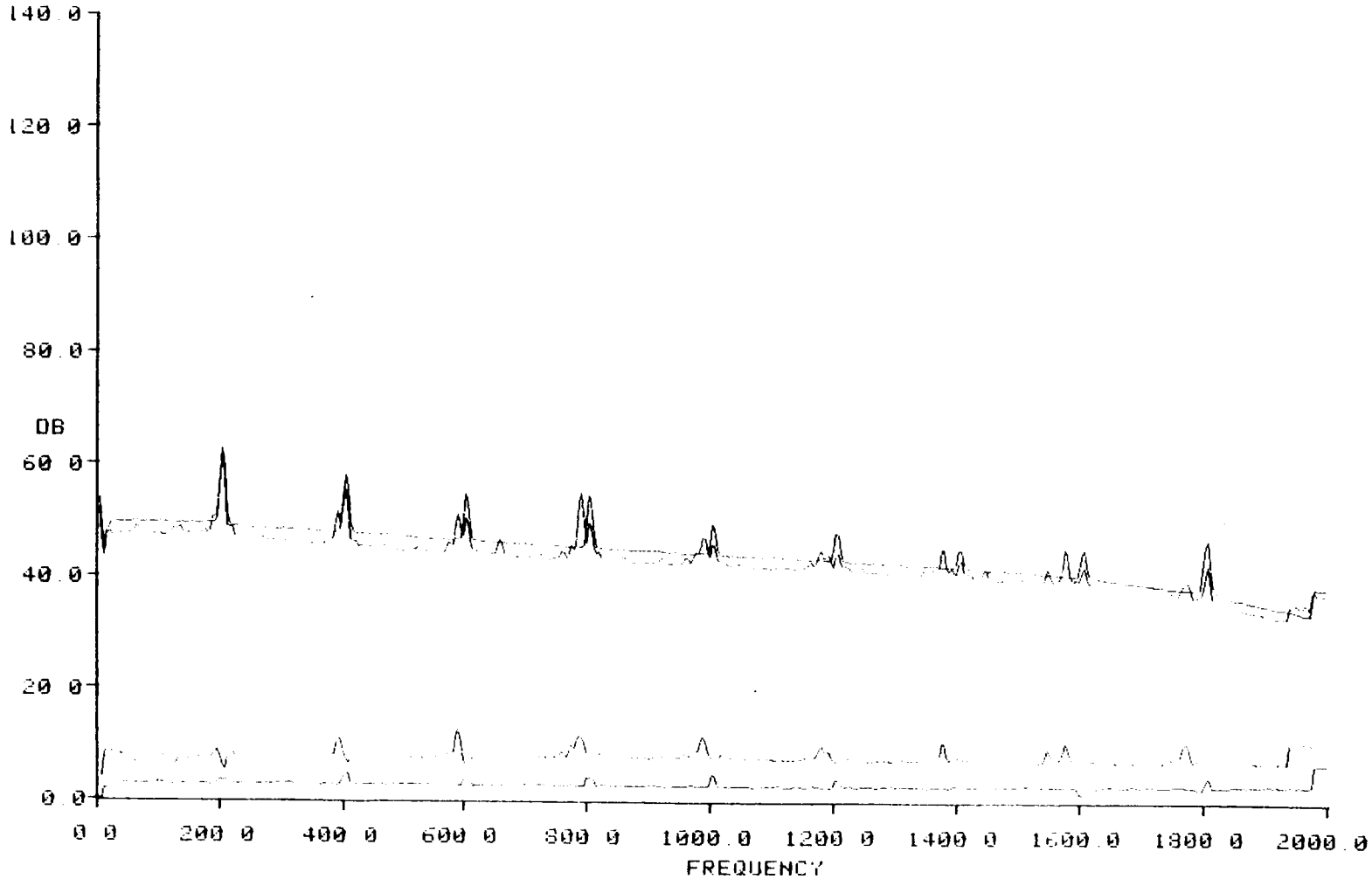

LIKELIHOOD RATIO WEIGHTS

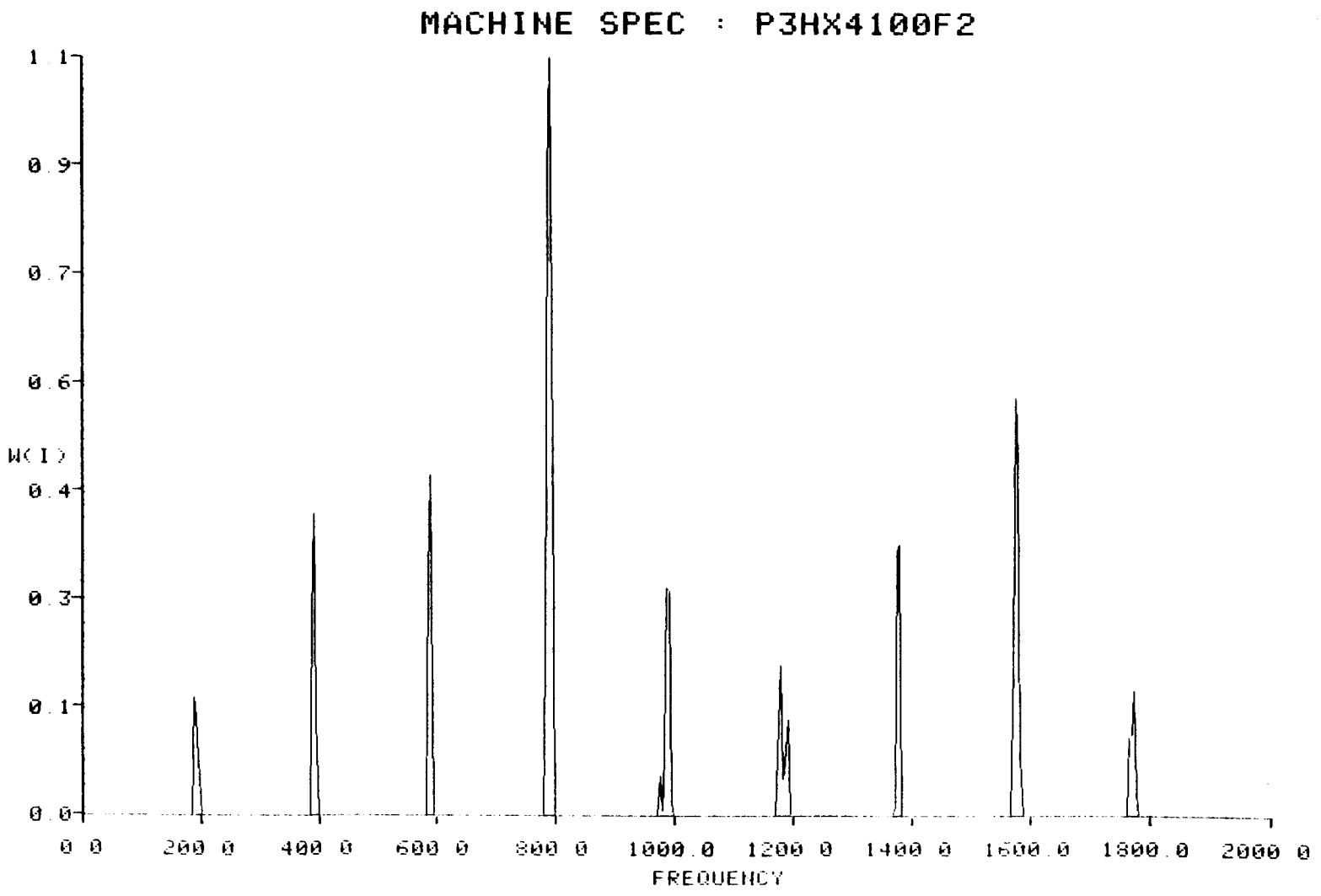

OPTIMUM SIGNATURE ANALYSIS DETECTION: Inner Race Fault - Multiple Three Phase Pumps

P_D for P_{FA} = 0.1

Baseband	HFD
.99 (unmodified weights)	.47 (modified weights)
.997 (modified weights)	

OUTER RACE FAULT-MULTIPLE THREE PHASE PUMPS

TEST DESCRIPTION: Outer Race Fault - Multiple Three Phase Pumps

A series of tests was performed in which a single outer race fault was introduced into the front bearing of six three phase pumps. The methodology of the test procedure for fault introduction was the same as was described in the inner race fault description for three phase pumps. Both baseband and high frequency demodulation data were obtained simultaneously.

Results Presented:

Baseband - P3BX4000F.2

1) Mean and standard deviationof the baseline and faulted refits.
2) "Modified" likelihood ratio weights (contribution by DC and FRF components set to zero).
3) Multiple frequency detection (weights assigned value of one at BPFO and harmonics; zero everywhere else).

High Frequency Demodulation - P3HX4000F.2

4) Mean and standard deviation of the baseline and faulted refits.
5) "Modified" likelihood ratio weights (contribution by DC and FRF components set to zero).
6) Modified likelihood ratio weights (all weights set to zero except at BPFO and harmonics).

MEAN FOR FAULTED REFITS
MEAN FOR BASELINE REFITS
SIGMA FOR FAULTED REFITS
SIGMA FOR BASELINE REFITS

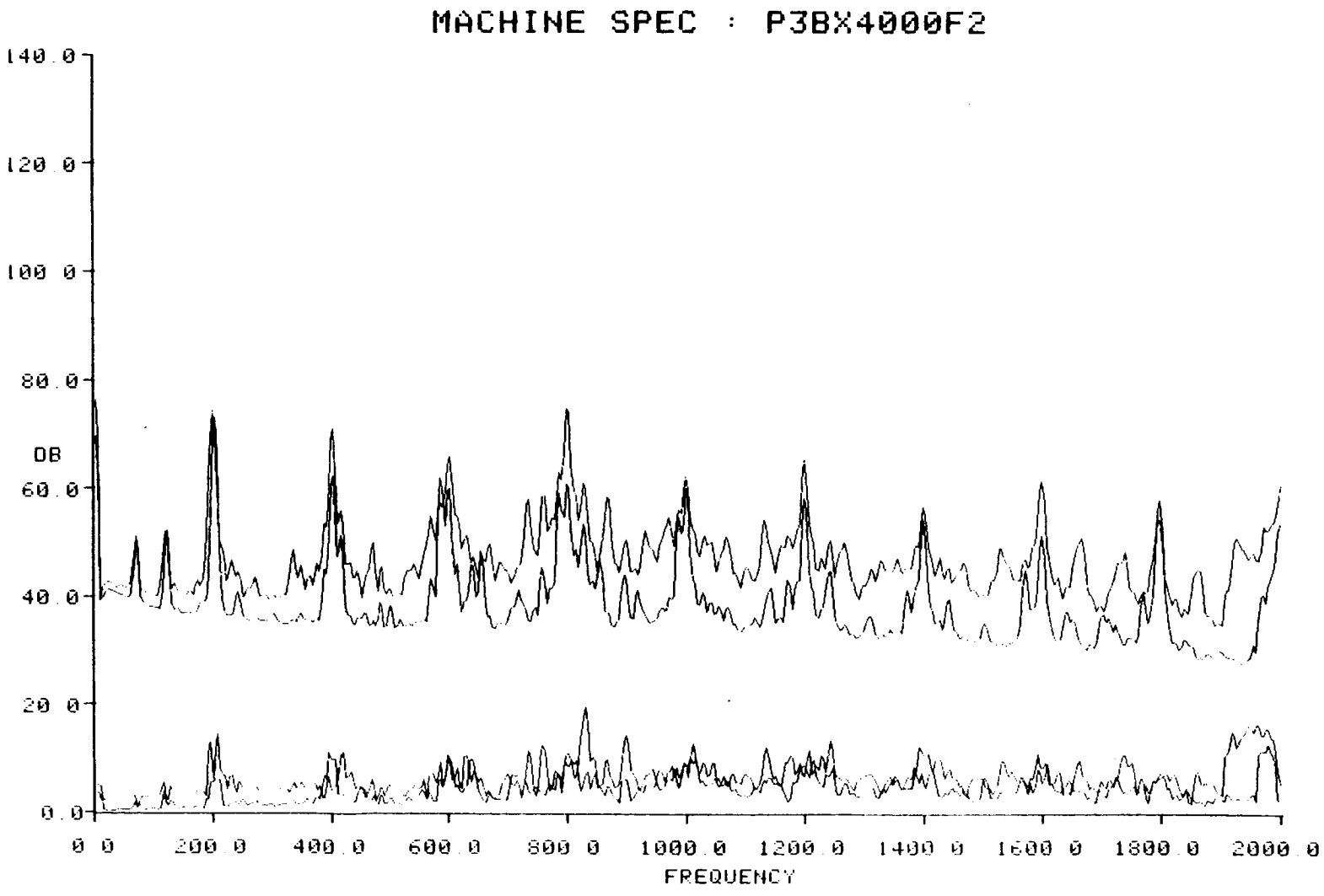

LIKELIHOOD RATIO WEIGHTS

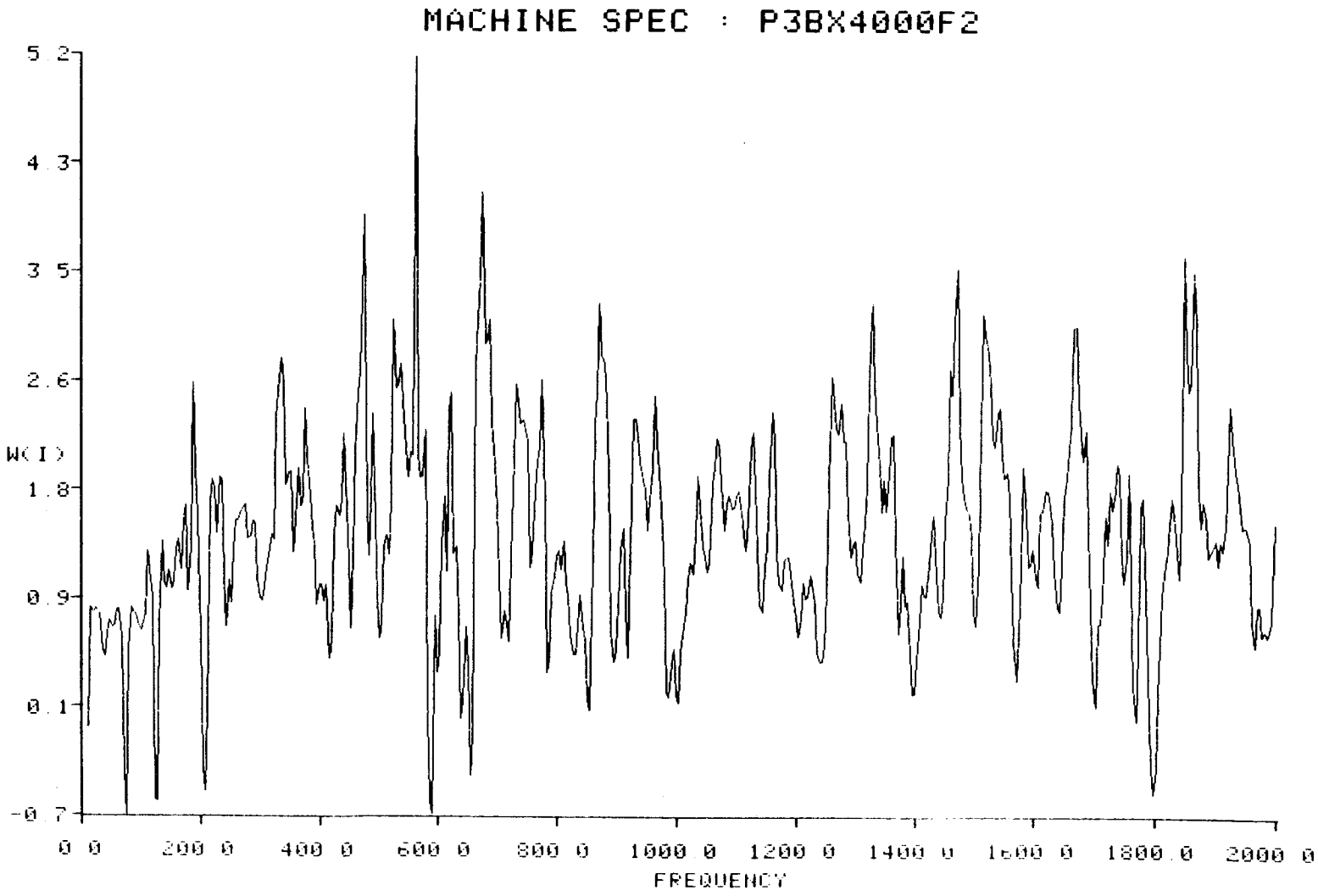

LIKELIHOOD RATIO WEIGHTS

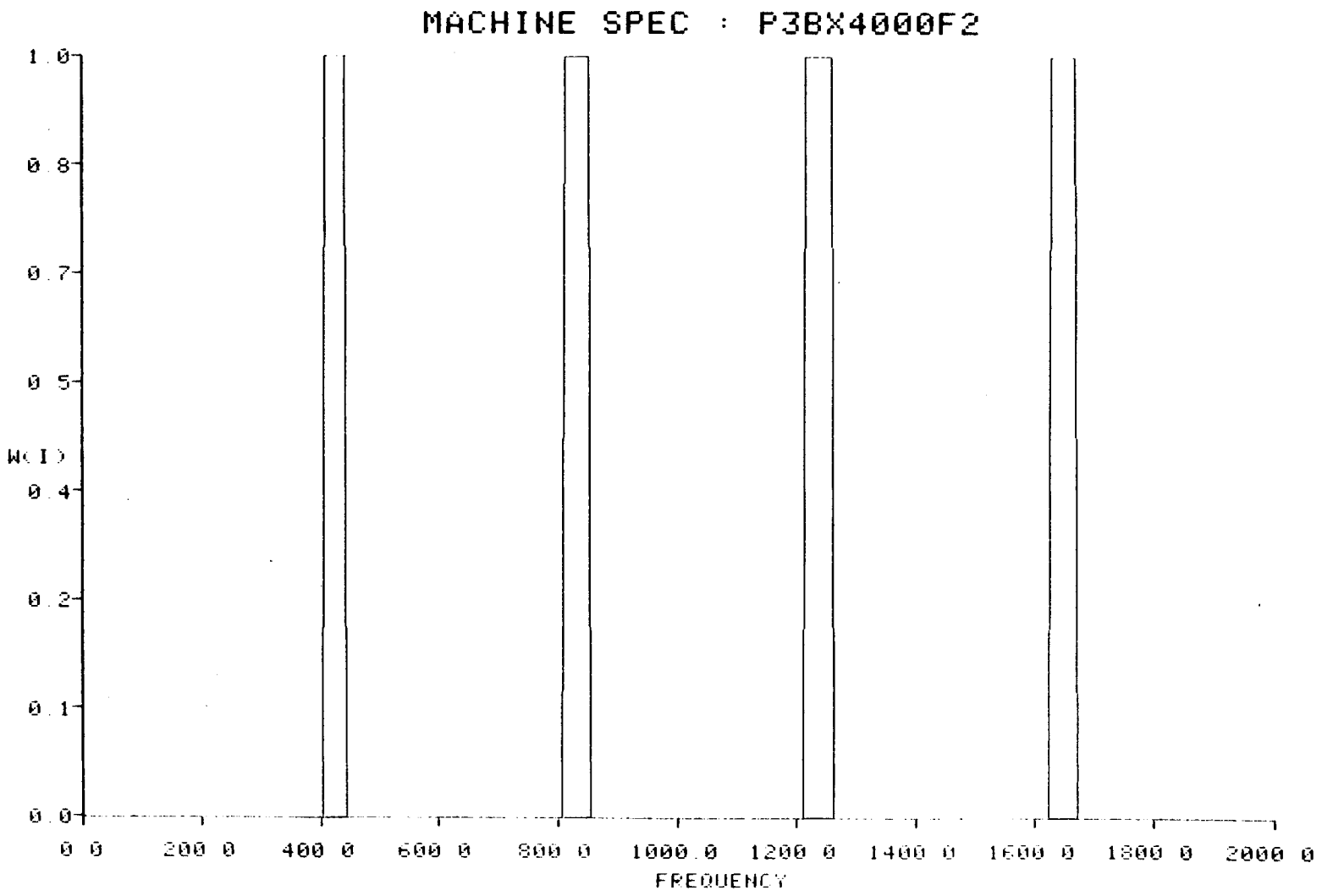

MEAN FOR FAULTED REFITS
MEAN FOR BASELINE REFITS
SIGMA FOR FAULTED REFITS
SIGMA FOR BASELINE REFITS

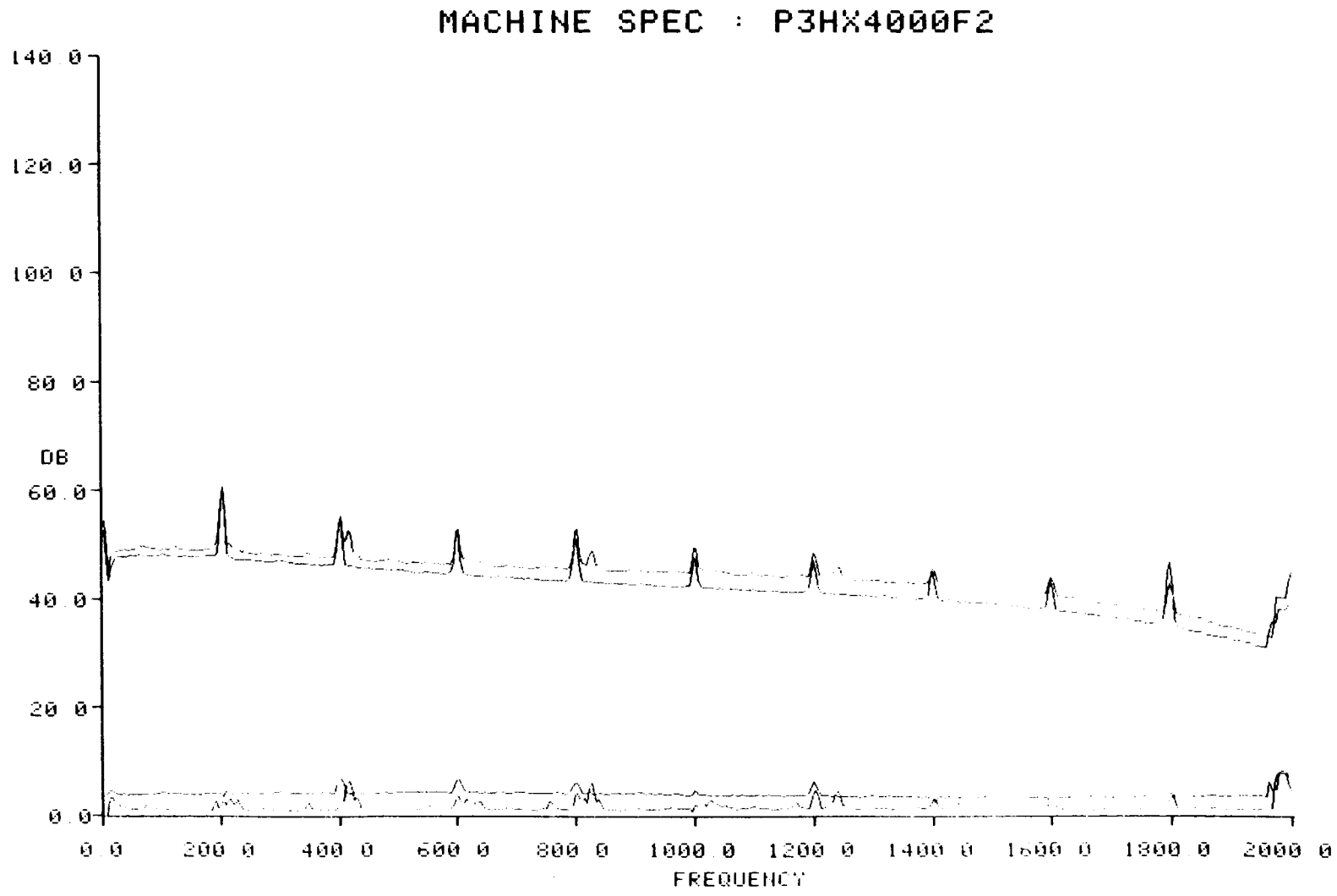

LIKELIHOOD RATIO WEIGHTS

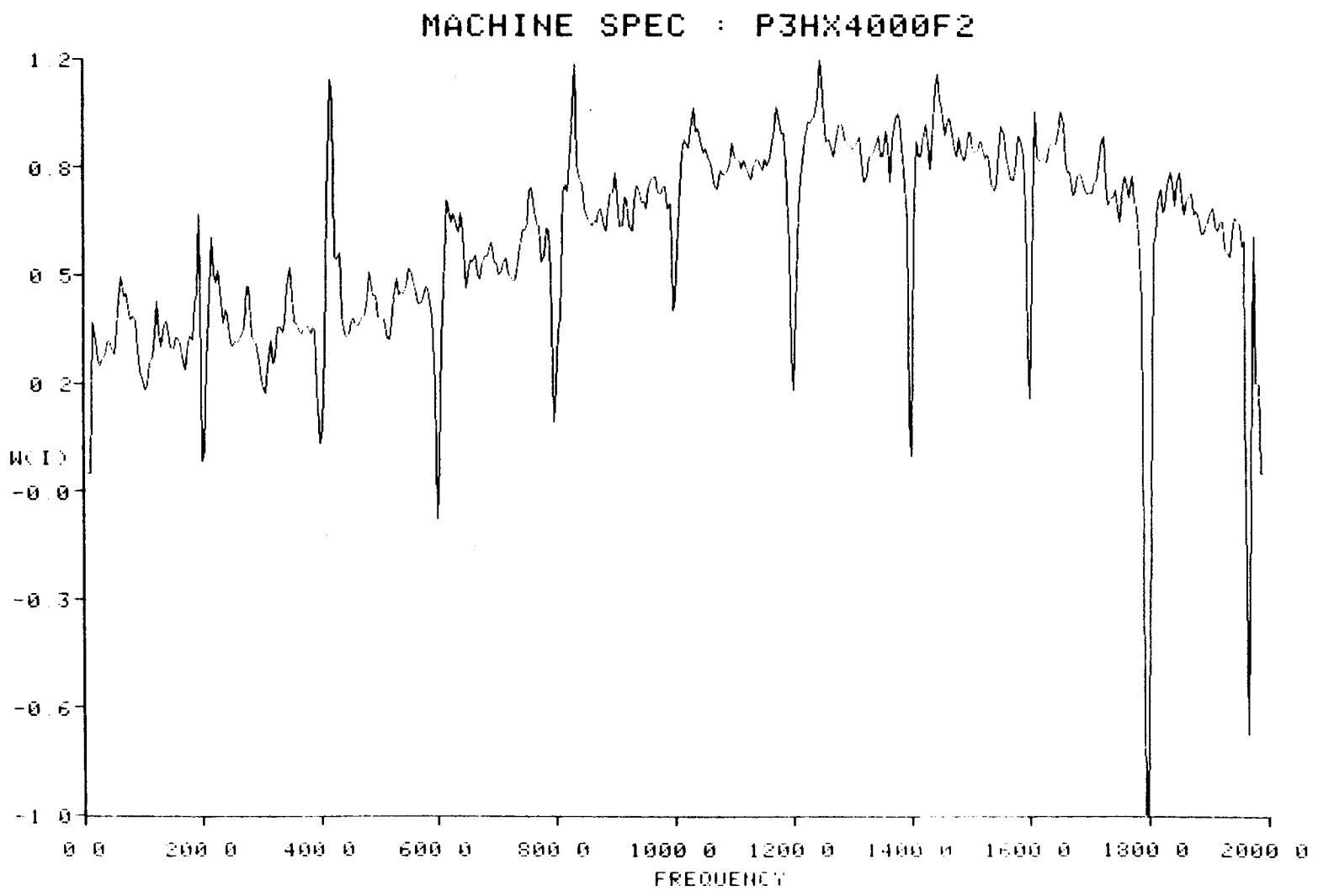

LIKELIHOOD RATIO WEIGHTS

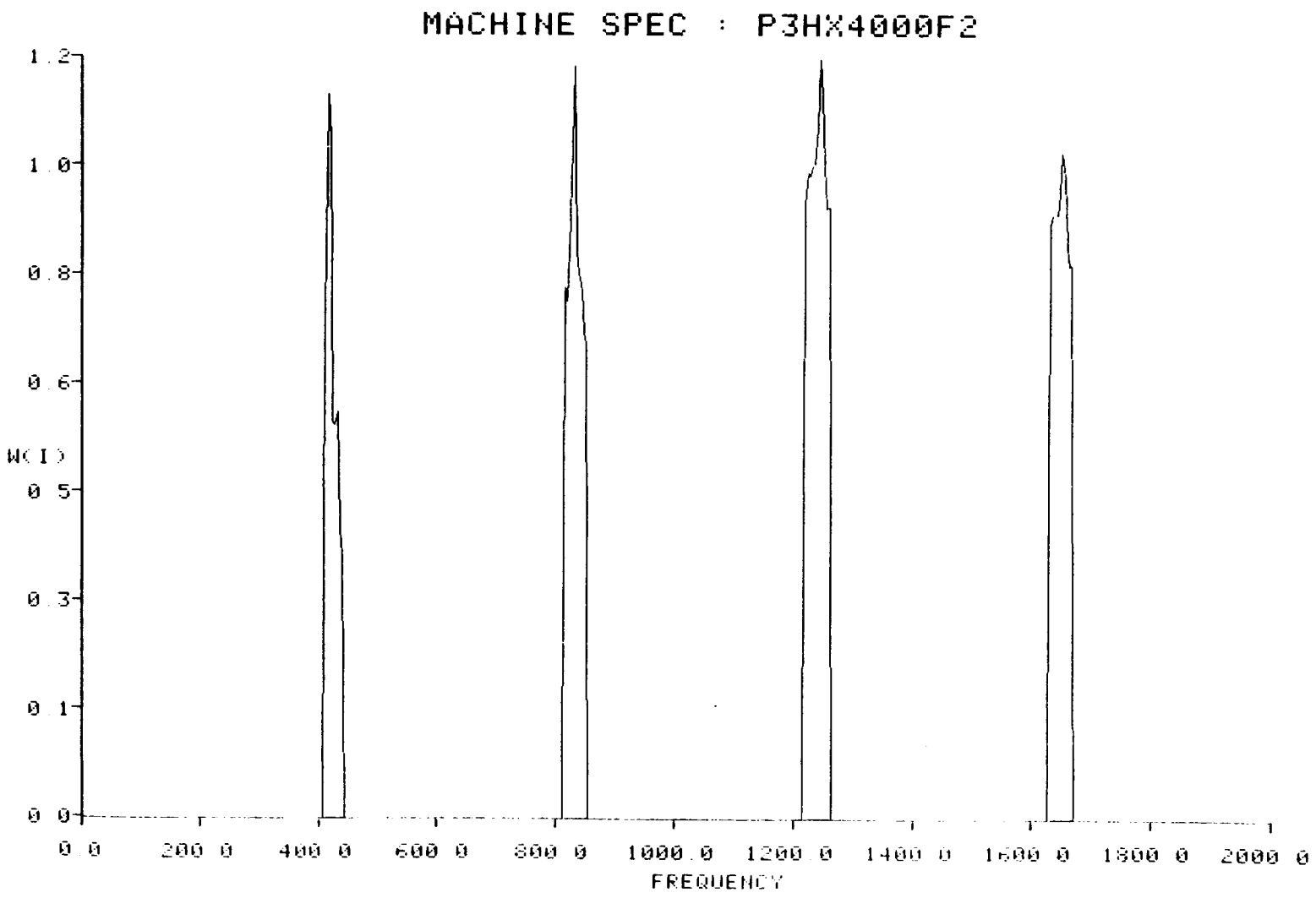

OPTIMUM SIGNATURE ANALYSIS DETECTION: Outer Race Fault - Multiple Three Phase Pumps

P_D for P_{FA} = 0.1

Baseband	HFD
0.97 (modified weights)	.05 (modified weight)
0.73 (multiple frequency detection)	.20 (modified weights @ BPFO)

PHASE LOSS - SINGLE THREE PHASE PUMP

TEST DESCRIPTION: Phase Loss - Single Three Phase Pump

A series of tests was performed in which the loss of a single - phase of the three phase power to a single three phase pump was evaluated. A baseline was obtained with the pump running normally, after which one of the phases was removed. Four baseline and four faulted conditions were obtained. The pump was left running during the entire test series. Both baseband and high frequency demodulation data were obtained simultaneously.

Results Presented:

Baseband - P3BX3400F.2

1) Mean and standard deviation of the baseline and faulted refits.
2) "Modified" likelihood ratio weights (contribution of DC and FRF components set to zero).
3) Modified likelihood ratio weights (all weights set to zero except at three largest weights).

High Frequency Demodulation - P3HX3400F2

4) Mean and standard deviation of the baseline and faulted refits.
5) Modified likelihood ratio weights (contributions of DC and FRF components set to zero).

MEAN FOR FAULTED REFITS
MEAN FOR BASELINE REFITS
SIGMA FOR FAULTED REFITS
SIGMA FOR BASELINE REFITS

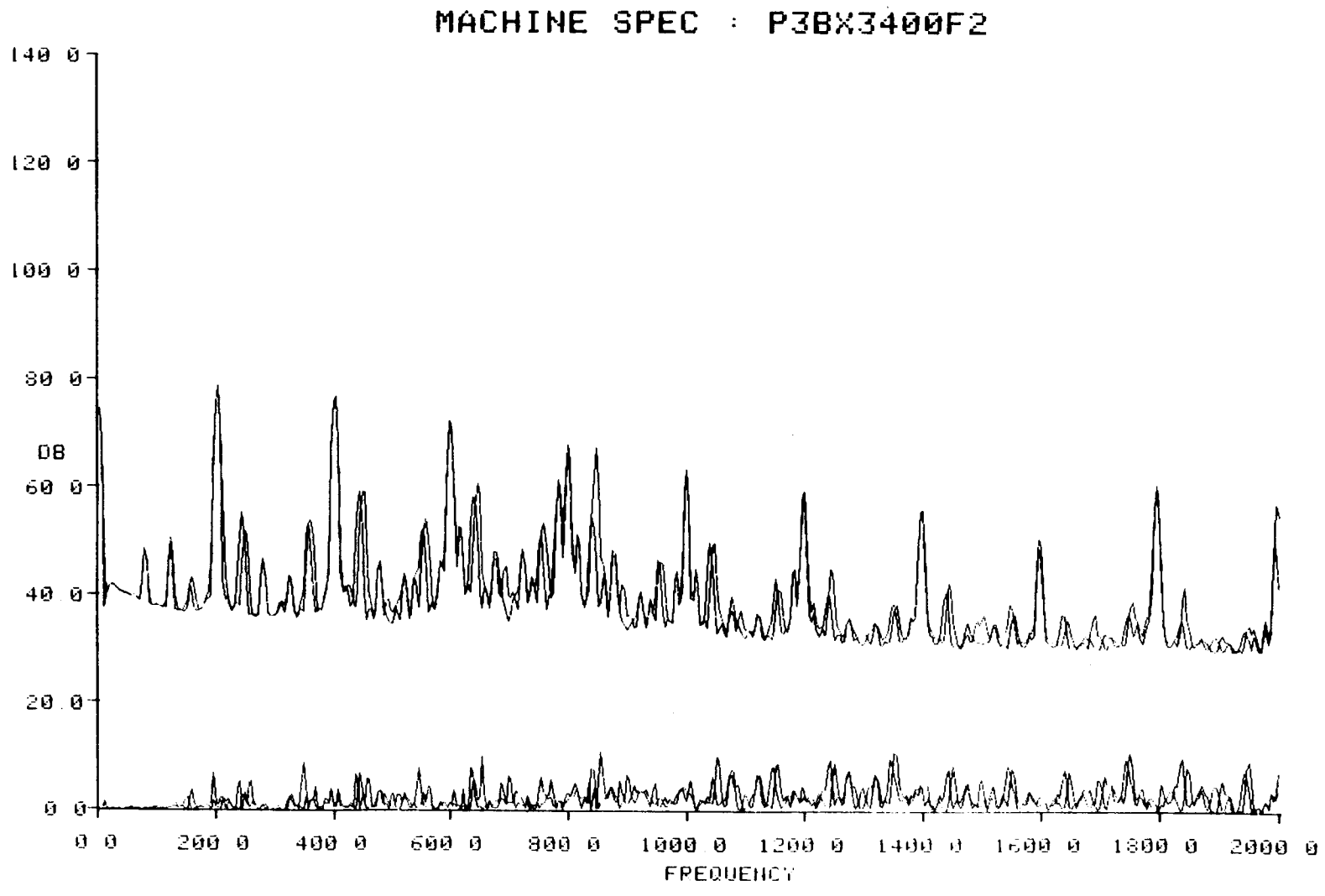

LIKELIHOOD RATIO WEIGHTS

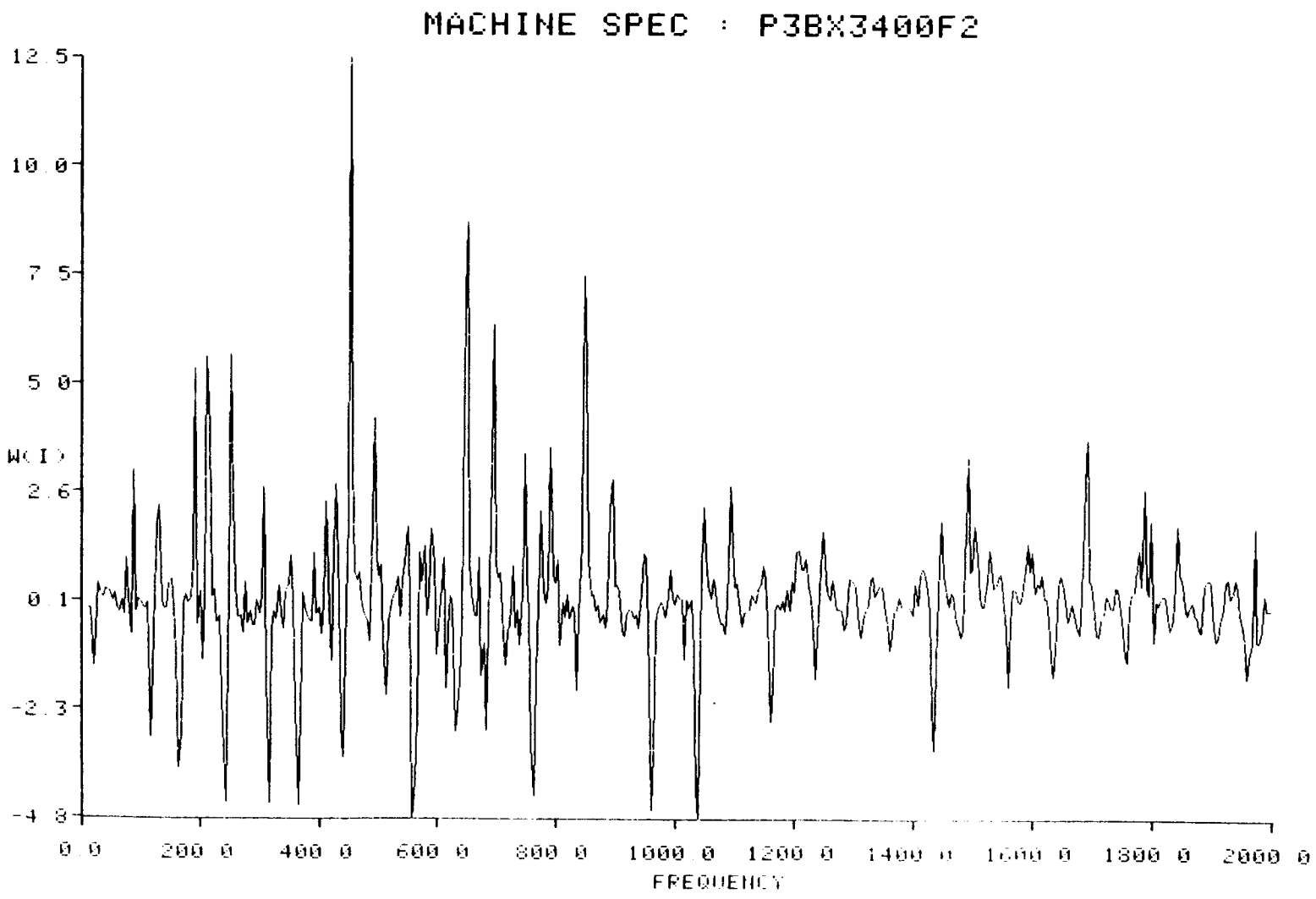

LIKELIHOOD RATIO WEIGHTS

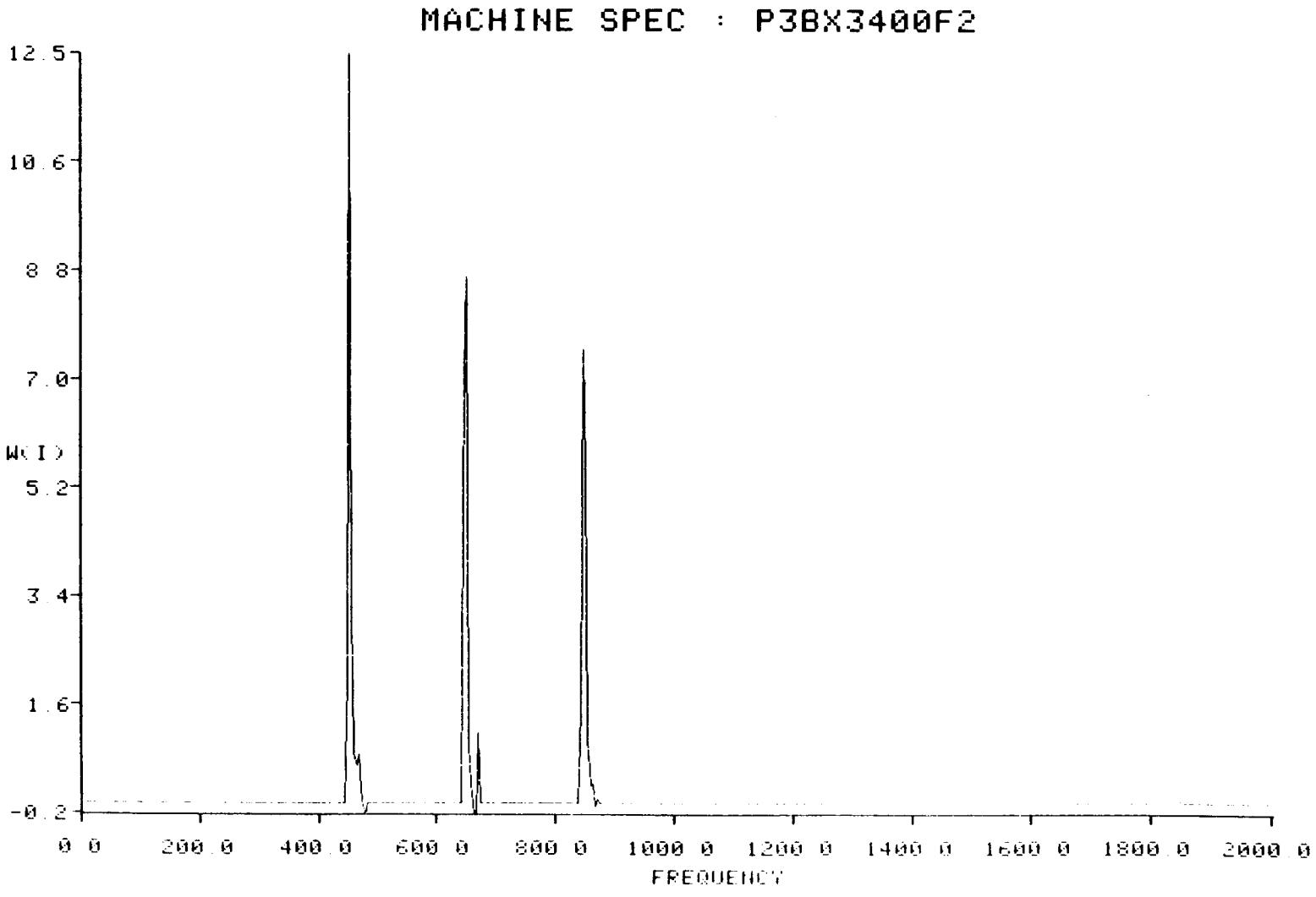

MEAN FOR FAULTED REFITS
MEAN FOR BASELINE REFITS
SIGMA FOR FAULTED REFITS
SIGMA FOR BASELINE REFITS

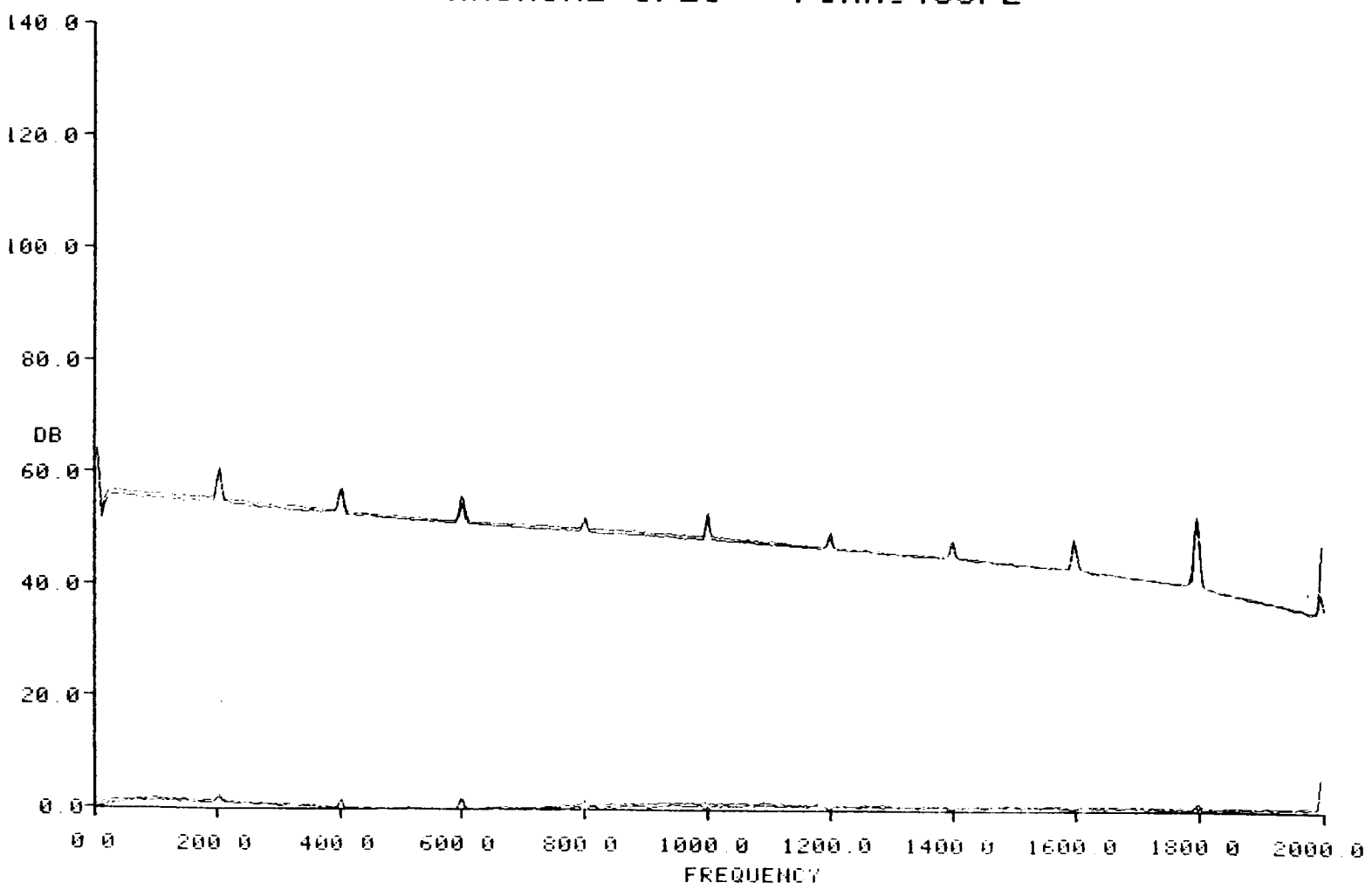

LIKELIHOOD RATIO WEIGHTS

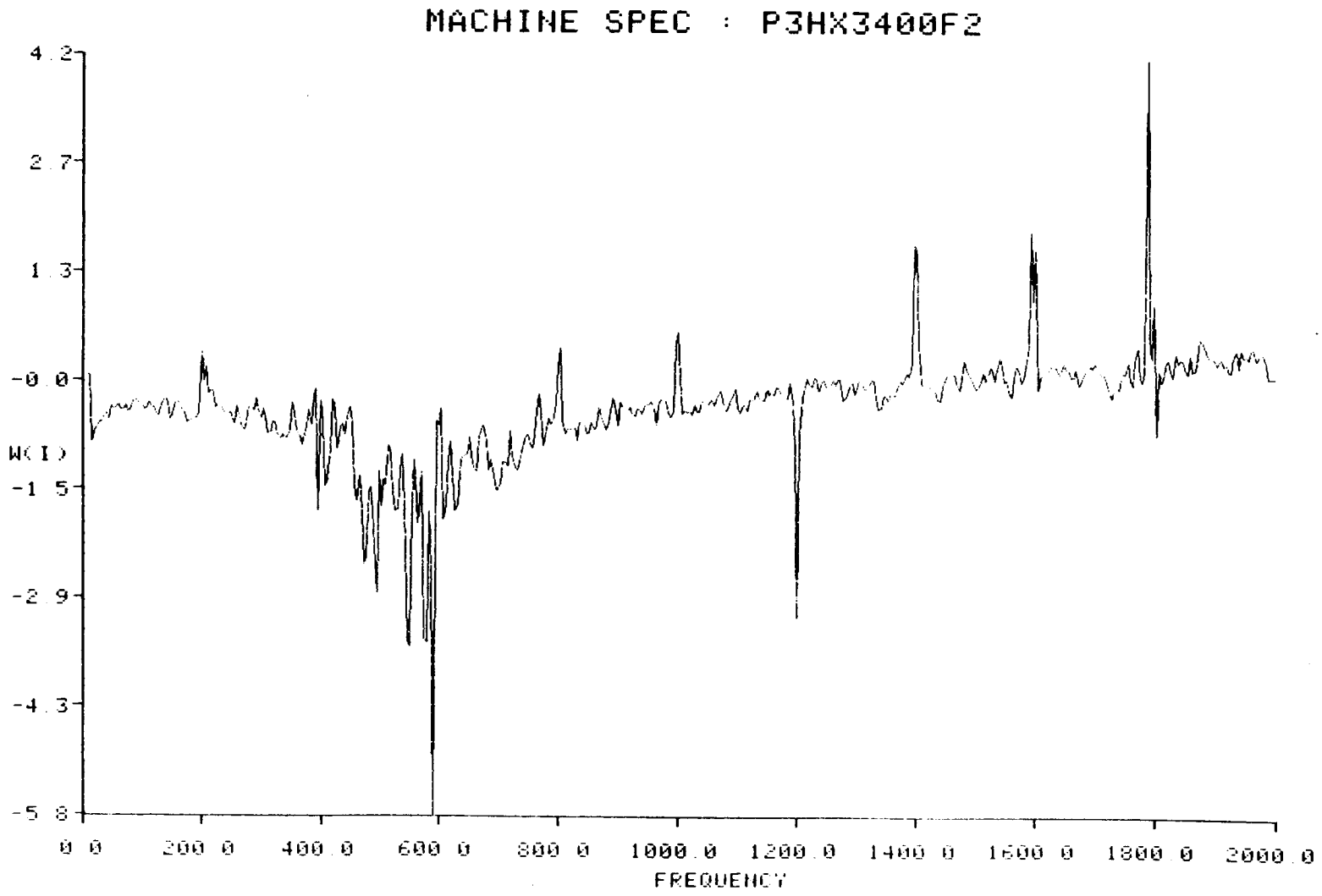

h-2

OPTIMUM SIGNATURE ANALYSIS DETECTION: Phase Loss - Single Three Phase Pump

P_D for P_{FA} = 0.1

Baseband	HFD
1.0 ("modified" weights)	.59 (modified weights)
1.0 (modified weights)	

LOAD CONDITIONS - SINGLE ONE PHASE PUMP

TEST DESCRIPTION: Load Conditions - Single One Phase Pump

A series of tests was performed in which a high and low discharge pressure for a single one phase pump was evaluated. Baseline readings were obtained while the pump was operating normally at a nominal discharge pressure of 40 psig. The discharge pressure was then increased to twice nominal pressure (80 psig) and a set of faulted readings obtained. The discharge pressure was decreased to one-half nominal pressure (20 psig) and another set of faulted readings recorded. Four baseline and two sets of four faulted conditions were obtained. The pump was operating continuously during the experiment. Both baseband and high frequency demodulation data were obtained simultaneously.

Results Presented:

I. Discharge Pressure = 80 psig

Baseband - P1BX35A0B2

1) Mean and standard deviation of the baseline and faulted refits.
2) "Modified" likelihood ratio weights (DC contribution set to zero)
3) Modified likelihood ratio weights (all weights set to zero except at 1XRPM, 2XRPM, and gear mesh frequency).

II. Discharge Pressure = 20 psig

Baseband - P1BX35AUB2

4) Mean and standard deviation of the baseline and faulted refits.
5) "Modified" likelihood ratio weights (contributions by DC and FRF component set to zero)

Note: The gear mesh frequency weight is high with a 80 psig discharge pressure and is very small at 20 psig.

MEAN FOR FAULTED REFITS
MEAN FOR BASELINE REFITS
SIGMA FOR FAULTED REFITS
SIGMA FOR BASELINE REFITS

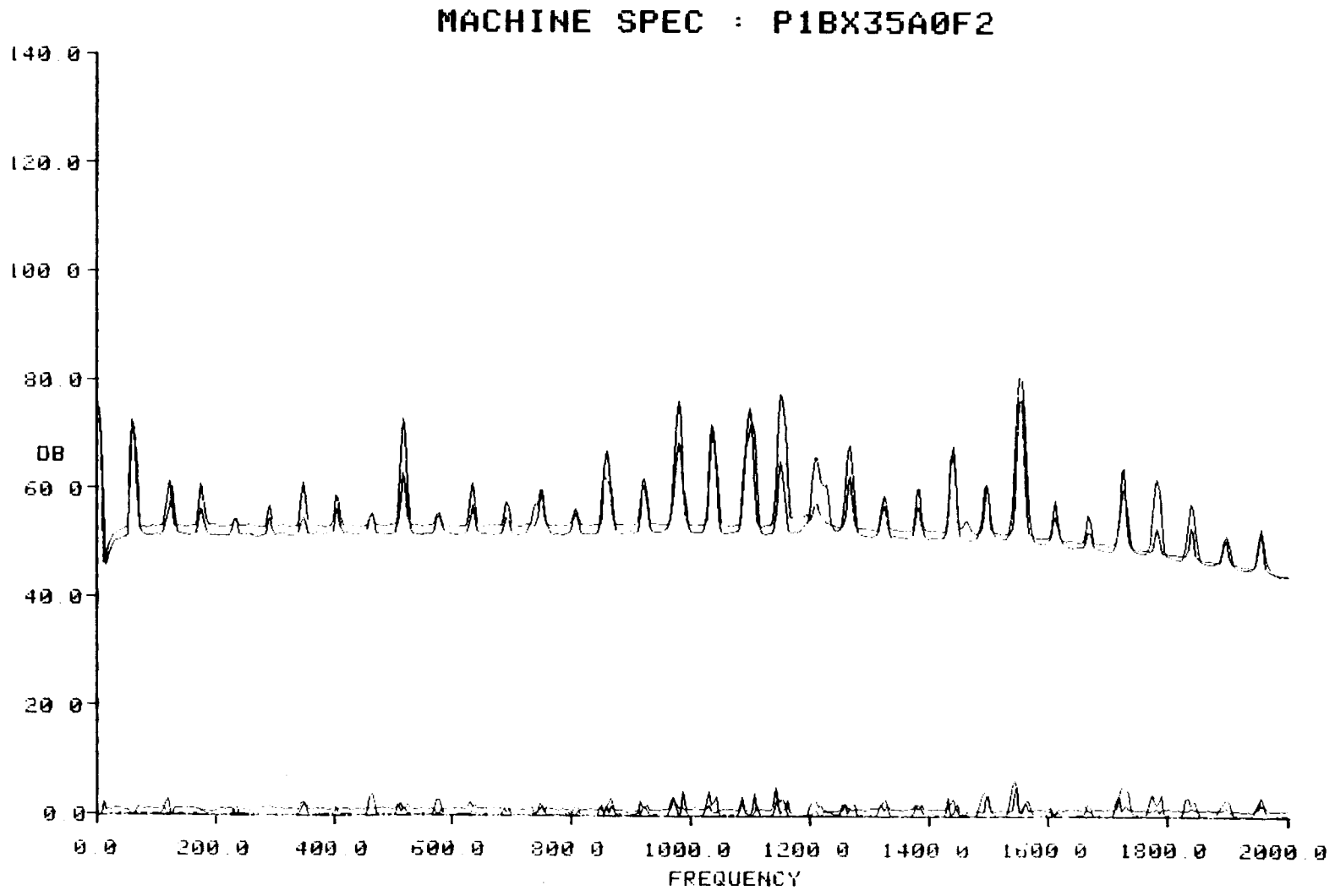

LIKELIHOOD RATIO WEIGHTS

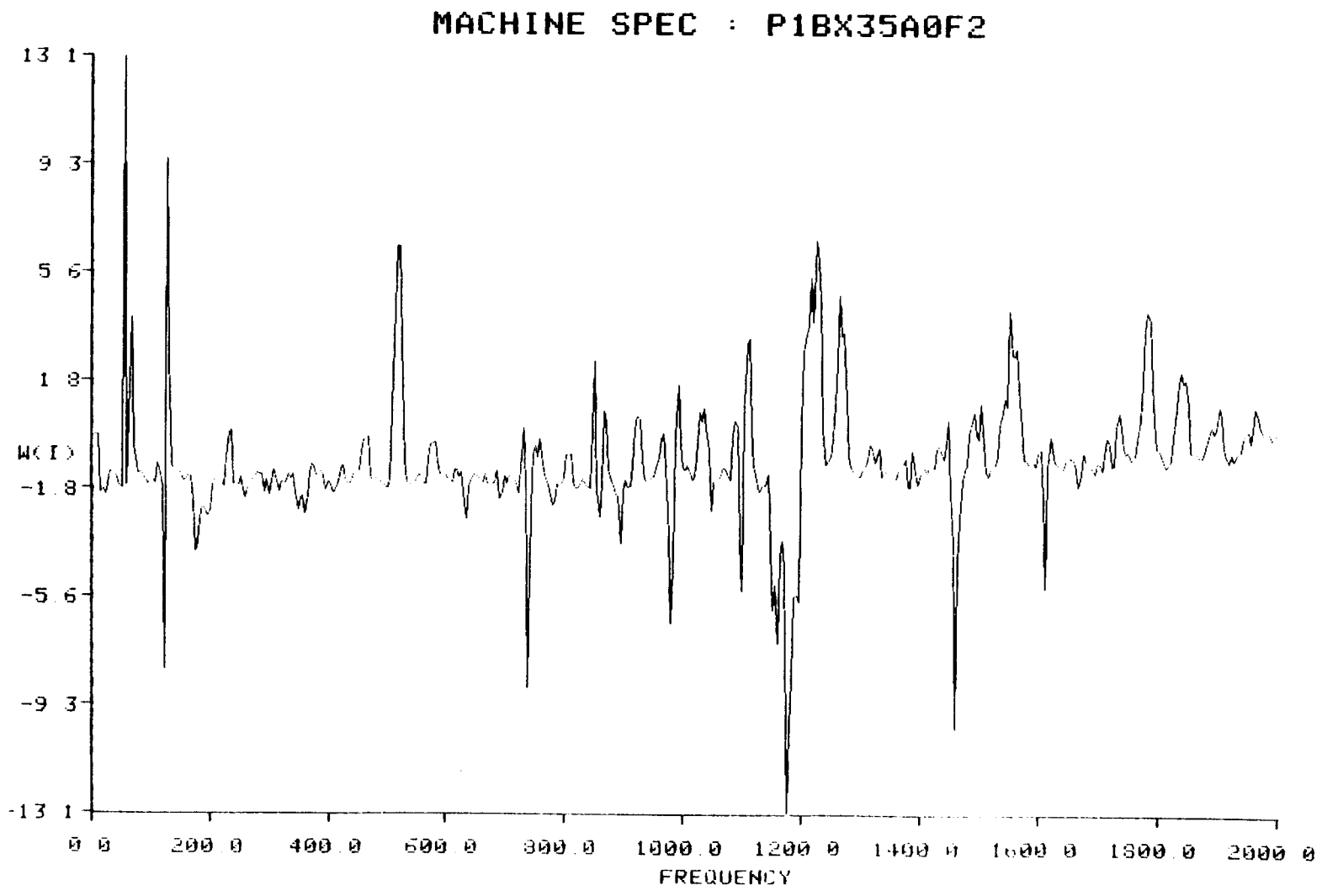

LIKELIHOOD RATIO WEIGHTS

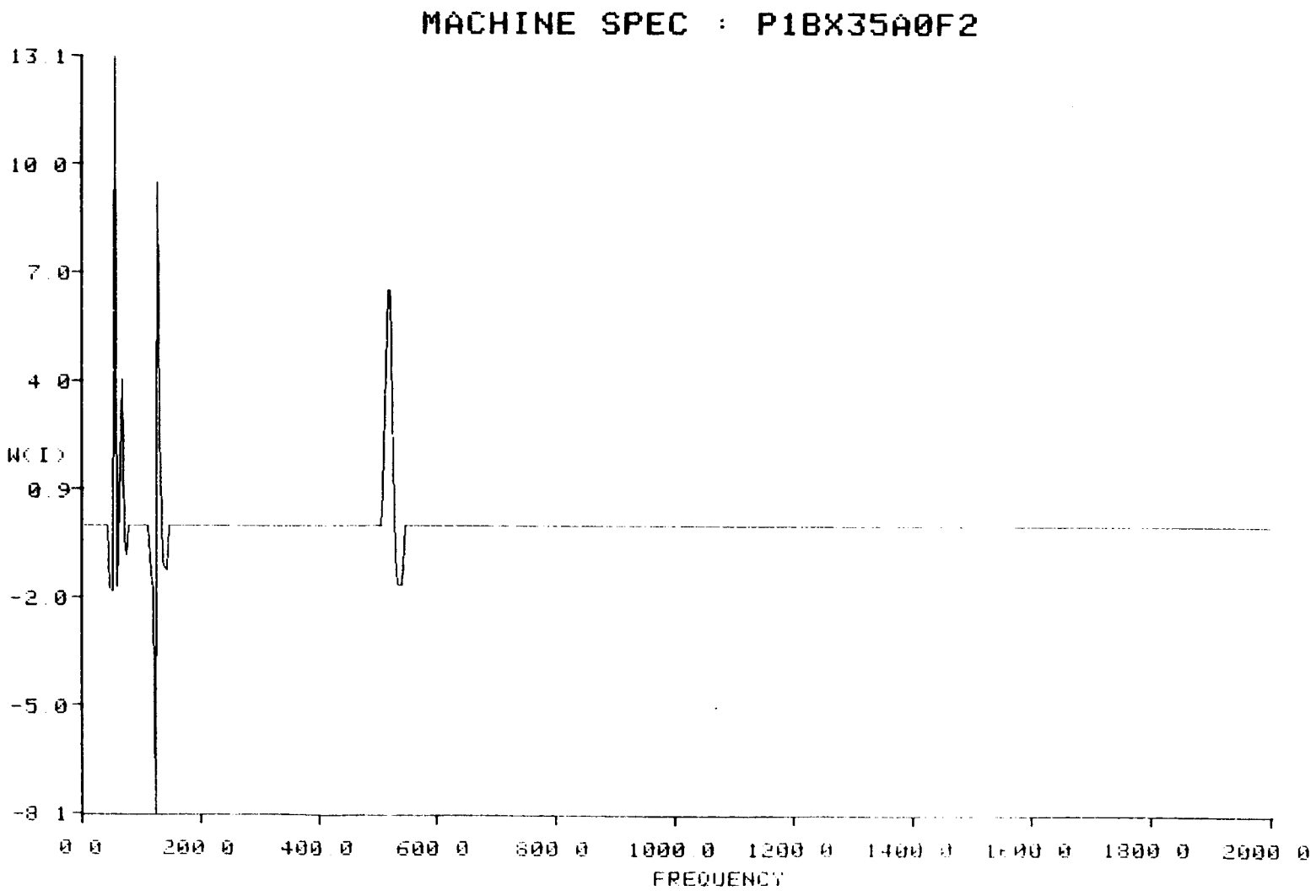

MEAN FOR FAULTED REFITS
MEAN FOR BASELINE REFITS
SIGMA FOR FAULTED REFITS
SIGMA FOR BASELINE REFITS

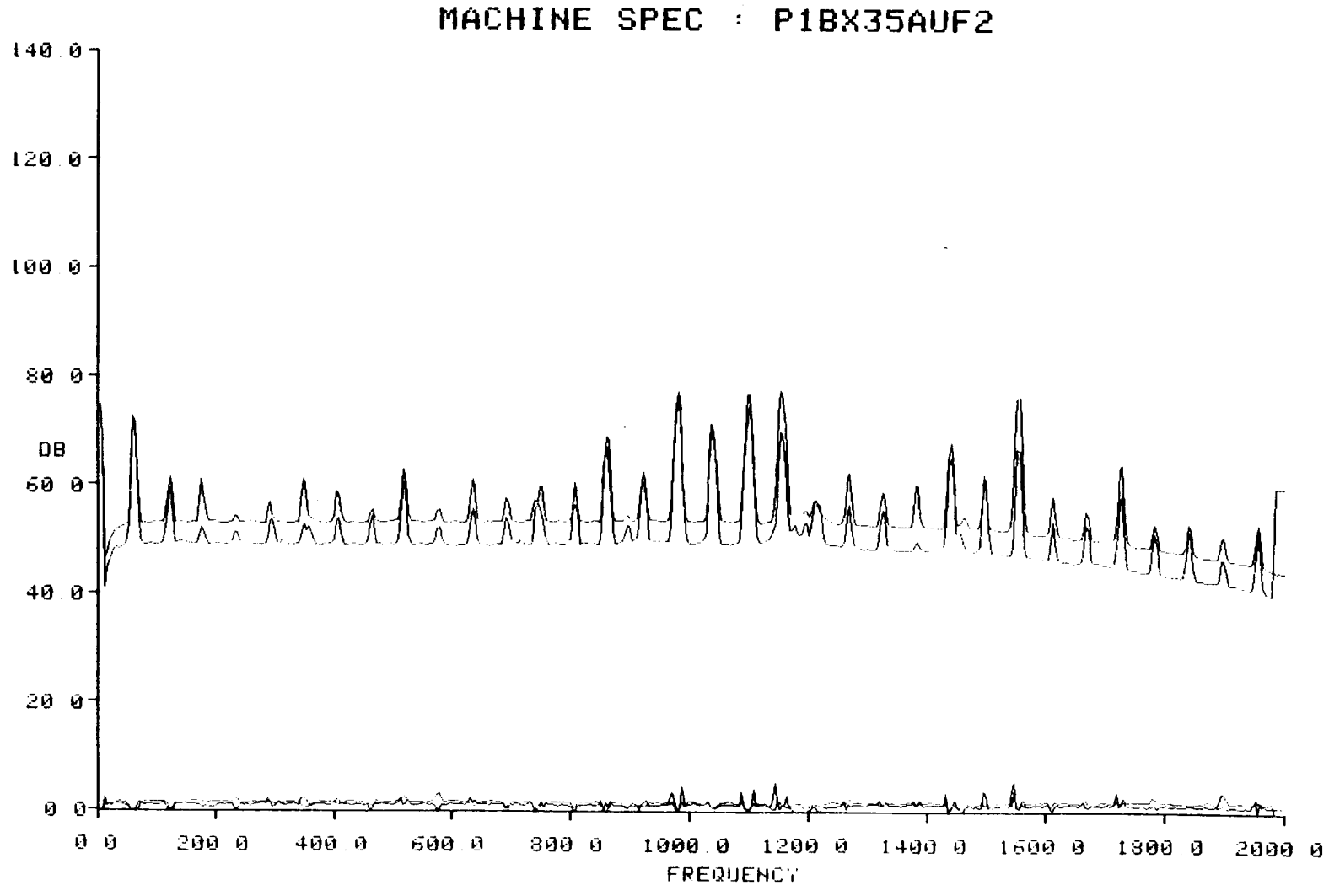

LIKELIHOOD RATIO WEIGHTS

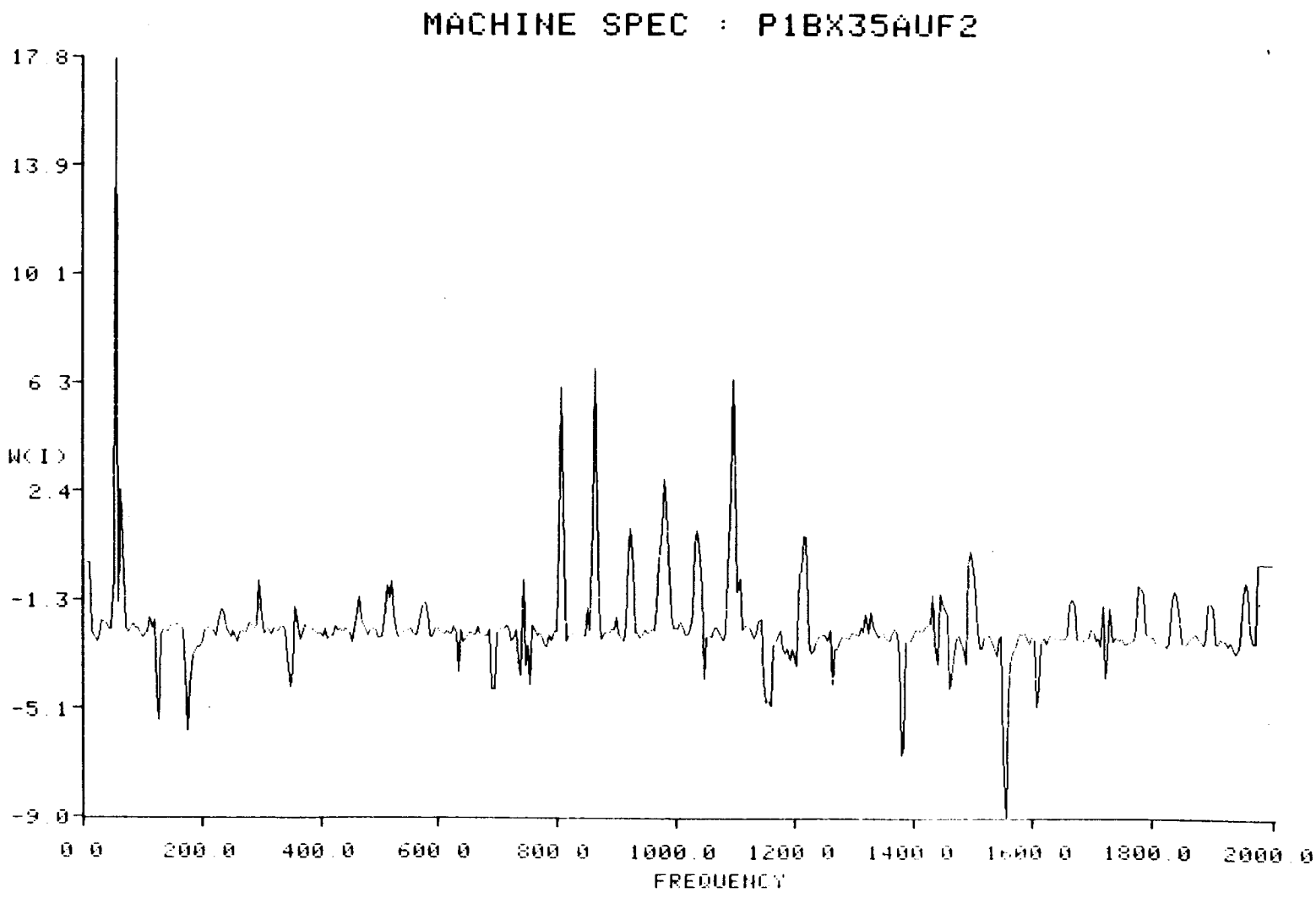

OPTIMUM SIGNATURE ANALYSIS DETECTION: Load Conditions
Single One Phase Pump

P_D for P_{FA} = 0.1

Discharge Pressure	Baseband	HFD
80 psi	1.0 ("modified" weights)	.99
	1.0 (modified weights)	
20 psi	1.0	1.0

INLET AIR RESTRICTIONS -- SINGLE FAN

TEST DESCRIPTION : Inlet Air Restrictions -- Single Fan

A series of tests was performed in which the inlet air to a single TRW fan was restricted. Restricted air flow can occur with a dirty or partially blocked air filtration device upstream of a fan in actual service. A baseline reading was obtained under normal operating conditions, after which approximately 25% of the free inlet area of the fan was blocked. A set of faulted data was then obtained. The inlet area was then further restricted to approximately 75% of the free inlet area and another set of faulted data was obtained. This test procedure was performed on the test fan four times. The fan remained in operation during the entire experiment. Both baseband and high frequency demodulation data was obtained simultaneously.

Results Presented:

I. 25% Blockage of Inlet

Baseband -- F0BX2500F.2

1) Mean and standard deviation of the baseline and faulted refits
2) "Modified" likelihood ratio weights (contributions by FRF components set to zero only)

II. 75% Blockage of Inlet

Baseband -- F0BX25A0F.2

3) Mean and standard deviation of the baseline and faulted refits
4) "Modified" likelihood ratio weights (contributions by FRF components set to zero)
5) Modified likelihood ratio weights (weights above 250 Hz set to zero retaining area of large positive weights)

MEAN FOR FAULTED REFITS
MEAN FOR BASELINE REFITS
SIGMA FOR FAULTED REFITS
SIGMA FOR BASELINE REFITS

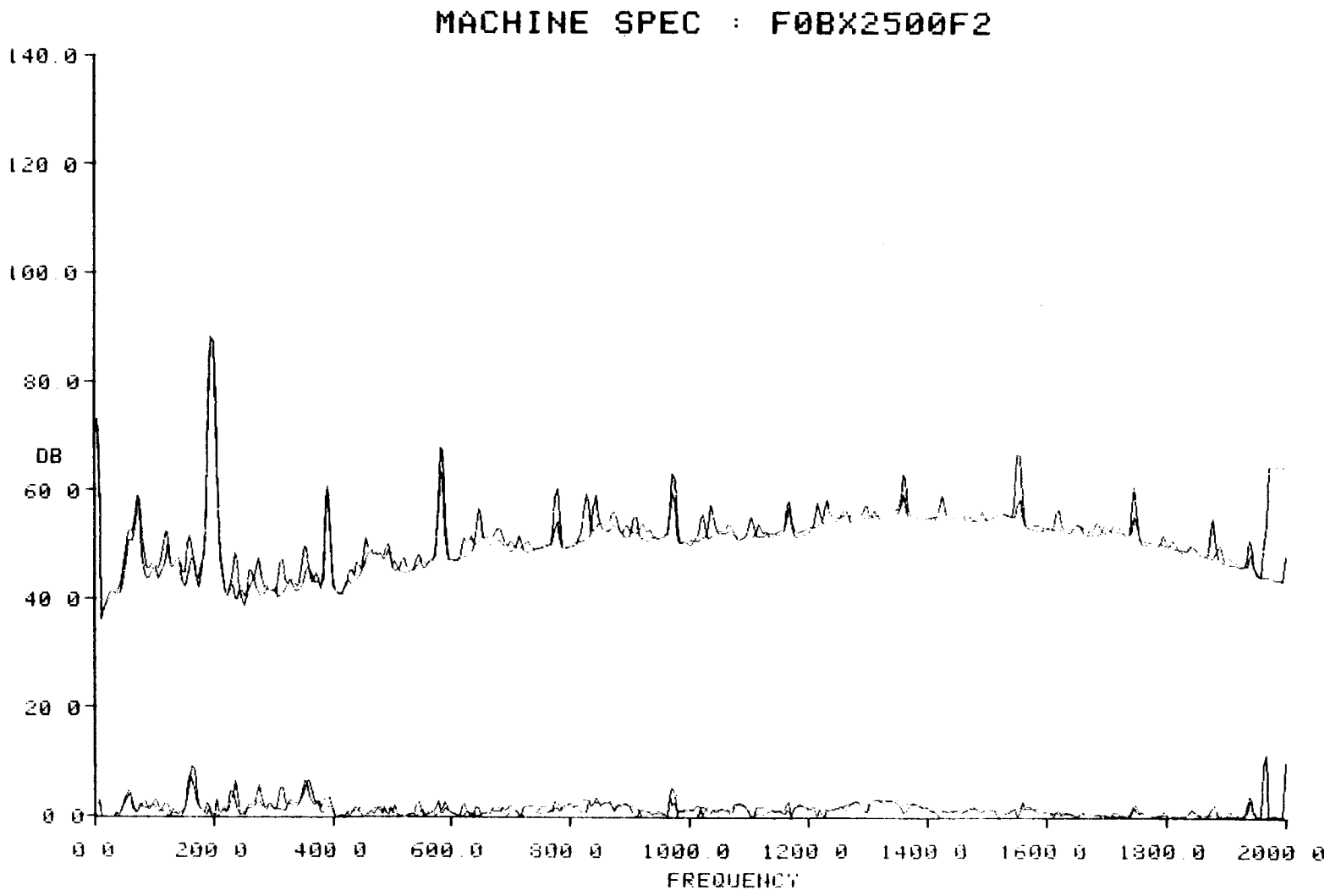

LIKELIHOOD RATIO WEIGHTS

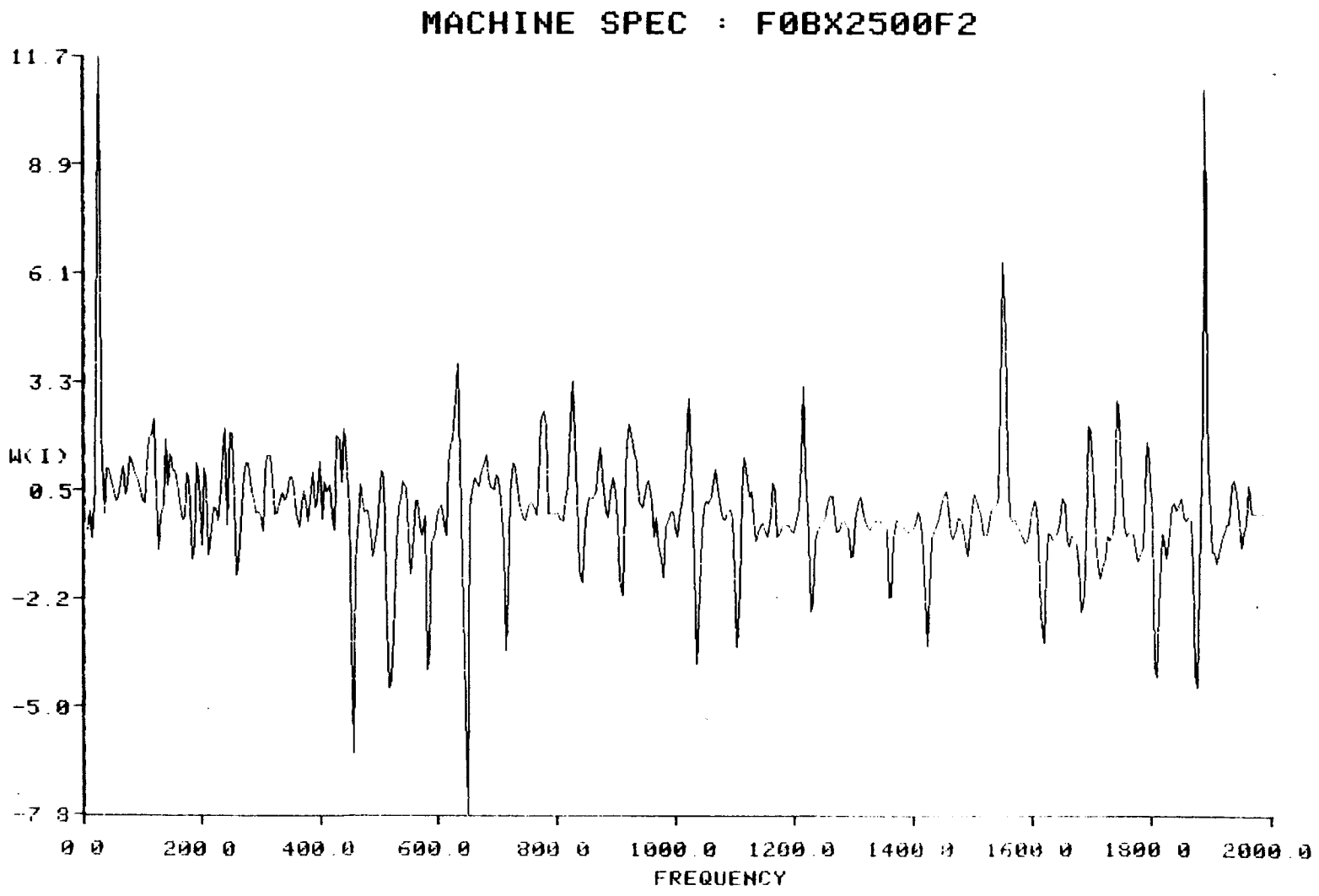

MEAN FOR FAULTED REFITS
MEAN FOR BASELINE REFITS
SIGMA FOR FAULTED REFITS
SIGMA FOR BASELINE REFITS

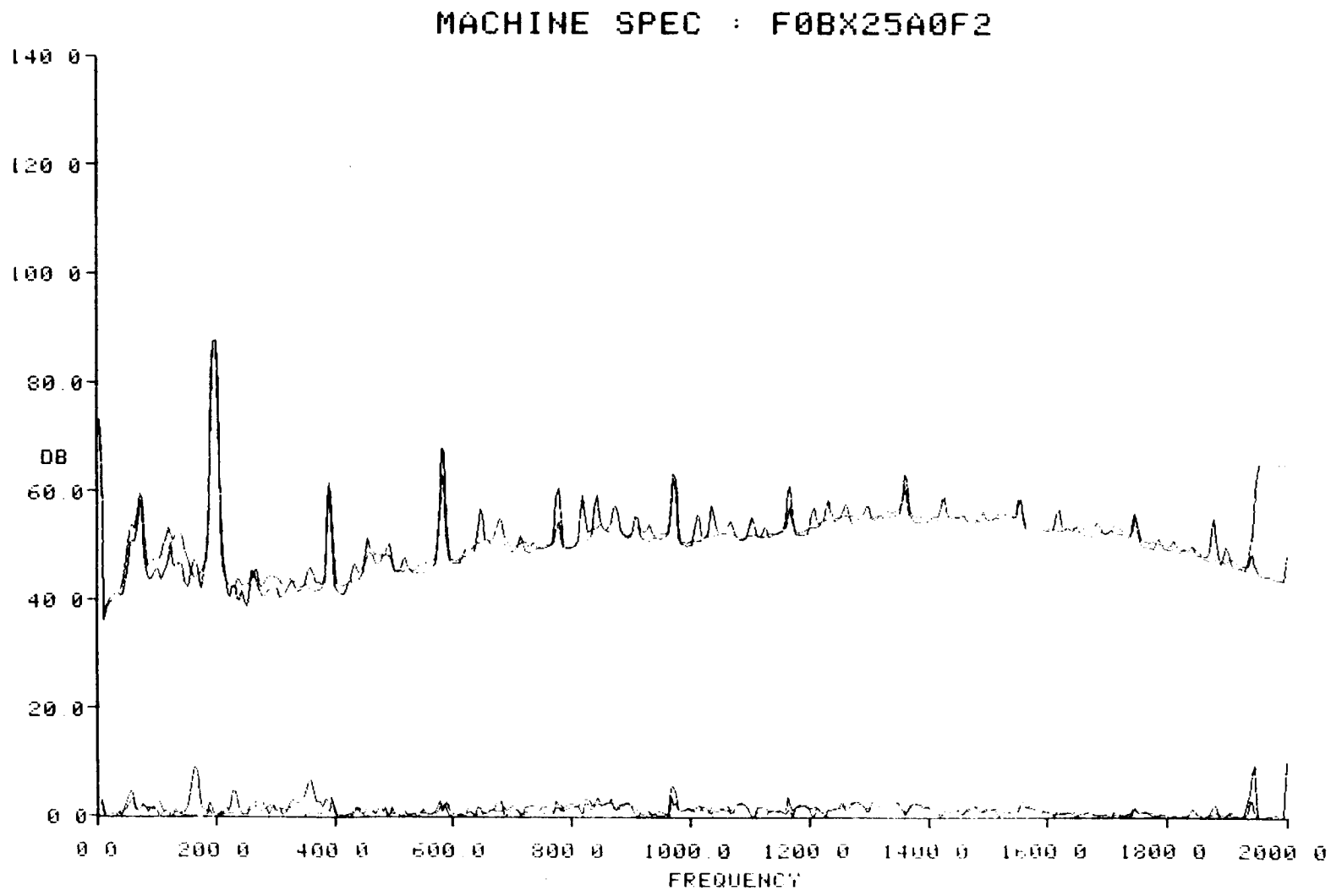

LIKELIHOOD RATIO WEIGHTS

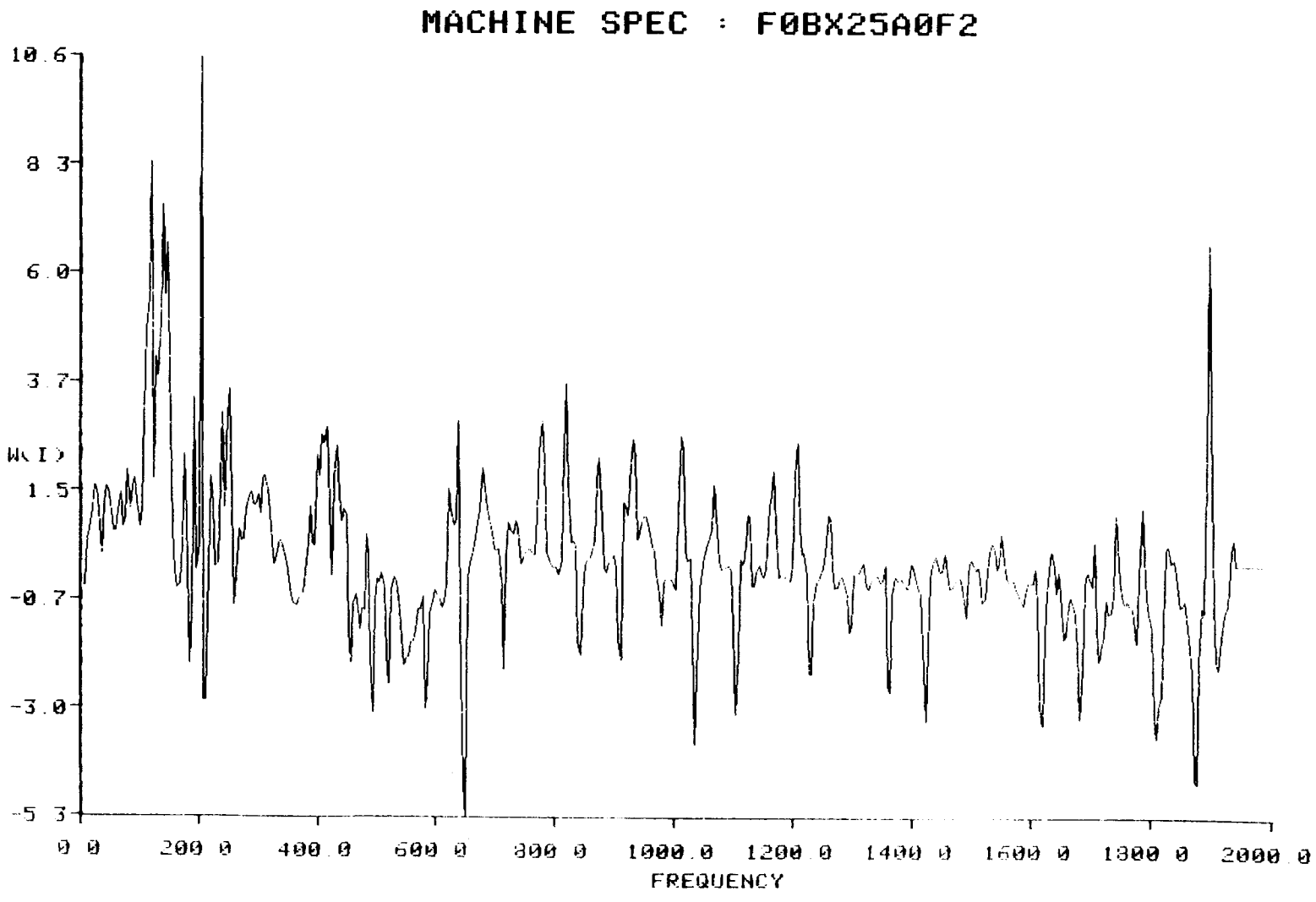

LIKELIHOOD RATIO WEIGHTS

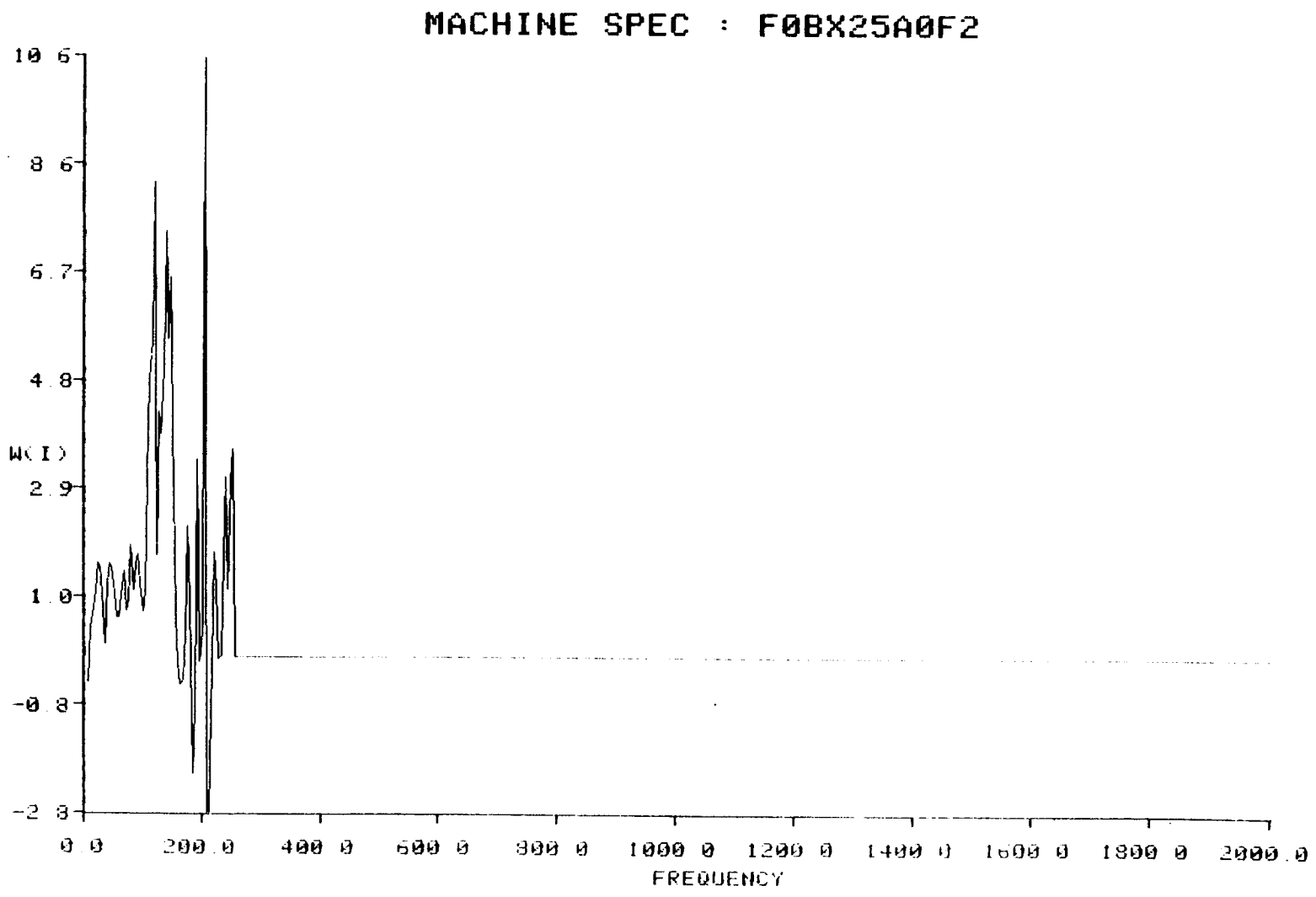

Optimum Signature Analysis Detection : Inlet Air Restrictions -- Single Fan

P_D for $P_{FA} = 0.1$

Inlet Test Condition	Baseband	HFD
25% Blockage	1.0	0.80
75% Blockage	1.0	0.90

COUPLING IMBALANCE -- SINGLE THREE-PHASE PUMP

TEST DESCRIPTION: Coupling Imbalance -- Single Three-Phase Pump

A series of tests was performed in which two conditions of coupling imbalance on a single three-phase pump was evaluated. The pump head was decoupled from the motor for the tests, with the accelerometer mounted vertically on the motor housing. A baseline was first obtained with the unit running normally. The motor was then stopped and a small imbalance weight weighing 0.035 grams was attached to the magnetic coupling at a radius of approximately 14 mm from the shaft centerline. The unit was restarted and a set of faulted data obtained. After collection of the small imbalance data, the motor was stopped and a larger imbalance weight weighing 0.173 grams was attached at the same location as was used for the small imbalance test. The large imbalance faulted data was then obtained. This fault introduction procedure was repeated on the same unit four times. Both baseband and high frequency demodulation data was obtained simultaneously.

Results Presented:

I. Small Coupling Imbalance

Baseband -- P3BX3700F.2

1) Mean and standard deviation of the baseline and faulted refits
2) Unmodified likelihood ratio weights

II. Large Coupling Imbalance

Baseband -- P3BX37L0F.2

3) Mean and standard deviation of the baseline and faulted refits
4) Unmodified likelihood ratio weights

High Frequency Demodulation -- P3HX37L0F.2

5) Mean and standard deviation of the baseline and faulted refits

6) "Modified" likelihood ratio weights (contributions by DC and FRF components set to zero only)

MEAN FOR FAULTED REFITS
MEAN FOR BASELINE REFITS
SIGMA FOR FAULTED REFITS
SIGMA FOR BASELINE REFITS

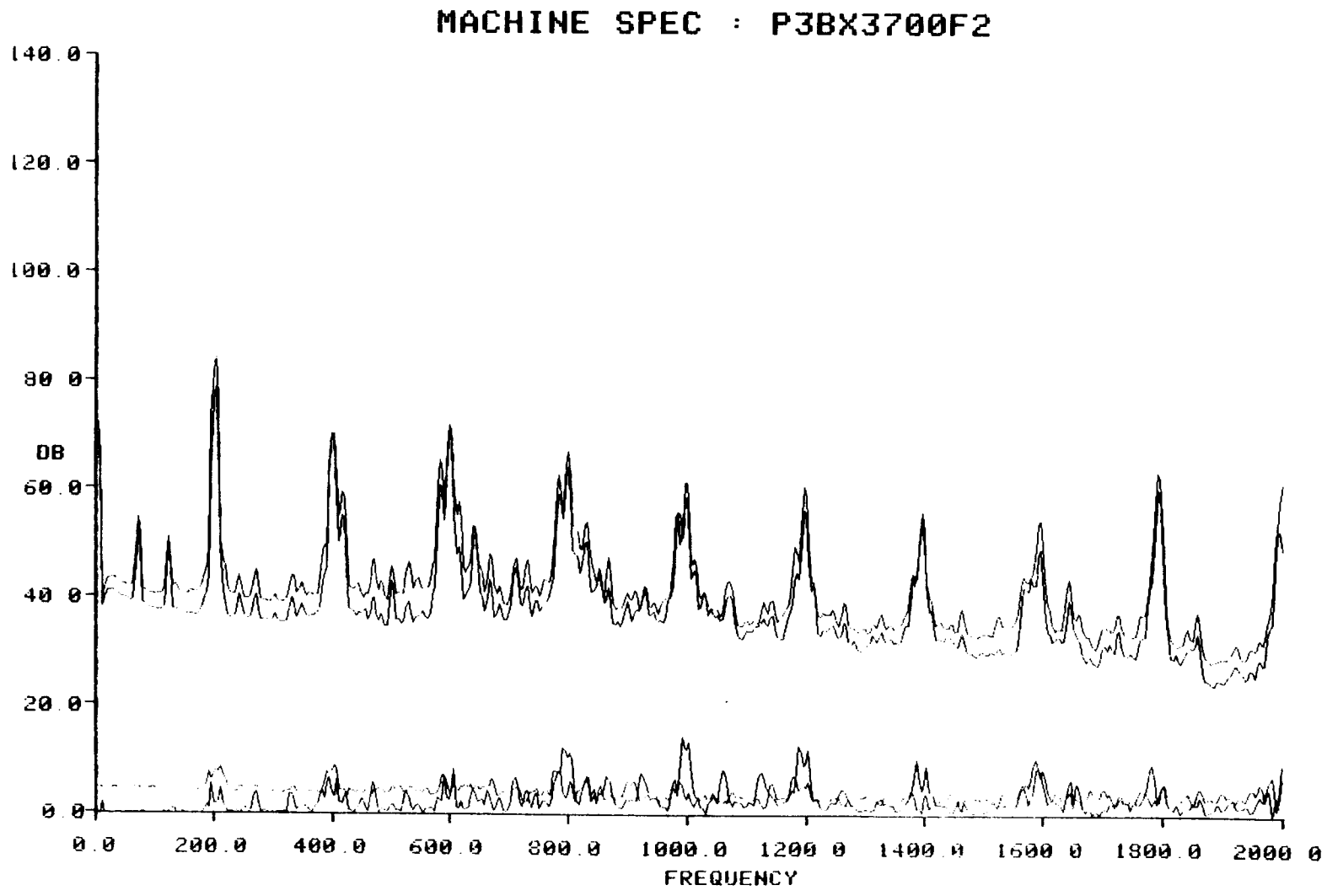

LIKELIHOOD RATIO WEIGHTS

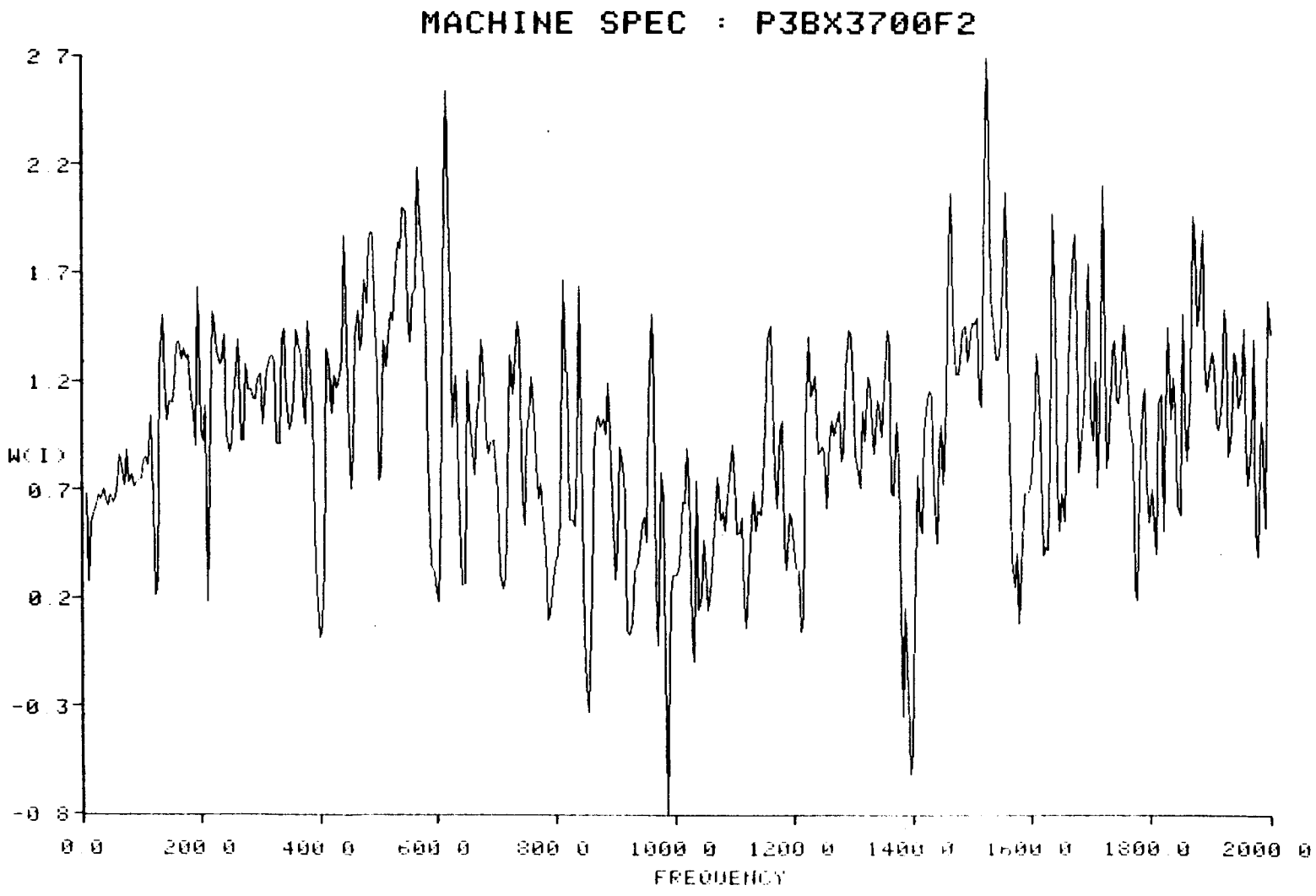

MEAN FOR FAULTED REFITS

MEAN FOR BASELINE REFITS

SIGMA FOR FAULTED REFITS

SIGMA FOR BASELINE REFITS

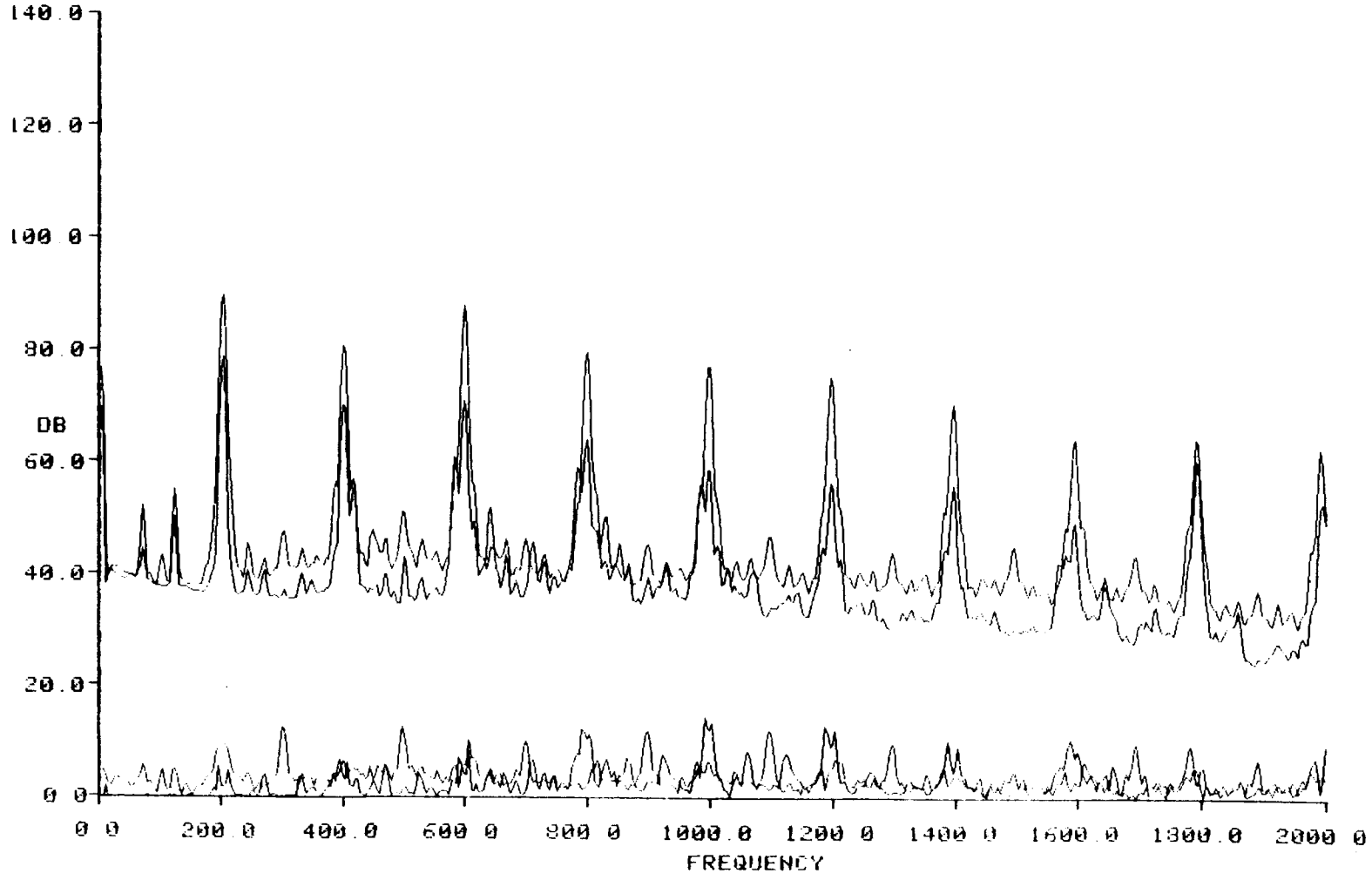

LIKELIHOOD RATIO WEIGHTS

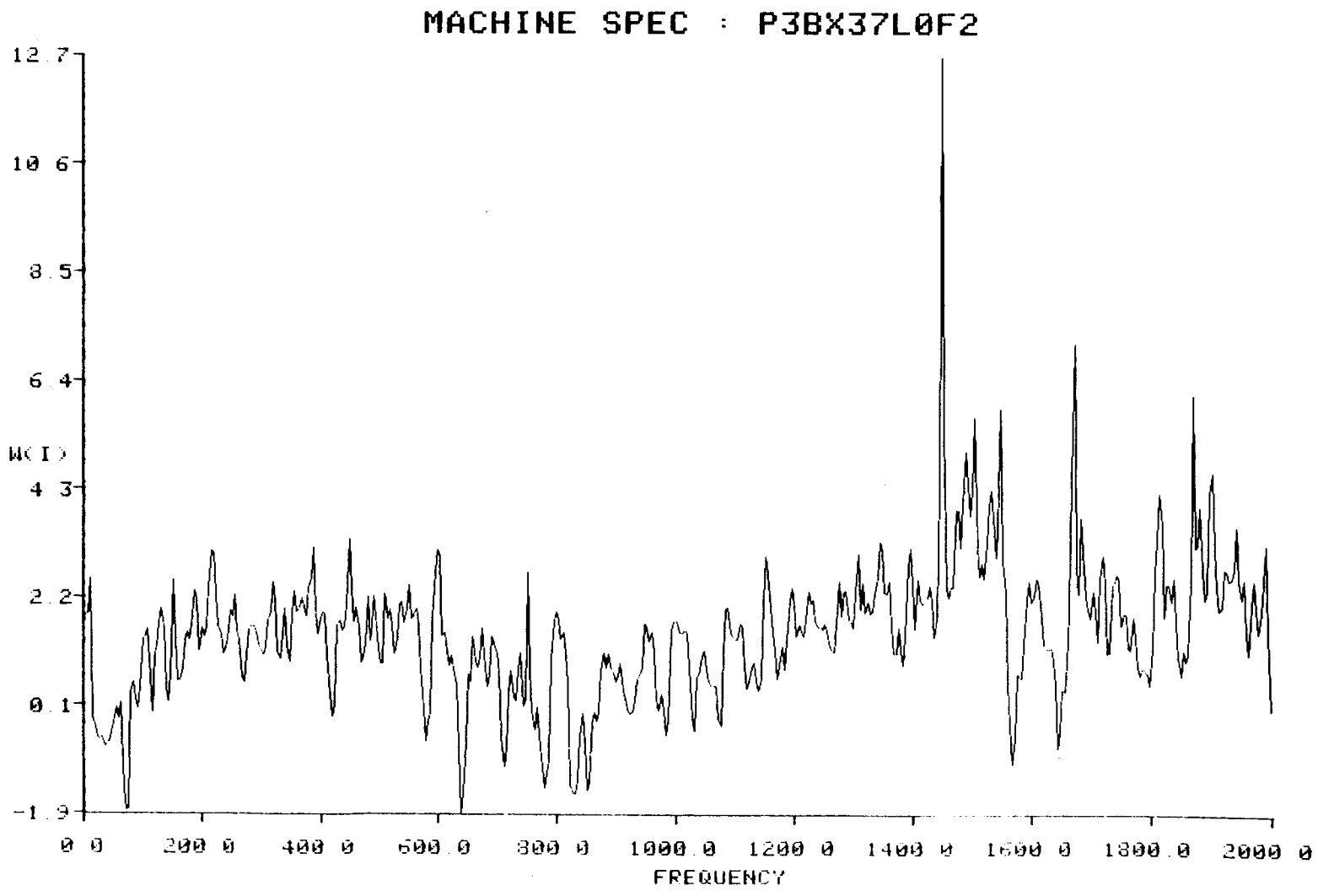

MEAN FOR FAULTED REFITS
MEAN FOR BASELINE REFITS
SIGMA FOR FAULTED REFITS
SIGMA FOR BASELINE REFITS

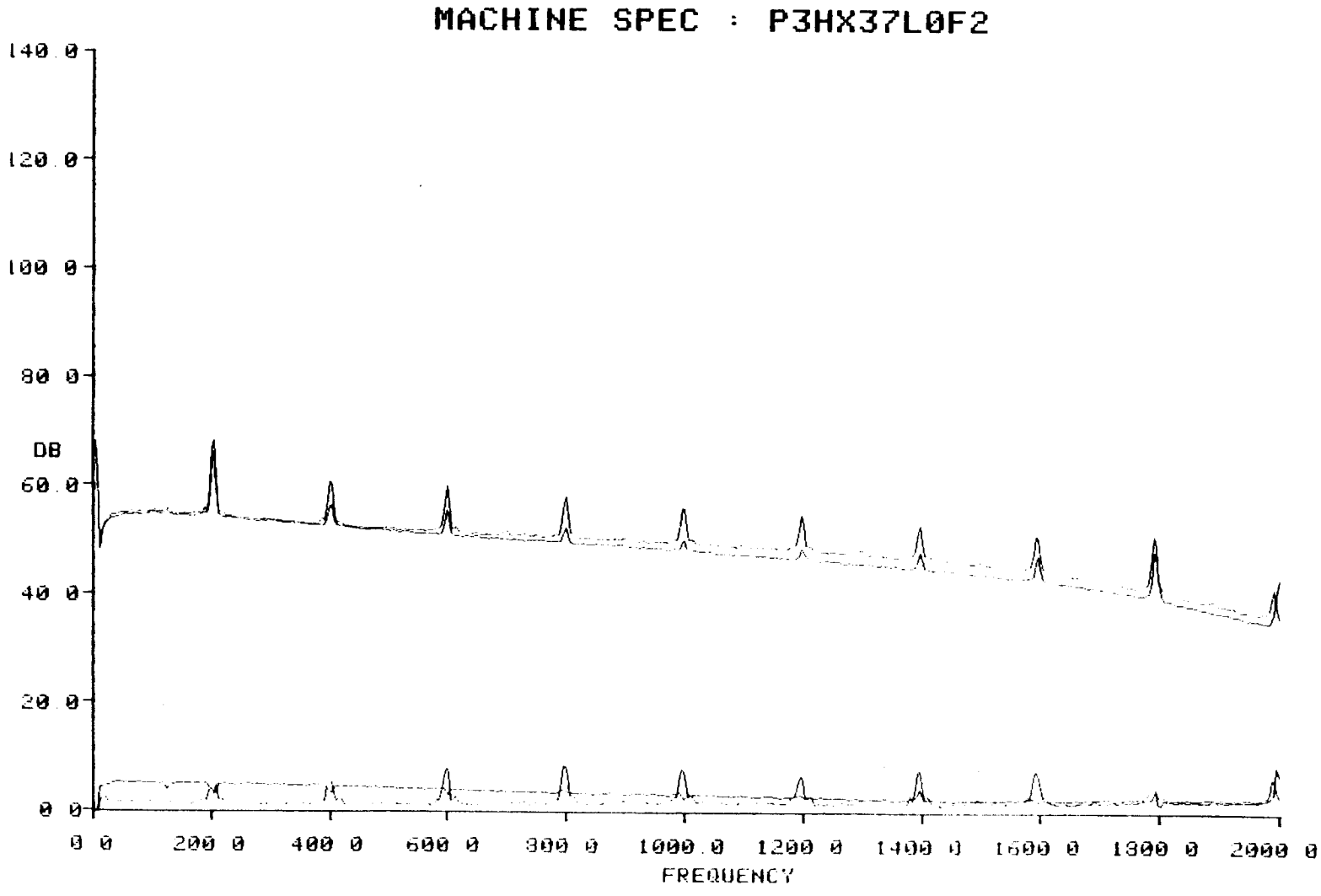

LIKELIHOOD RATIO WEIGHTS

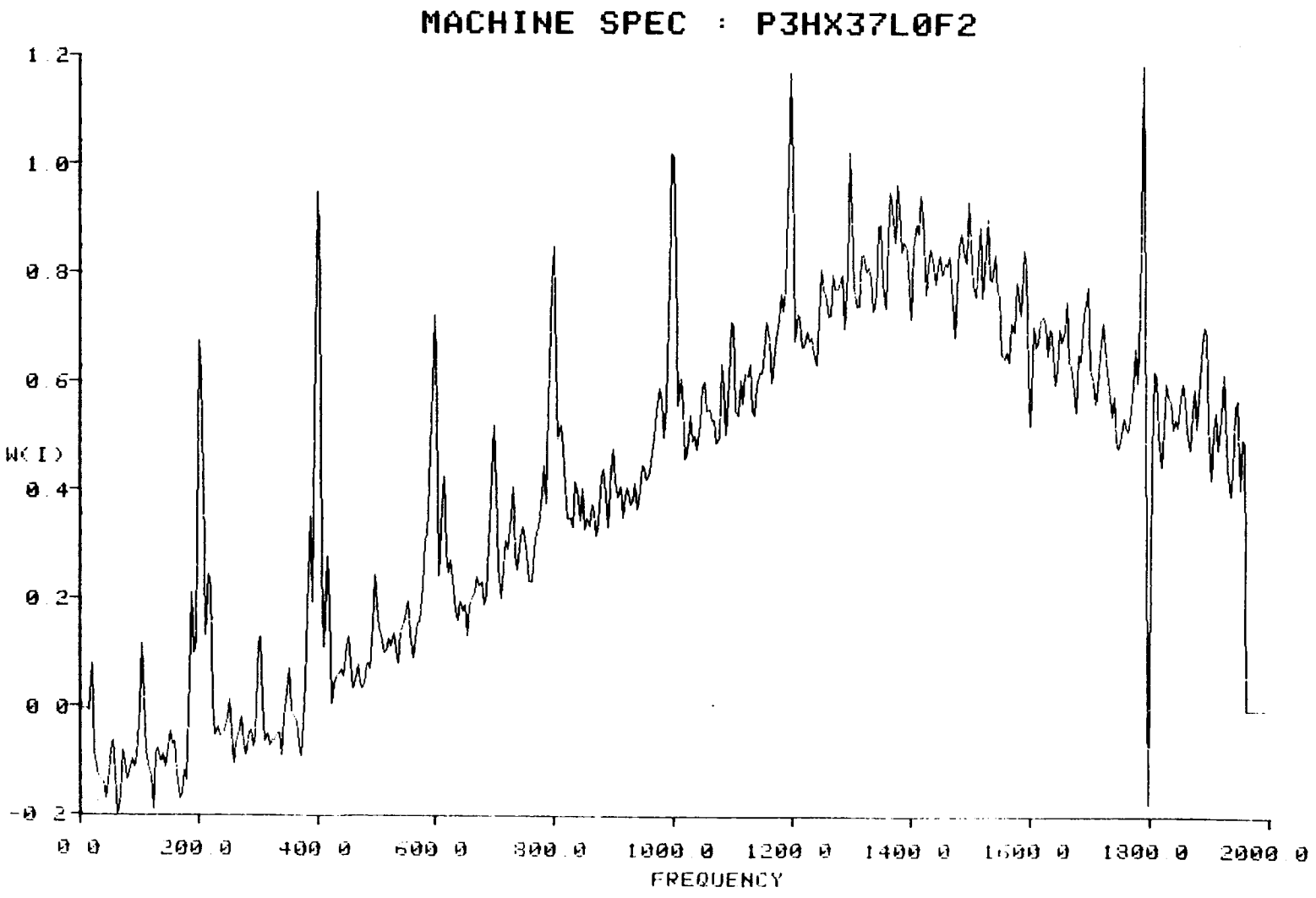

Optimum Signature Analysis Detection: Coupling Imbalance -- Single Three-Phase Pump

P_D for $P_{FA} = 0.1$

Test Condition	Baseband	HFD
Small Imbalance	0.76	0.69
Large Imbalance	0.99	0.32

VOLTAGE CHANGE -- SINGLE ONE-PHASE PUMP

TEST DESCRIPTION: Voltage Change -- Single One-Phase Pump

A series of tests was performed in which an over and under voltage condition on a single one-phase pump was evaluated. A baseline was recorded at the normal operating voltage (120V) after which the voltage was increased approximately 10% to 135V and a set of faulted data was obtained. The voltage was then reduced approximately 10% under nominal voltage to 105V, and a second set of faulted data was again obtained. This procedure was repeated on the pump four times with the pump remaining in operation during the entire experiment. Both baseband and high frequency demodulation data were obtained simultaneously.

Results Presented:

I. Under Voltage (105V)

Baseband -- P1BX35BUF.2

1) Mean and standard deviation of the baseline and faulted refits
2) Unmodified likelihood ratio weights

II. Over Voltage (135V)

Baseband -- P1BX35B0F.2

3) Mean and standard deviation of the baseline and faulted refits
4) "Modified" likelihood ratio weights (contribution by FRF component set to zero only)

High Frequency Demodulation -- P1HX35B0F.2

5) Mean and standard deviation of the baseline and faulted refits
6) "Modified" likelihood ratio weights (contribution by FRF component set

to zero only)

Note: The test pump remaining on during the experiment resulted in a low standard deviation in the test spectra. The large positive detection weight values are a result of this small data variability.

MEAN FOR FAULTED REFITS
MEAN FOR BASELINE REFITS
SIGMA FOR FAULTED REFITS
SIGMA FOR BASELINE REFITS

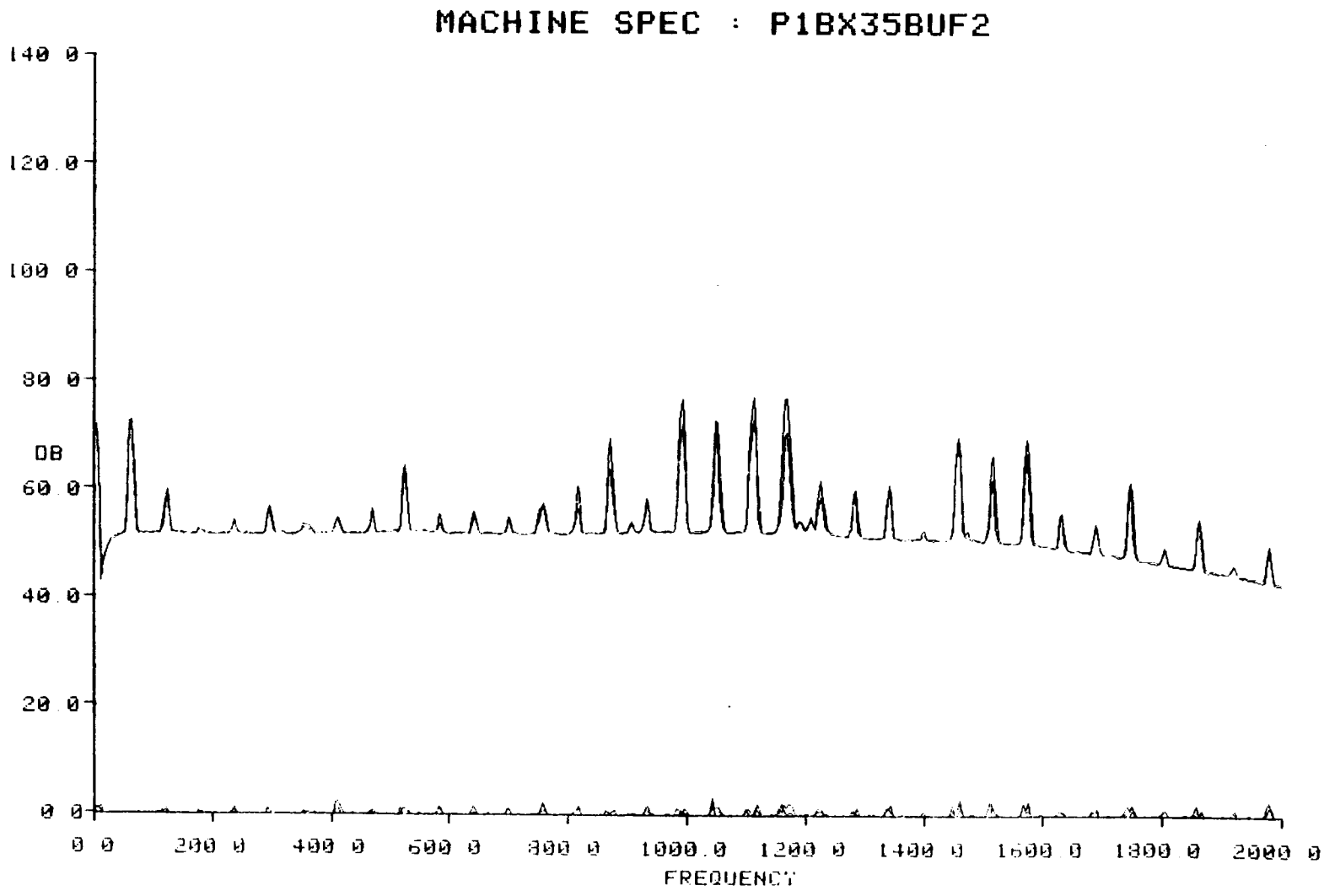

LIKELIHOOD RATIO WEIGHTS

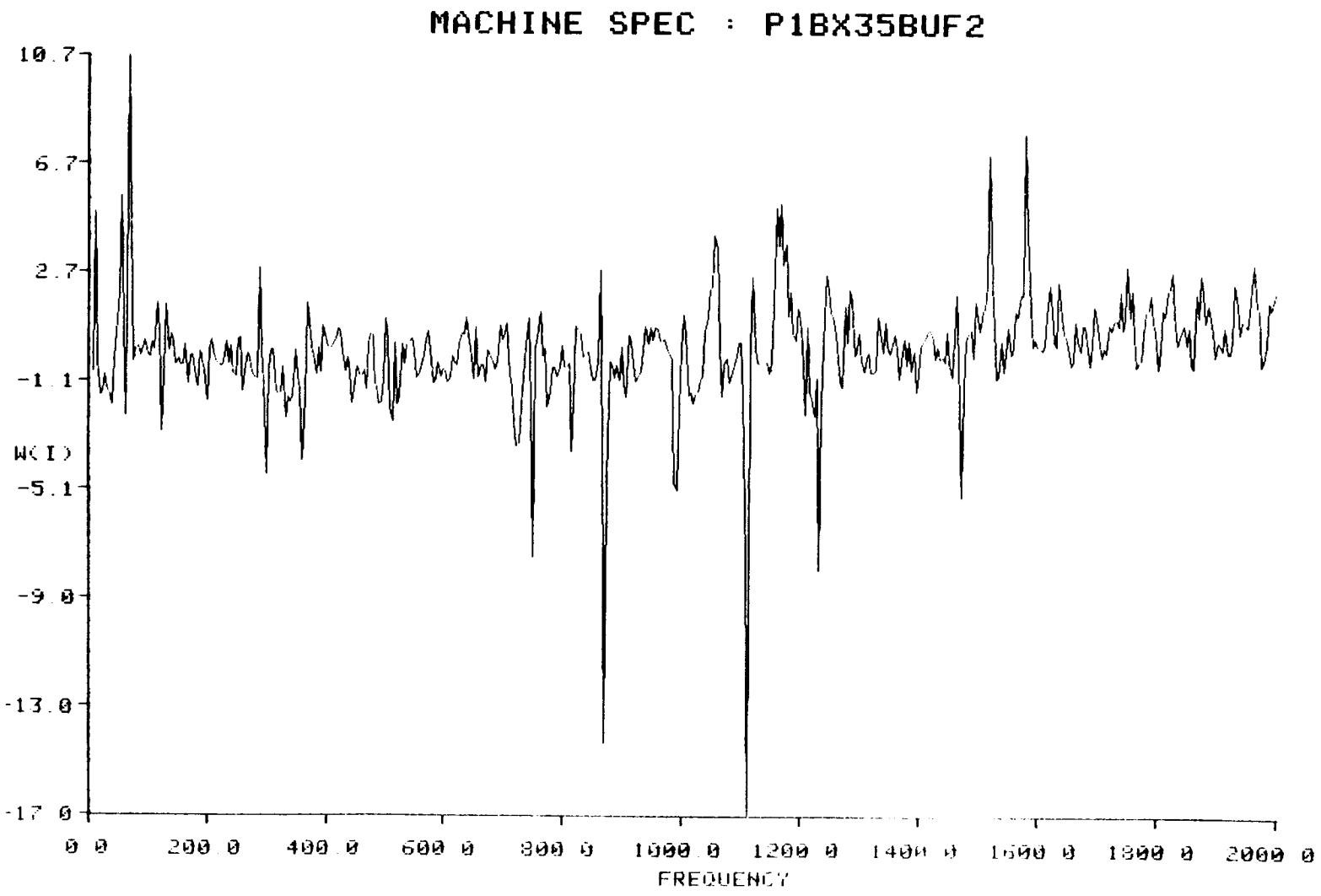

MEAN FOR FAULTED REFITS
MEAN FOR BASELINE REFITS
SIGMA FOR FAULTED REFITS
SIGMA FOR BASELINE REFITS

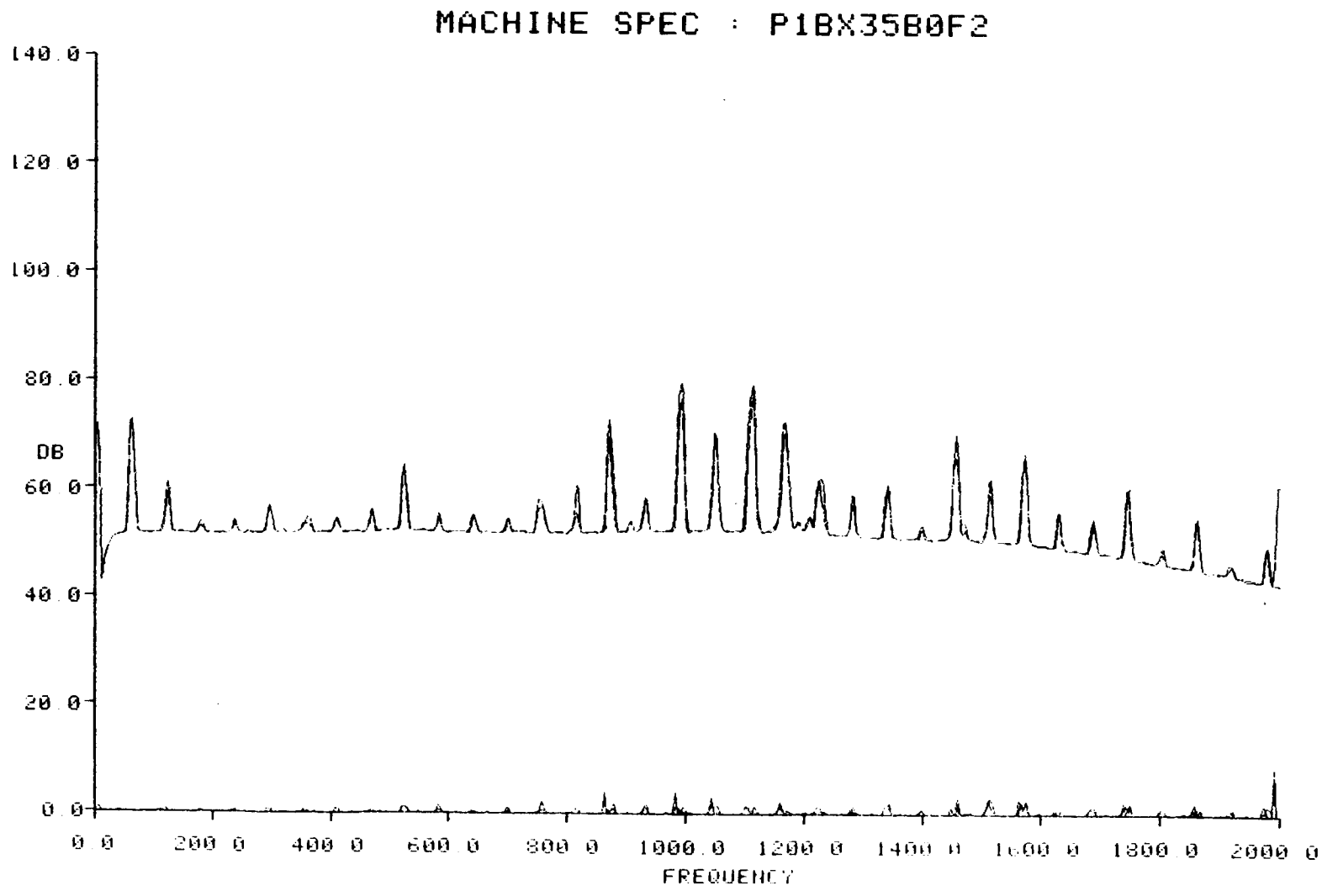

LIKELIHOOD RATIO WEIGHTS

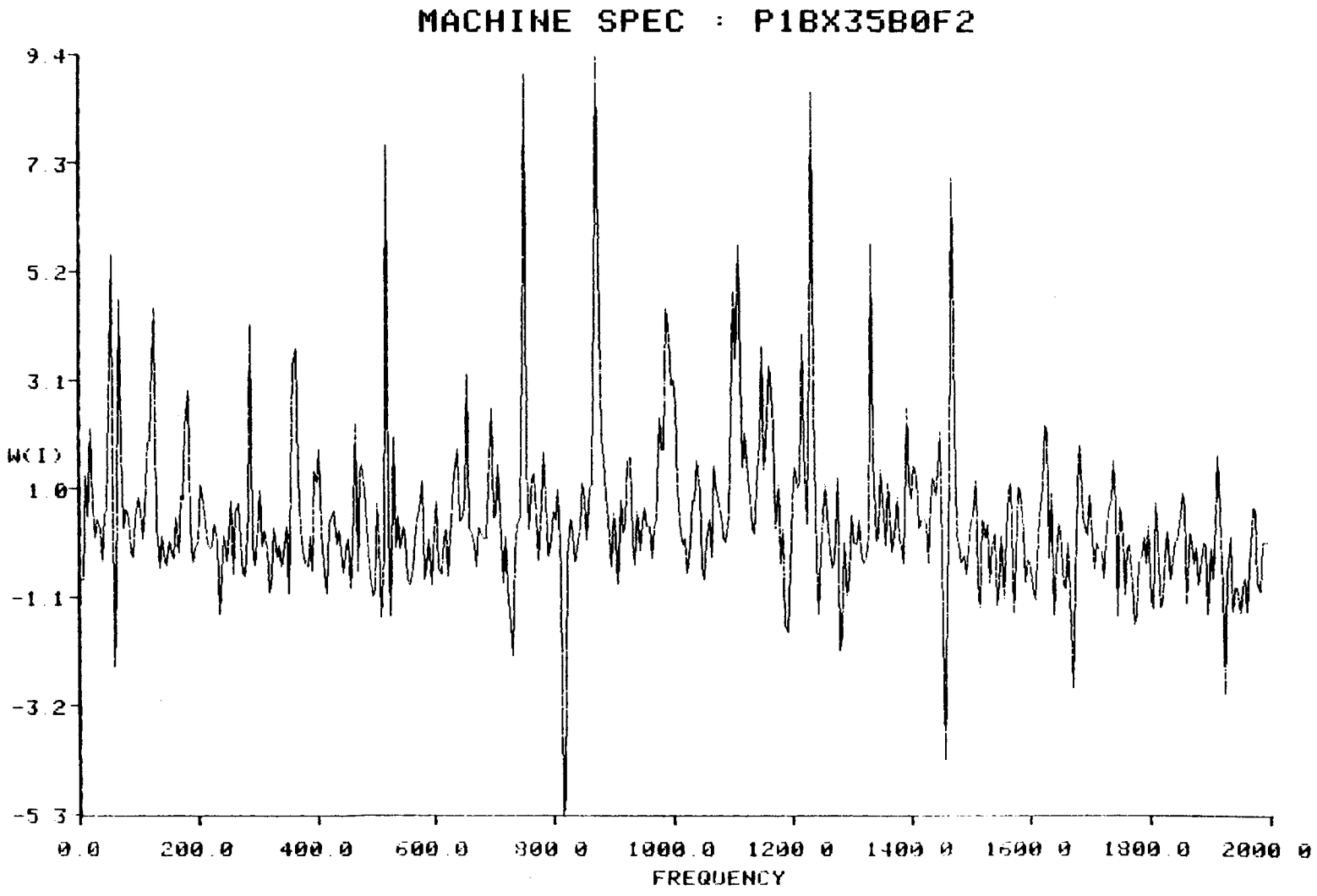

MEAN FOR FAULTED REFITS
MEAN FOR BASELINE REFITS
SIGMA FOR FAULTED REFITS
SIGMA FOR BASELINE REFITS

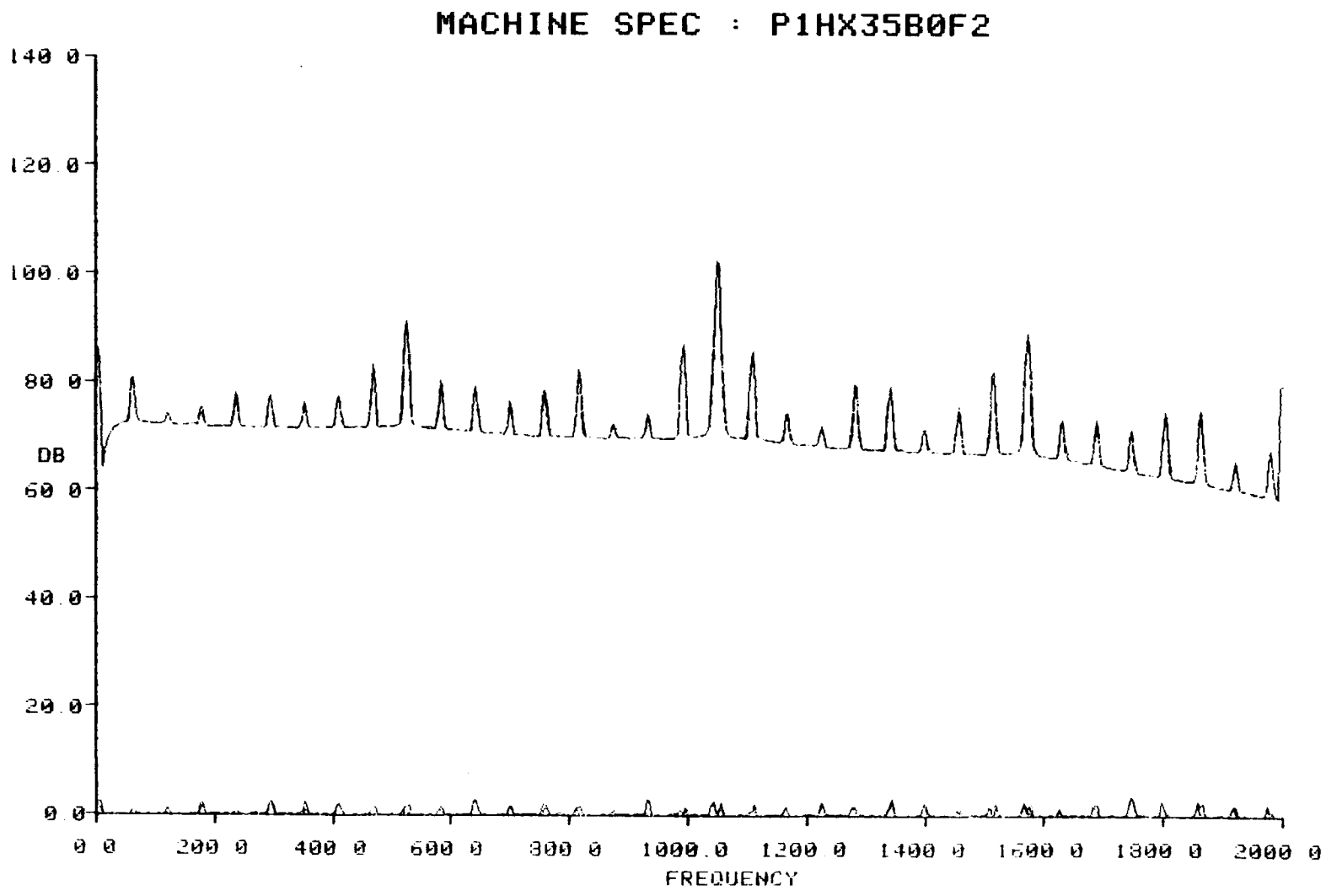

LIKELIHOOD RATIO WEIGHTS

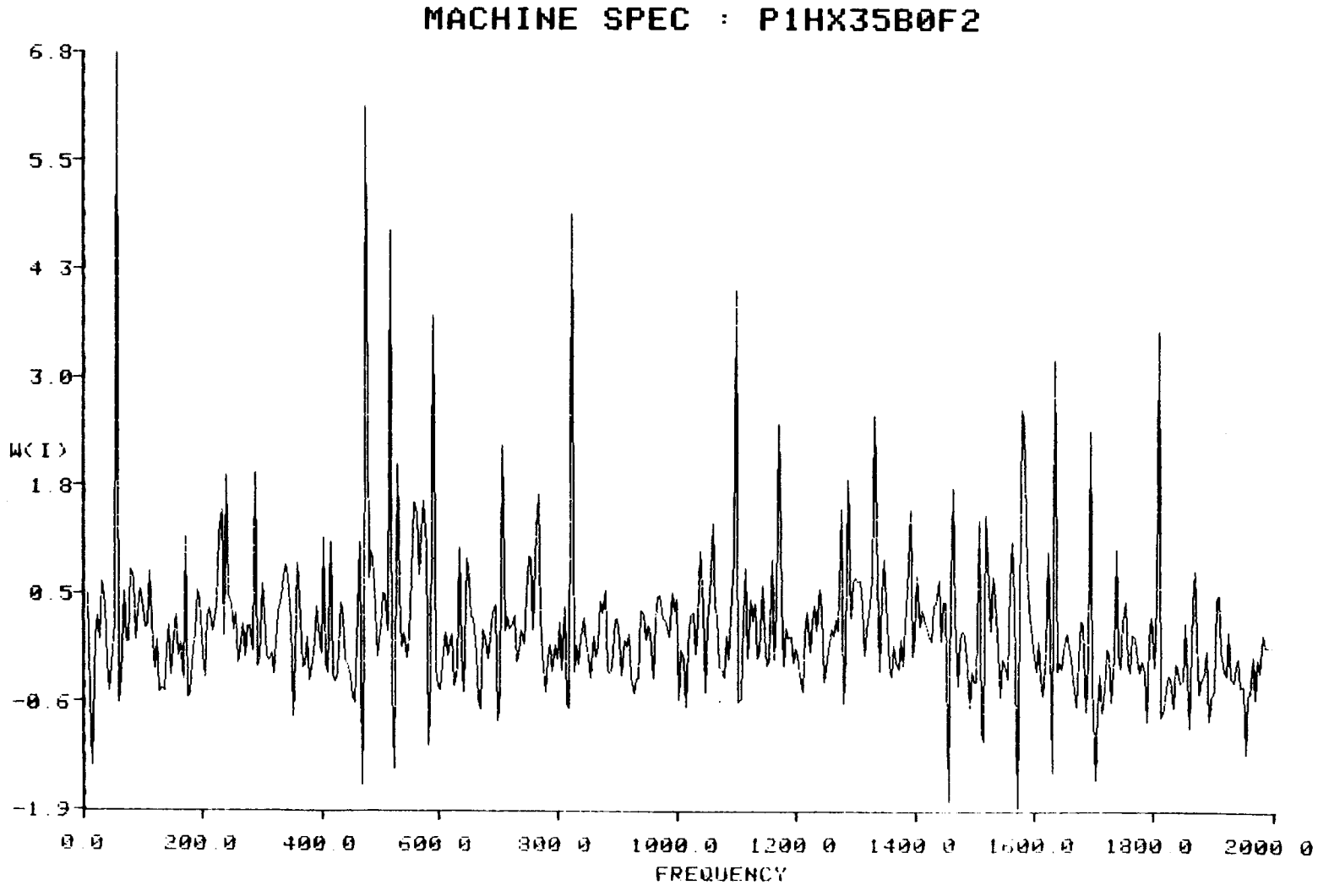

Optimum Signature Analysis Detection : Voltage Change - Single One-Phase Pump

P_D for $P_{FA} = 0.1$

Test Condition	Baseband	HFD
Under Voltage	1.0	1.0
Over Voltage	1.0	1.0

Appendix E

Likelihood Ratio Test For
Analysis of Machinery Vibration Spectra

ABSTRACT

The following appendix contains derivations and applications description for the likelihood ratio weighting technique for analysis of vibration spectra.

1.0 APPLICATION OF BAYES CRITERIA TO ANALYSIS OF MACHINERY VIBRATION SPECTRA

In order to provide an analysis technique with minimum reliance on specific spectral features and more dependent on global spectral behavior, an "optimal" binary hypothesis test based on Bayes criterion was investigated. The test known as the "likelihood ratio test", is described in this appendix.

1.1 Likelihood Ratio Test

1.1.1 Definition - The definition of the likelihood ratio derived from Bayes criterion for binary hypothesis tests (e.g. see reference 1) is given by:

$$\Lambda(x) \triangleq \frac{P(x/H_0)}{P(x/H_1)} \qquad (1)$$

where

$\Lambda(x) \triangleq$ likelihood ratio,

$P(x/H_1) \triangleq$ Probability density function of the observable x given hypothesis H_1, and

$P(x/H_0) \triangleq$ Probability density function of the observable x given hypothesis H_0.

It is often more convenient to use the natural logarithm of $\Lambda(x)$ given by,

$$\ln [\Lambda(x)] = l(x) = \ln [P(x/H_1)] - \ln [P(x/H_0)] \qquad (2)$$

since the logarithm is a monotonic function and allows multiplicative terms for joint probabilities to be converted to sums.

The "optimal" estimate of condition H_1 or H_0 is obtained by computing $\ell(x)$ for a given observation and comparing $\ell(x)$ with a threshold (see reference 1).

1.1.2 Application to Machinery Vibration Spectra - The problem of interest in this study is modeled by the binary hypothesis tests as given by:

H_1 Δ Spectrum indicates "clearly good" machine

H_0 Δ Spectrum is not indicative of "clearly good" machine (e.g. "questionable", or "bad" machine or faulty data).

The data necessary to compute estimates of the necessary probability functions are available. The next section describes the method of approach and assumptions used to derive the likelihood ratio processor from the vibration spectral data.

2.0 ASSUMPTIONS AND METHOD OF APPROACH

2.1 Gaussian Density and $\ell(x)$

The density function of the log amplitude of the vibration power spectra for a machine was assumed to be of Gaussian form, and the two hypothesis alter the density by variations in mean level only. Furthermore, the power estimates at each frequency or bin are assumed to be independent* so that the covariance matrix is diagonal. These assumptions allow the densities to be expressed as,

$$P(S_i/H_1) = \prod_{i=1}^{M} \left(\frac{1}{\sqrt{2\pi}\,\sigma_i}\right) \exp\left(-\frac{(S_i - m_{1i})^2}{2\sigma_i^2}\right) \quad (3)$$

$$P(S_i/H_0) = \prod_{i=1}^{M} \left(\frac{1}{\sqrt{2\pi}\,\sigma_i}\right) \exp\left(-\frac{(S_i - m_{0i})^2}{2\sigma_i^2}\right) \quad (4)$$

where,

S_i Δ Amplitude of machine vibration power spectrum in dB at frequency i for a given refit.

m_{1i} Δ Average log amplitude at frequency i of the machine vibration spectrum for data indicative of "clearly good" machine.

m_{0i} Δ Average log amplitude at frequency i of the machine vibration spectrum for data other than "clearly good", (i.e. "questionable", "bad", "faulty data").

* This assumption has been investigated in detail in previous studies and the results indicate that the independent bin assumption is not valid. However, the performance of the algorithm is not strongly dependent on this assumption.

$$\sigma_i^2 \triangleq \text{variance of } S_i \tag{5}$$

Given the definition of the likelihood ratio,

$$\Lambda(S_i) \triangleq \frac{P(S_i/H_0)}{P(S_i/H_1)} \tag{6}$$

the log likelihood ratio is given by:

$$\ell(S_i) = \frac{1}{2}\left[\sum_{i=1}^{M}\left(-\frac{(S_i - m_{0i})^2}{\sigma_i^2}\right) - \sum_{i=1}^{M}\left(-\frac{(S_i - m_{1i})^2}{\sigma_i^2}\right)\right] \tag{7}$$

Completing the square operations and canceling common terms in equation (7) yields,

$$\ell(S_i) = \sum_{i=1}^{M} \frac{S_i\,(m_{1i} - m_{0i})}{\sigma_i^2} + K \tag{8}$$

where k is a constant dependent on the mean values and may be combined with the threshold in processing the data.

2.2 Analysis of Vibration Data

Equation (8) of Section 2.1 indicates that the likelihood ratio processor consists of a weighted sum of the spectral values, where the weights are given by the ratio of the mean differences ("clearly good" versus not "clearly good") divided by the variance of the spectral values. The required mean and variance values are of course, not known apriori. However, the database collected during repeated experiments of good versus faulted machines may be used to estimate the required statistics.

A single machine type and accelerometer position is selected from the database. The data are then divided into the "good" and "not good" groups. The mean

and variance values for each group are computed as well as the mean and variance for the combined groups.

A given experiment was selected for analysis and the following quantities were computed,

$$m_{0i} = \frac{1}{N_0} \sum_{j=1}^{N_0} S_{0i}, \qquad i = (1, 2, ...,.500) \quad (9)$$

$$m_{1i} = \frac{1}{N_1} \sum_{j=1}^{N_1} S_{1i}, \qquad i = (1, 2, ...,.500) \quad (10)$$

$$\sigma_{0i}^2 = \frac{1}{N_0 - 1} \sum_{j=1}^{N_0} (S_{0i} - m_{0i})^2, \qquad i = (1, 2, ...,.500) \quad (11)$$

$$\sigma_{1i}^2 = \frac{1}{N_1 - 1} \sum_{j=1}^{N_1} (S_{1i} - m_{1i})^2, \qquad i = (1, 2, ...,.500) \quad (12)$$

$$\sigma_i^2 = \frac{\sigma_{0i}^2 + \sigma_{1i}^2}{2} \qquad i = (1, 2, ...,.500) \quad (13)$$

where,

N_0 = number of measurements for faulted machines.

S_{0i} = Amplitude of spectra in dB at frequency i for each good machine spectra.

m_{0i} = Mean value for faulted machine spectra at frequency i.

σ^2_{0i} = Variance value for faulted machine data.

$N_1, S_{1i}, m_{1i}, \sigma^2_{1i}$ Δ are the corresponding parameters for baseline machine spectra.

N = total number of spectra available (baseline and faulted).

σ^2_i = Variance at frequency i for all spectra.

The next step in the performance analysis of the likelihood ratio processor was the computation of the value of $\ell(S_j)$ for each j^{th} spectrum as given by:

$$\ell(S_j) = \sum_{i=1}^{500} (S_{ij} - m_i)\,\omega_i \qquad (14)$$

where,

$$m_i = \frac{m_{0i} + m_{1i}}{2} \quad \text{and}$$

$$\omega_i = \frac{m_{1i} - m_{0i}}{\sigma_i} \qquad (15)$$

The values of ω_i correspond to the likelihood ratio weights derived in Section 2.1 except that normalization is by σ rather than σ^2 to reduce the dependence on noisy estimates of σ^2.

The final step consisted of computing the values of mean and standard deviation for (S_j) over j (j = number of experiments) for both the baseline (B) and faulted (F) data sets. Values of μ_F, σ_F and μ_B, σ_B were then used to estimate the probability of detection (P_D) and probability of false alarm (P_{FA}).

Two basic techniques were used to obtain estimates of P_D and P_{FA}. The primary technique consisted of evaluation of Gaussian integrals of the following form,

$$P_D(T) = \int_T^{\infty} \left(\frac{1}{\mu_F \sqrt{2\pi}} \right) \exp - \left[\frac{(x - \sigma_F)^2}{2\sigma_F^2} \right] dx \qquad (16)$$

$$P_{FA}(T) = \int_T^{\infty} \left(\frac{1}{\mu_B \sqrt{2\pi}} \right) \exp - \left[\frac{(x - \sigma_B)^2}{2\sigma_B^2} \right] dx \qquad (17)$$

The value of assumed threshold T was varied to obtain corresponding values of P_D and P_{FA}. The second technique involved Monte Carlo simulation to account for uncertainties in the estimates of mean and standard deviation and is described in the main body of the report.

References

1. G.M. Milner, "Vibration Power Spectra Screening Analysis Final Report - Volume 1.0", 30 July 1985, Tracor Document No. T85-01-9518-U.

APPENDIX F

Harmonic Series Identification by Clustering

ABSTRACT

The following appendix describes the algorithm developed for this study to automatically identify and analyze harmonic series in narrowband spectral data.

1.0 INTRODUCTION

The clustering algorithm may be described in a series of fourteen algorithmic steps. A description of each of these steps is provided in this appendix.

2.0 ALGORITHM DESCRIPTION

1. Define $S_R(fi)$ as the spectral values of a measured spectrum after normalization for rotation rate.

2. Pass the spectrum $S_R(fi)$ through a tone identification algorithm. The operation of the tone identification algorithm is as follows:

   1) The noise spectral equalization (NSE) output spectra (prewhitened spectra) are processed by differencing all values to obtain local maxima which are determined by a positive difference followed by a negative difference.

   2) Each maxima is compared to a threshold (selectable with a default of 5 dB) and all values greater than threshold are retained. If the number of peaks is less than thirty, all peaks are retained. If the number is greater than thirty, then the absolute values of the peaks (before NSE) are compared and the thirty largest values are selected.

The index of each tone found is noted and stored as T (T = 1,2, ... M) and $M \leq 30$).

   3) Store the frequency index and amplitude of each tone.

T	Freq. Index [F(T)]	Amplitude [S(fi)]
1	21	70
2	42	82
3	58	91
4	69	56
.	.	.
.	.	.
.	.	.
M	408	64

(Note: The maximum value of M is 30.)

4) Compute an upper triangular matrix $\Delta F(S, T)$ for all differences in tone index as,

$$\Delta F(S, T) = F(S) - F(T) \qquad S = 1, 2, \ldots M; \quad T = 1, 2, \ldots S-1.$$

5) Certain values of ΔF are identified for a machine as ΔF_K $(K = 1, 2, \ldots N)$ (e.g. $\Delta F_1 = 59$, $\Delta F_2 = 102$, etc.).

6) The computations in step 4 are grouped according to ΔF_K. That is, N groups are formed. A given value of $\Delta F(S, T)$ is placed in group K if

$$\Delta F(S, T) = \Delta F_K \pm 1.$$

7) The pair S,T is saved as the ith member of group K if $\Delta F(S,T)$ satisfies the equation in step 6.

Grouping of Pairs

K =	1	2	3	4	5 . . . N
(ΔF_K =	(59)	(102)	.	.	. .)

i	S,T	S,T	S,T			
1	4,3	.	.	.	.	.
2	5,4	.	.	.	.	.
3	6,5	.	.	.	.	.
4	8,7	.	.	.	.	.
5	12,8	.	.	.	.	.
.	.	.	.	.	.	.
.	.	.	.	.	.	.
.	.	.	.	.	.	.
MAX_K						

Notes:

1. S > T, and the i index of pair S,T must correspond to increasing values of S. That is, if j > i, then Sj > Si.
2. MAX_K = the number of pairs contained in the Kth group.
3. MAX_K may equal zero for some or all K values.

8) Define,

S(K,i) = S value for ith pair of Kth group.
T(K,i) = T value for ith pair of Kth group.

9) Groups are formed according to the following algorithm:

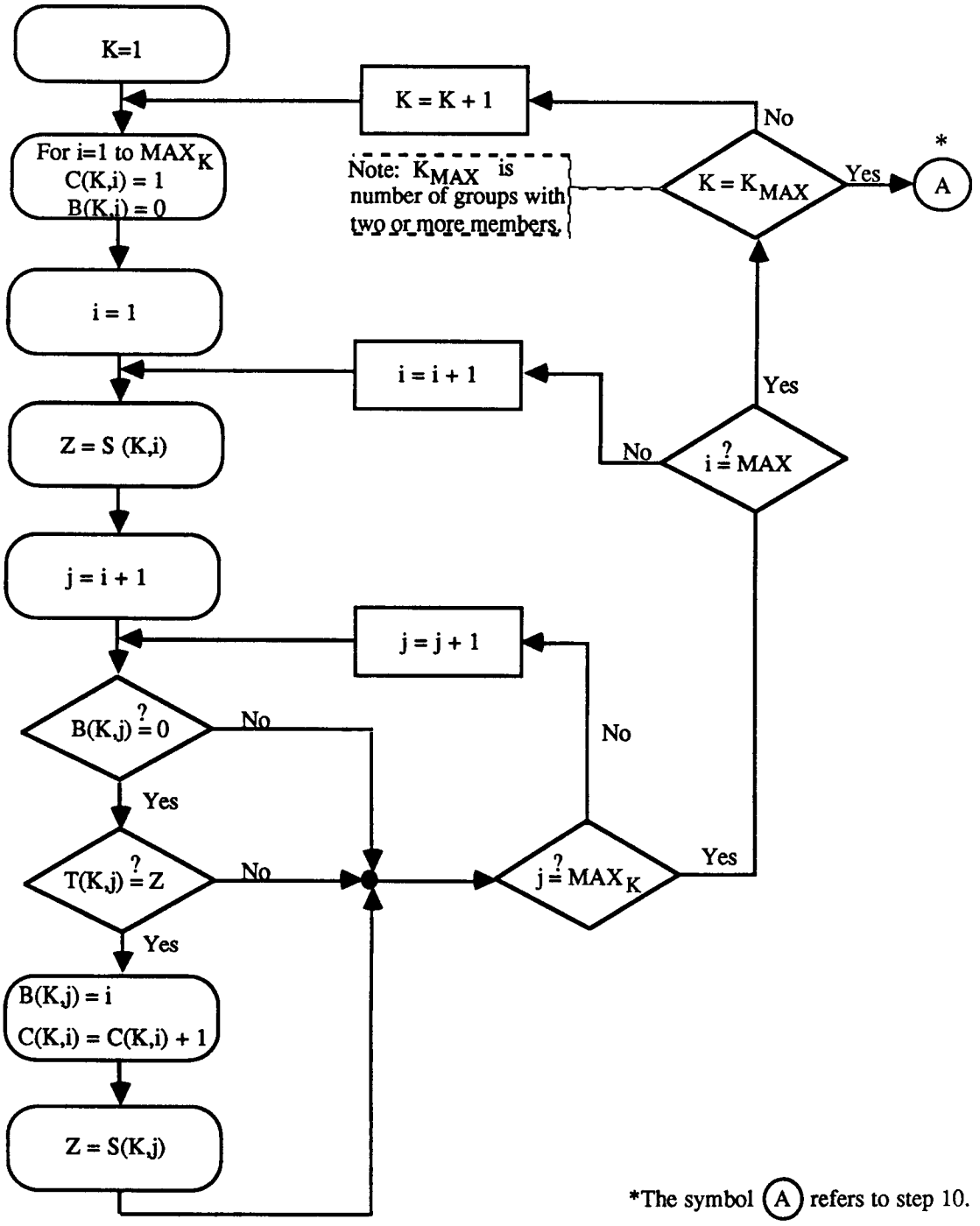

Figure F-1 - Algorithm for Harmonic Series Identification

10) For all C(K,i) $\geq$ 2, obtain a list of all unique tone index numbers in grouping K,i. The index values should have the minimum T value and maximum S value in a group. For example, if K,i contains index pairs (3,2), (4,3), and (6,4), then the index values associated with group K,i are 2, 3, 4, and 6.

11) Find the three largest (in amplitude) values of SR(fi) for each K,i group.

12) Obtain the average amplitude of all SR(fi) values in each group K,i.

13) Obtain the average ΔF for all pairs in group K,i.

14) Compute additional statistics of interest.